

Summer 2010



energie atomique • énergies alternatives

A person in a dark lab coat is working in a laboratory setting, illuminated by blue light. The person is positioned in the center-left of the frame, leaning forward. The background is dark and out of focus, suggesting a laboratory environment. The text is overlaid on the right side of the image.

Materials
*at the core of the process
of innovation*



Clefs CEA No. 59 – SUMMER 2010

Main cover picture

Most of the programs conducted by CEA entail, as a prerequisite, mastering innovative materials. Aware as it is of the challenges involved, but equally of the importance of the issues that must be met, with regard to such materials, standing at the core of component performance, CEA has set up a crosscutting program for that purpose.

P.-F. Grosjean/CEA – P. Avavian/CEA – P. Stroppa/CEA – Artechnique/CEA

Inset

top: The ultra-high-voltage (UHV) electron microscope, set up at CEA/Saclay, stands as a quite unique facility, for the purposes of simulating/observing some of the effects of in-service neutron irradiation on cladding materials, and other core components, be it in LWRs, fast reactors, or GFRs.

P. Stroppa/CEA

bottom: Tubular HTE cells. Development work on 600-cm² cells, featuring an innovative coaxial architecture. Electrode deposition by a coating process.

P. Stroppa/CEA

Pictogram on inside pages

A typical composite architecture for a hydrogen tank fabricated by filament winding. This technology allows a succession of resin-impregnated carbon-fiber plies to be laid, at varying angles, determined so as to ensure optimum thermomechanical behavior for the structure.

P. Stroppa/CEA

Review published by CEA

Communication Division

Bâtiment Siège

91191 Gif-sur-Yvette Cedex (France)

Phone: + 33 (0)1 64 50 10 00

Fax (editor's office): + 33 (0)1 64 50 17 22

Executive publisher

Xavier Clément

Editor in chief

Marie-José Loverini

Deputy editor

Martine Trocellier

martine.trocellier@cea.fr

Scientific committee

Bernard Bonin, Christian Charissoux, Gilles Damamme, Céline Gaiffier, Étienne Klein, François Papat, Gérard Sanchez

Iconography

Florence Klotz

Production follow-up

Lucia Le Clech

Subscription

Subscription (printed French version) to *Clefs CEA* is free.

Requests for subscriptions should be addressed, preferably via Internet, by using the form available at the site:

<http://www.cea.fr>

or by fax to: + 33 (0)1 64 50 20 01

Translated into English by

Jean-François Roberts

ISSN 1625-970X

Clefs CEA (CD-Rom)

Design of electronic media

Calathea – Paris

Phone: + 33 (0)1 43 38 16 16

With the exception of illustrations, all information in this issue of *Clefs CEA* may be freely reproduced, in whole or in part, subject to agreement by the editors and mention of the source.

© 2010 CEA

RCS Paris B 775 685 019

Head office: Bâtiment Le Ponant D, 25, rue Leblanc, 75015 Paris (France)

Materials at the core of the process of innovation

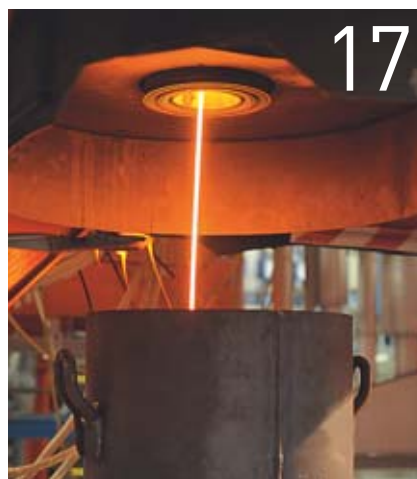
- 2 Foreword,
by Bernard Bigot
- 4 Challenges, avenues for advances,
and priorities for CEA's crosscutting
program on advanced materials,
by Frédéric Schuster

I. NUCLEAR MATERIALS

- 8 Introduction, by Bernard Bonin

- 10 **Innovative materials
for light-water reactor fuel
assemblies,**
by Jean-Christophe Brachet,
Marion Le Flem and Didier Gilbon

- 14 **Numerical experiments**
Multiscale modeling of materials:
from *ab-initio* calculations to kinetic
simulations,
by François Willaime, Thierry Deutsch
and Pascal Pochet



- 17 **Cold-crucible fabrication
of nuclear glasses,**
by Roger Boën
- 22 The long-term behavior of glasses
for waste containment purposes,
by Stéphane Gin
- 24 **Deciphering structures**
Solid-state NMR for the observation
of glasses at the atomic scale,
by Thibault Charpentier

- 26 **SiC/SiC composites
for GFR fuel claddings,**
by Patrick David, Fabienne Audubert,
Valérie Chaumat, Cédric Sauder and
Lionel Gélébart



- 31 **ODS alloys for structures subjected
to irradiation,**
by Yann de Carlan

- 35 **Experimental simulation**
Investigating the irradiation behavior
of nuclear materials: the contribution
of the JANNUS platform,
by Patrick Trocellier, Sandrine Miro
and Yves Serruys

- 38 **Environmental barriers for extreme
environments,**
by Frédéric Sanchette, Cédric Ducros,
Karine Wittmann-Ténèze, Luc Bianchi
and Frédéric Schuster

- 42 **The benefits of mesoporous solids
for the nuclear industry,**
by Xavier Deschanel,
Frédéric Goettmann, Guillaume Toquer,
Philippe Makowski and Agnès Grandjean

- 47 **Surface exploration**
Atomic-force microscopy:
a powerful, multipurpose technique
for the investigation of materials,
by Jacques Cousty





Foreword

Making available materials able to meet ever more searching specifications stands at the core of the process of innovation that CEA is committed to. The specifications involved relate to such requirements as specific technical performance, reliability, fabrication costs, durability, environmental impact, recyclability... This capacity for innovation is fostered on the basis of the original design of advanced components for new technologies. These new technologies include those under development for defense and global security purposes, and equally the new energy technologies, information technology or biomedical technology. In all of these areas, it is often found that materials are key. Aware as it is of these issues, CEA has always sought to further materials science, to meet the many challenges set by the programs it is engaged in. The forms of organization implemented at CEA for that purpose may have varied over time. Throughout, however, materials have remained a strong and constant concern for CEA, as the reviews contained in this issue will show.

Since 2006, crosscutting activities, in this area, have come under the "Advanced Materials" Program. This program is charged with driving the impetus for such activities, and providing a structure for them. Indeed, such a crosscutting character is found to be a requisite, in order to nurture novel ideas and new concepts, which often call for contributions from a number of disci-

plines. The program has the purpose, in particular, of bolstering the connection between front-end research and technological development work. It further has the remit of fostering or strengthening the indispensable alliances, to be set up with the best partners at hand in the field.

In the energy sector, CEA has been very active, in two domains, in contributing to R&D of different kinds. These R&D efforts on materials do exhibit a number of common features. Such common features include drawing on the best science available, while complying with clear, relevant roadmaps. On the other hand, these R&D programs do involve quite crucial differences. These differences do not stem from contrasting cultures, rather they are indeed intrinsic, though not to the point of precluding cross-fertilization. In the area of nuclear energy, operational feedback for an industrial application is, of its very nature, long in coming. Projects extend over the very long term. In this context, the development of a predictive science of the long-term behavior of materials is seen to be a requisite. This must go hand in hand with devising accelerated experiments, for the purposes of simulating e.g. the effects of materials irradiation. This science of nuclear materials further calls for resource-hungry fabrication facilities and suitable characterization resources. Indeed, characterization must be effected, preferably, at scales that will allow comparisons to be made with the results yielded by simulation.

In the sector of materials for new energy technologies, feedback from experience is found to be swifter. At the same time, competition is severe between the many players in the field. These technologies include photovoltaics, energy storage, the hydrogen pathway... While the timescales involved are indeed different, there are areas where cross-fertilization between new energy technologies and nuclear power is desirable. This is true, in particular, for fabrication processes, numerical simulation or advanced characterization techniques. Numerical simulation for materials has made, over the past 15 years or so, tremendous advances related to the predictive character of electronic structure calculations. CEA is active in this field and stands on a par with the best players worldwide. In the areas of information technology and biomedical technology, the specific physical and chemical properties exhibited by the materials involved are, likewise, crucial to the way devices operate. This is fundamental for the design of these devices to meet requirements stemming from industry and society

“As a whole, such advances in the field of materials are not viewed by CEA in isolation. Rather, in many instances, they are fostered through close partnerships: joint laboratories, technology platforms, alliances...”



L. GODART/CEA

at large. The rise of nanotechnologies, for the purposes of materials engineering, is set to bring in many advances. These will make it possible to expand considerably the range of properties exhibited by materials. Most importantly; they will also allow savings to be achieved in terms of raw materials. This is anticipated to result in benefits in terms of costs and the sustainable availability of resources. This research effort on nanomaterials is being conducted, at CEA, in a deliberately “integrated” manner, taking on board risk control, from the outset, together with consideration of the overall life cycle of materials. This approach is fully in tune with CEA’s engineering culture.

As a whole, such advances in the field of materials are not viewed by CEA in isolation. Rather, in many instances, they are fostered through close partnerships: joint laboratories, technology platforms, alliances... The players participating in France’s National Alliance for the Coordination of Energy Research (ANCRE:

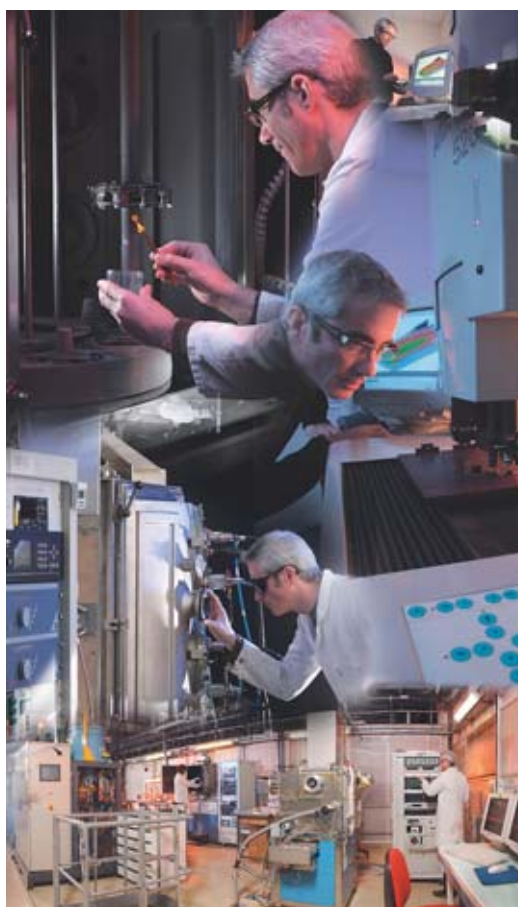
Alliance nationale de coordination de la recherche pour l’énergie) have clearly identified materials as a strategic sector for energy technologies as a whole. The same is true on the international scene, in particular within the European Energy Research Alliance (EERA), as in a number of European technology platforms.

I should like to extend the warmest thanks to all of those who have contributed to the writing, and editing of this issue, of the highest interest as it is. I wish every one of those reading it may find in it sources of inspiration, and a rekindled zest for materials science. For this is truly an area for which France, as indeed Europe as a whole, needs must step up the efforts, and resources devoted to it.

➤ **Bernard Bigot**
Chairman, CEA

Challenges, avenues for advances, and priorities for CEA's crosscutting program on advanced materials

Most of the programs run by CEA – in particular those answering the purpose of laying the ground for the energy sources of the future (fission, fusion, alternative energies, energy efficiency) – **entail, as a prerequisite, mastering innovative materials**, be it as regards synthesis, predicting, and controlling their properties, or ensuring predictable behavior under a variety of stresses, which may be severe, over the long term. Aware as it is of the challenges involved, but equally of the importance of the issues that must be met, with regard to such materials, standing at the core of component performance, CEA has set up an “Advanced Materials” Crosscutting Program.



A vacuum coating facility, used for the purposes of environmental barrier applications.

CEA's “Advanced Materials” Crosscutting Program has set itself the remit of articulating the production of scientific, or technological knowledge – at the front end – and applications-oriented programs, in those areas where there is still a potential for cross-

fertilization (in terms of processes, [simulation](#), characterization). It further aims to ensure continued vitality, ongoing evolution, and ability to adjust to changing requirements, with regard to CEA's technological capability, in the field of advanced materials. Often seen as they are, by designers of complex systems, as the supporting “stuff” that just needs to be supplied, materials yet stand at the very core of the process of innovation, particularly as regards the energy sources of the future. As such materials are seldom to be procured ready-made, “off the shelf,” researchers thus need to design them in order to suit the target application, while keeping to an acceptable cost, in environmentally compliant conditions, and meeting requirements for maximum raw materials conservation.

Arising as it did as the outcome of a thoroughgoing examination, and analysis of the strengths, but equally of the weaknesses at hand, together with the risks, and opportunities involved, the “Advanced Materials” Crosscutting Program has drawn up a strategy, articulated across ten priorities. Each one of these has the purpose of fostering an integrated approach, for research, but equally of building bridges between a variety of materials-related disciplines, which are often found to be highly insulated from one another – for breakthrough innovation tends to arise at crossover points between diverse cultures. In order to promote a consistent approach in key areas, the “crosscutting program” initiated the drawing up of four development plans, involving all of the centers of expertise at CEA, in the fields of high-performance metallurgy, advanced [composites](#), and [ceramics](#), surface engineering, and, finally, as regards the [synthesis](#), and incorporation of [nano-meter](#)-scale structures. A scientific task force has been set up, to drive these development plans. As of now, this brings together more than 450 research scientists at CEA.

P. Avramian / CEA

Materials for the reactors of the future

In the French context, the ongoing development, and growth of nuclear energy increasingly calls for in-depth knowledge, and understanding of the constituent materials used for the structures, and **fuel assemblies** being designed for nuclear reactors. CEA must anticipate how these structures will age, with regard to the lifetime extension of such reactors. Whether it be for **fourth-generation reactors**, or the **fusion** reactors of the future, catering for the operation of these installations entails designing, fabricating, and qualifying high-performance materials that extend the envelope, as regards strength, and resistance, to allow their employment in highly aggressive environments, which, in many cases, involve a combination of high temperature, strong **irradiation**, and heavy **corrosion**.

Pushing back the current boundaries of our understanding of structural, and fuel materials, at the **submicron** scale, is seen as an indispensable step, to enable:

- an improved prediction ability, as regards the robustness of materials behavior, in areas where experimental data acquisition remains fraught with difficulties;
- the development of innovative materials, affording the ability to meet peculiarly stringent specifications, as drawn up for the reactors of the future (Generation IV, fusion), while directing the research effort in such a manner as to steer clear of overlong, excessively expensive research and development stages, while bringing down lead times for materials qualification.

These major challenges call for two, complementary lines of approach. One, empirical approach is grounded on experimental knowledge, and the identification of behavioral laws; while the second, theoretical approach entails gaining a systematic understanding of the physical phenomena involved, and **modeling** these, so the experiments may be better directed, that will serve to validate the models.

High-performance metallurgy looms large, for the purposes of meeting the issues raised by the optimization of second-, and third-generation nuclear systems, but equally with regard to the development of materials able to withstand the extreme conditions prevailing in the fourth generation of **fission** reactors, as in the coming fusion reactor. The main goals set for this development plan include, first of all, setting up an industrial technology line, for the fabrication of nanoreinforced steels. This covers – very much at the front-end level – investigations as to the evolution of the metallurgical characteristics exhibited by materials, as a function of the fabrication parameters involved, or in materials subjected to extreme stresses, e.g. irradiation. The plan is further concerned with highly technological aspects, e.g. the extrapolation, to a pilot, or even to an industrial scale, of mechanical alloying processes, or the development of solid-state (i.e. below melting point) welding techniques. Finally, the plan provides for the investigation of alternative metallurgical routes to grinding, involving the use, in many cases, of processes originating in the area of surface treatment.

Another part of this plan covers the evaluation of new powder consolidation, and **sintering** technologies (e.g. spark plasma sintering), near-net-shape production technologies (direct manufacturing), and technologies for the fabrication of materials featuring a compo-



P. Stroppa / CEA

Fabrication of nanostructured coatings by thermal spraying.

sition gradient, and thus a property gradient. Finally, the plan must address the development of characterization techniques catering for the various scales involved in numerical simulation, together with tools for *in-situ* characterization, as for characterization in operating environments.

Ceramics: from aerospace to nuclear power

As regards the development of advanced composites, and ceramics, the main thrust, initially, concerns the development of ceramic-matrix composites (CMCs). These must meet the extreme requirements entailed by nuclear applications, which involve, in many cases, far more severe constraints than dedicated aerospace applications, for instance – in particular, with regard to the issue of tightness, with respect to fission gases. Indeed, such nuclear applications may not take up directly **silicon**-carbide-based products (SiC/SiC), as originally produced for the aerospace industry, since their properties are found wanting. This has led to the development of specific, nuclear-grade materials, exhibiting suitable **thermomechanical** properties, in terms of fission-gas-tightness, and nonreactivity with respect to nuclear fuel. With a view to steering away from conventional fabrication routes, e.g. **chemical vapor infiltration (CVI)**, researchers are exploring novel, alternative routes – e.g. rapid heating processes, or processes involving the use of nanopowders. Finally, CEA is keeping up an active technological watch, with regard to ceramics exhibiting a “ductile character” at high temperature, together with a strategic watch with respect to mastering the fabrication of key components, e.g. high-performance ceramic fibers.

High-performance surface engineering

With regard to the programs conducted at CEA, this is a discipline of strategic importance. The initial goal being set, in this respect, is to aim for the development of very-high-performance environmental barriers, to cater for extreme environments: corrosion, high temperature, irradiation, components in contact with **plasma**, in the case of fusion reactors... Any of which diverse stresses may occur, in some cases, in combination. Researchers are going for a less empirical approach, for the development of new surface treatments, by drawing on the contribution from numerical

Carbon nanotubes – laid out here in superposed mats – afford a wealth of applications, from industry (for flat screens, or fuel-cell membranes) to defense (they provide highly efficient chemical pollutant sensors, when filtering molecules are grafted onto them).



C. Dupont / CEA

simulation, to design “customized” surfaces, to suit a given operating environment. This surface engineering sector has undergone major changes, and advances, over the past 20 years. This is due, in particular, to the emergence of high-ionization-rate **physical vapor deposition (PVD)** processes, to the development of thermal spraying technologies – used to spray suspensions of nanopowders – or **chemical vapor deposition (CVD)** technologies, involving the direct injection, in pulsed-pressure mode, of liquid precursors, for instance. At the present time, the moment is seen to be opportune, to carry out a detailed review of the technologies at hand, but equally to go for the development of hybridized processes – since no single technology can yield a universal solution.

Finally, the extraordinary rise of advanced materials for alternative energy purposes, in particular for **thin-film photovoltaics**, means such technologies are now seen as eminently strategic in their own right.

From research to industry

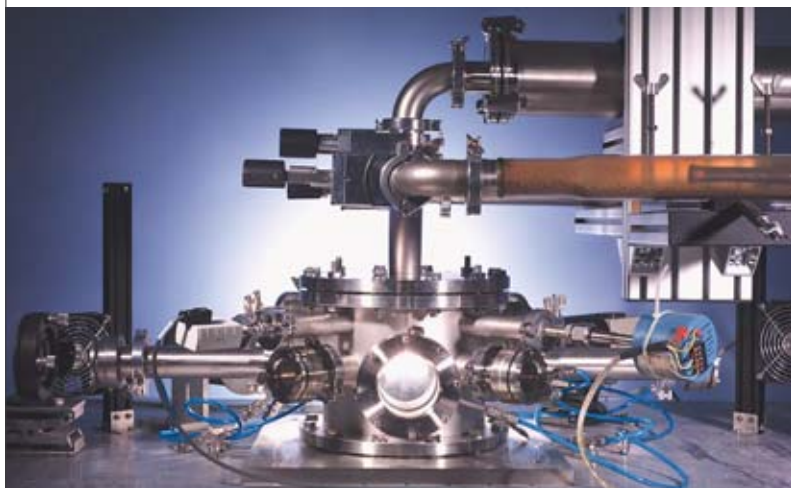
Many of the dedicated materials, or components for energy applications of the future – in particular in the areas of photovoltaics (so-called third-generation cells), energy storage (by **electrochemical** means, in

particular), or for the **hydrogen** pathway – already call for, or will be calling for the synthesis, and incorporation of nano-objects (nanopowders, nanotubes, nanowires), for the purposes of future developments. The fourth development plan, at CEA, is predicated on a twofold orientation. First of all, the aim is to evaluate, with the greatest objectivity possible, the technologies available for the synthesis of nano-objects (vapor-phase, liquid route...), while bearing in mind the requirement that they must lend themselves to going over to the industrial scale. Second, this plan is also intended to bring about a responsible, safe development of nanomaterials. In this respect, CEA stands as a precursor, with the *NanoSafe* program, dedicated to the safe production, and utilization of nanomaterials in an industrial environment. This global approach to risk control entails working on, at one and the same time:

- areas relating to the development of nano-object monitoring techniques, with regard both to measuring workforce exposure, and ensuring a detailed control of fabrication processes;
- the elaboration of ever more integrated synthesis processes, to eliminate, as far as feasible, any discontinuity;
- nano-object toxicology;
- the lifecycle – taken in its entirety – of nanostructured materials, down to, and including, the protocols for ultimate destruction, or recycling.

Further, participation in, and contribution to, standardization organizations is seen as one of the major aspects, in this newly emerging field of activity, and one which relates to manufacturers as a whole. As part of this evolution, tools are being developed for the techno-economic evaluation of nanomanufacturing, for the purposes, in particular, of evaluating the costs of safety measures, and the economic viability of certain processes.

In order to boost collaborative research efforts, by bringing in complementary expertise, both at the front-end, and industrial levels, a dynamic of projects in partnership has been set in motion, involving France’s National Research Agency (**ANR: Agence nationale de la recherche**), the competitiveness clus-



A. Bonin / CEA

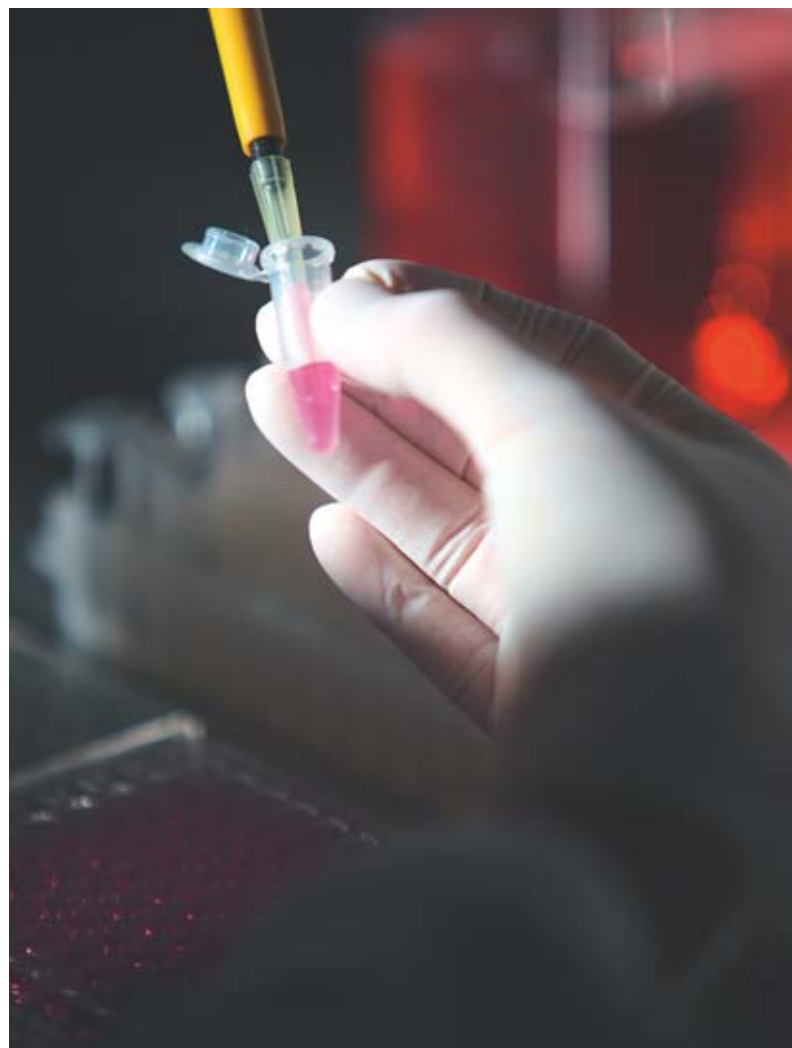
A laboratory setup for the synthesis of nanopowders, using laser pyrolysis technology.

ters (*pôles de compétitivité*) set up under national government auspices, the European Union's Framework Programs, the OSEO funding agency... Likewise, in order to optimize R&D efforts, reduce costs, minimize delays in accessing scientific, and technical results, a particular effort has been initiated, and must be driven forward, to ensure CEA is able to strike up the most useful alliances, both at the front end – with support given to a number of research groups (on spark plasma sintering, the Glasses research group, the PAMIR [Physique et applications de la matière sous irradiation: Physics of, and Applications for, Irradiated Matter] group) – and with industry. In the area of materials technology, the effort must be ongoing. The evolution affecting fabrication technologies, and technological utilizations, with regard to such advanced materials, entails that new developments be monitored, particularly attentively, in emerging technologies, enabling savings to be made in terms of raw materials, and energy, and seen to be readily reconfigurable, and environmentally compliant. The crosscutting program is constantly bolstering CEA's technological capability, though the setting up of joint laboratories, in partnership with industry, or academe, and technology platforms.

As is happening in other areas, the materials sector calls for a heightened effort, to maintain a scientific, technological, and strategic watch. For instance, the watch concerned with the development of integrated sensors, affording the ability to provide information, in real time, as to the state of aging, in a material being operated in a given environment, stands as a crucial field of investigation – bearing in mind the costs generated by installation outages, and maintenance operations. With regard to the prospects concerning component durability, a major area of investigation takes its cue from the watch monitoring the development of self-healing materials. In a context marked by the globalization of research, information technologies afford quick, ready access to the entire scientific, and technical production, worldwide. Indeed, the watch instrument yields gains, in terms of productivity, that are quite considerable, and thus serves to redirect the allocation of scientific resources, and exploratory research.

The setting up, under the auspices of the crosscutting program, of a “Materials Challenge” for exploratory research serves to promote funding for highly innovative projects, the taking up of novel issues, and exploration of new avenues. It is conducive to risk-taking, through the funding of “probe studies,” on issues of breakthrough innovation.

The “Materials Challenge” yields innovations that feed into all four development plans, by funding breakthrough research topics. It also ensures an ongoing flow of front-end research in areas that, while less broadly crosscutting (glasses, for instance), are resonant with societal concerns, since they are involved, in particular, in nuclear waste conditioning, and the prediction of long-term behavior as regards matrices used for waste disposal purposes. Finally, one general priority, for the crosscutting program, concerns numerical simulation, enabling as it does researchers to achieve savings in terms of time, and thus of experimental costs, which may loom quite large. Developed to the highest standards, numerical simulation makes



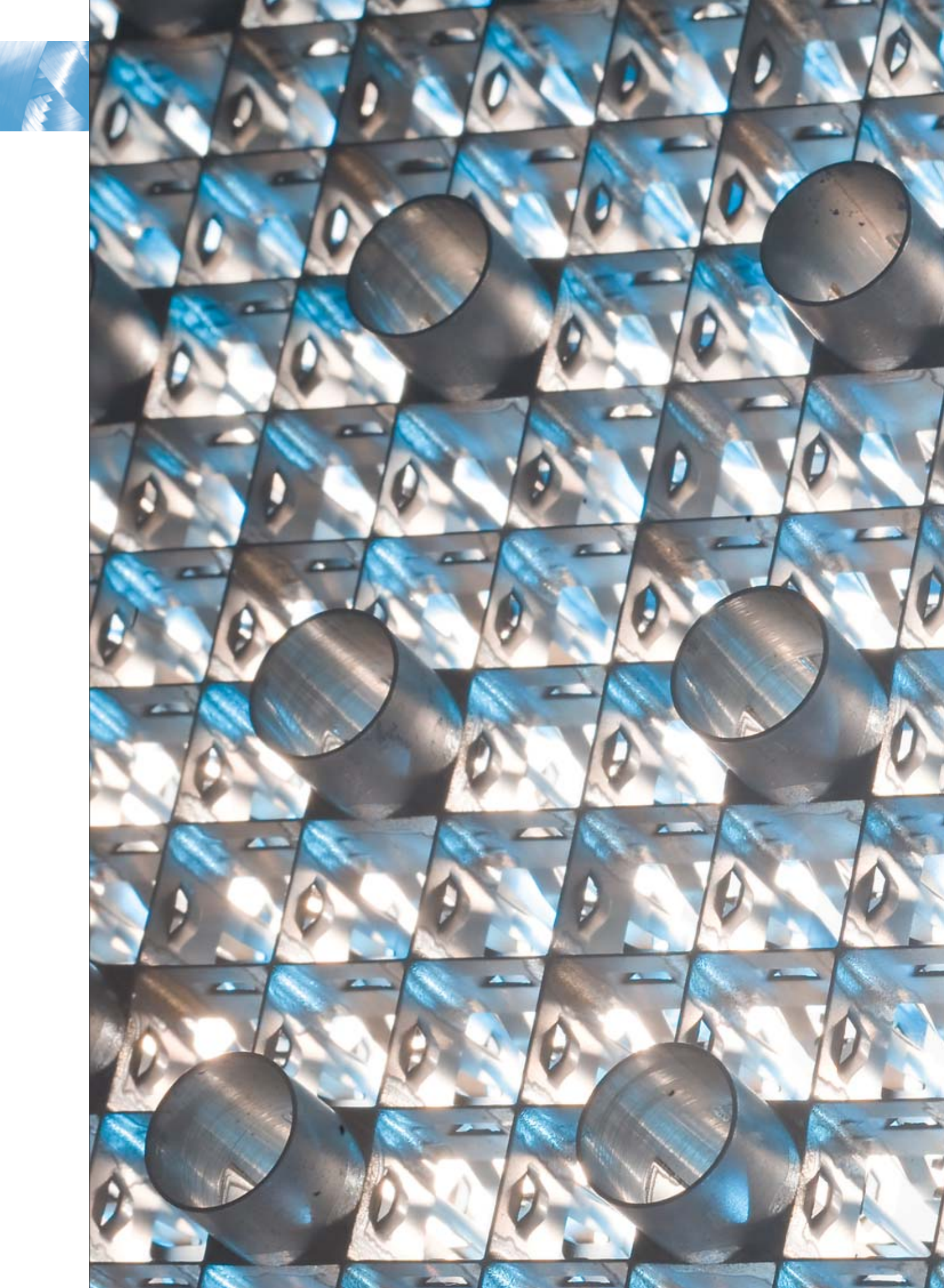
C. Dupont / CEA


Miniaturization of toxicity tests. Cells are exposed to nanomaterials inside a microbiological safety cabinet, to ensure work is carried out under sterile conditions.

a substantial contribution to the design of new materials: e.g. catalysts, electrolytes used in electrolyzers, novel architectures for photovoltaic cells, self-healing materials for extreme environments... It is likewise involved for the purposes of predicting behavior in an operating environment (irradiation, modeling corrosion...), and optimizing fabrication processes (in particular, as regards the switching over to an industrial scale of such key processes as mechanical alloying, assembly technologies, new densification, and consolidation processes...).

CEA is intent on bringing all of these investigations to the market, by ensuring they help promote France's industrial competitiveness, but equally through its communications effort, to “make its know-how known,” for the purposes of disseminating materials technologies, either directly to the existing industrial fabric, or by supporting the emergence of startups. Such are the challenges, and issues – hard to meet indeed, but altogether exciting – and such the priorities on which the “Advanced Materials” Crosscutting Program has elected to focus its action, and bring its resources to bear.

> Frédéric Schuster
 Director, “Advanced Materials”
 Crosscutting Program
 CEA Saclay Center





Spacer grid, to hold the rods of a 17×17 fuel assembly.
Nuclear materials are subjected to the coupled effects
of mechanical, thermal, chemical, and irradiation stresses.

P. Stroppa / CEA

I. NUCLEAR MATERIALS

Materials are of crucial importance, for the civilian nuclear sector. The behavior of materials under irradiation, thermal, mechanical, and chemical stresses determines the lifetime of existing reactors, and stands as the condition for their safety, and performance. All four types of stress are coupled with one another, and interconnected by the “time” variable: materials that fulfill their function as anticipated, for the entire lifetime of the installation – that is what is required! Nuclear waste management, likewise, is intimately dependent on the materials serving to condition such waste: glasses, cements, bitumens. These materials have the purpose of confining the waste’s radioactivity, and ensuring that waste takes on a solid, stable form, such as to allow handling, and ultimate disposal. Nuclear waste management raises the twin issues of the fabrication of the matrices and packages required, and of their long-term behavior, in storage, or in deep underground disposal. As is the case for reactor materials, the chief concern is to control corrosion, fatigue, creep, embrittlement, and swelling in these materials, when subjected to irradiation, be they metals, alloys, or ceramics.

The design of the nuclear reactors of the future is, in turn, closely bound up with the materials that are to be employed for their structure, and fuel. What is at stake here is not only these reactors’ performance, but indeed their very feasibility. In the coming fast reactors, materials will be subjected to grueling conditions, owing to neutron fluxes, and operating temperatures markedly higher than those prevailing in current water reactors. The coolant fluids under consideration raise highly specific corrosion issues. If they are to cater for more energetic neutrons, and larger heat flows, materials will have to cater for stringent constraints.

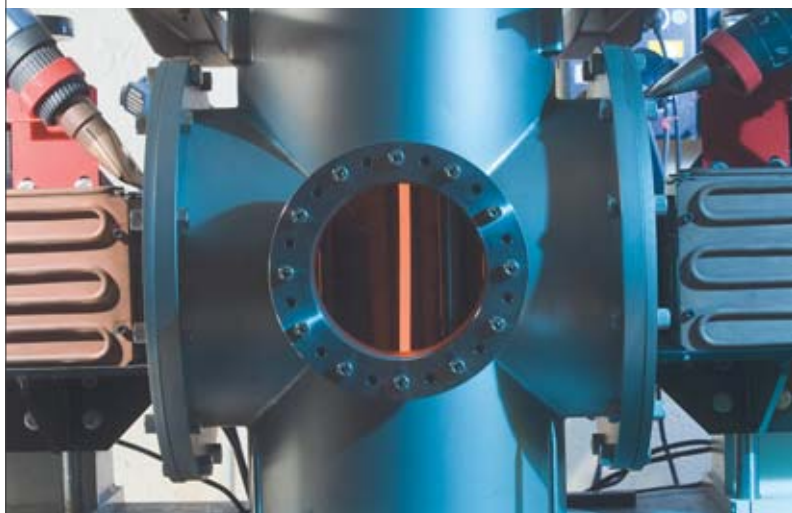
To take up these challenges, materials of all types are being investigated: metals, and alloys will go on being employed, owing to their ductility, mechanical strength, and the flexibility their use enables. Ceramics are being considered for their mechanical strength, and thermal, and chemical resistance. Their only drawback – albeit a major one – is their brittleness. For that reason, many of the materials of the future will be composites, since they make it possible to combine the qualities exhibited by their constituents, without their failings.

The development, and qualification of a novel nuclear material is a long-drawn-out affair. First, the ability must be achieved, of ensuring its *fabrication*, from the laboratory stage through to the industrial stage; then, of effecting its *characterization*, at the macroscopic scale, down to the atomic scale. This area has witnessed major advances, over the past few years, with the advent of near-field microscopy techniques. Then, the material must be *tested*. Neutron irradiation experiments are, as a rule, protracted, and costly, and the facilities to carry them out are few. Finally, there must be the ability to *model* the material. With the rising power of supercomputers, it becomes possible to envisage interconnecting the various modeling scales, to lay the foundations for the behavioral laws governing materials on a firm physical basis, at the microscopic scale. Such modeling will provide a framework, to gain an understanding of materials, and to predict their behavior. Meanwhile it will also be used as reference for their design, and to achieve their qualification with a limited number of experiments.

► **Bernard Bonin**
Scientific Directorate
Nuclear Energy Division
CEA Saclay Center

Innovative materials for light-water reactor fuel assemblies

Over the past few years, R&D efforts have allowed significant improvements to be achieved, as regards the performance of materials for light-water reactor fuel assemblies, thus securing sizeable operating margins. Nevertheless, fuel cladding – standing as it does as the first containment barrier for radioactive fission products and fission gases – is being addressed in sustained fashion. Thus, avenues for innovation are being explored, to secure further improvements yet, in terms of cladding robustness in nominal conditions, as in hypothetical accident situations.



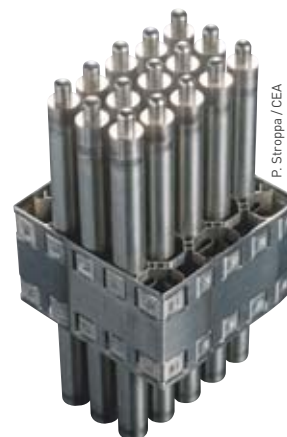
P. Stroppa / CEA

Cladding burst tests, in high-temperature accident conditions, are carried out in the “EDGAR” facility at the Applied Metallurgical Research Service (Service de recherches métallurgiques appliquées: CEA/DMN/SRMA). Part of the cladding, heated by Joule effect, may be seen through the observation port.

In light-water nuclear reactors (LWRs), the fuel assembly (see Figure 1) plays a paramount role, with regard to reactor efficiency, and safety. In particular, fuel cladding materials must meet stringent, demanding specifications, for many reasons: not only does the cladding stand as the first containment barrier, for radioactive fission products and fission gases, but it further contributes to the dimensional stability of the assembly as a whole, while ensuring the transfer of heat from the fuel itself, to the coolant fluid (water). LWR fuel cladding materials, involving as they do zirconium- (Zr) based alloys, are thus required to withstand, as best may be achieved, the various operating stresses arising, such as: corrosion due to water from the primary circuit environment, relatively high temperatures, the effects of neutron irradiation, and mechanical loadings⁽¹⁾ that may occur. All of which has led – for many years now – CEA, and its partners in industry, to investigate, and qualify “novel” fuel cladding materials, with the

aim of enhancing their performance and ensuring operating margins are maintained in nominal conditions, as in incident, or accident situations. Thus, over the past 20 years, industrial development work, carried out in particular by Areva NP, in partnership with CEA, has allowed significant improvements to be achieved, with regard to LWR fuel assemblies. As regards cladding materials, mention should be made – amongst other efforts – of the development, qualification, and deployment of Areva NP’s M5™ alloy. Indeed, this alloy [Zr base–1% Nb (niobium)–O (oxygen)] exhibits corrosion resistance, in operational conditions, that is markedly higher than that of Zircaloy–4 – i.e. the cladding material used for the reference fuel,⁽²⁾ an alloy going back some years now, of the Zr–1.3% Sn (tin)–0.2% Fe (iron)–0.1% Cr (chromium)–O (oxygen) type – as shown in Figure 2.

Figure 1. Part of a pressurized-water reactor (PWR) fuel assembly, comprising short fuel cladding segments fitted with endplugs, and part of one of the spacer grids. An actual fuel assembly may comprise as many as 17 × 17 rods, each more than 4 m long.



P. Stroppa / CEA

(1) Mechanical loadings: stresses applied to the material/component during operations, and/or in accident conditions, due to thermal and/or mechanical causes. For instance, when in operation, the fuel cladding tube is subjected to internal pressure, due to the initial pressurization gas, and fission gases, along with outside pressure, due to the pressurized water (155 bars). Moreover, once closure of the initial pellet–cladding gap has occurred (beyond 1–2 operating cycles), further stresses set in, exerted by the fuel pellet itself, which tends to undergo swelling, owing to the generation within it of fission gases.

In the longer term, however, researchers are aiming to achieve yet further improvements with regard to the performance and robustness of LWR fuel assembly materials. One particular purpose is to enable improved handling characteristics and an increase in the number of operating cycles and/or of fuel discharge burnup, while guaranteeing adequate safety margins, in possible accident situations in particular. The supporting R&D effort calls for the investigation of materials behavior, from very small scales (to gain an understanding of the physical processes involved) through to more macroscopic scales (operational behavior, semi-integral tests in accident conditions...). At the same time, advanced models must be developed, for the purposes of simulating – in the best feasible manner – the behavior of fuel cladding materials, thus making “predictive tools” available.

Innovative fuel cladding concepts

A number of avenues are thus being explored, with a view to securing innovations for fuel assembly materials. Forward-looking studies, for the purposes of evaluating – over more or less extended timescales – innovative cladding concepts, affording improvements with regard to some of the desired properties, for future LWR fuel assemblies, are currently being conducted at CEA.

A “composite” cladding

This is aimed at achieving a significant enhancement of mechanical strength, at high temperatures, for fuel claddings, through to the elevated temperatures liable to be reached, in some hypothetical accident scenarios, e.g. the loss of primary coolant accident (LOCA). One of the concepts that won acceptance involves the development of composite claddings, combining a conventional, metallic cladding material (zirconium-based alloys) – ensuring cladding tightness – with a ceramic material, exhibiting higher strength at high temperatures. Among the ceramic materials being considered, mention should be made of magnesium spinel, selected for its compatibility with regard to the required neutronic properties and its irradiation behavior, which, at first blush, does not involve any unacceptable drawbacks. Prototype stratified metal–ceramic composite claddings were thus fabricated, by plasma spray deposition. That pathway has been abandoned, however, for the time being, since the high-temperature sintering step, indispensable as it is for the purposes of densifying the sprayed material, induces interdiffusion phenomena, resulting in major degradation of the interfaces between the various strata of materials. At the same time, at the lower temperatures characterizing nominal operating conditions, the presence of layers of ceramic material causes a drop in thermal conductivity, and an overall falloff in ductility in the fuel cladding, such as might prove unacceptable in operational conditions. On the other hand, it should be said that a

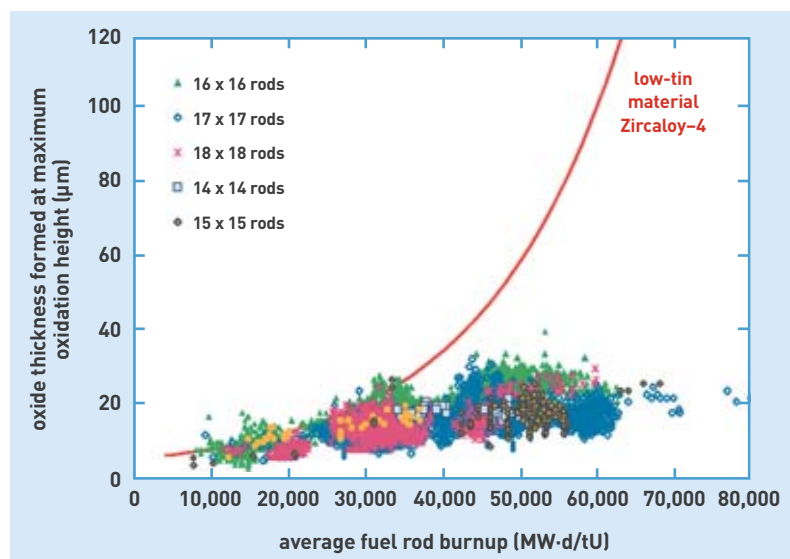


Figure 2. Evolution of the oxide thickness forming, during operations, on PWR fuel cladding materials (at the hottest axial level), as a function of burnup. [D. KACZOROWSKI *et al.* “Corrosion behavior of alloy M5®: experience feedback and understanding of phenomenological aspects”, Water Reactor Fuel Performance Meeting 2008 [WRFPM 2008], Seoul, Korea, 19–23 October 2008.]



Cladding samples, after undergoing burst testing in high-temperature accident conditions in the “EDGAR” facility.



Quench dilatometry test being carried out on a cladding sample, subjected to dynamic heating, and subsequent cooling ramp conditions (up to 100 °C/s).

(2) Reference fuel: the standard UOX fuel, in light-water reactors, consists of uranium oxide, enriched in terms of uranium-235.



Testing apparatus used for cladding burst tests from internal pressure in nominal conditions (around 350 °C), and picture of cladding segments subsequent to testing.



“ceramic–ceramic” concept, of the SiCf/SiC type (silicon carbide, SiC, matrix, reinforced with long SiC fibers), is being investigated in some laboratories in other countries, with a view to future LWR applications. This concept takes its cue from development work being carried out for the cladding of

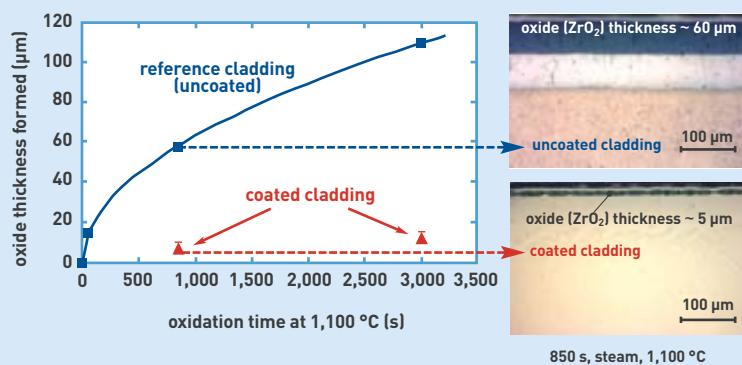


Figure 3. Behavior of fuel cladding segments during oxidation in high-temperature (1,100 °C) steam, simulating hypothetical accident conditions, e.g. in a loss of primary coolant accident (LOCA).

the forthcoming gas-cooled fast reactors (GFRs), which is one of the reactor lines under consideration for the fourth-generation nuclear reactors.

A coated cladding

Another avenue for innovation involves seeking to enhance corrosion resistance in nominal conditions – albeit more particularly in high-temperature accident (LOCA) conditions – by means of an *ad-hoc* coating, taking advantage of state-of-the-art deposition technologies such as physical vapor deposition (PVD), and chemical vapor deposition (CVD) processes. Early on, researchers elected to go for metallic, rather than ceramic linings, owing in particular to issues of physicochemical and thermomechanical compatibilities between the lining, and the zirconium-alloy substrate. A whole range of deposits is being investigated, in particular of the submicron multilayer type. Increasing the number of layers makes it possible, on the one hand, to associate different types of coating materials, in alternation, while, on the other hand, enhancing coating tightness, in the event of faults, and/or cracking arising in some of the sublayers.

Initial results are encouraging. In particular, for various types of multilayer deposits, a quite significant gain in high-temperature oxidation resistance – when simulating hypothetical accident conditions – was found (see Figure 3). The behavior of such deposits has yet to be investigated under irradiation, however, together with their potential for transposition to a more industrial scale.

An erbium-“poisoned” cladding

In order to raise fuel discharge burnup values and/or extend operating cycle length, fuel enrichment, in terms of fissile isotopes, needs to be increased. Such an evolution necessarily entails the availability of enhanced negative reactivity, with regard to neutrons. For that purpose, one of the means adopted, in conventional practice, involves directly adding, within fuel pellets, a burnable neutron poison, as a rule gadolinium oxide (Gd_2O_3). This is then referred to as heterogeneous neutron poisoning, since only a few rods in each fuel assembly are involved. This concept type indeed stands as the reference, for the assemblies of the forthcoming European Pressurized-Water Reactor (EPR).

One alternative, targeted by a currently ongoing R&D effort, now involves inserting the neutron poison into the cladding material, rather than into the fuel pellets. It was decided to go for erbium (Er), owing to its neutronic characteristics, which were deemed to be more suitable for the concept being considered. As is usually the case, with any development of novel materials, the first problems to be addressed concerned the “fabricability” aspects. In a subsequent stage, the issue is one of verifying compliance, for the properties achieved, with the specifications set for the application at hand.

In order to carry out the fabrication of prototype zirconium-based claddings featuring an erbium insert, the physicochemical compatibility of a rare earth, viz. erbium, with respect to a zirconium-based matrix first had to be verified. An initial fabrication pathway, by means of powder metallurgy, was

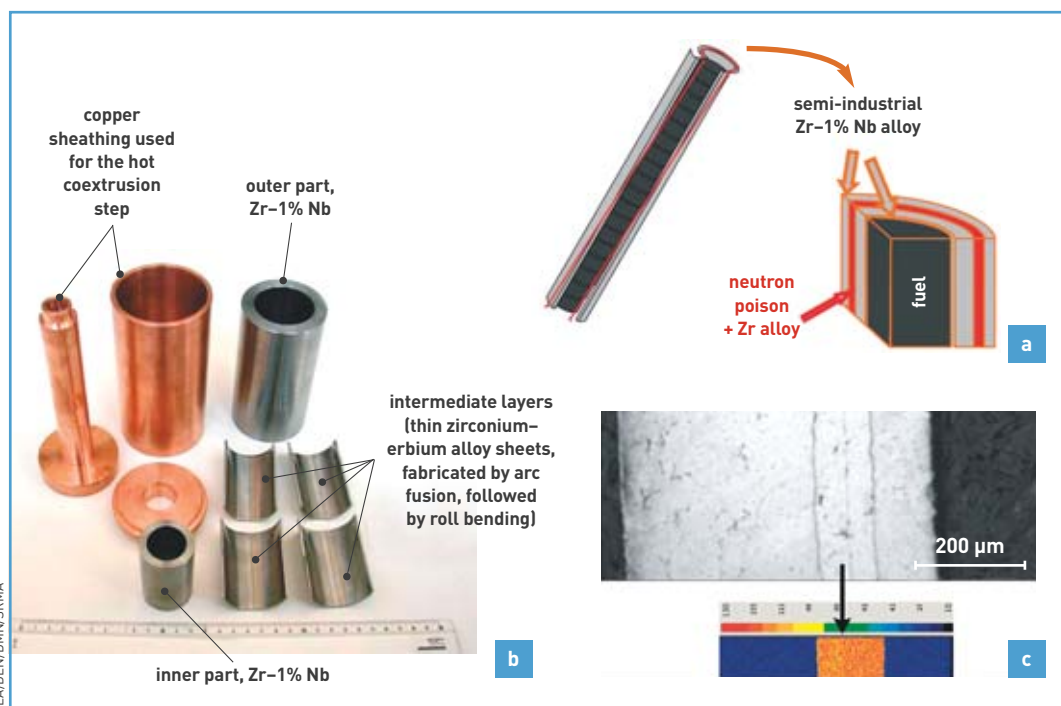


Figure 4.
(a) Schematic of the “Triplex” zirconium-based cladding with erbium insert.
(b) The various components of the blank, prior to the hot coextrusion step. (c) Optical micrograph, and X-ray cartography of the final cladding, with a thickness of some ~ 600 μm. The X-ray map [obtained by means of electron probe microprobe analysis] shows the erbium distribution across the thickness of the cladding.

employed at first, using the facilities available at CEA. This allowed an initial production run of “Triplex” – i.e. three-layered – claddings to be completed, in which erbium is inserted in the form of an intermediate zirconium–erbium alloy layer, sandwiched between two layers of industrially proven Zr–1% Nb (niobium) alloy. More recently, a semi-industrial fabrication run, based on processes involving **hot coextrusion**, followed by cold rolling, was successfully brought out, by way of a collaboration with **Areva Np/CEZUS**, resulting in the fabrication of nearly 10 meters of prototype cladding tubing (see Figure 4). With initial results proving encouraging, two successive CEA patents were registered. Such work has yet to be extended, however, to cover behavior under neutron irradiation, representative of the conditions prevailing during operation, as indeed in hypothetical accident situations. Finally, a more thorough techno–economical study needs to be conducted, to assess the benefit accruing from transfer to a more industrial scale.

From the laboratory to industrial production: a long-term endeavor

Forward-looking studies, aimed at evaluating innovative LWR fuel cladding concepts have thus allowed a number of avenues of interest to be identified, some of which have resulted in patents being filed. Evaluations carried out at a more industrial scale, along with investigations of irradiation behavior are planned, for the coming years. It should be borne in mind, on the other hand, that the development, and qualification of novel materials, intended for nuclear reactor fuel assemblies, must meet stringent safety constraints, and consequently rely on extensive operational feedback. This latter point calls for, in particular, irradiations carried out in research reactors, as in industrial power reactors, and subsequent examinations in hot laboratories. All of which stages induce quite extended timescales, typically some 10–20 years, before it becomes feasible to go over from the laboratory scale, on to an industrial level, and operational qualification.



General view of the “Castaing” electron microprobe, which makes it possible to quantify, in particular, the distribution, at the micron scale, of added elements, and impurities, within fuel claddings.

> **Jean-Christophe Brachet,**
Marion Le Flem and **Didier Gilbon**
Department of Materials for Nuclear Energy
Nuclear Energy Division
CEA Saclay Center

FOR FURTHER INFORMATION

Nuclear Fuels, a CEA Nuclear Energy Division Monograph, Editions Le Moniteur (2009).

CLÉMENT LEMAIGNAN, *Science des matériaux pour le nucléaire*, “Génie atomique” Series, EDP Sciences (2004).

NUMERICAL EXPERIMENTS

Multiscale modeling of materials: from *ab-initio* calculations to kinetic simulations

A *ab-initio* calculation methods, for the purposes of computing electronic structures, have made it possible, since the early 1990s, to simulate the properties of perfect crystalline materials – i.e. of materials free of any defect. By improving such methods, and with the increasing power of supercomputers, it has now become feasible to simulate the properties of elementary defects, which may seldom be accessed directly through experiments. This has opened up a vast, fruitful field of multiscale simulations, where such data yield the basis for realistic simulations of the kinetics of materials evolution. The kinetic Monte-Carlo method thus provides the means to model phenomena acting at the scale of a second, or even of a year.

The multiscale method

The strategy adopted involves concatenating a variety of methods, to rise up in the scale of the system sizes, as of the timespans simulated. At the *smallest scale*, *ab-initio* methods, based on quantum mechanics – more specifically, on density-functional theory⁽¹⁾ – afford the ability to predict, for a wide range of materials, to a precision of a few percent, most of the properties amenable to simulation in terms of a volume of several hundred atoms. These methods have the huge advantage of involving no parameter to be adjusted, even though they are by no means free from approximations. They do require, on the other hand, the use of massively parallel supercomputers, since they are highly resource intensive, in terms

of computing power. Considerable work has been carried out, over the past few years, for the purposes, on the one hand, of bringing down total computation time, by way of the simultaneous use of up to several hundred processors, and, on the other hand, of enhancing precision, for the properties computed, with regard to ever more complex defects. *Ab-initio* methods make it possible to compute, to a precision that proves as a rule adequate, for the purposes of physical metallurgy applications, energy differences between different atomic configurations, as e.g. between two crystal phases, or between

(1) Density-functional theory: a theory based on the existence of a universal functional, making it possible to compute the energy of a quantum system of n particles, on the basis of electron density.



The Titane supercomputer at CEA's Research and Technology Computing Center (CCRT: Centre de calcul recherche et technologie), one of the components of CEA's scientific computing complex, based at the Bruyères-le-Châtel site, near Paris (DAM-Île-de-France Center). Realistic, high-performance simulations are carried out at the site, to gain a better understanding of materials behavior, particularly under irradiation.

P. Stroppa / CEA

a perfect crystal, and a crystal featuring a defect (defect formation energy), or between the upper, and lower bounds of the energy barrier a defect must cross in order to migrate (defect migration energy). Going over to *larger scales* – for samples of the order of 1 cubic micrometer (μm^3), and times longer than 1 second – involves the use of statistical physics models, of the kinetic Monte-Carlo type. The name “Monte-Carlo” stems from the fact that the occurrence of elementary events, and their duration – be it a defect jumping along the crystal lattice, or two defects reacting by *diffusion* – are derived by generating random numbers. Such models chiefly take into account the energies involved for the various elementary diffusion mechanisms, and afford the ability to simulate spatio-temporal evolutions as regards the chemistry of, and defects in, a material. Such simulations prove far less costly, in terms of computation time. Such coupling between *ab-initio*, and kinetic Monte-Carlo methods allows highly realistic “numerical experiments” to be carried out, which may be directly compared to actual experimental findings. This approach will be illustrated for two cases: *self-diffusion* in silicon, and *irradiation defects* in iron.

Self-diffusion in silicon

For more than 50 years, self-diffusion in silicon has been addressed by numerous studies, both experimental, and theoretical. This phenomenon, simple though it may be at first blush, has given rise to much debate. From an experimental standpoint, the difficulty stems from the competition arising between *vacancy*, and *interstitial* mechanisms, together with their sensitivity to temperature, stresses, or *doping*. From a theoretical standpoint, the issue arises owing to the Jahn–Teller effect,^[2] and the various charge states exhibited by the vacancy.^[3] In this particular case, the resort to *ab-initio* methods is thus unavoidable, as they precisely reproduce such electronic effects. Thus, on the basis of Monte-Carlo simulations, computational physicists at CEA showed that the vacancy–vacancy interaction must be taken into account, if the experiments carried out at various temperatures, and in diverse *thermodynamic* conditions (doping, or intensive *irradiation*) are to be correctly reproduced. This results in a form of diffusion that does not conform to an Arrhenius law:^[4] three temperature regimes arise, the existence domains for which are strongly dependent

on defect concentration (see Figure 1). On the basis of these simulations, a phenomenological model may be put forward, linking the diffusion energy E to the vacancy concentration C_v , and temperature T – $[E(C_v, T)]$ –, allowing the various experiments to be reconciled. This phenomenological model may then be used in industrial simulators of the *computer-aided technological design* type, to determine the optimum conditions for the fabrication of *nanometer*-size devices, for which the control of diffusion is a key parameter. This is then referred to as point-defect engineering. The effect of a biaxial stress on diffusion is one further phenomenon that needs to

be taken on board, if these fabrication conditions are to be accurately determined. Thus, experiments carried out in 1994 evidenced a speeding up of vacancy diffusion under compression and a tailing

- (2) Jahn–Teller effect: this effect corresponds to a distortion of a system (crystal lattice, nonlinear molecule...), resulting in the removal of the degeneracy for some electronic levels (i.e. that occupy the same energy level), and a lowering of that system's energy.
- (3) In insulating materials, vacancies may exhibit an electric charge state that is neutral, positive, negative, doubly negative, doubly positive...
- (4) I.e. the logarithm of the quantity measured does not vary in linear fashion with the inverse of temperature.

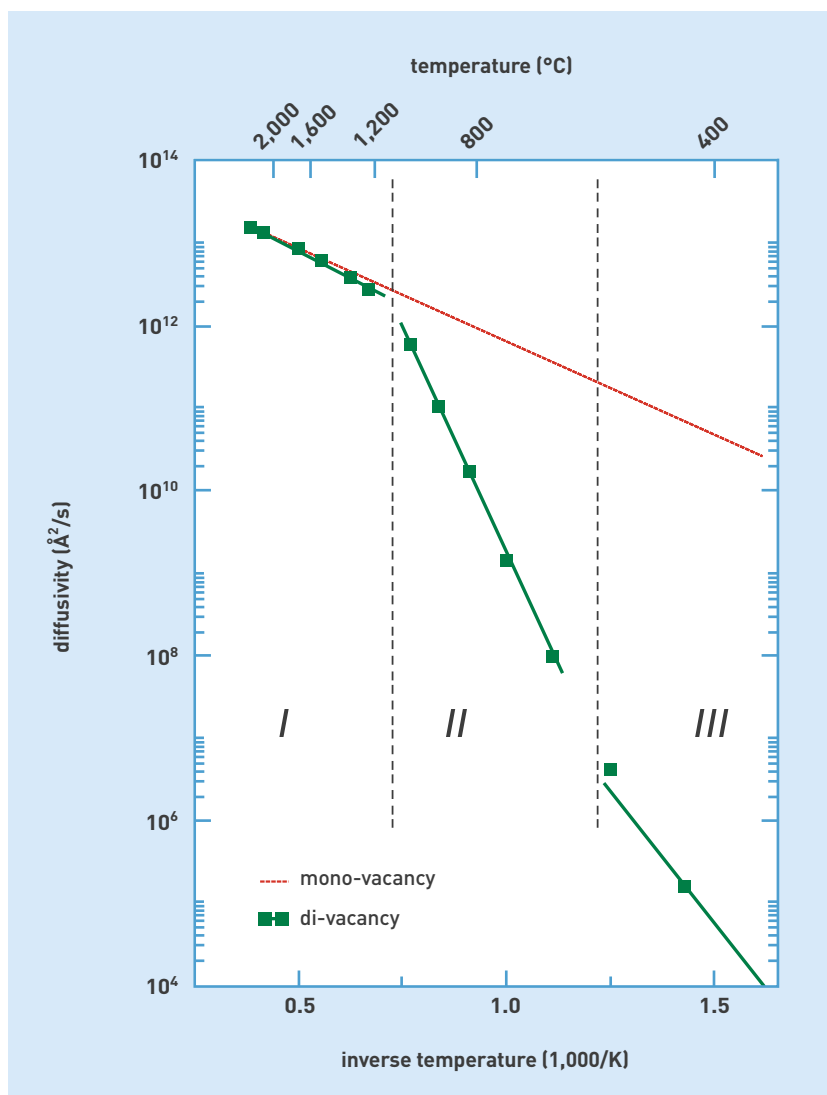


Figure 1. Diffusivity in silicon, as a function of temperature. The red dotted line plots the case of an isolated vacancy (mono-vacancy), this merging with the simulated curve at high temperature. The slopes of the green segments are a measure of effective diffusion energy, which may be compared with experimental findings. A di-vacancy corresponds to the aggregation of 2 vacancies.

NUMERICAL EXPERIMENTS

off under tension, and, conversely, a speeding up of interstitial diffusion under tension and a falling off under compression. *Ab-initio* calculations performed at CEA made it possible to predict an asymmetrical behavior as regards the intensity of this effect, with respect to tensile, and compressive stresses. This purely electronic effect (Jahn-Teller effect) had been disregarded up to now. This new analysis thus reconciled the various experimental measurements that had appeared somewhat scattered.

Irradiation defects in iron

A material subjected to irradiation by high-energy **neutrons** undergoes alteration, both structurally, through ballistic damage, and in terms of its chemical composition, owing to **nuclear** reactions. These two effects may be "simulated" in speeded up fashion, without **activating** the material, by means of **ion** beams (see *Investigating the irradiation behavior of nuclear materials: the contribution of the JANNUS platform*, p. 35), by reproducing, within a few hours, and in highly realistic fashion, the damage that would be generated by neutrons over several decades. The state of the material will depend – aside from this flux of defect, and **transmutation** product generation – on the evolution kinetics of the defects, liable as this is to result in the formation of **dislocation loops**, cavities, or **precipitates**, or to cause a segregation of **alloying elements** at **grain boundaries**. These phenomena are the causes of the dimensional changes observed under irradiation (**swelling**, growth), or of the degradation found, in terms of thermomechanical properties (**hardening**, embrittlement). By raising the temperature, the various thermally activated processes that control this defect evolution kinetics may be speeded up in like manner to the speeding up of their generation. However, the connection between thus diverse irradiation conditions may only be achieved by way of multiscale modeling. Such coupling, between *ab-initio* calculations, and kinetic Monte-Carlo simulations, is one of the keys to the strategy adopted by the research program units on Basic Scientific and Technological Research (RSTB: Recherche scientifique et technologique de base), and Simulation, at CEA's Nuclear Energy Division, for the purposes of gaining a better understanding of materials behavior under neutron irradiation.

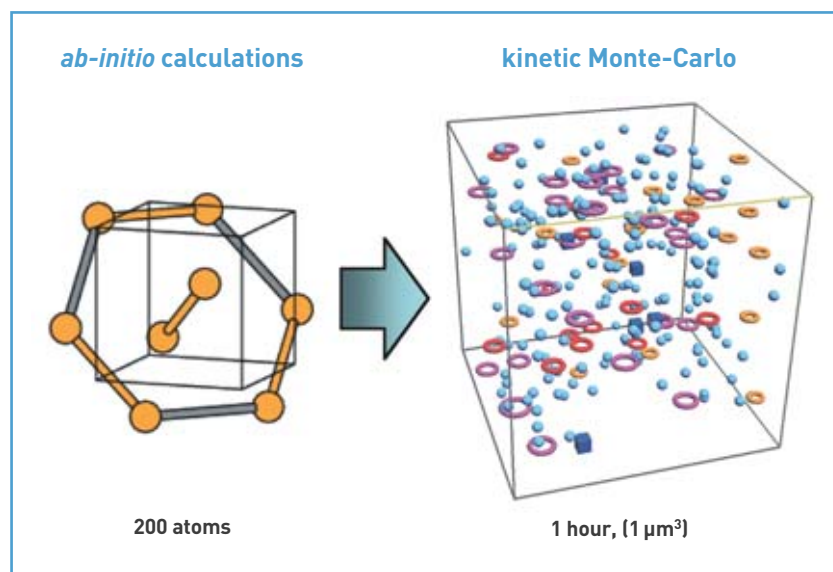


Figure 2.

Multiscale modeling of irradiation defects in iron. At left, a cluster of 4 self-interstitials, in the form of dumbbells (orange), as obtained by *ab-initio* calculation. At right, snapshot of the evolution of a population of defects, as acquired by kinetic Monte-Carlo simulation. The rings, the blue spheres, and blue cubes represent, respectively, interstitial clusters, vacancies, and vacancy clusters.

In iron-based materials exhibiting a **body-centered cubic structure** – including **ferritic steels** – one of the bottlenecks, as regards modeling this kinetics, is the mobility of small defect clusters. A number of barriers have been overcome, over the past few years, by means of simulation. First, *ab-initio* calculations made it possible to identify the structure of the **self-interstitial** in iron, and its migration mechanism. It proved feasible to simulate a complete experiment, involving the **annealing** of defects in ultrapure iron, after irradiation by electrons at low **dose**, by the kinetic Monte-Carlo method, on the basis of the migration, and dissociation energies of small vacancy clusters, and interstitial clusters, as derived by *ab-initio* calculation. This multiscale simulation yielded the ability to reproduce, for the first time, all four annealing stages observed experimentally, suggesting that the energy landscape yielded by *ab-initio* calculations was indeed a plausible one. This made it apparent, in particular, that the defects that become mobile around 300 K – a matter for much controversy for more than 20 years – are indeed mono-vacancies. It is apparent, at the same time, that clusters of 3 or 4 vacancies are far more mobile than single vacancies. These findings are of particular importance, with regards to materials subjected to neutron irradiation, in which such defects are liable to form

directly in **atomic displacement cascades**. Finally, it is clear that a fraction at least of the small interstitial clusters remain immobile (see Figure 2). A multiscale study, combining **molecular dynamics** and *ab-initio* calculations, resulted in lines of research being identified, as regards the structure of these defects.

A successful coupling

The coupling of *ab-initio* calculations, and kinetic Monte-Carlo simulation has notched up a number of further successes. On the one hand, the modeling of the precipitation kinetics of copper in iron highlighted the unexpected contribution of small copper clusters, which prove more mobile than single **solute** atoms. And, on the other, the modeling of the **desorption** kinetics of **helium** showed the crucial part played by residual **carbon** content.

➤ **François Willaime**
Department of Materials
for Nuclear Energy
Nuclear Energy Division
CEA Saclay Center

➤ **Thierry Deutsch and Pascal Pochet**
Nanosciences
and Cryogenics Institute (INAC)
Physical Sciences Division
CEA Grenoble Center

Cold-crucible fabrication of nuclear glasses

Vitrification has stood the nuclear industry in good stead, for many years now, as a safe long-term conditioning technology for high-level waste. Major advances are nonetheless still being made, with the development of the cold-crucible technology, affording as it does new possibilities, in terms of volume reduction, and of extending the range of waste products amenable to incorporation. Indeed, by allowing higher melting temperatures to be achieved, this process opens the way to a considerable increase in glass production capacities, and the fabrication of novel matrices, involving higher incorporation rates than current glasses.



Glass pouring from the Upgradeable Vitrification Prototype (PEV: Prototype évolutif de vitrification), fitted with a cold-crucible furnace, set up at CEA/Valrhô-Marcoule.

As early as the late 1950s, decision makers at CEA became aware of the issue raised by future evolutions, as regards **fission product (FP)** solutions, and set in train a research program to address it. Such fission product solutions, pre-concentrated as they are, to limit their volume, are held in interim storage in **stainless steel** tanks, which are kept constantly cooled and agitated. The **activity** of these solutions, related as it is to the **burnup** achieved for the **fuel** undergoing **treatment**, may be as high as $3.75 \cdot 10^{13}$ Bq/L, and the amounts of power released are considerable (up to 7 W/L). These nitric solutions⁽¹⁾ (1–2 N) are charac-

terized by their high complexity, in physicochemical terms. Their chemical composition includes, as a rule, inactive **elements**, such as corrosion products [iron (Fe), **nickel** (Ni), **chromium** (Cr)], added elements [**aluminum** (Al), sodium (Na)...], **solvent** degrada-

(1) Nitric solution: nitric acid is a highly corrosive chemical compound, of formula HNO_3 . It is used, as a rule, in aqueous solution: $\text{HNO}_3 + \text{H}_2\text{O} \rightarrow \text{H}_3\text{O}^+ + \text{NO}_3^-$, the concentration in hydronium ions, H_3O^+ , released into the solution being noted N (so-called normal concentration).

By way of example, for 1 mole nitric acid in 1 liter of solution, solution concentration will stand at 1 N.

tion products [phosphorus (P)], and elements originating in **cladding** materials [aluminum, magnesium (Mg), **zirconium** (Zr)...]. The range of **radioactive** elements – fission products, and **actinides** – is quite large, covering as it does more than 40 elements, from **germanium** (Ge) (atomic number 32) to californium (Cf), with atomic number 98.

Glass, a choice containment material

Conditioning fission product solutions has the purpose of making the **waste** pass from the liquid to a solid form, of bringing down the volume taken up in **storage**, and subsequently in **disposal** facilities, and, lastly, to obtain a material that meets the safety requirements entailed by storage, and ultimate disposal. The material serving for the conditioning of such solutions must exhibit highly specific properties, owing to the complexity of the problem at hand. Initial lines of research, which had at first looked into **crystalline** materials, of the mica, or feldspar type, switched, in 1960, to focus on the fabrication of vitreous materials. In the 1960s, **glass** was selected, in France, and by the international community, to serve as **containment** material for fission product solutions, owing to the flexibility exhibited by its disordered structure, which enables this material to contain many chemical elements. **Radionuclides** become part of the glass structure: this is no mere encapsulation, therefore, rather what occurs is containment at the **atomic** scale (see Figure 1). Further, glass features good properties in terms of thermal stability, chemical durability, and resistance to self-irradiation.⁽²⁾

Seeking to arrive at a glass composition entails a tradeoff between the properties exhibited by the material and the technological feasibility of fabricating that



P.-F. Grosjean / CEA

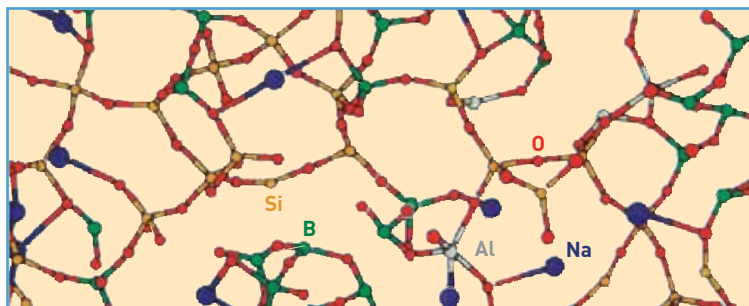
A block of containment glass (R7T7 glass).

material at the industrial scale. The French authorities opted for alumino–borosilicate glasses as containment materials for the fission product solutions yielded by the treatment of fuels from the **natural uranium–graphite–gas** (UNGG) reactor line, and **light-water reactors** (LWRs). As regards solutions yielded by LWRs, the glass manufactured by **Areva NC** at the La Hague (Manche *département*, western France) plant, under product reference **R7T7**, consists, to some 80%, of oxides of **silicon** [SiO_2 (silica)], **boron** [B_2O_3 (boric oxide)], aluminum [Al_2O_3 (alumina)], and sodium (Na_2O). Silicon, aluminum and boron act as glass formers, i.e. they serve to **polymerize** the glass network, through the strong bonds they induce. **Alkali metals**, in turn, act as modifier elements, depolymerizing the glass network. They make it possible to lower the melting point, and have a favorable effect on the **viscosity** and reactivity of the molten glass, thus facilitating fabrication. The incorporation fraction, for fission product oxides, is restricted, nowadays, to 18.5% (see Table). Apart from the **platinoids**⁽³⁾ and a fraction of the tellurium (Te) – these occurring in the glass in the form of **ruthenium** oxide (RuO_2) crystals, and as metallic phases [**palladium** (Pd), rhodium (Rh), tellurium] – R7T7 glass, subsequent to fabrication and natural cooling, is homogeneous at the microscopic scale. Its physicochemical properties have been determined for inactive **simulant** glass, and subsequently validated on samples of radioactive glasses fabricated in the laboratory, or samples from the industrial workshops at La Hague.

The continuous, two-step vitrification process

The main operations that make it possible to pass from the liquid to obtain glass include water **evaporation**, **calcination**, and **vitrification**. The calcination step

basic constituents of the glass matrix: SiO_2 , Na_2O , B_2O_3 , Al_2O_3



incorporation of fission products (FPs) in the form of oxides (FP_2O_3 ...) into the glass matrix

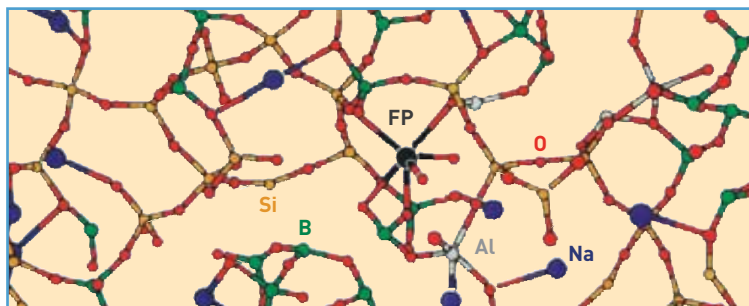


Figure 1.
Principle of the containment of elements in a vitreous structure.

(2) Self-irradiation phenomenon: the **radioactive decay** of radionuclides tends to disrupt the matrix holding them, owing to the emission of radiation, with concomitant generation of heat.

(3) Platinoids: this group comprises platinum (Pt), along with palladium (Pd), rhodium (Rh), ruthenium (Ru), **iridium** (Ir) and osmium (Os), which all exhibit characteristics close to those of platinum. Platinoids are also referred to as noble metals, owing to their high resistance to corrosion, and oxidation.

oxides	specified range for industrial operations (wt%)		average composition of industrial glasses (wt%)
	mini	maxi	
SiO ₂	42.4	51.7	45.6
B ₂ O ₃	12.4	16.5	14.1
Al ₂ O ₃	3.6	6.6	4.7
Na ₂ O	8.1	11.0	9.9
CaO	3.5	4.8	4.0
Fe ₂ O ₃		< 4.5	1.1
NiO		< 0.5	0.1
Cr ₂ O ₃		< 0.6	0.1
P ₂ O ₅		< 1.0	0.2
Li ₂ O	1.6	2.4	2.0
ZnO	2.2	2.8	2.5
(FP + Zr + actinide) oxides + fines in suspension	7.5	18.5	17.0
actinide oxides			0.6
SiO ₂ + B ₂ O ₃ + Al ₂ O ₃	> 60		64.4

Table.
Chemical composition range for R7T7 glasses, as produced in Areva NC's industrial workshops at La Hague.

converts most of the elements present into oxides, through decomposition of the nitrates,⁽⁴⁾ except for the alkali metals, and some of the *alkaline earths*. This takes place over a temperature range extending from 100 °C to 400 °C. Vitrification is carried out by way of the reaction of the calcine obtained from the previous operation with raw materials that chiefly provide substances acting as formers of the glass network, e.g. silica. These raw materials take the form, as a rule, of already formed glass, known as glass frit. These reactions require temperatures ranging from 1,050 °C to 1,300 °C, depending on the composition of the glass being fabricated. These steps must be effected by means of a process associated to technology that is sufficiently straightforward to be compatible with operating in *high activity* conditions.

To achieve productivity levels consonant with the requirements of fuel treatment plants, CEA has developed a continuous process, along with its associated technology. This involves an evaporation–calcination step, to which fission product solutions are subjected, followed by a vitrification step, applied to the calcine obtained. The two steps are carried out in continuous fashion, in two distinct items of equipment (see Figure 2).

The *calciner unit*, comprising a rotating tube, heated by a resistance furnace, also takes in reagents, and a recycled solution, yielded by offgas treatment. The unit serves to carry out the operations of evaporation, and partial conversion of the nitrates occurring in the solutions into oxides. The *vitrification furnace*, inside which the glass fabrication reactions take place, takes in the calcine produced by the rotary tube, together with glass

frit. This furnace is constructed, in current practice, around an inductively-heated metal melting pot. Glass is poured in discontinuous fashion, one load at a time, into *refractory* stainless-steel canisters (2 × 200-kg melts per canister, in the Areva NC vitrification workshops at La Hague).

Subsequent to fullscale validation, using inactive *simulants*, this continuous, two-step vitrification process was deployed in 1978, at Marcoule (Gard *département*, southeastern France), in the Marcoule Vitrification Workshop (AVM: Atelier de vitrification de Marcoule), associated to the UP1 treatment plant; in 1989 and 1992, at La Hague, in the R7 and T7 workshops, associated to the UP3 and UP2–800 plants⁽⁵⁾ respectively; in 1990 at Sellafield (United Kingdom), in the Windscale Vitrification Plant (WVP). The R7, and T7 workshops are each set up with three vitrification lines, with an initial solution treatment throughput of 60 L/h, and a glass fabrication capacity of 25 kg/h per line.

This vitrification technology does however labor under some limitations. On the one hand, the lifetime of the metal pots, set at around 5,000 hours, means they are a source of secondary waste. And, on the other hand, their glass fabrication capacity calls for the presence of several lines, operated concurrently. Finally, the options, as regards containment *matrix* compositions, are restricted to glasses involving fabrication temperatures lower than 1,150 °C.

(4) Nitrates: salts (i.e. ionic compounds, consisting of *cations* and *anions*, forming a neutral product, bearing zero net charge) of nitric acid, HNO₃. The nitrate ion has the chemical formula NO₃⁻.

(5) UP2–800: a plant, operated from 1994 on by Areva NC at La Hague (Manche *département*), where the greater part of spent fuels from the French nuclear power reactor fleet undergo treatment. The plant is the outcome of the refurbishment of the UP2–400 unit, which, taking over from the UP1 plant at Marcoule (Gard *département*), was dedicated to treatment of spent fuels from the UNGG reactor line. Fuels from other countries undergo treatment at the UP3 plant, commissioned in 1990–92.

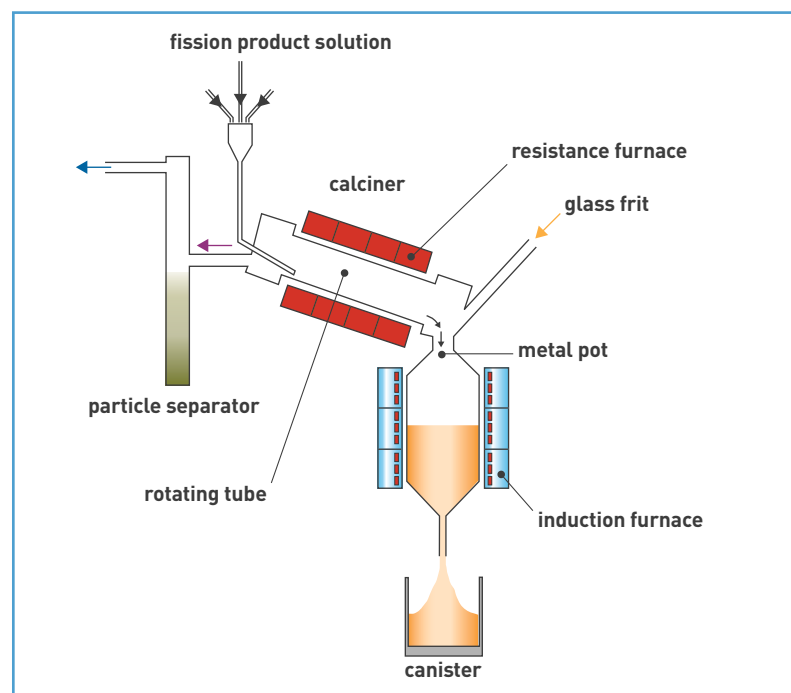


Figure 2.
The continuous, two-step vitrification process.

Cold-crucible vitrification, a technology for the future

To overcome these barriers, a new glass fabrication technology, by direct-induction melting in a cold crucible, has been developed.

Advantageous characteristics

Direct-induction melting involves placing the glass that is to be heated in an alternating **electromagnetic** field, generated by an inductor. The frequency for this alternating field stands at a few hundred **kilohertz** or so. As liquid glass is an **electrical conductor** (exhibiting as it does a **resistivity** of 1–10 **ohm-centimeters**), the alternating electromagnetic field generates, within it, induced currents, which dissipate energy by the **Joule effect**. In this type of induction, the point is to directly heat the material that is meant to undergo melting, not the crucible. The latter component is made of metal, stainless steel for instance. It is cooled by water circulation, and segmented, to ensure relative “transparency” to the electromagnetic field (see Figure 3).

Where the glass comes into contact with the cold wall, a thin layer of solidified glass forms, with a thickness of 5–10 mm, interposing itself between the molten glass, and the cold metal wall. Thus, the metal forming the crucible does not come into contact with the molten glass, which is held entirely inside this solidified glass “skin,” or “skull:” hence the term “self-crucible” (or “skull melter”). Since glass is an electrical insulator material at ambient temperature, a glass load must be preheated, if induction is to be initiated. This preheating is effected, for nuclear application purposes, by positioning a **titanium (Ti)**, or zirconium ring over the initial glass load. This ring heats up, under the effect of the electromagnetic field: thereafter, its **oxidation** yields energy to the glass, making it possible for the glass to melt. By the end of this induction-priming stage, the metal, now fully oxidized, becomes a constituent of the glass. The furnace subsequently operates on a semi-continuous basis. The feed of melt stock is continuous, while pouring the fabricated glass into canisters is carried out on a sequential basis. Pouring is effected by way of a cooled metal valve. At the end

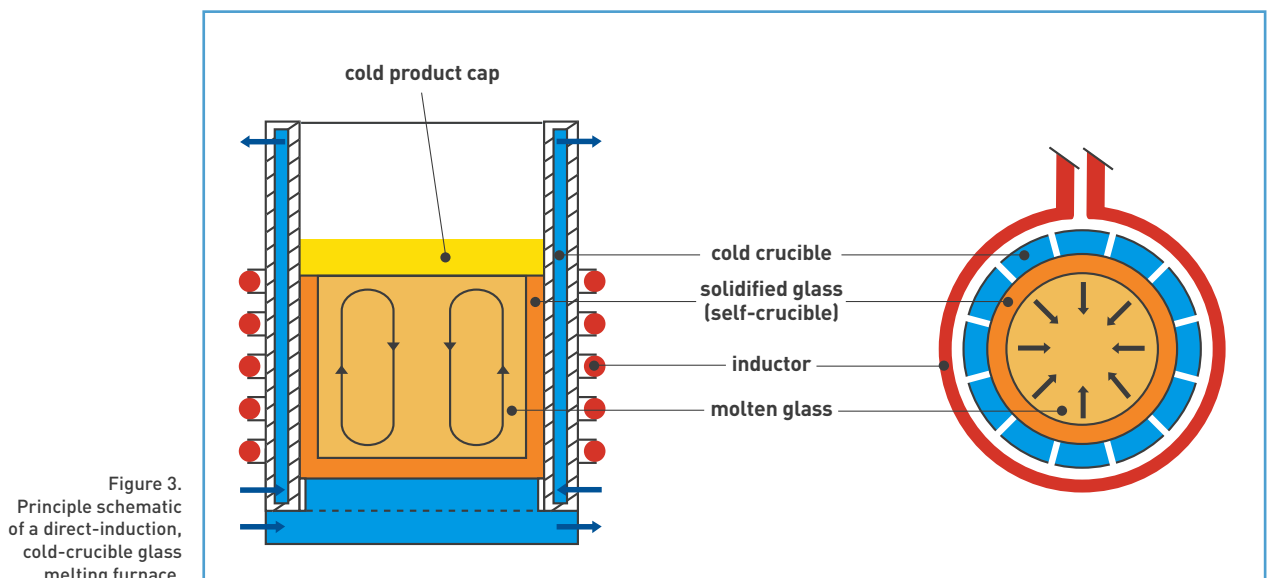
of each pouring operation, a sufficient volume of molten glass is retained inside the furnace to maintain induction, and sustain melting. A mechanical agitator, together with a gas-bubbler system, ensures thorough stirring of the molten glass bath, allowing a good level of thermal, and chemical homogeneity to be obtained in the glass.

In the context of nuclear applications, furnaces for cold-crucible induction glass fabrication were developed with a view to putting their two chief characteristics to advantage. First, cooling the crucible results in the formation of a thin solidified glass layer, keeping the crucible away from the molten glass, this precluding corrosion. Crucible lifetime is thus considerably extended, even when highly corrosive materials are fabricated in molten form. Second, heating by direct induction within the molten glass bath makes for an increased glass fabrication capacity, and allows high fabrication temperatures to be achieved. This characteristic opens up further prospects, as regards the development of new containment materials, involving higher incorporation rates, not amenable to production by the current process.

Development of an optimized crucible

Development of this technology has been pursued at CEA/Valrhô–Marcoule for more than 20 years. A major milestone was reached with the hooking up of a fullscale furnace – crucible inner diameter: 650 mm – to the calciner and offgas treatment system of the inactive prototype set up in one of the vitrification units at La Hague (Upgradeable Vitrification Prototype [PEV: Prototype évolutif de vitrification]).

Once the technology was deemed to have reached sufficient maturity, a tripartite working group, bringing together **Areva**, **SGN**, and CEA, specified the chief technological design options associated to the development of the cold-crucible vitrification process, in an environment of the type found at the La Hague vitrification workshop. The trials, and development work carried out led to the specification of an optimized crucible, exactly along the lines of the one set up at La Hague in 2009, and brought





General view of the Upgradeable Vitrification Prototype (PEV: Prototype évolutif de vitrification), fitted with a cold-crucible furnace, set up at CEA/Valrhô-Marcoule.

on stream in active mode in April 2010. A fullscale pilot of the cold crucible was constructed and connected up to the existing PEV calciner, in place of the former furnace, thus making available, in inactive operation, a fully representative setup for the process due to be operated at La Hague.

This technology provides the means to achieve higher melting temperatures (1,200–1,400 °C), laying the ground for a significant enhancement of production capacity for R7T7 glass, and the fabrication of novel containment matrices. Mention may be made, e.g., of the following: a glass–crystalline material, bearing 13 wt% molybdenum oxide (MoO_3), developed for the purposes of the containment of old solutions, yielded by the treatment of the $\text{UMo}^{(6)}$ fuels from UNGG reactors; a contain-

ment glass for low- and intermediate-level sodium-rich solutions, and, in the longer term, novel glasses, making it possible to consider higher fission product incorporation rates.

Further cold crucible applications

In the context of the technology dissemination initiatives conducted by CEA, two furnaces, 60 cm, and 1.20 m in diameter respectively, were constructed under license by the French EFD corporation, and brought on stream by FERRO corporation at Saint-Dizier (Haute-Marne *département*, eastern France). The 1.20-m-diameter furnace ensures production of 40 tonnes/month of enamel, or glass frit. The benefits of this technology, as regards enamel production – used for enameled sheet metal fabrication – are the absence of contamination from the refractory material, the ability to carry out melting with no temperature limitation, the ease of halting operations, and starting up again, to switch to another glass composition, and furnace reliability.

Unquestioned qualities

The cold-crucible vitrification technology not only opens the way to the fabrication of novel containment matrices, it equally makes it possible to anticipate on the future evolutions of spent fuel treatment plants. It meets the aims of achieving simplification, and lower operating costs, and of catering for a wider variety of wastes. Cold crucibles likewise afford potential benefits with regard to many nonnuclear applications, owing to their reliability, and flexibility of operation.

> Roger Boën

Waste Treatment and Conditioning
Research Department
Nuclear Energy Division
CEA Valrhô-Marcoule Center

⁽⁶⁾ UMo fuel: this consists of uranium (U) metal, alloyed with molybdenum (Mo).



A block of glass–crystalline material, used for the containment of old solutions yielded by the treatment of UMo fuels from UNGG reactors.

The long-term behavior of glasses for waste containment purposes

In France, under the aegis of the Act of 29 June 2006 on the sustainable management of **radioactive waste** and materials, one of the milestones set involves selection of a site for the **disposal** of **ultimate waste** in a **geological environment**, so that the repository may be commissioned by 2025. The demonstration of safety for a geological disposal facility for **long-lived** radioactive waste is to be carried out in 2013–14 by **ANDRA**, the host rock being considered being the **Callovo-Oxfordian** argillites⁽¹⁾ found in the northeastern parts of the Paris Basin. This demonstration will take the form of an iterative process, relying on phenomenological **modeling**, and **simulation**, bearing in mind the extremely long timescales that have to be taken on board (typically, from a few tens to several hundreds of thousand years, to arrive at a significant reduction in radiological risk). In the disposal concept currently considered, in argillaceous formations, the waste takes the form of the **glass** block (the borosilicate glass **containment matrix**, in its metal canister, made of **stainless steel**), protected by an overpack, made of **carbon steel**, about 55 mm thick. These objects will be held inside tunnels, at a depth of some 500 m below ground.

Alteration due to water

Numerous theoretical and experimental studies have converged in the conclusion that the properties exhibited by the glass will not undergo alteration in the short, medium, or long term, whether owing to temperature – causing negligible **crystallization** – or **irradiation** – this causing only minor evolutions in macroscopic proper-

ties. On the other hand, once water resaturation occurs across the geological site, and the metal envelopes become corroded, the water present in the underground environment will be liable to alter the glass, and release some of the **radionuclides** it contains. The long-term behavior of such **vitrified** waste, once it comes into contact with water, thus raises a major query, regarding the **source term** for these radionuclides. The issue thus is that of determining at what rate glass degradation will take place, and by which mechanisms.

The research work serving to formulate an answer relies on multiscale **mechanistic** studies, carried out for the purposes of constructing a kinetic **model**. The ability of this model to be used in a predictive manner is evidenced by studies conducted on **natural and archeological analogs**. The difficulties encountered, in such an exercise, are chiefly due to the large timescales – both temporal, and spatial – considered, but equally to the large number of parameters involved: glass composition (some 30 oxides, with diverse contents), temperature (varying across space, and time), water chemistry, and rate of water renewal close to glass surfaces, the nature of solid bodies in the vicinity of the glass, glass fracturing, due to mechanical **stresses** set up by the cooling of the glass, subsequent to pouring. Notwithstanding such difficulties, it is yet possible to bank on the fact that nuclear glasses undergo alteration by way of physicochemical processes altogether similar to those acting on natural silicate glasses, or minerals.⁽²⁾ To that extent, their study can thus draw on the theoretical concepts developed for the latter group of materials.

The results so far established

In the presence of water, nuclear glasses undergo reactions that may be attributed, in part, to the nature of the chemical bonds set up within the glass structure, and – as regards other reactions – owing to the properties of the solute species. The main reactions involved include **ion** exchanges, these chiefly involving **alkali metals**, weakly bonded as these are to the glass network, **silicon hydrolysis**–condensation reactions, resulting in the formation of a **porous** hydrated layer, gradually taking on a **passivating** role, along with the **precipitation** of crystallized secondary phases. At the temperatures of interest in the disposal context (25–90 °C), such secondary phases mainly involve clay minerals (see Figure 1).

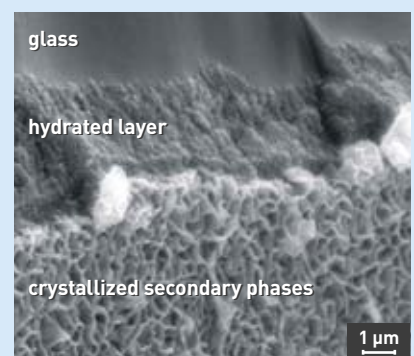


Figure 1. Semi-profile view, under **scanning electron microscopy**, of alteration products formed on SON68 nuclear glass (inactive R7T7), after 4 months in pure water at 150 °C.

Fundamental research studies, conducted to gain an understanding of the mechanisms involved, have highlighted the existence of a strong coupling, at the **mesoscopic** scale, between the aforementioned chemical reactions, and **solute** transport, the hydrated layer having the ability to take on a passivating role, as its porosity closes. The high degree of chemical complexity exhibited by such alteration layers is due, to some extent, to the nature of the glass itself, but equally to the environment, this supplying exogenous, potentially disturbing **elements**, as e.g. magnesium (Mg), and iron (Fe).

The various kinetic regimes governing the alteration of nuclear glasses are set out, in simplified fashion, in Figure 2. The **initial rate** is limited by hydrolysis of the silicate network (breaking of Si–O–Si chemical bonds). The **rate drop** is associated to the formation of a dense, passivating zone within the hydrated layer. The **residual rate** is due to dissolution of the hydrated layer, by a reaction driven by the renewal of the solution, and the precipitation of the secondary phases taking up the constituents that make up that layer. Finally, a possible **alteration resumption** may be observed in particular cases, where the secondary phases are liable to undergo bulk precipitation. In the conditions prevailing for disposal in the geological environment, it is anticipated that glass will alter in the residual rate regime (a few tens of



Glass–iron–clay integral experiment. This has the purpose of investigating the degradation mechanisms acting on the containment matrix for radioactive waste (glass), subsequent to water resaturation at the disposal site (clay formation), and corrosion of the metal (iron) canister, and overpack.

P.-F. Grosjean / CEA

(1) Argillite: a detrital sedimentary rock, chiefly consisting of argillaceous minerals.

(2) Silicate minerals: minerals the skeleton of which essentially consists of an array of silicon (Si) and oxygen (O) tetrahedra, with additions of **aluminum** (Al), magnesium (Mg), iron (Fe), calcium (Ca), potassium (K), sodium (Na), and other elements. Silicates make up 97% of the Earth's crust.

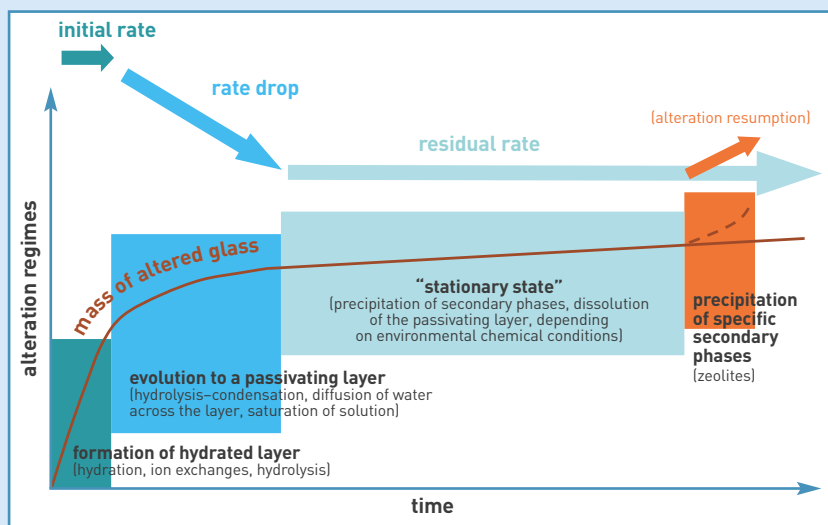


Figure 2.
Relationships between nuclear glass alteration kinetics and reaction mechanisms.

nanometers per year), after a transient stage, involving a higher rate (several micrometers per year). This stage, relatively short-lived as it is, is thought to be due to the strong reactivity of the surrounding materials.⁽³⁾

GRAAL: set to rule over glass alteration mechanisms

A new model, doing away with some of the empirical character attaching to previous approaches, has been developed at CEA, for the purposes of determining more precisely the influence of chemical, and hydrodynamic conditions prevailing within the repository environment, on the residual rate of glass alteration. This model, going

by the name GRAAL (for Glass Reactivity with Allowance for the Alteration Layer), includes an explicit description of the four chief alteration mechanisms acting on glass: formation of the passivating layer by glass hydration, diffusion of water across that layer, dissolution of that layer over its outside surface, and precipitation of crystallized secondary phases. The equations may either be solved analytically, for simple cases, or be integrated into a geochemical code, to cater for chemistry-transport couplings, and simulate complex systems. These equations involve four parameters, all amenable to measurement by way of independent experiments. As applied to laboratory experiments, using a single set of parameters, this model affords adequate precision, when simulating the release into the solution of the major constituents of the glass. This study, presently conducted on a reference glass, is currently being transposed to other glass compositions, and chemical conditions representative of the repository – with water taken from the site of ANDRA's Underground Research Laboratory at Bure (Meuse/Haute-Marne départements, northeastern France), for instance. For that purpose, relations must be determined between the chemical composition of the passivating layer, its thermodynamic stability, and its protective capability.

The model's long-term validity was tested on an archeological glass, subjected to

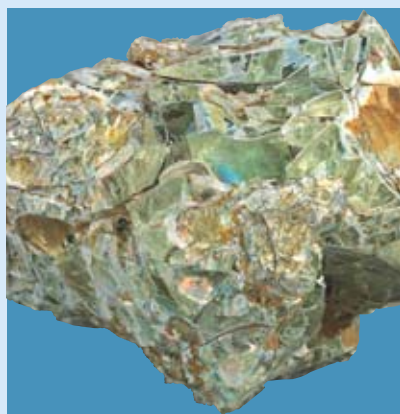
alteration by seawater for 1,800 years. The study covered fractured glass blocks – fracturing being due to the selfsame cause⁽⁴⁾ as in nuclear glasses – weighing several kilograms, that had been lying on the seabed. A mechanistic and kinetic study allowed the similarity to be evidenced, of the reactions involved with those taking place in nuclear glasses, and model parameters to be determined, for this glass – involving as it does a highly distinctive composition, compared to its radioactive counterparts. When set against observables, the model is found to account, quantitatively, for the variability observed in the alteration facies identified by a thorough characterization of the block. Finally, when used in predictive fashion, the model tells us that the contribution of the network of cracks – even though that network does initially present water with a surface area 90 times larger than would a dense monolith – to the block's alteration will have but a minor impact over the long term, since alteration of such blocks is controlled by the dissolution, at the maximum rate, of outside surfaces exposed to constant water renewal. More generally, this exercise highlights the significance of chemistry-transport couplings, with regard to the durability of materials held in conditions far from thermodynamic equilibrium.

The GRAAL model has not yet been applied to the disposal in a geological environment of conditioning glasses for high-level (high-activity) waste, since development is not fully finalized (this being the task set for the two coming years). Be that as it may, performance calculations were carried out in 2005, in the context of the initial demonstration of safety for disposal in a clay environment.

On the basis of conservative assumptions, i.e. allowing for safety margins, these calculations predict lifetimes, for glass packages, of some 1 million years. As has been made clear, these timescales will be more precisely determined for the next safety demonstration. In any event, these findings already make it apparent that the glass matrices used for the containment of high-level waste, yielded by spent fuel treatment, will significantly contribute to bringing down the potential impact of disposal in a geological environment.

> Stéphane Gin

Waste Treatment and Conditioning
Research Department
Nuclear Energy Division
CEA Valrhô-Marcoule Center



P.-F. Grosjean / CEA

Archeological glass from Les Embiez Island (off the south coast of France, Var département), which had remained close to 1,800 years at the bottom of the Mediterranean Sea. Such archeological glasses undergo alteration due to water, through mechanisms very similar to those acting on nuclear glasses, their widely differing compositions notwithstanding. Such studies helped demonstrate the long-term validity of the GRAAL model.

(3) On this topic, see "What long-term behavior for nuclear waste packages", *Clefs CEA* No. 53, Winter 2005–2006, pp. 51–56.

(4) Mechanical stresses, arising from the thermal shock related to rapid cooling of the objects involved.

DECIPHERING STRUCTURES

Solid-state NMR for the observation of glasses at the atomic scale

Nuclear magnetic resonance (NMR) is a form of spectroscopy, the – relatively simple – physical principle involved being based on the interaction of the magnetic moment of an atomic nucleus with an external magnetic field (Zeeman effect). This gives rise to the phenomenon known as Larmor precession: the nuclear magnetic moment precesses about the axis of the magnetic field, at a frequency that is specific to that nucleus, its so-called Larmor frequency, proportional to the magnitude of the applied magnetic field.⁽¹⁾ Now, around the nucleus, this field is subject to perturbations from internal magnetic fields, due to a variety of physical causes. These include a shielding phenomenon due to the atom's electron cloud, resulting in the chemical shift affecting the frequency; coupling with the electric charges lying around the atom considered (quadrupole interaction); or magnetic dipole interactions with neighboring atoms. These perturbations result in shifts in the Larmor frequency. The NMR spectrum is then made up of resonances, arising at positions that are

characteristic of the various local environments of the nucleus being observed. These chiefly depend on the number, and nature of neighboring atoms, or of the atoms entering in a chemical bond with the one observed, or even on the local geometry, or the motions of the atom, or the molecule. While for liquid samples the rapid motions affecting molecules (Brownian motion) in the solvent allow very narrow – and thus quite finely resolved – resonances to be obtained, in the solid state, the rigidity of the atomic lattice, and the multiplicity of interactions involved result in considerable broadening of the resonances, which overlap one another. In such conditions, it is no longer possible to separate the various resonances making up the spectrum.

A magic angle to refine the spectrum

Spinning the sample about an axis set at a specific value (the so-called magic angle 54.7°), relative to the static magnetic field, i.e. magic-angle spinning (MAS NMR), currently stands as the standard technique

making it possible to do away with such broadening. However, the technique is effective only for nuclei involving a nuclear spin of $\frac{1}{2}$, as shown in Figure 1. By judiciously combining this motion, imparted to the sample, and a modulated radiofrequency irradiation of the nuclear spin – leading to a two-dimensional experiment – physicists are then able to remove the residual broadenings for nuclei of spin higher than $\frac{1}{2}$ (see Figure 1). These recent, so-called high-resolution techniques are undergoing constant ongoing refinement. This is achieved, first and foremost, by means of technical advances, such as magnetic fields of ever higher intensities (currently higher than 20 T), or increased sample spinning frequencies (now reaching 70 kHz!). And, second, this is due to the ingenuity of NMR physicists, who are forever devising radio-frequency irradiation sequences involving increasingly complex modulations, but which prove ever more robust, and effective!

(1) On this topic, see “NMR, an ever-advancing spectroscopic technique”, *Clefs CEA* No. 56, Winter 2007–2008, pp. 56–60.



The magnet of the high-magnetic-field solid-state NMR spectrometer used for the purposes of investigating the structure of materials. The resonance frequency for the hydrogen nucleus, i.e. the proton, stands at 500 MHz in this magnet.

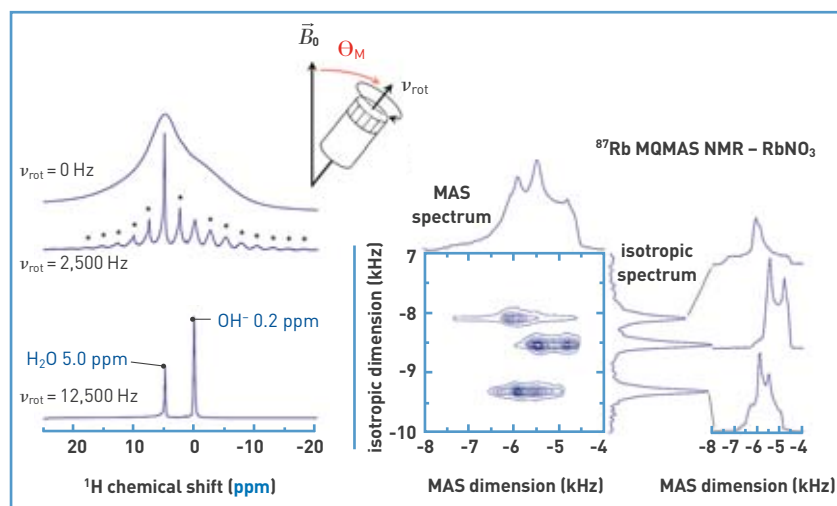


Figure 1.

Rapidly spinning the sample, about an axis set at the magic angle ($\theta_M = 54.74^\circ$), with respect to the axis of the magnetic field, makes it possible to refine the spectrum, for a nucleus having a spin of $\frac{1}{2}$, in this case the hydrogen nucleus, i.e. the proton, ^1H (at left). In the case of nuclei involving a nuclear spin higher than $\frac{1}{2}$, in this case the rubidium-87, ^{87}Rb , nucleus, it becomes necessary to resort to two-dimensional experiments, such as multiple-quantum magic-angle spinning (MQMAS), to achieve resolution of the sites. The MAS dimension corresponds to a standard NMR acquisition, while the isotropic dimension yields the high resolution. In the MAS spectrum, lines retain a certain breadth, owing to the anisotropies involved in the interactions. In the isotropic spectrum, only isotropic terms are retained, this yielding narrow lines (right).

An irreplaceable tool for glass investigation purposes

While NMR has now fully made its mark as a proven technique in the fields of organic chemistry, and molecular biology,^[2] all of these advances have served to turn solid-state NMR into a, by now, irreplaceable tool for the purposes of materials investigations, especially with regard to glasses. Such **amorphous** materials, indeed, exhibit no medium- or long-range order, as regards atomic configurations (they are known as *disordered-structure* materials), and thus call for specific analytical tools. In the NMR context, since the interactions being probed are local, at the atomic scale,

(2) On this topic, see "NMR for protein analysis", *Clefs CEA* No. 56, Winter 2007–2008, pp. 52–55.

such structural, and chemical disorder results in a broadening of resonances, around an average characteristic frequency. The need to take into account this broadening is a further difficulty, to be taken on board for the purposes of **modeling**, and interpreting experimental glass spectra. Be that as it may, by way of advanced, multidimensional techniques, a nucleus such as that of oxygen-17 (¹⁷O) yields a multiplicity of information, as to the structure of oxide glasses (see Figure 2). This makes it possible to identify the various chemical bonds making up the skeleton of the glass structure (in the example shown in Figure 2, the *bridging* oxygens in Si–O–Si, Si–O–B, B–O–B), but equally **depolymerized** regions where **alkali metal** and **alkaline earth ions** (Ca⁺⁺, Na⁺) are located, causing

the emergence of the *non-bridging* oxygens, Si–O[–], that are indispensable, for electric charge compensation purposes. Non-bridging oxygen concentration is directly related to many macroscopic properties (**viscosity**, **conductivity**, mechanical strength, chemical durability...), evidencing the importance of the relationships found, in glasses, between physicochemical properties and local structure. In this respect, NMR is a science that has yet to show its full potential.

Combining simulations, and experiments

Figure 3 shows that the **boron-11** (¹¹B) spectrum from a glass sample (taken as the simplified model of a **nuclear glass**) subjected to external **heavy-ion** irradiation is altered, with respect to the spectrum from an undamaged glass sample. NMR clearly evidences the evolution of boron **coordination numbers**, but equally a broadening, suggestive of alteration (greater disorder) in the glass structure. Relating a particular environment to an observed resonance is a task that can prove altogether fraught with difficulty. As a rule, comparing the frequency of the resonance being looked at with those – available in tabulated form – for **crystalline** compounds of known structure allows such an interpretation to be arrived at. This, however, is an approach that has its limitations, its prerequisite being the existence of such databases. Quite recently, significant advances, achieved in the area of the **ab-initio** calculation of NMR parameters, have made it possible to **simulate** NMR spectra, on the basis of atomistic models of glasses. Direct comparison with experimental data then yields a wealth of information. The first task is that of identifying, and quantifying the local environments, the second stage being one of seeking to arrive at a better understanding of the structural disorder evidenced, e.g., by the distribution of geometric parameters – e.g. bond angles. These novel approaches are still but at their early stages, however, when combined with the entire range of increasingly sophisticated methods afforded by NMR, they are set to contribute to the continued enhancement in structural resolving power that is being achieved for solid-state NMR.

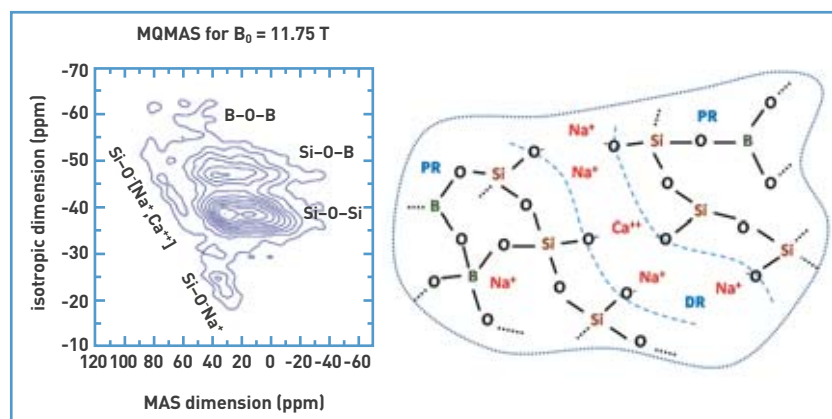


Figure 2. Notwithstanding the disordered structure exhibited by the material being investigated, in this case a borosilicate, sodocalcic glass (consisting of oxides SiO₂, B₂O₃, Na₂O, CaO), the MQMAS NMR technique (spectrum shown at left) has the ability to resolve the various environments involved for oxygen. It then allows virtually direct reading of the glass structure, as shown schematically at right, in **polymerized** (PR), and depolymerized regions (DR).

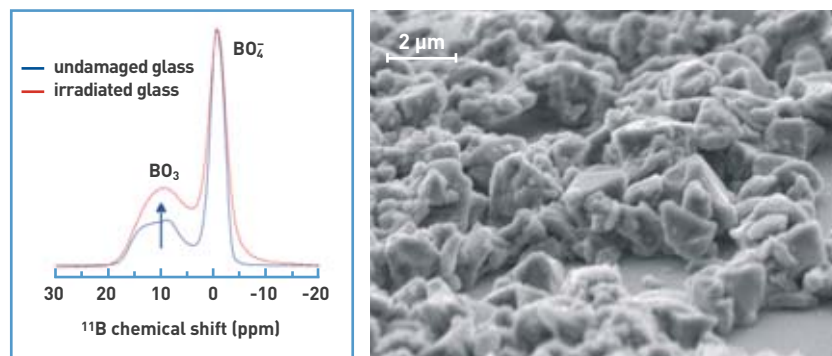


Figure 3. In borosilicate glasses, MAS NMR of boron-11 (¹¹B) is a very powerful technique, for the purposes of probing the various environments of boron, occurring in this case as 3-coordinated, BO₃, and 4-coordinated boron, BO₄. Comparison of spectra from **micrometer**-scale grains of a simple glass, before (blue), and after (red) heavy-ion beam irradiation evidences the alteration in terms of boron coordination numbers, and increased structural disorder. (This study was carried out in collaboration with S. Peugot at CEA/Nuclear Energy Division/Valrhô–Marcoule Center.)

> Thibault Charpentier
Radiation–Matter Institute,
Saclay (IRAMIS)
Physical Sciences Division
CEA Saclay Center

SiC/SiC composites for GFR fuel claddings

Owing to their satisfactory behavior at high temperature and under irradiation, SiC/SiC composites are being considered for the fabrication of fuel claddings for the gas-cooled fast reactors of the future. Development of SiC/SiC claddings stands as a real challenge, calling for advances to be made on a wide variety of materials issues, involving both technological, and scientific aspects.

Preparations for the densification, by CVI treatment, of a tubular SiC-fiber architecture, obtained by filament winding. At bottom right, close-up view of the tube, ready to be introduced into the furnace.



CEA/DEN/DMN

The specifications to be complied with, as regards fuel claddings for fourth-generation gas-cooled fast reactors (GFRs), set a challenge for materials science. Indeed, exceedingly severe constraints of various kinds are compounded in this respect: operation at 900 °C, in an intense neutron flux, for several years, while exhibiting satisfactory mechanical, and thermal properties; tightness to be maintained at up to 1,600 °C, while subjected to internal, or external overpressure of 70 bars; and retention of fuel element geometry up to 2,000 °C, to ensure proper cooling. Many potential candidates, e.g. refractory metals, or alloys, or monolithic ceramics, had to be ruled out. The only candidates still in the running are SiC/SiC composites, consisting of high-performance silicon-carbide fibers, and a matrix likewise of silicon carbide. However, existing industrial materials are the outcome of development efforts that were rather directed at the aerospace industry, thus calling for numerous optimizations, if they are to serve for the intended application. Reinforcement architectures

must be adapted, to suit the geometry of fuel elements of the pin type. Achieving control of geometric tolerances, and surface states, and ensuring tightness are imperative requirements. The fiber-matrix interphase⁽¹⁾ must allow for sufficient rupture elongation. Over the past three years, investigations have been conducted jointly by laboratories from various divisions at CEA, along with the Thermostructural Composites Laboratory (LCTS: Laboratoire des composites thermostructuraux), for the purposes of securing advances in this area.

Development of reinforcement architectures

A material, when organized in fiber, or filament form, may exhibit outstanding mechanical properties, related to specific microstructures (orientation, texture, very low defect content), developed at the synthesis stage. Such fibers are obtained, as a rule, in

(1) Interphase: the interfacing material standing between two phases of a medium.



Braiding machine, serving for the fabrication of triaxial braids.

the form of continuous yarn – coming in spools of tow comprising several hundred, or several thousand filaments – ready to be used directly, or to undergo a variety of preparatory operations, such as assembly in tape form, rupturing,⁽²⁾ covering,⁽³⁾ and cutting, to fabricate the reinforcement for the composite material. Available reinforcement structures are, as a whole, carried over from conventional textile techniques: braids, woven fabrics, knits, felts, needled or wound structures. Determining the ideal structure for the target application may be a highly complex undertaking. This involves not only a search on the basis of the desired mechanical, and thermal properties, but equally taking on board constraints stemming from the textile techniques used, e.g. achievable geometries, the ability of filaments to be formed, together with the structure's ability to undergo densification.

For pin-type claddings, the braiding technique does seem well suited for the purposes of achieving small-diameter tubular shapes, however it is not the only one. Filament winding is another technique, affording particular ease of operation, currently being evaluated. Braiding affords the further benefit of its use lending itself to simple solutions, with regard to fuel element closure, however these solutions have not as yet been qualified. Braiding parameters include braid angle, ranging from 20° to 60°, braid pattern (see Figure 1), and number of layers. The studies conducted since 2007 have addressed a number of points:

- control of geometry, through control of the inner diameter, by way of a **graphite** mandrel, during the braiding step; and of the outer diameter, through the addition of a sacrificial layer, machined away after densification;
- achieving a smooth surface state, and tightness, through integration of a dense layer, and/or a metal liner⁽⁴⁾ during braiding;

(2) Rupturing: effecting a break by stretching.

(3) Covering: the operation whereby a textile yarn is wound around a twisted strand.

(4) Liner: a coating, or internal layer, of moderate thickness, serving to ensure tightness.

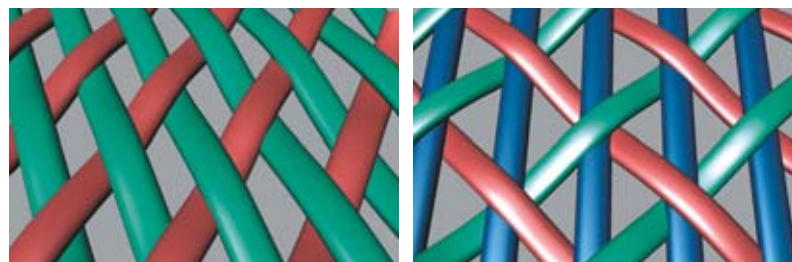


Figure 1.

At left, a biaxial braid. The yarns cross over, running in two directions, the $+\theta$ and $-\theta$ directions (θ being the braid angle), relative to the tube axis. Right, a triaxial braid. A further set of yarns is inserted, running parallel to the tube's axis.

- development of a braid closure solution;
- comparison of densification behavior for the various braids considered.

Characterization studies, and mechanical and thermal **modeling** efforts, for high temperature conditions, will be required, to decide which architectures afford the best performance.

Fabrication of an interphase and matrix

Aside from exhibiting satisfactory resistance under fast-neutron flux conditions, a GFR **cladding** material must bring guarantees with regard to damage tolerance. As regards SiC/SiC composites, this is achievable only by interposing an interphase material between fiber, and matrix, having the function of deflecting the cracks arising in the latter phase. All of the studies carried out, the world over, and over many years now, have shown that the reference material, in this respect, is **pyrocarbon**. In fact, this material occurs in a wide variety of grades. This textured, lamellate material exhibits marked variations in its properties, depending on the direction of applied stress (anisotropy). Its characteristics mean it is able to act as an outstanding crack “deflector,” allowing, in situations of mechanical stress, multicracking to develop in the matrix, with no propagation to the fiber reinforcement (see Figure 2). Featuring as it does, at the same time, good chemical compatibility with SiC, up to high temperatures, pyrocarbon stands as the ideal interphase, in SiC/SiC composites, irrespective of the application considered, even in **oxidizing** atmospheres. It has been shown that, if mechanical strength is to be retained under fast-neutron flux conditions, up to large **dose** values, the thickness of the interphase must be restricted to a maximum of 150 **nm**. On the other hand, apart from this criterion, the fibers' surface chemical

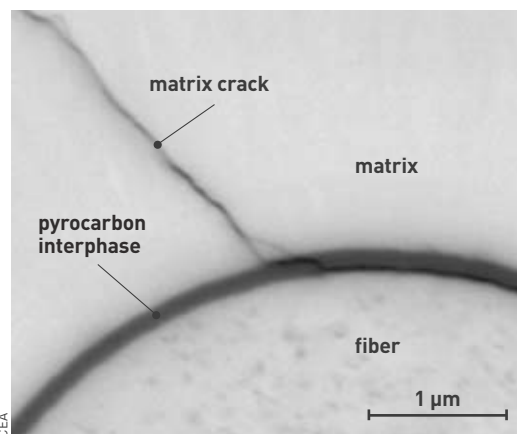
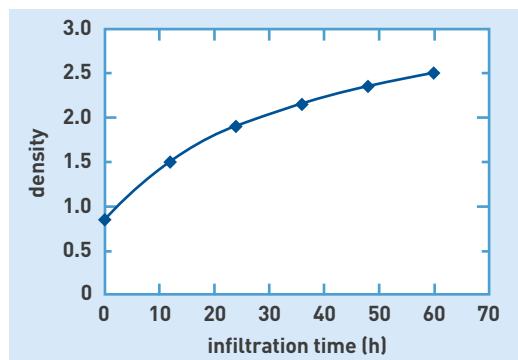


Figure 2. Deviation of a matrix crack at the pyrocarbon interphase, within a SiC/SiC composite. Deviation first occurs at the interphase–matrix interface, and subsequently at the fiber–interphase interface.

Figure 3.
Evolution of density
for a composite densified
by chemical vapor
infiltration (CVI),
as a function of
infiltration time.



composition, and surface roughness play a paramount role, with regard to fiber–matrix coupling, within SiC/SiC composites. For that reason, numerous studies are currently ongoing, to identify the parameters governing the nature of the fiber–matrix coupling, for the purposes of optimizing mechanical behavior in these materials.

As regards the matrix, and thus fabrication of the end-object from fiber preforms, densification studies, involving [chemical vapor infiltration \(CVI\)](#), are currently being carried out independently, with the acquisition of a dedicated CVI furnace. Such CEA fabrication runs will be compared to industrial fabrication runs, initiated concurrently, for the purposes of evaluating the CEA products. To increase fiber content, and ensure control of outer “cylindricity,” the parts are secured, at the outset of the densification step, in a rig allowing gas diffusion to take place. Density increases, initially, in linear fashion, as a function of infiltration time, increasingly slowly thereafter, tending to an asymptotic limit, corresponding to the theoretical density (see Figure 3). This may be accounted for by the fact that diffusion (i.e. [pore](#) diameters), and deposition surface areas (i.e. intra- and inter-yarn surfaces) decrease with time. Final density stands at close to 2.5 (as against a theoretical value of 3.2), corresponding to a [porosity](#) of some 20–25%. To ensure tightness, and low inner surface roughness, one solution involves using, at the braiding stage, a mandrel first coated with a dense silicon carbide layer, the mandrel being subsequently done away with, after densification. Machining of an outer sacrificial layer results, in components 100 mm long, in an accuracy, with regard to the outer diameter and straightness, of 30 [microns](#), in accordance with specifications (see

Figure 4.
A silicon-carbide braid
(at right), seen after
densification (middle),
and after the machining
operation to remove the
outer sacrificial layer
(left).



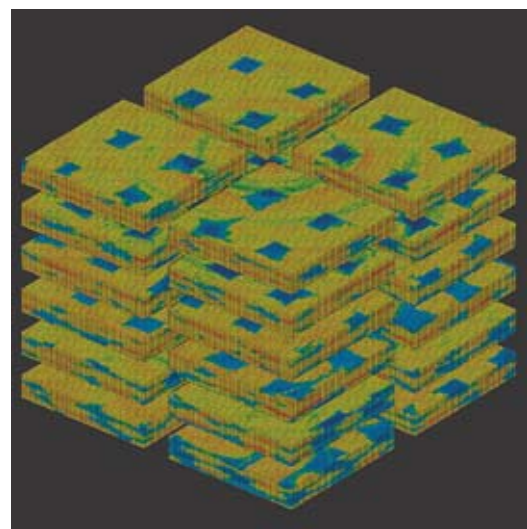
P. Stroppa / CEA

Figure 4). Concentricity measurements, and accuracy measurements for inner diameters are less readily obtained.

Modeling the mechanical behavior

The chief benefit of using ceramics in the composite form is that of turning a “brittle” material into a “damage-tolerant” material. In the former type, a single crack propagates abruptly, resulting in nonreproducible behavior, evidencing very low rupture strain. In the latter form, cracks are deflected at the fiber–matrix interfaces, and a multicracking process sets in, giving rise to reproducible mechanical behavior, and larger rupture strain. On the other hand, the use of complex microstructures (woven architectures, different nested scales) results in a highly [anisotropic](#) material behavior, which does not readily lend itself to modeling.

For the purposes of determining a relation between fabrication process, microstructure, and mechanical behavior, CEA is bringing forward a multiscale approach of thermomechanical behavior. The aim is to derive the material’s macroscopic behavior, on the basis of the behavior, and spatial distribution of the various constituents. The approach being developed lays emphasis, in particular, on the influence of the porosity present within the material, at various scales: the microporosity extending between fibers, within yarns, and the macroporosity occurring between woven yarns. The effects of porosity, within the material, are twofold. It makes for freer elastic behavior in the material, in certain privileged directions, however it also results in a concentration of local stresses, liable to cause cracking in the material. In order to characterize the three-dimensional spatial distribution of this porosity, the material was analyzed by [X-ray tomography](#), at the [European Synchrotron Radiation Facility \(ESRF\)](#), in Grenoble (France). By way of example, Figure 5 shows various [meshes](#), derived on the basis of a 3D image, obtained at ESRF. Each of these meshes was used, to evaluate the anisotropy in elastic behavior induced by macroporosity.



CEA - ESRF

Figure 5.
Meshes derived on the basis of the X-ray tomography characterization – carried out at ESRF (Grenoble, France) – of a SiC/SiC composite. Such meshes are used to quantify the influence of the three-dimensional distribution of porosity on elastic behavior anisotropy.

Optimization of thermal conductivity

Cladding materials are required to ensure an optimum transfer of heat, from the fuel to the coolant fluid. As regards a composite material, a **thermal conductivity** higher than 10 W/m·K is expected, in operational conditions. One of the major drawbacks of SiC/SiC materials stems from their low thermal conductivity, this being related, in part, to their inhomogeneity, and inherent porosity, but equally to the evolution of SiC thermal conductivity at high temperature and under **irradiation**. Indeed, a fall in SiC/SiC thermal conductivity is found to occur, as a rule, at higher temperatures – it may then become lower than 10 W/m·K at 1,000 °C – and in neutron flux conditions. If the dimensioning criteria for fuel cladding materials are to be met, the composite's thermal conductivity thus needs to be optimized.

A number of avenues may be considered, for the purposes of enhancing the thermal conductivity of composites. An attempt may be made to reduce porosity, or the use of more highly conducting fibers may be looked into, or an optimization may be sought of fiber preform architectures. However, whilst every one of these avenues is liable to bring about an increase in thermal conductivity at ambient temperature, it is very much the inherent behavior exhibited by SiC at high temperature, under irradiation, that acts as the greatest limitation to thermal conductivity, in SiC/SiC composites. In such conditions, one alternative involves substituting, for the SiC matrix, a novel matrix, exhibiting higher thermal conductivity than that of SiC under irradiation, at high temperature.

A study, conducted in the context of a doctoral thesis at LCTS, has been carried out on **titanium** carbide (TiC), this being a possibly advantageous material, in view of its specific properties. Indeed, owing to the metallic character of some of its **atomic** bonds, TiC exhibits a rise in thermal conductivity with temperature. Consideration is thus being given to substituting, for the SiC matrix of SiC/SiC composites, a TiC matrix, to obtain a SiC/TiC composite, which would exhibit, in a range of temperatures extending from 800 °C to 1,000 °C, under irradiation, a higher thermal conductivity than SiC/SiC. TiC thermal conductivity measurements, at high temperature, were carried out with SiC/TiC microcomposites, and the findings were compared with those acquired for SiC/SiC microcomposites. The outcome was that the thermal conductivity exhibited by TiC, as fabricated by CVI, is slightly higher than that of SiC, fabricated by the same process. Studies were also conducted on TiC irradiated by **ion implantation**, at France's GANIL (Grand Accélérateur national d'ions lourds: National Large Heavy-Ion Accelerator) facility, in a variety of conditions (simulating neutron irradiation). They showed that, subsequent to irradiation at ambient temperature, in the **nuclear** interaction domain – this being the characteristic region, for neutron damage – the thermal conductivity exhibited by TiC, at high temperature, is higher than that of SiC. This behavior is accounted for by the greater structural stability retained by TiC under irradiation, which is understood to be related to the **carbon** hypo-stoichiometry, and the strength of **covalent bonds** arising in TiC. Bearing in mind that, in a reactor, operating temperature, at the cladding surface, will stand at around 800 °C, cladding damage must also be



A rig used to measure the thermal conductivity of microcomposites, set up at the Thermostructural Composites Laboratory.

evaluated in high-temperature conditions. For that reason, irradiations were carried out at higher temperatures, at 500 °C, this being the highest temperature currently achievable, at GANIL. It was found that, in such conditions, TiC undergoes greater damage than SiC (formation of **dislocation loops**), while SiC thermal conductivity is higher than that of TiC, at ambient temperature. On the other hand, owing to the differing evolutions of thermal conductivity with temperature, for SiC and TiC, at 1,000 °C, TiC thermal conductivity becomes higher than that of SiC, in the nuclear interaction domain.

These investigations have thus shown that, subsequent to irradiations, whether carried out at ambient temperature, or at 500 °C, high-temperature thermal conductivity is higher in TiC than in SiC. Based on these findings, TiC would appear to be a good candidate, with regard to enhancing thermal conductivity in ceramic-matrix composites (CMCs). Further, complementary studies have yet to be carried out, before SiC/TiC composites can be put forward as GFR cladding materials. These studies will cover the characterization of the thermal properties of materials irradiated at higher temperatures (800–1,000 °C), under a neutron flux, together with research on the fabrication of such composites, and characterization of their mechanical properties.

Brazing complex SiC and SiC/SiC composite structures

With regard to the leaktight sealing of ceramic claddings, solutions have been investigated at CEA, using the BraSiC® process, involving **brazes** consisting in the main of silicon. Such brazes prove unreactive with respect to SiC-based materials, and ensure good wettability in the presence of such substrates. The braze selected for this study requires a **brazing** temperature in the 1,420–1,440 °C range, and is employed under **helium**. Process optimization was carried out for a fuel in the form of honeycomb-cell plates, however this may be readily adapted to cater for pin-type cladding

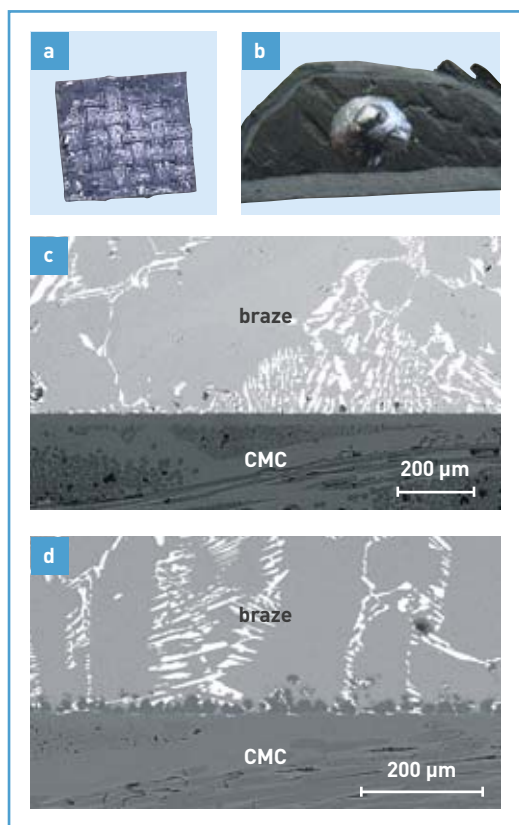


Figure 6. Droplet test, involving a braze droplet placed on the composite, and the observation, according to the environment, of the reactivity found between braze, and composite. (a) The overlain droplet has completely infiltrated the uncoated composite. (b) The overlain droplet has solidified on top of the composite coated with a presealing deposit. (c) The interface between braze, and ceramic-matrix composite (CMC) in a metal furnace. (d) The braze-composite (CMC) interface, in a graphite furnace.

tubes, this being the currently prioritized concept. Assembly involves a honeycomb structure, in β -SiC (exhibiting a **face-centered cubic** structure), and SiC/SiC ceramic-matrix composite (CMC) plates, supplied by the French **Safran/SPS** company. Initially, braze behavior with respect to the composite was investigated in terms of wetting, reactivity, and infiltration, since this material exhibits considerable **open porosities**. These studies highlighted the need to deposit, over the composite, a final pre-sealing SiC coating, to ensure tightness (by **chemical vapor deposition** [CVD]), to seal the macroporosities, thus precluding any braze infiltration into the material being brazed (see Figures 6a, 6b). It was shown that composite-braze reactivity depends on the environment (graphite, or metal brazing furnace), and on the stoichiometry of the SiC surface deposit. Indeed, should

the SiC deposit be carbon-rich, the latter element may be partly dissolved into the liquid braze, and, depending on conditions, yield SiC **precipitates** as cooling takes place. This is what occurs in treatments carried out in a graphite furnace, during which the furnace atmosphere is not sufficiently oxidizing to remove residual carbon from the SiC deposit. The joint formed during the brazing operation is then heterogeneous, exhibiting a composition varying as braze advances between the components (see Figure 6d). This configuration is not acceptable, since it may result in alterations in properties, liable to impair the strength of the assembly. For cases where the material exhibits residual surface carbon, it is then preferable to go for brazing in a metal furnace, in which the presence of even low oxygen content in the helium used is sufficient to limit carbon content in the braze, thus precluding the formation of SiC precipitates (see Figure 6c). Braze sealing of SiC honeycomb structures was validated in a metal furnace (see Figure 7). The influence was evidenced, of the geometrical characteristics (flatness, surface roughness) of the composite plates on the thickness of the brazed joints. For the composites used in this initial evaluation, thickness was found to be greater than 75 μm . To minimize this tolerance, it would appear crucial to optimize the characteristics of the composite plates, with particular regard to the weaving method used.

In the coming years, to meet all of the stipulations set out by the GFR specifications, a new, more refractory braze composition will have to be arrived at, and the brazing process will need to be validated for a pin-type configuration.

The 2012 target

Owing to the stringent specifications set for GFR fuel elements, development of SiC/SiC claddings stands as an ambitious target, both from the technological, and scientific standpoint. High-temperature tests will make it possible to work in actual conditions consistent with the target performance. Innovative solutions will doubtless be required, if fabrication is to be achieved, by 2012, of an initial pin prototype, featuring the chief functionalities required for the GFR fuel elements of the future.

> Patrick David

Materials Department
Military Applications Division
CEA Le Ripault Center

> Fabienne Audubert

Fuel Research Department
Nuclear Energy Division
CEA Cadarache Center

> Valérie Chaumat

LITEN Institute (Innovation Laboratory for
New Energy Technologies and Nanomaterials)
Technological Research Division
CEA Grenoble Center

> Cédric Sauder and Lionel Gélébart

Department of Materials for Nuclear Energy
Nuclear Energy Division
CEA Saclay Center

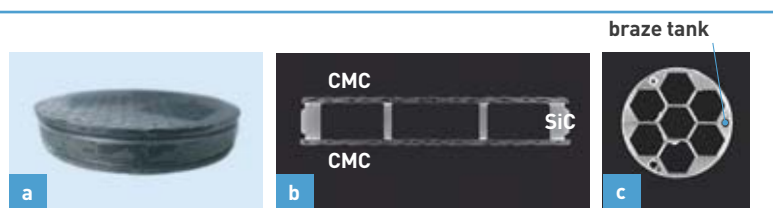


Figure 7. A honeycomb structure, brazed between two ceramic-matrix composite (CMC) plates, and control views obtained by **tomography**. (a) The sealed assembly. (b) Tomography of the assembly, showing the braze (white). (c) Tomographic view of a joint.

ODS alloys for structures subjected to irradiation

Of the various solutions available for consideration, for cladding purposes, with regard to fuel elements for the fourth-generation sodium-cooled fast reactors, ODS materials – i.e. oxide-dispersion-nanoreinforced materials – afford many benefits. Indeed, these high-performance materials combine, at the same time, remarkable mechanical strength, in hot conditions, and outstanding irradiation behavior.

Of the various options available, for the purposes of constructing a fourth-generation fast-neutron reactor, the sodium-cooled fast reactor (SFR) concept is the one that can draw on the widest operational feedback. In order to enhance the neutronic performance of such reactors, the core design, for this reactor line, calls for a closer-packed fuel-element bundle, i.e. one involving larger-diameter fuel pins, fitted with thinner spacer wires, inserted between the cladding tubes, than were used in the Phénix⁽¹⁾ or Superphénix⁽²⁾ (SPX) fast reactors (see Figure 1). To preclude any excessive deformation of the fuel pins, it is essential that the cladding material should exhibit little swelling under irradiation. At the same time, in order to achieve optimization in economic terms, the burnup values being considered will result in doses higher than those allowed for the cladding material used in Phénix, namely 15–15 Ti austenitic steels. New alloys thus must be developed, e.g. oxide-dispersion strengthened (ODS) steel grades, exhibiting better performance levels than the last-generation austenitic steels designed for deployment in the Phénix, and Superphénix reactors. ODS materials afford not only negligible swelling under irradiation, owing to their “ferritic” body-centered cubic structure – by contrast to austenitic grades, which feature a face-centered cubic structure – but equally outstanding creep properties, owing to the nanoreinforcements present in the matrix.

(1) Phénix: an experimental reactor, in the sodium-cooled fast reactor line. Sited at Marcoule (Gard département, southeastern France), this reactor initially went critical in 1973, being shut down on 1 February 2010. It has made it possible, amongst other achievements, to gain knowledge as to the irradiation behavior of materials being considered for the reactors of the future.

(2) Superphénix: a prototype sodium-cooled fast reactor, sited at Creys-Malville (Isère département, southeastern France), currently undergoing dismantling. It reached its full power rating in 1986, being shut down in 1998. The core held 364 assemblies, each comprising 271 fuel pins, containing a stack of U–Pu mixed-oxide fuel pellets.



Cladding (billet), raised to a high temperature – about 1,100 °C – containing ODS powder. The billet is ready to undergo hot extrusion, using a press.

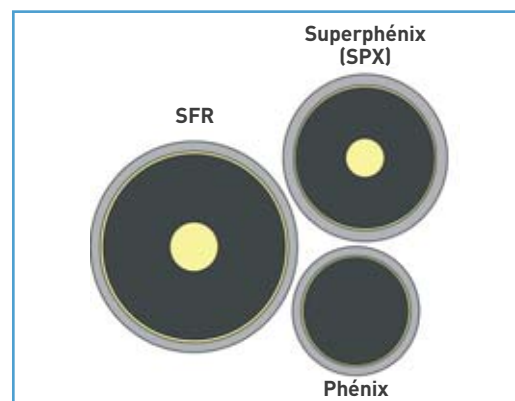


Figure 1. Sectional view of the fuel and cladding used for the Phénix and Superphénix fast reactors, and for the future SFR. The fuel is shown in black, the metal cladding in gray, while the central cavity, holding no fuel, is shown in yellow.

The first commercial ODS steels were brought out in the 1970s, the grades offered being **nickel**- (Ni), or iron- (Fe) based. Conventional metalmaking techniques, involving processes of the melt type, followed by casting of the grade, do not allow materials containing fine oxide particles to be obtained. When oxides are introduced into the material at the molten stage, they either react with the furnace crucible and are no longer to be found after casting, or they **coalesce** within the liquid bath, yielding oxides that are too bulky to result in a reinforcement effect in the material. It is thus necessary to go for mechanical synthesis, using a pathway hailing from **powder metallurgy**, commonly known as *mechanical alloying*.

ODS metallurgy

The standard fabrication sequence, for ODS materials, involves several steps (see Figure 2). ODS materials are obtained by powder metallurgy, the first fabrication step involving cogrinding a metal powder together with **yttrium** oxide (Y_2O_3) powder. At this stage, an iron oxide may also be added, or an yttrium-(Y) rich intermetallic compound,⁽³⁾ to provide the amounts of yttrium, and oxygen (O) required for the formation of nano-oxides. The metal powder consists of a powder prealloyed to the chemical composition of the desired material – apart from yttrium, and oxygen – or it may comprise a number of metal powders, featuring different chemical compositions, which, when ground, will yield a powder exhibiting a homogeneous distribution of all of the **elements** involved. This mechanical alloying step yields a powder which may be described, as a first approximation, as a metallic matrix, holding all of the alloying elements in a solid solution. CEA has embarked on a number of collaborations with manufacturers, in particular with **Mecachrome**, through the joint CEA–Mecachrome laboratory known as MATPERF (Matériaux hautes performances: High-Performance



P. Stroppa / CEA

Hot extrusion press, serving to effect the consolidation of materials, set up at the Extreme Materials Technology Laboratory (DEN/LTMEX: Laboratoire de technologie des matériaux extrêmes), at CEA/Saclay. This installation is used both for R&D work on ODS-alloy cladding for fourth-generation reactor fuel elements, and for some of the innovative investigations regarding second- and third-generation **PWR** fuel-element cladding.

Materials), with a view to ensuring that the industrial fabric will have the ability to meet the demands of the nuclear power industry, in terms of large-scale production, to supply the tonnes of ODS materials that will be required for the fabrication of fuel assemblies.

Once the powder has been obtained, consolidation of the ODS materials is achieved either by **hot extrusion**, or by **hot isostatic pressing**. In some fabrication sequences, extrusion is carried out subsequent to an initial consolidation step, by hot isostatic pressing. For the purposes of tube production, proceeding with an extrusion operation does appear to be inescapable. These steps are followed by transformation operations in cold conditions, through cold rolling, or pilgering process and possibly by heat treatments, for stress relief⁽⁴⁾ purposes.

The micrographs reproduced at Figures 3 and 4 show typical **microstructures**, observed in ODS iron-base alloys, during fabrication. It is now generally agreed that the mechanisms involved in the formation of nanophases, in ODS alloys, include the dissolution of yttrium oxides, Y_2O_3 , during grinding, and a **precipitation** of nanophases (Y, Ti, O) during the hot consolidation step.

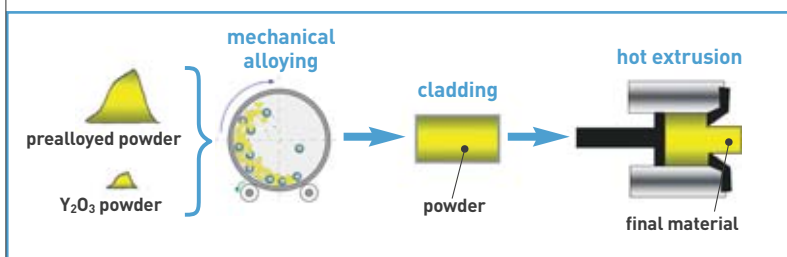
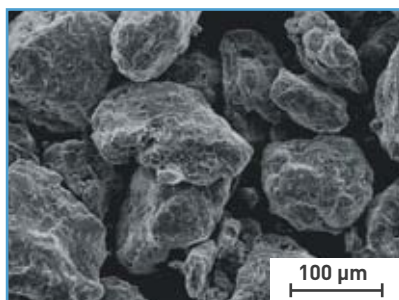
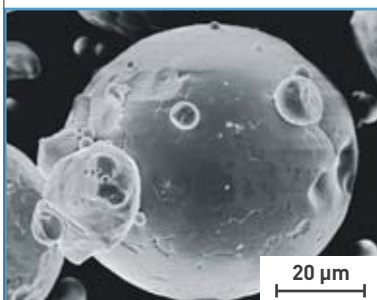


Figure 2.
The various steps involved in the fabrication of an ODS material, in this case featuring Y_2O_3 nanoreinforcements.



CEA/DMN

Figure 3.
Micrographs, obtained under **scanning electron microscopy (SEM)**, of powders observed before (left) and after (right) cogrinding.

(3) Intermetallic compound: a metallic compound featuring a specific type of crystal structure, formed by combining several metals.

(4) Stress relief: a heat treatment having the purpose of bringing down internal stresses, while causing no notable structural alteration.

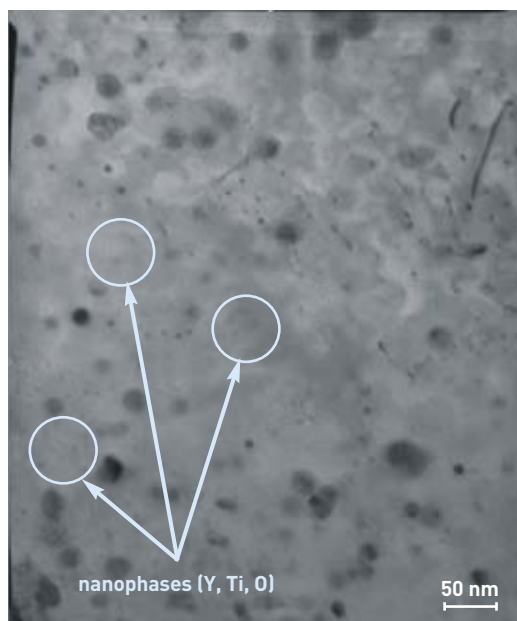


Figure 4. Micrograph, obtained under **transmission electron microscopy (TEM)**, of a ferritic ODS featuring **titanium- (Ti)**, **yttrium- (Y)**, and **oxygen- (O)** rich nanoreinforcements.

This fabrication process is the only one, currently, to have reached the industrial stage, allowing the mass-production (several tens of tonnes annually) of ODS materials featuring **nanometer-scale** reinforcements. Be that as it may, other techniques are being explored, around the world. Mention may be made, for instance, of the endeavors pursued by the **OCAS** research center, within the **ArcelorMittal** group (Belgium), to produce ODSs through injection, into molten steel droplets, of nanometer-size oxide particles, by way of a side nozzle. Once **doped** with yttrium oxide, the droplets solidify, yielding an ingot, which may then be transformed. Likewise, methods involving **electron-beam physical vapor deposition (EB-PVD)** are being investigated at the Harbin Institute of Technology (China).

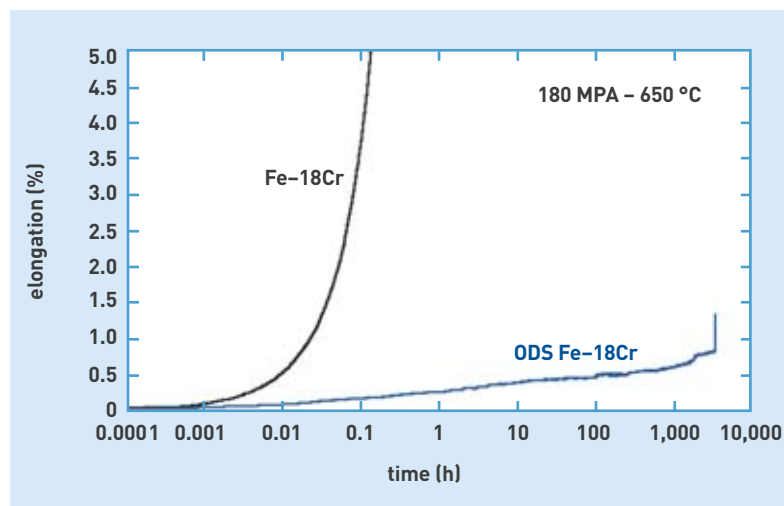


Figure 5. Graph plotting the creep found in a non-nanoreinforced ferritic alloy, compared to that for a nanoreinforced Fe-18Cr (iron base, 18% chromium) ODS material.

Specific mechanical properties

Ferritic, or **martensitic** ODS grades exhibit remarkable thermal creep resistance, for this class of materials (see Figure 5). At the same time, the presence of nanoreinforcements, together with fabrication by mechanical alloying, and subsequent extrusion do result in quite specific microstructures, and mechanical properties. For instance, ODS grades exhibit virtually no tertiary creep,⁽⁵⁾ this entailing far-reaching modifications to the way cladding tubes are to be dimensioned, compared to the approaches previously adhered to, for the austenitic steels employed in the Phénix and Superphénix reactors. The ODS materials selected for cladding purposes involve a matrix featuring a body-centered cubic structure. They involve – as indeed all ferritic, or martensitic materials – a **ductile–brittle transition temperature**, which needs to be evaluated. For conventional steels, martensitic

(5) Tertiary creep: this creep stage occurs in the time interval leading up to rupture, when the strain rate is found to increase with time.



The cold rolling step, for ODS-alloy tubes, has the purpose of shaping the extruded blank, to obtain thin tubes, exhibiting the desired geometry.

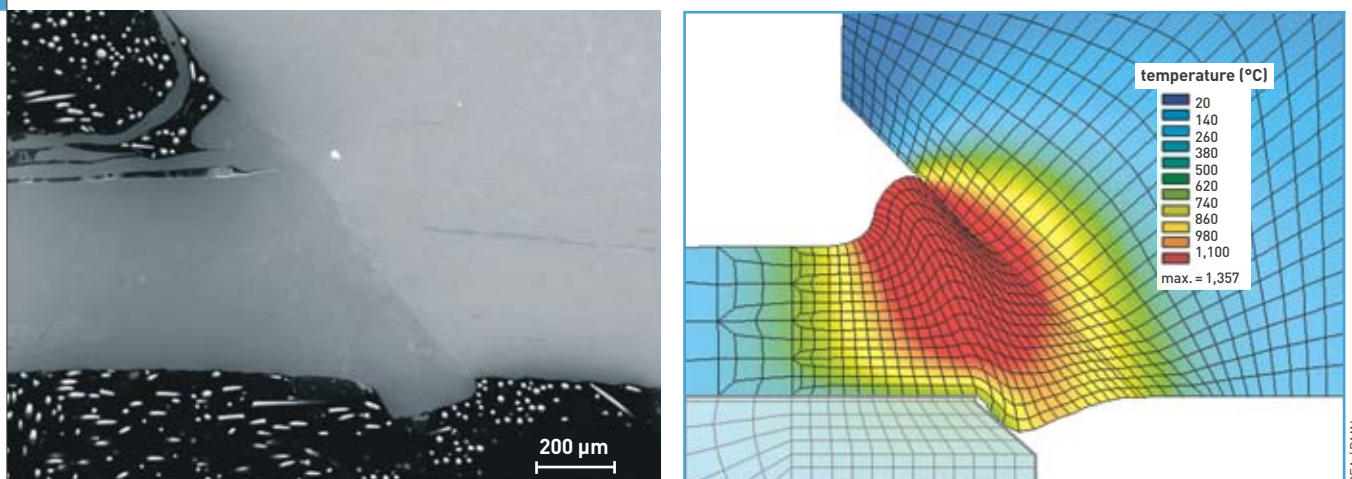


Figure 6. Shown at left, the image, as obtained under scanning secondary-electron microscopy, of a cladding–endcap weld, effected by resistance welding. Right, an instance of the result achieved by way of electrothermomechanical coupling.

grades in particular, this temperature is sufficiently low, both before and after irradiation, not be a cause for concern in operational conditions. With regard to ODS grades, depending on the fabrication sequence selected, the ductile–brittle transition temperature may show quite notable variations, a point that is peculiarly critical for such materials.

The qualification of ODSs as cladding materials entails carrying out specific mechanical tests, on tubes made of these materials. Such tests are currently being developed at CEA.

Weldability of ODS tubes

The constraints related to endcap–cladding weldability are crucial. The endcap is a solid steel component, serving to ensure fuel pin tightness, while enabling pin handling operations. An operational process must be qualified, allowing for use in glovebox conditions – owing to fuel handling constraints – and guaranteeing pin tightness, both before and after irradiation, while withstanding applied mechanical stresses. During the welding operation, it is thus crucial that the ODS base metal's initial microstructure be altered as little as feasible, by precluding any alteration, or agglomeration of nanometer-size “dispersoids,” and any microstructural evolution (grain size, and shape), or segregation of elements at interfaces. Solid-state welding techniques are thus the favored solutions. These should prove robust with respect to changes in geometry, or material (switching to other ODS grades). Further, welds should be readily amenable to inspection by nondestructive testing.

Various solid-state welding processes were evaluated, with the PM 2000 ODS steel produced by the Plansee Group: diffusion welding by uniaxial pressing [uniaxial diffusion welding (U–DW)], spark plasma sintering (SPS), friction stir welding, and resistance welding. The latter technique was used, in the 1980s, by teams at Dour Metal Corporation, in Belgium, to weld the pins in two ODS fuel assemblies, irradiated in Phénix; and, more recently, by JAEA, to weld pins made of an Fe–9Cr (iron base, 9% chromium) ODS alloy, currently

undergoing irradiation in the BOR–60 fast reactor (Dimitrovgrad, Russia). Resistance welding is seen as the favored process, however U–DW could provide an advantageous alternative, whereas SPS welding is seen as being altogether more difficult to employ. Figure 6 shows an instance of the results of resistance welding, for a cladding–endcap configuration.

Gradual deployment

Qualification of a novel cladding requires that all of the fabrication steps and all of the stages in the material's lifetime be taken into account, making sure no one point is found to be unacceptable. For instance, the material's irradiation behavior must be evaluated, and likewise cladding behavior, subsequent to in-reactor time, during assembly cleaning operations, and fuel treatment operations. The qualification of such novel grades may only be achieved over the medium term. The fuel assemblies required for the startup, and operation of the initial cores planned for the ASTRID (Advanced Sodium Technological Reactor for Industrial Demonstration) Reactor, a prototype fourth-generation reactor, will use 15–15 Ti austenitic steels, the most advanced grade in particular, known as AIM. This will provide the ability for operations up to doses that have yet to be determined, but such as will allow many concepts to be validated, for the reactors of the future. Deployment of high-performance ODS-alloy claddings will occur at a later date, in a gradual manner, depending on the stage reached in the qualification of these materials. The aim is to introduce, at the earliest time feasible, an assembly featuring one ODS cladding into the ASTRID prototype, in the first core for instance.

> Yann de Carlan

Department of Materials for Nuclear Energy
Nuclear Energy Division
CEA Saclay Center

Investigating the irradiation behavior of nuclear materials: the contribution of the JANNUS platform

Whatever the nuclear application involved, the physicochemical phenomena induced by irradiation within a material will tend to destabilize its atomic architecture, and bring about, over time, alterations in its microstructure and chemical composition. These alterations will result in modifications in mechanical behavior, physical properties such as thermal conductivity and density, and corrosion resistance.

Notwithstanding the advances achieved, in materials science, over the past 50 years, it is not as yet feasible to predict the effects of a given irradiation on the behavior of materials, as a function of the irradiation parameters (nature of the particles involved, spectrum hardness, flux, dose...). On the other hand, these advances have made it possible to account for the behavior of the material, on the basis of the characteristics and properties exhibited by its microstructure, and of the evolution of this microstructure under stress: there is thus

great benefit to be drawn from the detailed scrutiny of the microstructural alterations induced by well-defined irradiations. Coupled with theoretical developments and numerical modeling at the atomic scale, such investigations seek to provide a firmer basis, in physical terms, for the codes used to predict the irradiation behavior of materials, so that the best advantage may be extracted from the feedback from experience. Using beams of charged particles makes such approaches feasible, for small samples, in fully controlled irradiation conditions. This is an undemanding, flexible, high-performance experimental setup. Once the relationship has been determined, between irradiation damage sustained at the atomic scale and the consequent behavioral modifications exhibited by the material, it becomes possible to extrapolate, or interpolate the result, depending on irradiation conditions, in particular with regard to extending it to cover neutron irradiation, the effects of



P. Siroppe/CEA

The JAPET tandem Pelletron™ accelerator. Its source delivers beams of electronegative elements – e.g. chlorine, or iodine – or beams of metallic ions, e.g. silicon, or gold ions.

which may only be ascertained by way of in-reactor experiments, which prove much more cumbersome to set up.

Researchers are then able to perform the experimental simulation of a material's behavior under irradiation, by bombarding it by means of one, or more accelerated ion beams, and monitoring, *in situ* or *ex situ*, the evolution of its microstructure, of its chemical composition, and thermal, mechanical, or electrical properties.

The JANNUS accelerators

The JANNUS platform (Jumelage d'accélérateurs pour les nanosciences, le nucléaire et la simulation: Joint Accelerators for Nanosciences and Nuclear Simulation) comprises two experimental complexes, one located at Saclay, the other nearby at Orsay (Essonne département, near Paris), at the Center for Nuclear Spectrometry and Mass Spectrometry (Centre de spectrométrie nucléaire et de spectrométrie de masse), run under joint CNRS-IN2P3 and Paris-Sud (Paris-XI) University supervision. The Saclay facility stands as one of the major instruments for the Basic Scientific and Technological Research (RSTB: Recherche scientifique et technologique de base) program, conducted by CEA's Nuclear Energy Division. It brings together three electrostatic particle accelerators: one single-ended, 3-MV Pelletron™ accelerator (EPIMETHEE), one tandem 2-MV Pelletron™ (JAPET), and one single-ended 2.5-MV Van de Graaff accelerator (YVETTE), set up around a common experiment chamber.



P. Siroppe/CEA

The JANNUS platform's triple-beam experiment chamber, at Saclay. The beamline from EPIMETHEE lies in the horizontal plane, in the foreground, while that from JAPET is at the back. The beamline from YVETTE may be seen in the lower region, center. The first experiment in triple-beam mode was successfully carried out in March 2010.

EXPERIMENTAL SIMULATION



The beamlines from JAPET (left), YVETTE (center), and EPIMETHEE (right), converging onto the triple-beam experiment chamber, located behind the wall.

EPIMETHEE is fitted with a **multicharged-ion** source of the **ECR** type, delivering ions in multicharged electric states, from gases, or volatile **organometallic compounds**. JAPET features a charge-exchange ion source, using cesium vapor sputtering. This source delivers beams of **electronegative** ions, of **elements** such as **chlorine**, or iodine, which cannot be obtained with an ECR source, or ion beams of elements such as **silicon**, or gold, for which the compounds that may be used in an ECR source are not appropriate. The YVETTE accelerator is fitted with a **radiofrequency** ion source, having the ability to deliver beams of protons ($^1\text{H}^+$), deuterons ($^2\text{H}^+$), and helium-3 ($^3\text{He}^+$) and helium-4 ions ($^4\text{He}^+$).

The Orsay facility features one mixed-mode 2-MV accelerator (ARAMIS), and one 190-kV **ion implanter** (IRMA), both being coupled to a 200-kV **transmission electron microscope**. This setup allows the evolution of the sample's microstructure to be observed *in situ*, while it is undergoing irradiation, in single- or dual-beam configuration.

How ions simulate neutrons

A typical irradiation experiment, in triple-beam configuration, matches the conditions required, e.g., by applications in the area of **fusion**. The multicharged **heavy-ion** beam delivered by EPIMETHEE serves to simulate the atomic displacements caused, within the material, by neutrons. YVETTE provides **helium** (^4He), and JAPET **hydrogen** (^1H), as yielded by nuclear reactions (n, α) and (n, p). Such irradiations make it possible to investigate, independently, the part played by the **damage dose** – i.e. by **fluence** – or by **damage dose rate** – i.e. by **flux** – and by irradiation temperature, total concentration of injected gases (^4He , ^1H), and by the paths followed by ions inside the material.

Characterization

One key stage in the study involves the characterization, as precisely as feasible, of the irradiated sample. This characterization – whether structural, chemical, or mechanical – may be carried out during irradiation (*in situ*), or immediately subsequent to it (*ex situ*). Materials science can now avail itself of an altogether comprehensive panoply of physicochemical analysis techniques, e.g. electron microscopy, **atom-probe tomography**, **X-ray diffraction** and **absorption**... Light-ion beams – involving protons ($^1\text{H}^+$), deuterons ($^2\text{H}^+$), helium-3 ($^3\text{He}^+$), and

helium-4 ($^4\text{He}^+$) ions – likewise afford the ability for *in situ* characterization of concentration profiles, by way of Rutherford backscattering spectrometry,⁽¹⁾ elastic recoil detection analysis,⁽²⁾ or nuclear reaction analysis.

The behavior of two advanced materials under irradiation

Two examples are set out in the following paragraphs, illustrating the contribution made by the JANNUS platform to our understanding of the irradiation behavior of nuclear materials. The first example concerns hexagonal silicon **carbide** (6H-SiC), the second one an **ODS ferritic-martensitic alloy**, having the composition Fe-16Cr (by weight), reinforced by a dispersion of **yttrium oxide** (Y_2O_3) **nanoparticles**, to 0.37%.

(1) Rutherford backscattering spectrometry: this technique involves analyzing the backscattering of helium-4 ions directed onto a sample. It makes it possible to ascertain the sample's local composition, close to the surface.

(2) Elastic recoil detection analysis (ERDA): this technique involves analyzing the recoil of surface atoms, subsequent to their collision with helium-4 ions. This allows the sample's local composition to be ascertained, close to the surface.

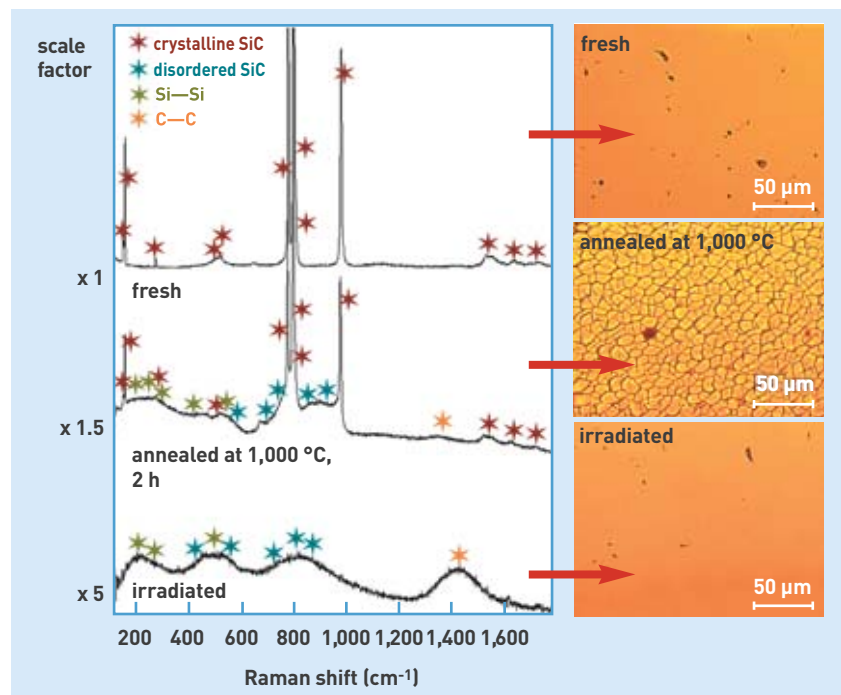


Figure 1. Raman spectra, and micrographs of a 6H-SiC single crystal, irradiated by means of a 0.92-MeV nickel-ion (Ni^+) beam at ambient temperature, to a dose higher than the amorphization threshold; of the fresh single crystal; and of the sample after annealing at 1,000 °C for 2 hours. This study was the outcome of a collaboration between all three services at the Department of Materials for Nuclear Energy (J.-M. Costantini, L. Gosmain, and S. Miro).



P. Stroppa / CEA

The control and monitoring station for the three accelerators used in the JANNUS platform.

The 6H-SiC **single crystal** was irradiated by means of a 0.92-MeV **nickel-ion** ($^{58}\text{Ni}^+$) beam, at ambient temperature, to a dose higher than the **amorphization** threshold. Figure 1 shows the **Raman spectra** for the fresh crystal, for the irradiated sample, and for the same sample, after **annealing** at 1,000 °C for 2 hours. Subsequent to irradiation, the characteristic bands from **crystalline** SiC have altogether disappeared, while bands corresponding to Si-Si, and C-C bonds are now apparent. Annealing results in a degree of restoration of the initial crystal system, as characterized by the reemergence of Si-C bands and diminished intensity for the Si-Si and C-C bands.

Further, this recrystallization involves a concomitant surface “fragmentation” phenomenon.

The ODS alloy, in turn, was irradiated at 425 °C in dual-beam mode, using 24-MeV iron ions ($^{56}\text{Fe}^{8+}$), and helium-4 ions ($^4\text{He}^+$), subjected to energy dispersion over the 1.7–1.1 MeV range, by means of thin **graphite** films. Damage rate stood at 30 dpa, while injected helium concentration stood at 0.0025 at.%/dpa. The transmission electron microscopy images shown in Figure 2 evidence the emergence of a bimodal distribution (i.e. involving two components, in terms of size) of helium bubbles, in a region featuring a low density of yttrium oxide

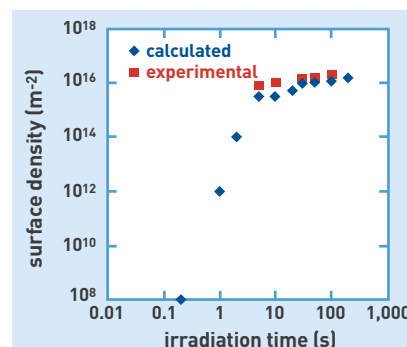
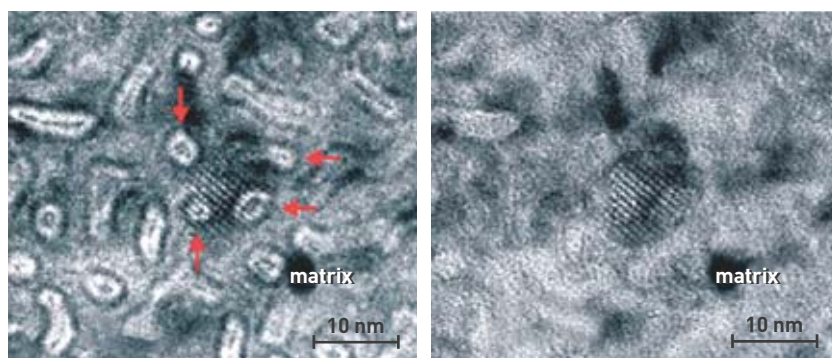


Figure 3. Variation in the surface density of interstitial loops forming in high-purity tungsten, irradiated with helium-4 ions, as a function of time. The comparison of calculated densities (diamonds), and experimental measurements (squares) shows excellent agreement. This study was the outcome of a collaboration between Kyushu University and Kyoto University (Japan) [Y. Watanabe, H. Iwakiri, N. Yoshida, K. Morishita, and A. Kohyama].

nanoparticles. Further, it is apparent that the oxide nanoparticles act as traps, with respect to helium bubbles.

Comparing experiment and numerical simulation

Investigations of this type fulfill a twin purpose: understanding the behavior of materials subjected to irradiation, and testing the ability of theories and multiscale modeling to account for experimental findings. Figure 3 shows a significant instance of the comparison of experiment and numerical simulation, as regards the formation of **interstitial loops** in high-purity tungsten (W), irradiated with 8-keV helium-4 ions ($^4\text{He}^+$) at ambient temperature, involving a flux of $2.6 \cdot 10^{13}$ ions/cm²/s. In order to compute the surface density of interstitial loops, an adjustment must be made to the parameter corresponding to the binding energy arising between an **interstitial** tungsten atom and a pair comprising one helium atom, and one tungsten **vacancy**. When the value for this parameter is set at 0.7 eV, as suggested by previously published **molecular dynamics** calculations, the agreement between experimental findings and simulation is found to be outstanding.



L. Hsiung / LLNL

Figure 2. Images, taken under transmission electron microscopy, showing the distribution of helium bubbles in an ODS Fe-16Cr steel, irradiated in dual-beam mode. The image at left shows up the presence of 4 helium bubbles (3–5 nm in diameter) associated to an oxide grain 10 nm in diameter, which may be seen in the right-hand image. The elongated cavities, on the other hand, are the outcome of the **coalescence** of smaller bubbles. This study was the result of a collaboration set up between Lawrence Livermore National Laboratory (USA) [L. Hsiung, M. Fluss, S. Tumey, J. Kuntz, B. El Dasher, M. Wall, W. Choi], Kyoto University (Japan) [A. Kimura], and CEA.

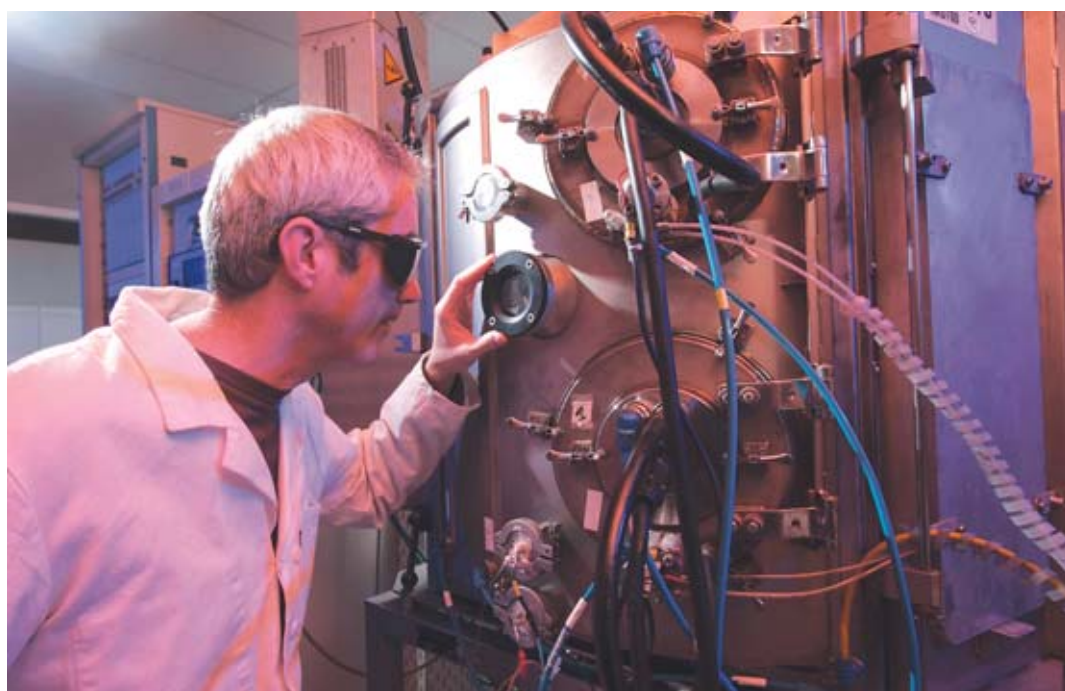
> **Patrick Trocellier, Sandrine Miro and Yves Serruys**

Department of Materials for
Nuclear Energy
Nuclear Energy Division
CEA Saclay Center

Environmental barriers for extreme environments

The emergence of novel technologies calls for the development of materials affording ever-higher performance levels. **This goes hand in hand, in most cases, with the requirement to protect such materials against an extreme, aggressive environment**, be it for applications in the nuclear industry, or in the aerospace and automotive sectors. The evolution undergone by deposition processes has helped make possible the development of nanostructured coatings, exhibiting remarkable properties, in terms of wear, corrosion, and high-temperature resistance, in exacting conditions.

Fabrication of nitride-based hard nanostructured layers in the vacuum arc evaporation reactor set up at CEA/Grenoble.



P. Avarian / CEA

The protection of materials by way of an environmental barrier must meet a set of specifications, associated to a particular application. Indeed, there is no universal coating, such as would stand as an effective barrier, guarding against corrosion in highly aggressive environments, high temperatures, mechanical stresses, diffusion, or any combination of such extreme conditions. The development of such barriers is thus strongly contingent on the properties looked for. Fabrication methods are then selected for this coating, on the basis of these properties. Thus, a variety of industrially mature deposition techniques may prove to be complementary, for the purposes of meeting the various requirements at hand. **Thermal spraying**, a process used for the dry deposition of thick coatings (a few hundred microns), at atmospheric pressure, is employed, for instance, for the fabrication of thermal barriers in aerospace applications. Such barriers have the ability to shield the substrate at high temperatures (typically 1,200 °C), in burnt kerosene⁽¹⁾ atmospheres. The development of dry deposition technologies, able to operate under reduced pressure, and the concurrent evolution

undergone by reactors have allowed the fabrication to be achieved of thin coatings (a few microns thick), having the ability to act as effective barriers, with respect to strong mechanical stresses.

In this context, nanomaterials, coming to the fore as they have owing to the strong surge in nanotechnologies, have experienced a remarkable expansion, opening up altogether broad prospects, in a variety of industrial areas. Indeed, the nanometer-scale architecture of these materials endows them with highly advantageous properties, compared to those of conventional materials. In the area of materials durability, the application of surface treatments by spraying, or, in vacuum, by way of dry **physical vapor deposition (PVD)**, or **chemical vapor deposition (CVD)** has likewise markedly swung in that direction. Most of the coatings currently being developed involve nanometer-scale structures. Two main approaches are available, for the purposes of achieving the

(1) Kerosene: yielded by refining, this petroleum cut is chiefly used for the production of aviation fuel. Kerosene consists of a mix of **hydrocarbons**, containing alkanes (C_nH_{2n+2}), of chemical formulae ranging from $C_{10}H_{22}$ to $C_{14}H_{30}$.



The deposition chamber of the vacuum arc evaporation reactor, featuring a substrate holder able to move about three rotational axes.

synthesis, in vacuum, of a nanostructured coating. The first approach seeks to obtain nanometer-size precipitates, within a homogeneous matrix, which may be amorphous, or otherwise (for a deposit of the nanocomposite type). The second approach involves stacking a series of nanometer-thickness layers of various materials (deposit of the nanolayer type). Three examples are described in the following paragraphs. The first two highlight the influence of such nanostructuring on wear resistance and oxidation resistance in these coatings. The third example evidences the benefits to be gained from the fabrication of nanostructured thermal barriers, by an innovative suspension plasma spraying process.

Nanostructured coatings for abrasive wear resistance

The application under consideration here is the protection of tungsten carbide (WC) cutting tools against wear, in the context of machining operations on Inconel 718. This nickel (Ni), chromium (Cr), and iron (Fe) superalloy, exhibiting as it does superior mechanical qualities, is employed – among other uses – for the fabrication of nuclear reactor components. For applications of this type, multilayer coatings, involving nitride-based compositions – e.g. titanium nitride (TiN), chromium nitride (CrN), and mixed aluminum and titanium nitride (AlTiN) – were deposited, by cathodic arc evaporation. Going for this deposition process, involving as it does a physical pathway, is dictated by the requirement to achieve high levels of coating adhesion onto the tool, compatible with the very heavy stresses anticipated. Indeed, when cathodic arc evaporation is used, the ionization fraction, for the plasma-generating phase, is much larger than is the case, for instance, of a magnetron cathode sputtering plasma:

80% of the titanium being ionized in a cathodic arc discharge, as against a few percent in a sputtering discharge. This characteristic affords the ability to carry out ionic pickling, using ions of the material to be deposited, and condition the surface prior to coating.

Vacuum deposition techniques involve processes out of thermodynamic equilibrium, and generally result in materials containing metastable phases. Such materials may exhibit properties that are, in some cases, more advantageous than those of the conventional materials used in their fabrication. In this case, bringing down the thickness of TiN and AlTiN layers in a stack of 3 μm total thickness makes it possible to obtain a so-called “superlattice” structure (see Figure 1). A “superlattice” nanolayer deposit consists of a stack of epitaxially grown layers, characterized by continuity of the crystal structure across the interfaces. The hardening observed as the period – i.e. the thickness of two successive layers – becomes smaller (see Figure 2) is commonly attributed either

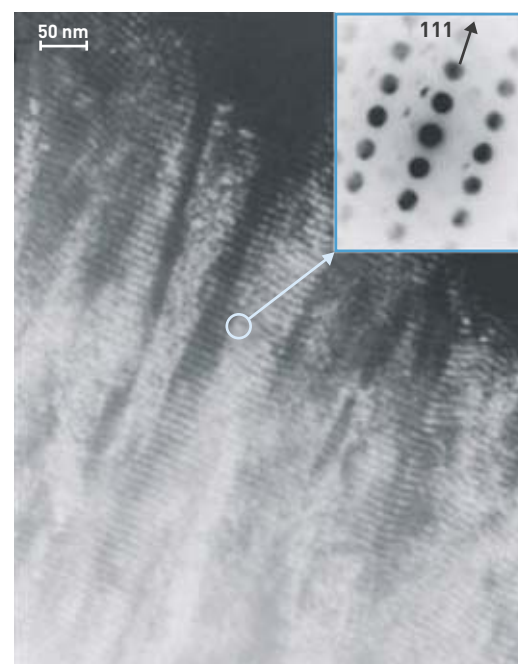


Figure 1. Bright-field image, under transmission electron microscopy, of a sectioned TiN–AlTiN superlattice coating, together with the associated electron microdiffraction image, evidencing growth along the [111] direction, perpendicular to the substrate surface. (Reproduced from C. DUCROS, C. CAYRON, and F. SANCHETTE, “Multilayered and nanolayered hard nitride thin films deposited by cathodic arc evaporation. Part 1: Deposition, morphology and microstructure”, *Surface and Coatings Technology*, vol. 201, Nos. 1–2, pp. 136–142. © 2006, Elsevier, with permission from the publisher.)

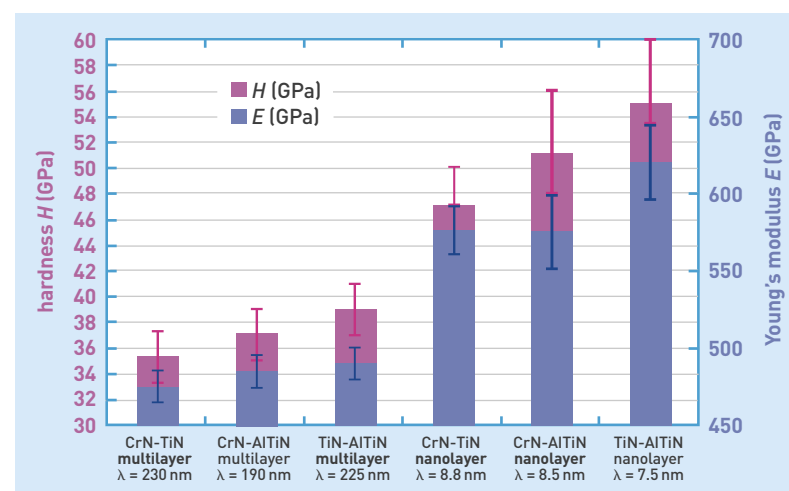


Figure 2. Hardness H , and Young's modulus E for multilayer coatings ($190 \text{ nm} < \lambda < 230 \text{ nm}$), and nanolayer coatings ($7.5 \text{ nm} < \lambda < 8.8 \text{ nm}$), for three systems: CrN–TiN, CrN–AlTiN, TiN–AlTiN. λ stands for the period, i.e. the thickness of two successive layers.

to the modulation of the **elastic moduli** (Young's moduli) across the two materials, or – to a lesser extent – to the alternating stress field arising as a result of the matching up of crystal lattices at the interfaces. In either case, hardening is thought to be due to a blocking of **dislocations** at the interfaces. Further, this hardening is strongly dependent on the period and the nature of the constituent materials in the stack. The increased coating **hardness**, inducing as it does greater resistance to abrasive wear, makes it possible to optimize machining performance (see Figure 3).

Nanostructured coatings to ensure oxidation resistance

As in the previous example, this instance concerns hard coatings, which could serve for a similar application: protecting tools used for transformation work (machining, forming). Be that as it may, the property for which improvement is being sought here is oxidation resistance, at temperatures that may rise to 1,000 °C, while retaining mechanical characteristics compatible with heavy stress levels. The fabrication of just such a nanocomposite is effected by way of the addition of **silicon** (Si) into a **transition-metal** nitride. Indeed, adding silicon to chromium nitride (CrN) can result in the **microstructure** shown in Figure 4. This evidences the presence of **nanoparticles** within an amorphous matrix, both phases containing all three **elements**, albeit in different compositions. Oxidation tests clearly show that the silicon addition, combined with nanostructuring, of the three-dimensional (3D) nanocomposite type, significantly enhances the high-temperature resistance of coatings (see Figure 5). This increased oxidation resistance was attributed to the **oxygen-diffusion barrier effect** due to the amorphous matrix of the nanocomposite.

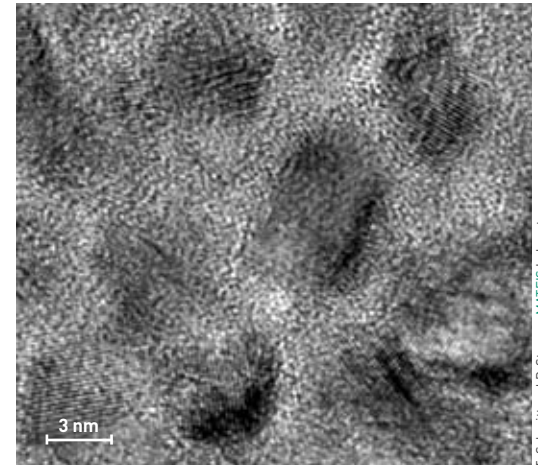


Figure 4. Bright-field image, obtained under high-resolution transmission electron microscopy. The nanoparticles are formed by a solid solution of silicon in chromium nitride (CrN).

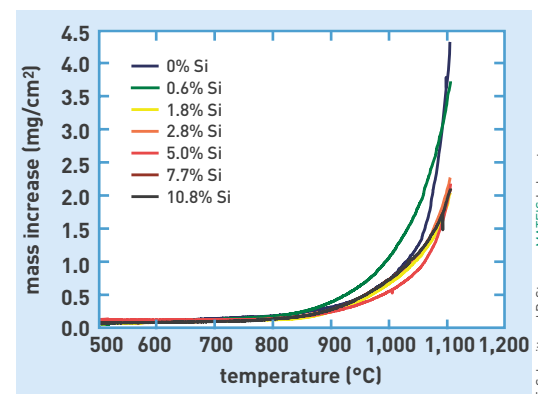


Figure 5. Oxidation resistance of Cr(Si)N coatings, as a function of silicon content. An improvement in oxidation resistance is observed, as characterized by lower activation energies, and weaker kinetics.

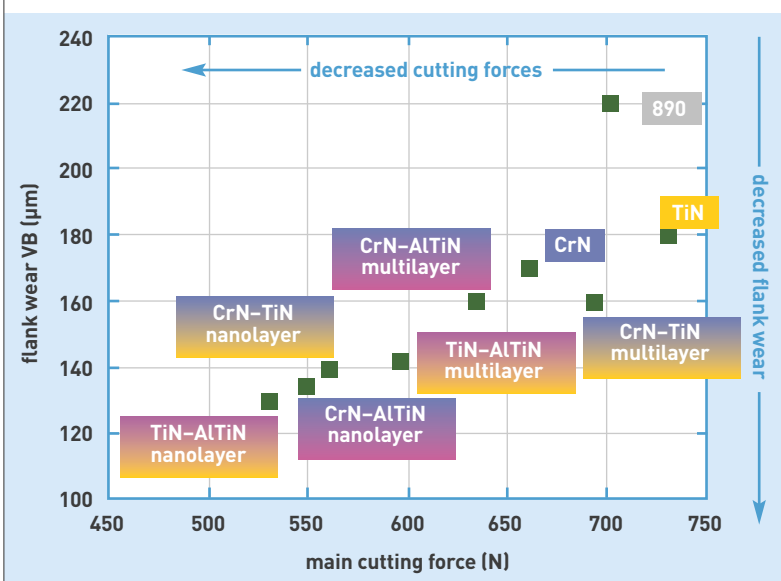


Figure 3. Evolution of tool **flank wear** (in µm), at the cutting edge, when coated with materials of different compositions and architectures, as a function of the main cutting force (in newtons [N]). The substrate (the tool) is a carbide insert, made of 890-grade tungsten carbide. The parameters of the finishing machining operation, on Inconel 718, are as follows: cutting speed 40 m/min; feed per revolution 0.2 mm/revolution; depth of cut (i.e. amount of material removed by the tool) 1 mm.

Optimization of thermal barrier performance

Yttria stabilized zirconia ($\text{ZrO}_2-x\% \text{Y}_2\text{O}_3$) coatings, fabricated by **plasma spraying**, are widely used to provide thermal barriers in the aerospace industry. They do however exhibit some weaknesses, commonly attributed to internal stresses, within the coatings, created during thermal cycling, and when cooling down after operations.

In the investigations currently being carried out, for the purposes of improving thermal barrier performance, and lifetime, promising results have been achieved with respect to nanostructured yttria stabilized zirconia coatings, fabricated by suspension plasma spraying (SPS). This innovative process allows to produce coatings, with thicknesses ranging from a few microns to several hundred microns, exhibiting a nanometer-scale microstructure. The principle involves introducing a stable suspension, acting as nanoparticles carrier, into a plasma jet, by means of a calibrated injector piece. Owing to the plasma's momentum,⁽²⁾ the incoming suspension jet is broken up into micrometer-sized droplets. Due

(2) Momentum: a quantity equal to the product of a body's mass by its velocity.



Suspension plasma spraying of ceramic nanopowders, carried out at CEA/Le Ripault.

to the high temperatures prevailing inside the plasma jet – close to 10,000 °C at the torch exit – the solvent of the droplets vaporizes, and the resulting nanoparticles are heated and accelerated during the flight phase. By modulating spraying conditions, it then becomes possible to promote the formation of dense, or porous nanostructured microstructures for the deposits (see Figure 6). Thermal diffusivity measurements, as set out in Figure 7, clearly evidence the benefit that can be gained from this type of microstructure, relative to conventional thermal barriers, fabricated from micron-sized particles.

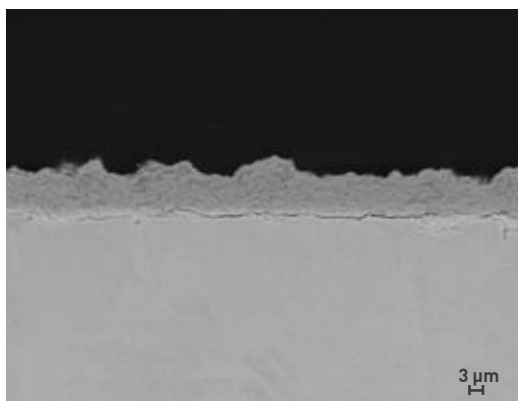
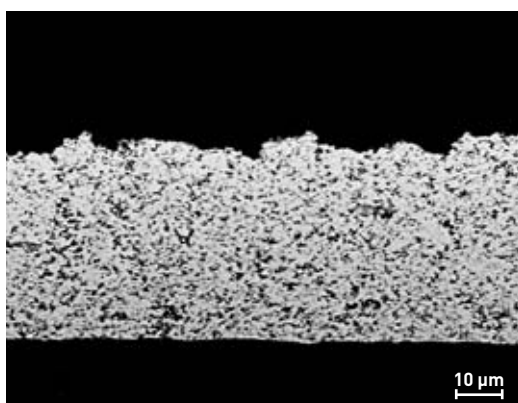


Figure 6. Yttria stabilized zirconia coatings, fabricated by suspension plasma spraying: views of polished sections, under scanning electron microscopy (top: porous microstructure; bottom: dense microstructure).

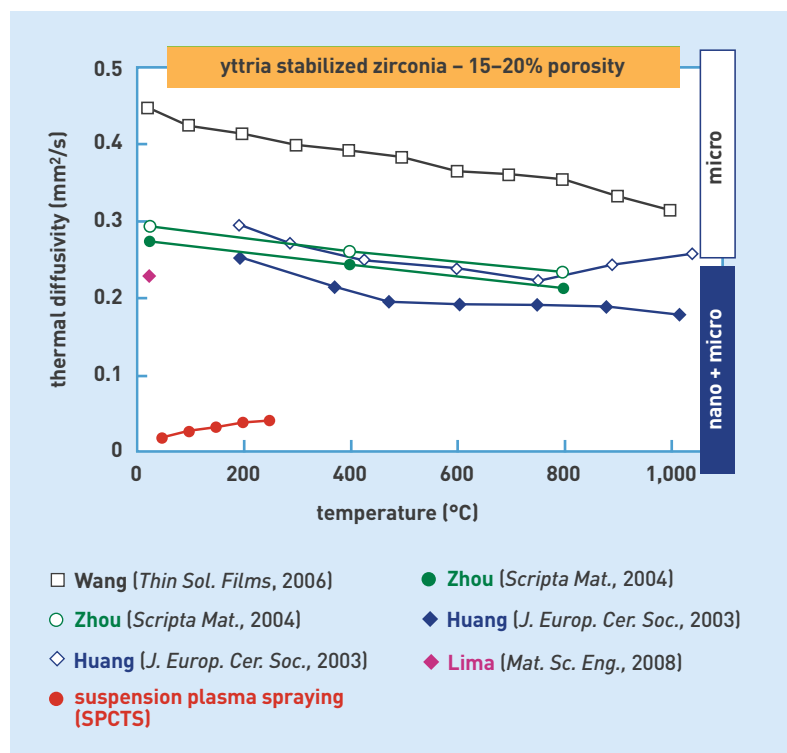


Figure 7. Comparison of thermal diffusivity in yttria stabilized zirconia deposits, as fabricated by agglomerated micro- or nanopowder spraying, with that of a deposit fabricated by suspension plasma spraying. The latter result was obtained, under the aegis of CEA's M08 corresponding research laboratory (LRC), by the SPCTS Laboratory.

Proven potential

The evolution undergone by deposition techniques has thus served to make possible the development of environmental barriers, which have become indispensable in many areas. Surface treatment processes as a whole, spray deposition and vacuum deposition processes in particular, have demonstrated their full potential as regards the fabrication of thermal barriers, diffusion barriers, corrosion-resistant barriers... The examples outlined here highlight the possibilities afforded, with regard to nanostructuring coatings, to optimize wear, oxidation, or high-temperature resistance, in demanding conditions. These materials were developed through the use of innovative technologies, lending themselves to being transferred to an industrial scale.

> Frédéric Sanchette

CEA/LERMPS Corresponding Research Laboratory
UTBM (Belfort-Montbéliard University
of Technology)

Cédric Ducros

LITEN Institute (Innovation Laboratory for
New Energy Technologies and Nanomaterials)
Technological Research Division
CEA Grenoble Center

> Karine Wittmann-Ténèze, Luc Bianchi

Materials Department
Military Applications Division
CEA Le Ripault Center

> Frédéric Schuster

"Advanced Materials" Crosscutting Program
CEA Saclay Center

The benefits of mesoporous solids for the nuclear industry

Over the past 20 years, mesoporous solids have literally pervaded the world of academic research, in the most diverse areas of chemistry and materials science. On the other hand, these materials have not, as yet, achieved a decisive breakthrough, in the field of nuclear research, even though they do afford strong potential, as materials of use not only with regard to the fuel cycle and waste conditioning, but equally for the investigation of radiation-matter interactions.

Recent advances in mesoporous materials synthesis have opened up a broad field of investigation, with regard to fuel cycles for fourth-generation nuclear reactors. Shown here, samples of mesoporous material precursors being examined.



P. Stroppa / CEA



Figure 1.
A French infantryman during the First World War, posing for the camera in the trenches, with his gasmask on: one of the first instances of the mass employment of a mesoporous solid.
<http://www.axsane.fr>

Numerous materials, present in everyday life, exhibit more or less extensive **porosity**. In the construction industry, for instance, concretes exhibit a **porosity fraction** ranging from 5% to 10%, while the baked clay used to manufacture bricks may involve a porosity value higher than 40%. The existence of such cavities is related to the fabrication techniques used, in effect owing to the removal of the water contained in these materials, as they dry out. The resulting porosity is poorly controlled. Some, more technological materials owe their functionality to their large **specific surface area**, a characteristic chemists seek to keep under close control, by acting on porosity formation. Such is the case, for instance, as regards zeolites – **crystalline ceramics** exhibiting pores smaller than 2 nm – which are used as **catalysts** in the chemical industry. Another class of materials, mesoporous solids (see Box), exhibiting porosities in the 2–50 nm range, has seen exponential growth over the past 20 years. And yet this type of material is anything but recent. Indeed, the activated carbon⁽¹⁾ pellets used in gas masks, during

World War I (see Figure 1) were already mesoporous solids. However, in the early 1990s, new synthesis methods were discovered, providing ways of obtaining mesoporous ceramics in large quantities, in perfectly controlled fashion. These scientific advances thus made it possible to bring in mesoporous systems in many fields of research, e.g. catalysis, gas detection, water decontamination... Somewhat surprisingly, the nuclear world stood relatively aloof from this veritable vogue, even though the properties exhibited by mesoporous solids turn out to be highly attractive, for the purposes of the various branches of research involved in this area.

Applications in separation chemistry

Controlling the industrial deployment of a nuclear **fuel cycle** entails, at various stages, having the ability

(1) Activated carbons: substances exhibiting a high adsorption capability, fabricated by pyrolysis from high-carbon-content substances (coal, wood...). The more volatile compounds are thereby removed, yielding a mesoporous carbon structure, with a specific surface area that may range from 300 m²/g to 1,500 m²/g.

How a mesoporous material is prepared

In the early 1970s, the **International Union of Pure and Applied Chemistry (IUPAC)**, becoming aware of the importance taken on by **porous** materials, in a great many applications, decided to classify these into three categories, as a function of pore size: **macropores** being pores with a width exceeding 50 nm, **mesopores** having a width between 2 nm and 50 nm, **micropores** a width not exceeding 2 nm. While synthesis processes to obtain both macroporous and microporous materials have been extensively investigated, the controlled preparation of ordered mesoporous materials presented far greater difficulties. A number of synthesis methods have been developed, over the past few years, the chief such methods being the use of **surfactant molecules** – namely **micelles** – as structuring agents, or templates (micelle-templated silicas [MTSs]), and the use of porous molds, likewise known as templates, in order to obtain a “negative” of the initial structure (nanocasting). MTSs, as a rule, are **silicates**, or **aluminosilicates**, yielded by condensation of an inorganic phase around an organic phase, of surfactant micelles. They may form, e.g., through the **polymerization** of silica (SiO_2) around organic, surfactant compounds. The surfactants are subsequently removed, by scrubbing, leaving in their stead pores, inside which controlled chemical, or physical reactions may then take place. The phases obtained are lamellar, hexagonal, or cubic, and pore size may be

controlled by using surfactants featuring **hydrophobic** chains of varying lengths. For instance, a chain with 8 carbon atoms will yield pores 1.8 nm wide, a chain with 16 carbon atoms pores 3.5 nm wide, when a **cationic** surfactant featuring an ammonium⁽¹⁾ head group is used. Many silica-based materials, but equally **transition-metal-oxide**-based materials – involving e.g. **titanium** oxide, TiO_2 , **zirconium** oxide, ZrO_2 , or niobium oxide, Nb_2O_5 – may thus be fabricated.

The second pathway again is based on the principle of using a template, albeit allowing a broader category of materials to be obtained, e.g. **carbons**, or transition-metal **nitrides** and **carbides**. This involves using a mesoporous matrix, consisting of a readily removable oxide (e.g. silica, or alumina [Al_2O_3]), as the template, and impregnating it e.g. with a carbon precursor, which condenses in the matrix. The template is subsequently dissolved by a chemical process, yielding a perfect inverse structure, which is porous likewise.

It is further possible to fabricate solids featuring surface functions, in the form e.g. of organic molecules, or metallic **nanoparticles**. To achieve this, such **functional** components may be **grafted**, or deposited, either during the synthesis of the porous matrix (this being the so-called “one-pot” route), or once the

porous material has been obtained (i.e. by the so-called “post-functionalization” route) (see Figure).

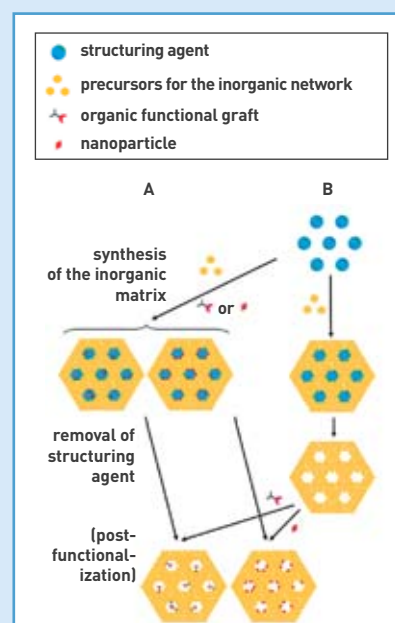


Figure. Two possible pathways, for the fabrication of a functional mesoporous solid. (A) The “one-pot” route, whereby the matrix precursor, and functional groups are mixed from the outset. (B) The “post-functionalization” route, whereby the porous matrix is synthesized in an initial step, and subsequently functionalized.

to separate **ions**, so as to be able to integrate, at a later stage, the **fissile** and **fertile** ions into the **fuel** – whether it be **uranium** extracted from mines, or recoverable **actinides** from **spent fuel** – while ensuring the **containment** of **elements** not recoverable for further use – e.g. **fission products** – and to decontaminate the resulting **effluents**, to reduce their toxicity. For the purposes of meeting the challenges set by such highly selective ion separation, in the context of what is generally referred to as **separation chemistry**, porous solids turn out to be choice materials (see Figure 2).

Actinide extraction

In 2000, a US team was the first to suggest using mesoporous silica (SiO_2) matrices, for the selective extraction of actinides from spent fuel. The hybrid, organic–inorganic extraction material selected was an organized mesoporous silica, featuring surface **functionalization** by means of quaternary ammonium groups.⁽²⁾ Extraction results, for **thorium** ions, were comparable to those achieved over conventional organic **ion-exchange resins**. At the same time, extraction selectivity, for thorium ions, relative to uranyl ions (UO_2^{2+}), was found to be higher.

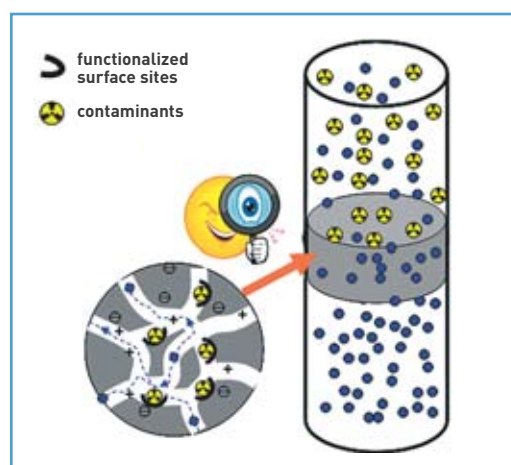


Figure 2. Operating principle of an ion separation membrane, or column. In this case, the membrane, schematically shown in gray, bears, within its porosity, a number of functionalized surface sites, serving to retain the contaminants to be removed from the effluent being decontaminated.

(2) Quaternary ammonium groups: an extensive family of chemical compounds, of general formula NR_4^+ , where N is a **nitrogen** atom, R an alkyl group (i.e. a radical obtained by stripping one **hydrogen** atom from a linear, or branched saturated **hydrocarbon** molecule).

Retention of radionuclides yielded by waste in disposal conditions

Irrespective of the **matrix** being considered, for the purposes of **radioactive waste disposal**, it may never afford optimum effectiveness for each and every ion species requiring immobilization. There will thus always be a small fraction of elements – so-called mobile elements – that will undergo early release – at the geological timescale – from the **conditioning** matrix. One solution to that problem would involve positioning, around the disposal matrix, functional mesoporous materials, having the ability to trap mobile **radionuclides**, thus precluding their diffusion into the environment. Thus, mesoporous **titanium** phosphates,⁽³⁾ fabricated by way of the techniques described in the Box, have been selected as **adsorbent** agents for such actinides as **plutonium**(IV) (Pu^{4+}), or **neptunium**(V) (Np^{5+}). Currently, mesoporous silicas, functionalized by self-organized organic groups, are being put forward for the purposes of effecting the selective **adsorption** of a wide variety of radionuclides (actinides, **lanthanides**, cesium [Cs], iodine [I]...).

Decontamination of radioactive effluents

When a fluid requires **decontamination**, in order to bring down its radiotoxicity, the solution that most readily comes to mind is to substitute the ions involved with other, less harmful ions – this is the ion-exchange concept – or to remove the unwanted ions by **precipitation**, or selective adsorption. Porous solids already stand as proven agents, as regards the ion-exchange and adsorption approaches. In some cases, a mesoporous material's chemical composition endows it with inherent extraction properties, thus requiring no further functionalization. In other cases, by contrast, it is essential that inorganic ion-exchange groups, or organic **complexants**, specific to the elements requiring extraction, be added onto the material's surface. This approach does entail, admittedly, finding adequate ion exchangers, or complexants, but it equally requires selecting the optimum substrate, to ensure effective separation in an unfavorable environment. Such substrates take

the form either of mesoporous powders, involving **grain** sizes suitable for use in column conditions, or mesoporous membranes.

Thus, a variety of mesoporous **zirconium** (Zr), tin (Sn), or cerium (Ce) **silicates** were directly tested as extraction materials, for a number of radionuclides, e.g. **molybdenum** (Mo), cesium (Cs), **strontium** (Sr), thallium (Tl)... At the same time, porous glasses, of the Vycor® type – these being disorganized mesoporous silicas, obtained by melting, controlled demixtion⁽⁴⁾ and dissolution – subsequently functionalized by means of **nickel** hexacyanoferrate ($\text{Ni}_3[\text{Fe}(\text{CN})_6]$) groups, were used as exchangers for the selective extraction of cesium.

A wide range of future applications

The emergence, over the past two decades, of mesoporous, and/or **nanostuctured** materials has thus already resulted in some positive spinoffs in the field of separation chemistry. At the same time, this opens up a much broader field of investigation, concerning all of the materials used in the nuclear sector. Apart from separation chemistry, waste conditioning, but equally the development of novel fuels and the investigation of materials subjected to intense radiation could benefit from advances made with mesoporous solids.

Mesoporous materials for the separation of radioactive elements

All of the existing instances of **radioactive** element separation, using functional mesoporous materials, rely on oxide matrices. However, these oxides exhibit limited thermal, chemical, and mechanical stability, in the operating conditions prevailing in nuclear applications (high acidity, high ionic strength,⁽⁵⁾ **irradiation**...). If such limitations are to be bypassed, ways must be found to use other matrices, e.g. **carbon**-, or **carbide**-, or **nitride**-based matrices. Of late, indeed, it has become feasible to obtain mesoporous carbon by way of a mesoporous silica replica, while **transition-metal** carbides and nitrides may be obtained through carburization, or nitridation of mesoporous oxides. New functionalization routes are being investigated, for these innovative matrices, giving grounds for their use being considered, for the purposes of radionuclide extraction, over very wide **pH**, temperature, and/or **solvent** ranges.

At the same time, irrespective of the matrix-extractant pair selected, the effectiveness, and kinetics of the ion separation effected by means of these materials are dependent on the ion transport properties prevailing within the system's porosity. Good knowledge of the physics of this transport, and appropriate **modeling**, as a function of the substrate's physicochemical properties – i.e. surface charge density, and distribution, **hydrophilic/hydrophobic** character, active site concentra-



A gas chromatograph, coupled to a **mass spectrometer** (GC-MS), serving to monitor the synthesis of organic functional grafts.

P. Stroppa / CEA

(3) Titanium phosphates: compounds of chemical formulae ATiP_2O_7 [A = sodium (Na), potassium (K), rubidium (Rb)], $\text{A}_2\text{Ti}_2(\text{PO}_4)_3$ [A = K, Rb], $\text{BaTi}_2(\text{PO}_4)_3$, $\text{Mg}_5\text{Ti}_4\text{P}_6\text{O}_{24}$.

(4) Demixtion: the spontaneous separation of a homogeneous mixture of liquids into a number of immiscible liquid phases.

(5) Ionic strength: the half-sum of the molar concentrations of all of the ion species present in a solution, each multiplied by the ion's valence number squared.



P. Stroppa / CEA

Synthesis furnaces, used for the structuring agent removal step (see Figure in Box).

tion, pore size and tortuosity... – are crucial, for the purposes of developing this type of radionuclide extraction process.

Mesoporous matrices for waste conditioning purposes

Consideration may also be given to using the self-same mesoporous matrices employed for ion extraction purposes, as waste conditioning matrices. Indeed, once the operation has been effected, whereby the ions requiring removal are adsorbed, the idea may be entertained, of selectively closing the extraction materials' porosity, to contain the radionuclides involved. With that purpose in mind, several classes of materials are being investigated:

- Vycor® glasses, these being materials that are industrially produced, at reasonable cost;
- mesoporous silicates, or **aluminosilicates**, synthesized in hydrothermal conditions (i.e. in an aqueous environment, at high temperature and pressure), which would allow incorporation – as and when required – of volatile radionuclides, e.g. iodine, or cesium, as early as the synthesis stage;
- materials exhibiting **nanometer**-scale organization (nanotubes), which could provide the ability to incorporate a wide variety of radionuclides into their structure, by confinement effects.⁽⁶⁾ **Carbon nanotubes** are the best known, however other compounds also exist, that are able to take on an organization with such a geometry (uranium compounds, **boron** nitride...).

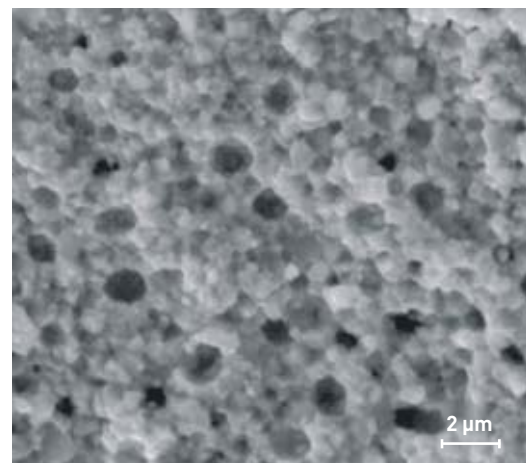
This is a promising pathway, as it involves none of the troublesome features found with conventional processes, such as **sintering**, and melting, which are carried out at high temperature – an unacceptable requirement, with regard to conditioning volatile products, as e.g. iodine, or cesium.

(6) Confinement effects: specific effects, related to the fact that, when one at least of the typical sizes involved, in a material, is very small, its physical properties are altered. For instance, bulk gold is yellow, whereas gold particles may show up in any color, depending on their size, among other parameters.

Controlling fuel porosity

Porosity is also found to be a crucial parameter, as regards the irradiation behavior of ceramic fuel, with regard, in particular, to the release of **fission gases**. The situations are somewhat different, depending on the fuel, and reactor type considered. **PWR** UO_2 (uranium dioxide) *fuel* is relatively cool. As a result, only a small fraction of the fission gases generated (< 1%) is released, up to a **burnup** of 30 **GW·d/tU**. Beyond this value, a larger fraction of fission gases (< 10%) diffuses along the **grain boundaries** in the thermally activated ceramic, and is released. In the peripheral region of the fuel **pellets**, i.e. in the cooler, less irradiated zones, the original oxide **grains** crack, and fission gases condense in the form of bubbles some 0.6 μm in diameter (see Figure 3).

Fast-reactor (FR) oxide fuel differs from PWR fuel, owing to the more severe operating conditions (higher temperature and **irradiation dose**). These conditions cause a restructuring of the ceramics,



CEA

Figure 3. **Microstructure** of the region that has undergone restructuring, as a result of irradiation, and of the thermal gradient, at the periphery of a UO_2 fuel pellet from a PWR (rim effect).

resulting in the formation of a central cavity and in the release of virtually all of the fission gases (> 90%) into the fuel **pin plenum**.

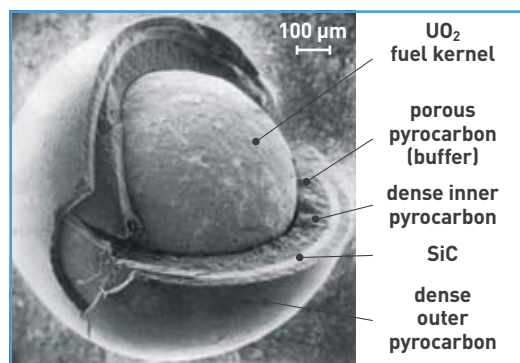
Particle fuel is another fuel concept. It is under consideration for *high- (HTRs), and very-high-temperature reactors (VHTRs)*, operating in a **thermal neutron spectrum**. Such fuel comprises a millimeter-size particle of fissile material, coated with several layers of carbon, and **refractory** compounds, of the **silicon** carbide (SiC), or zirconium carbide (ZrC) type (see Figure 4). The first coating layer may be thought of as a plenum, ensuring the retention of fission gases in its porosity. The subsequent layers have the function of providing closure for that porosity.

These examples serve to illustrate the importance of obtaining fuel that exhibits controlled porosity. All the more so, since, for **fourth-generation reactors**, actinide carbides are being considered as fuel. With this in mind, it may well be of relevance to investigate, as of now, how such carbides may be textured, to make them mesoporous.

Trapping defects in materials subjected to heavy irradiations

When a material is subjected to heavy irradiations, the size of **extended defects** (**point defect** clusters, **dislocation loops**) – related to the number of induced **displacements per atom (dpa)** – stands at around 1 nanometer, a size comparable to that of the **crystallites**, in a nano-organized material. The use of nano-organized materials may thus be seen as a promising avenue, to channel such defects. The interfaces would act as defect traps, bringing down the stresses generated by irradiations. One illustration for this argument is shown in Figure 5, where irradiated regions featuring nanometer-size grains undergo no **amorphization**, by contrast with those involving **micrometer-scale crystallites**.

Figure 4. Fractograph of a TRISO fuel particle, comprising a kernel of UO_2 fissile material, coated with four successive layers: porous **pyrocarbon**, dense pyrocarbon, SiC, dense pyrocarbon.



Observation of the microstructure, and composition control by **scanning electron microscopy (SEM)**, coupled with chemical analysis (**X-ray fluorescence**).

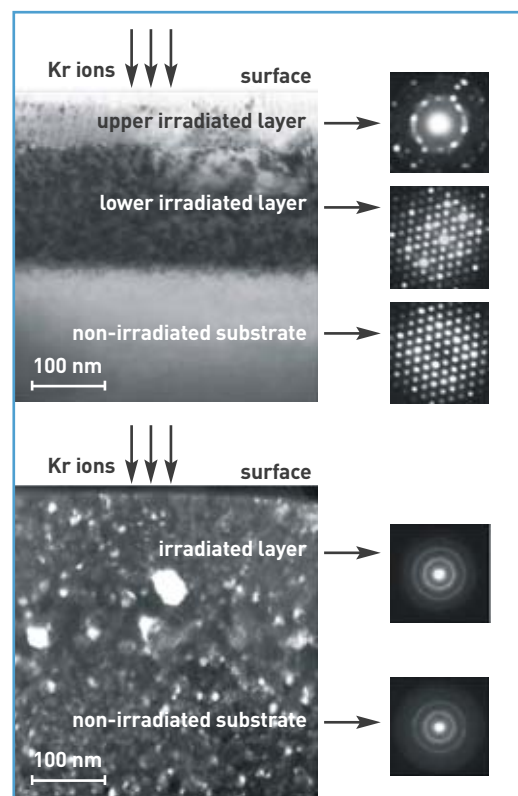
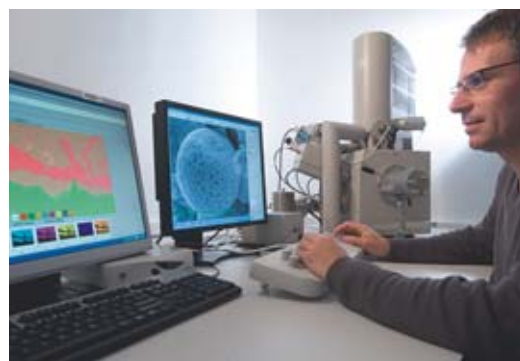


Figure 5. **Transmission electron microscopy** images, coupled with **diffraction** images, of MgGa_2O_4 materials featuring nanometer-size grains (top), and micrometer-size grains (bottom), irradiated with 300-keV krypton ions (Kr^{2+}). (Reproduced, with permission, from Tong D. SHEN, Shihai FENG, Ming TANG, James A. VALDEZ, Yongqiang WANG, and Kurt E. SICKAFUS, "Enhanced radiation tolerance in nanocrystalline MgGa_2O_4 ", *Applied Physics Letter* 90, 263115 (2007). © 2007, American Institute of Physics.)

Investigations of radiation-matter interactions

Concurrently, our understanding of radiation-matter interactions may be put to advantage, to look into radiation-induced reactions at the surface of mesoporous materials, or at the interfaces arising within meso-organized materials (e.g. in **graphite-oxide** hybrid materials). These thus stand as choice materials for the investigation of interactions at interfaces, e.g. **atom** migration, and for the determination of sensitivity thresholds, for the purposes of effecting radiation-induced chemical reactions, as e.g. SiC synthesis at the silicon-graphite interface.

The achievements, and prospects outlined in the present paper are in no way an attempt to provide an exhaustive overview; rather, their aim is to show that mesoporous materials have a place of their own, in the range of materials of interest, for the nuclear industry.

> **Xavier Deschanel, Frédéric Goettmann, Guillaume Toquer, Philippe Makowski and Agnès Grandjean**

Marcoule Separation Chemistry Institute (ICSM)
Joint CEA-CNRS-UM2-ENSCM Research Unit
Nanomaterials and Energy Laboratory
Valrhô-Marcoule Site

SURFACE EXPLORATION

Atomic-force microscopy: a powerful, multipurpose technique for the investigation of materials

Devised in the 1980s, local-probe microscopy techniques, such as [scanning tunneling microscopy \(STM\)](#), or [atomic-force microscopy \(AFM\)](#), yield unique information as to the surfaces of a wide variety of materials. The typical surface area explored by way of these techniques ranges from $2 \times 2 \text{ nm}^2$ to $100 \times 100 \text{ }\mu\text{m}^2$, in such diverse environments as air, vacuum, or a liquid, and at temperatures ranging from a few [millikelvins \(mK\)](#) to 1,000 K. Aside from these – anything but restrictive – experimental conditions, the advantage afforded by such instruments, for the purposes of materials science, is that they yield information as to topography, at scales comparable to those that can be attained by various types of [simulation](#). In particular, [atomic models](#) may be directly compared with experimental findings, since these microscopy techniques allow atomic [resolution](#) to be achieved. Further, as microscopists are

thus able to access topography in real space, these new techniques prove extremely powerful, for the purposes of investigating superficial defects. As regards AFM, this is supplemented by the ability to map variations in a local property, specific to the sample examined (whether electrical, magnetic, thermal...), at the same time as its topography is ascertained.

What is the operating principle of an AFM?

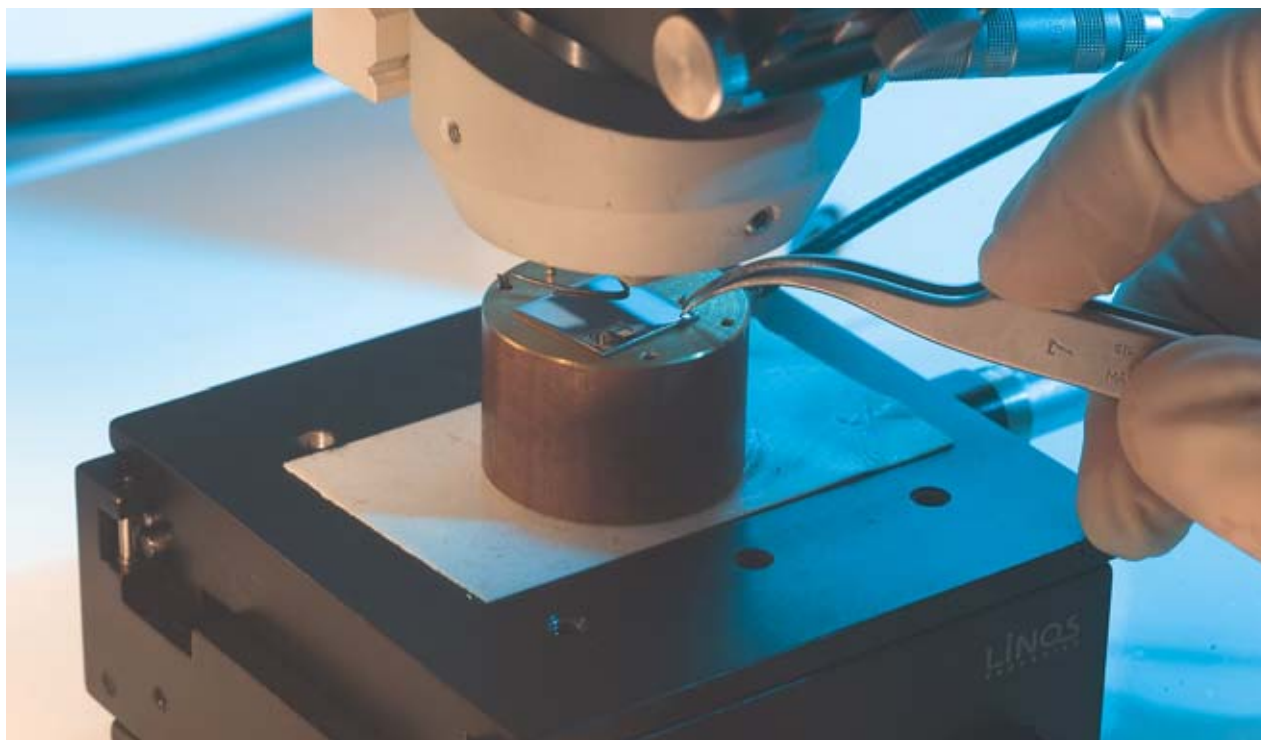
An atomic-force microscope comprises a probe (a tip) mounted at the free extremity of a spring of known stiffness, a control system, and a scanning system, which moves the probe across the sample's surface. The interaction between probe and surface (forces, or force gradient) is kept equal to a set value, by continuously adjusting the separation distance, via a feedback loop. An AFM image thus corresponds to a constant-interaction contour, obtained by

moving the tip along the surface. This contour matches, as a rule, the topography of the sample – which may be an insulator, or [conductor](#) material.⁽¹⁾ The contribution made by AFM to materials science is illustrated, in the following paragraphs, by way of a number of examples.

Observation of defects associated to irradiation of a crystal

The first example concerns the first observations of [irradiation](#) damage in an electrical insulator material, thus one not readily observable by means of conventional electron microscopes (be it a [transmission \[TEM\]](#), or [scanning electron microscope \[SEM\]](#)). As early as 1991, [defects](#) generated by high-energy [heavy ions](#), accelerated at France's GANIL (Grand

(1) For a fuller description of an AFM, see "Local-probe microscopy: contact and manipulation", *Clefs CEA* No. 52, Summer 2005, pp. 91–95.



P. Stroppa / CEA

Atomic-force microscope (AFM), set up at the Surface and Interface Physics and Chemistry Service, at CEA/Saclay. This tool – at the same time a simple, and multipurpose instrument – makes it possible to explore the surface of all and every type of material, to a high resolution.

SURFACE EXPLORATION

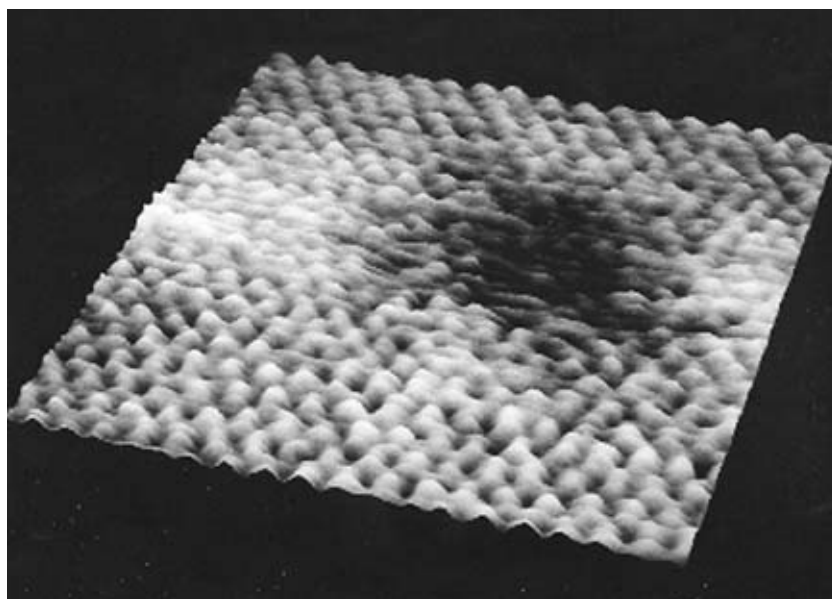


Figure 1.

Three-dimensional image of a cleavage surface of muscovite mica, through which a swift krypton ion has passed. The periodic structure observed in the lower part of the image corresponds to the crystal lattice of muscovite (period: 0.52 nm). The trace of the ion's passage is seen as a darkened, nonperiodic region, "softer," with respect to the AFM tip, than the part of the surface unaffected by irradiation. The Z-axis dynamics, i.e. the distance between the lowest, and the highest point, is equal to 1 nm. (F. THIBAUDAU, J. COUSTY, E. BALANZAT and S. BOUFFARD, "Atomic-force-microscopy observations of tracks induced by swift Kr ions in mica", *Phys. Rev. Lett.* 67 (1991), pp. 1582–1585).

Accélérateur National d'Ions Lourds: National Large Heavy-Ion Accelerator] facility, in a sample of muscovite mica,^[2] were investigated by AFM. Figure 1 shows a typical high-resolution image. The surface left undisturbed by the ion exhibits a periodic relief pattern (parameter: 0.52 nm), corresponding to the crystal lattice along the cleavage plane. The mark of the passage of a swift krypton-84 (⁸⁴Kr) ion (34.5 MeV/amu) through the material shows up in the form of a region where the periodic structure has vanished. This image thus provides a direct insight into the damage caused, in the crystal, by the passage of an ion.

Monitoring the emergence of defects due to plastic deformation in a metal

The second illustration relates to the plastic deformation observed in metals. It is known that a metal, when subjected to increasing tensile stress, deforms in elastic fashion (reversible elongation), and subsequently in a plastic manner (irreversible deformation). Such permanent elongation is the outcome of the formation, and displacement of line defects, known as dislocations. For many years now, dislocations in crystals have been targeted by TEM investigations, this involving complex prior

preparation of the sample [thin section]. By contrast, using AFM, the deformation of a bulk sample may be monitored, by way of the emergence of dislocations at the free surface of the sample, and likewise the evolution kinetics of these dislocations (number, density, cross-slips...). Figure 2 shows the morphological alteration, at the

polished surface of a two-phase stainless steel, consisting of austenite and ferrite grains, when it is subjected to traction. In the first stages of plastic deformation, parallel lines appear in the grains of the austenitic phase. These lines correspond to the relief associated to the emergence of dislocations, slipping along {111} planes within these grains. As the deformation rate increases, dislocation density rises inside the austenite grains, and the ferrite grains begin to undergo deformation. Thus, a detailed description of the deformation undergone by a bulk sample may be arrived at, at the nanometer scale. It becomes feasible to determine the evolution kinetics of emerging dislocations, in the ambient atmosphere, in a liquid, even in a corrosive medium, with the ability to observe *in situ* the defects generated.

Characterization of the electrical properties of an insulating layer covering a metal

The third example serves as an illustration of the capability afforded by AFM, of ensuring the acquisition of two types of information. Using an AFM fitted with a special module, the electrical resistivity of the passive layer that covers the surface of stainless steels was measured, concur-

(2) Micas are minerals consisting chiefly of aluminum and potassium silicates. Muscovite, having the formula $KAl_2(Si_3Al)O_{10}(OH,F)_2$, is a silvery mineral of the mica group, readily cleaved into laminae.

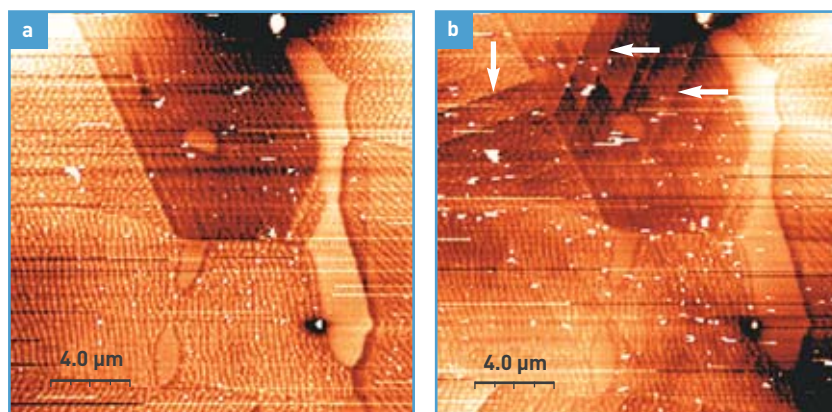


Figure 2.

Topographies, obtained by AFM, of the surface of a two-phase stainless steel sample, subjected to plastic deformation. (a) Prior to deformation. The clear domains correspond to ferrite grains. The superficial nanostructuring, due to polishing, makes it possible to make out the various austenite grains. (b) After deformation. Parallel lines may be seen in the austenite grains (arrowed). Each line corresponds to the emergence of several dislocations. The density of emergent dislocations rises with the deformation rate.

(Reproduced from S. FRÉCHARD, F. MARTIN, C. CLÉMENT and J. COUSTY, "AFM and EBSD combined studies of plastic deformation in a duplex stainless steel", *Materials Science and Engineering: A*, vol. 418, No. 1–2 (2006), pp. 312–319. © 2005, Elsevier, with permission from the publisher.)

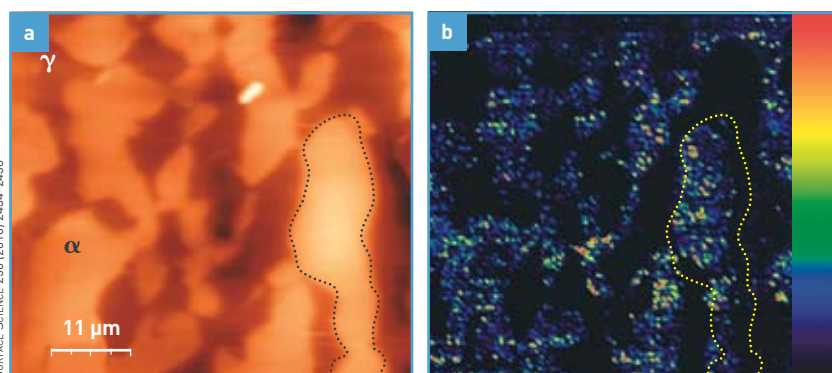


Figure 3. Topography and local electric characterization of the passive layer covering austenite and ferrite grains, in a two-phase stainless steel. (a) Topography of the surface. The ferrite grains, one of which is delineated with a dotted line, show up as clear regions (α -domains). (b) Cartography of electrical conductivity across the passive layer protecting both phases. The passive layer, where it covers ferrite grains, clearly exhibits strong variations in conductivity, as evidenced by the selfsame ferrite grain. By contrast, the passive layer covering austenite (γ -phase) grains is found to be homogeneous and an insulator. The current dynamics is indicated by the color scale, ranging from 0.1 nA (black) through to 8 nA (red).

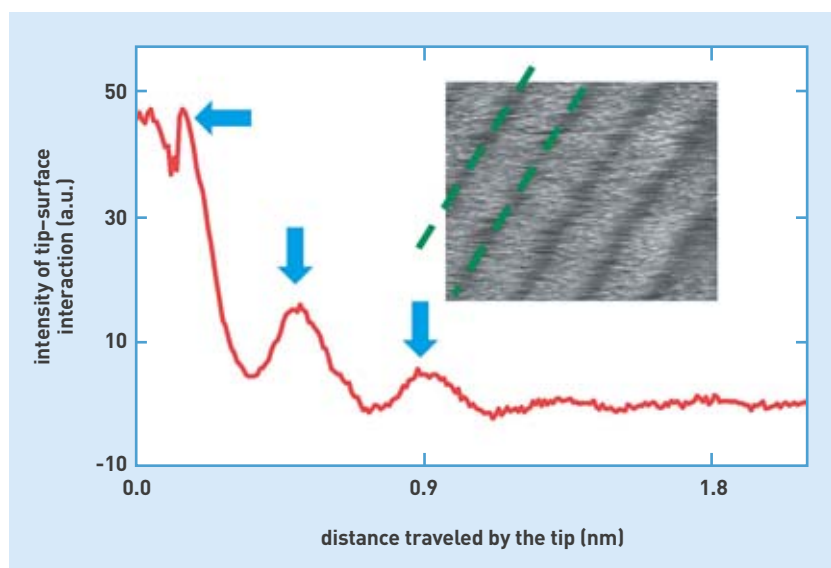


Figure 4. Structuring of molecular density in a liquid, in the vicinity of a solid. The curve plots the variation in intensity of the tip-surface interaction, related to hexadecane ($C_{16}H_{34}$) density, as a function of the distance between the apex of the AFM tip, and the graphite surface. Each peak (arrowed in blue) corresponds to a high molecular density, due to this structuring. The AFM image evidences the lamellar arrangement of the self-assembled hexadecane layer, across the graphite's cleavage surface. The width of a lamella (the distance between two green lines) corresponds to the length of one molecule (2.4 nm).

rently with the sample's topography. It is this thin oxide-hydroxide layer which protects these alloys, rendering them not readily oxidizable. In this setup, the tip acts as a conductor, while the metal sample is

polarized by means of a voltage $|V| < 3$ V. The intensity of the current circulating between these two electrodes is measured at every point of the topographical image. Figure 3 shows the two images obtained, over the same region of the freshly prepared sample. It was found that the passive layer, covering both phases as it does, exhibits quite diverse resistive

properties. Where it lies over austenite grains, the covering exhibits very high resistivity, at a remarkably constant value. By contrast, the passive layer protecting ferrite grains shows a wide dispersion in its local resistivity. After aging in the ambient environment for 3 months, the resistivity of the passive layer, where it covers ferrite, became less heterogeneous, while still exhibiting a number of fairly conducting regions. The nature of these heterogeneities, probably causing the initiation of pitting corrosion,^[3] is currently in the process of being identified.

Visualization of the arrangement of molecules at a liquid-solid interface

The final illustration concerns the three-dimensional self-organization of molecules at the interface between a solid and a liquid. In a standing liquid, molecular density remains constant over a long time, relative to the time interval between two successive encounters by neighboring molecules. On the other hand, the presence of a wall causes a local modification in this density, as shown by molecular dynamics simulations. In that case, density exhibits oscillations, dependent on the distance to the wall, associated to partial ordering of the molecules. AFM exploration of the interface between hexadecane ($C_{16}H_{34}$), and graphite evidenced two remarkable findings. On the one hand, periodic oscillations in molecular density are observed, as the distance between tip and surface decreases (see Figure 4), in agreement with the results from simulations. And, on the other hand, the molecular layer that comes into contact with graphite consists of a compact arrangement of self-assembled molecules, exhibiting a lamellar structure (two-dimensional crystal). Molecular disorder, in the other layers, rises as distance from the wall increases. AFM thus allows a three-dimensional description to be arrived at, of a liquid-solid interface. As a result, this technique does seem altogether suitable for the *in-situ* exploration of biological samples.

> **Jacques Cousty**

Radiation-Matter Institute, Saclay (IRAMIS)
Physical Sciences Division
CEA Saclay Center

(3) Pitting corrosion: localized corrosion, taking the form of the emergence of cavities, or pits, growing into the material from the surface down.



II. DEDICATED MATERIALS FOR NEW ENERGY TECHNOLOGIES

France is reassessing its energy strategy, in the light of concerns for energy security, and the effects of climate change. New energy technologies (NETs) are pointing the way to highly promising production, and consumption modes, involving the development of already existing processes, or the deployment of new energy carriers, such as hydrogen. In this context, CEA's strong commitment in the fields of electrically powered transportation, and solar energy has led it to face several challenges, arising in the area of materials. Flagship projects include the development of automotive electric powertrain, coupled to high-performance storage batteries, or hydrogen-powered fuel cells – a project that entails developing means of hydrogen production, and storage. As regards the storage of electrical energy, Li-ion technology currently affords the best performance levels, albeit still requesting further optimization, in terms of power, and energy density, if it is to be used in land transportation applications. This has led to the emergence of novel materials, as regards both electrode materials, and electrolytes, while complying with stringent constraints, in terms of cost, and safety. At the same time, the production of electricity from hydrogen, and oxygen, using a proton-exchange membrane fuel cell (PEMFC), operating at low temperature, involves numerous transfer mechanisms within a range of diverse materials. The deployment of such complex systems for transportation purposes requires innovative materials be developed, especially catalysts, or components of the membrane/active layer/gas diffusion layer assembly, forming the core of the fuel cell – such advanced materials will make it possible to achieve cost reductions, and extend fuel cell lifetime. Finally, CEA is developing a fiber-reinforced composite material, which, combined with a polymer liner to ensure gas-tightness, may serve for the manufacturing of compressed hydrogen storage tanks, operating at a pressure of 700 bars. The further issue arises, of hydrogen production, to be met by the high-temperature electrolysis (HTE) of steam, involving a system that produces the splitting of water molecules through the combined application of heat, and electricity. The stack of ceramic cores, and metal plates, operating as it does at high temperatures, is subjected to thermomechanical stresses, and corrosion phenomena, calling for leading-edge research efforts as regards the constituent materials.

Finally, as regards solar energy, CEA is conducting research efforts in both fields of thermal energy (i.e. the conversion of sunlight into heat), and photovoltaic energy (i.e. the conversion of sunlight into electricity). This last domain has to face stronger challenges, and, thus, will be the only one covered in the following pages. At the present time, the dedicated technologies related to the various types of photovoltaic cell exhibit varying levels of maturity, and are directed to different markets, depending on their performance (conversion efficiency), and cost. CEA is committed to supporting France's drive to secure a diversification of energy sources, to ensure the sustainability of energy supplies. Some 250 research scientists, engineers, and technicians at LITEN, in collaboration with all of the other expertise centers at CEA, are fully engaged in these R&D programs.

► **Hélène Burlet**

LITEN Institute (Innovation Laboratory
for New Energy Technologies and Nanomaterials)
Technological Research Division
CEA Grenoble Center

PEM fuel cells: a highly convincing solution

Intended as they are, primarily, for vehicle-mounted applications – automotive applications, in particular – **PEM fuel cells needs must look to a reduction in costs, and bulk, while achieving enhanced durability, and performance, in a highly competitive international context.** The challenge is indeed worth taking up, since, with regard to the current trend, for a diversification of clean primary energy sources, PEM fuel cells provide a highly convincing solution.

The GENEPAC
(Générateur électrique
à pile à combustible:
Fuel-Cell Electric
Generator) fuel cell,
developed by CEA, in
partnership with PSA
Peugeot Citroën, for a
forthcoming automotive
application.



Devised by British physicist Sir William Grove as early as 1839, the fuel cell's operating principle remained that of a laboratory device, up to the 1960s. Rescued from oblivion by the rise of the space programs, in which context it was used as an electric power generator, the fuel cell now stands as an effective solution, with regard to the policies being implemented, to curb **greenhouse gases**, and to promote the development of alternative forms of energy to petroleum-, natural gas-, and coal-based energies. Five main types of fuel cell currently share the market, one of these being the **proton** exchange membrane fuel cell (PEMFC). This type of fuel cell, based on the use of a proton exchange membrane, is more particularly dedicated to employment in electric vehicles, and consumer electronics.

A multiscale, multiphysics, multimaterial system

As to its principle, the PEM fuel cell may be defined as an **electrochemical** device, having the ability to convert into electrical energy the chemical energy contained in **hydrogen**, and oxygen (see Figure 1). Aside from delivering electricity, this type of fuel cell affords the additional benefit of yielding no further byproducts but heat, and water. It is thus a nonpol-

luting system, standing as a serious alternative to present-day heat engines.

As regards its configuration, the PEM fuel cell takes the form of a stack of basic fuel cells (see Figure 2), each comprising an **electrolyte**, and two **electrodes**: one anode, and one cathode, supplied with reactant gases by means of gas distribution manifolds, with may be either **porous** (foams), or involve channels (stamped metal plates, or molded graphite/polymer composite).

- The electrolyte consists of a **polymer** membrane, which has a twofold purpose: on the one hand, it ensures proton transport, from the anode to the cathode, where reactions take place, respectively, of hydrogen **oxidation**, and **oxygen reduction**; and, on the other hand, it serves to preclude transfers of electrons, and gases between anode, and cathode. At the present time, the materials exhibiting the best performance are polymers, albeit requiring to be kept sufficiently hydrated, if they are to fulfill their assigned role as proton conductors; moreover, they are unable to function at temperatures higher than 100 °C.

- The electrodes, in turn, involve two components. First, an active layer, within which the electrochemical reactions take place, consisting of **carbon** grains (to ensure **electron** transfer), onto the surface

of which the catalyst, in the form of platinum particles, is deposited (this being indispensable to ensure the electrochemical reactions occur), coated with an **electrolyte** (as a rule identical to that of the membrane, to effect proton transport). Once dry, this layer becomes porous, thus allowing gas transport. A second, **carbon-fiber**-based layer, known as the gas diffusion layer, forms a porous, carbon-fiber-base medium, fulfilling a number of roles: ensuring a homogeneous gas supply to the active layer, effecting water and heat removal, and collecting electrons (see Figures 1, 2).

Owing to the multiplicity of components involved, the basic cell, in a PEM fuel cell, is characterized by a wide diversity of geometrical scales: a few hundred square centimeters (cm^2) as regards the components' surface area, 5–200 μm as regards thickness, 10 nm –1 μm pore diameter in the active, and gas diffusion layers, 30–50 nm as regards carbon grain size, 2–5 nm for the catalyst grains (see Figure 3). The catalyst accounts for a large part of a PEM fuel cell's total cost: employment of this substance therefore calls for optimization.

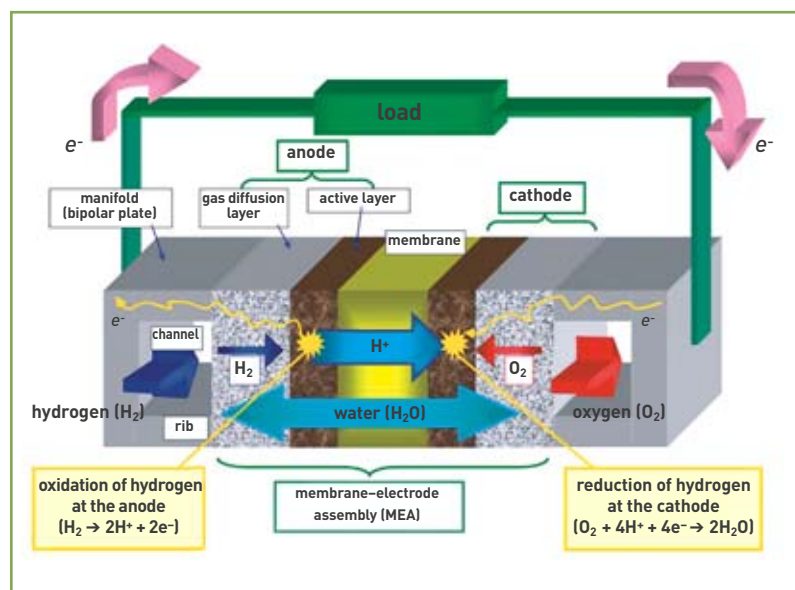


Figure 1.
Principle schematic of a basic cell, in a fuel cell of the PEMFC type.

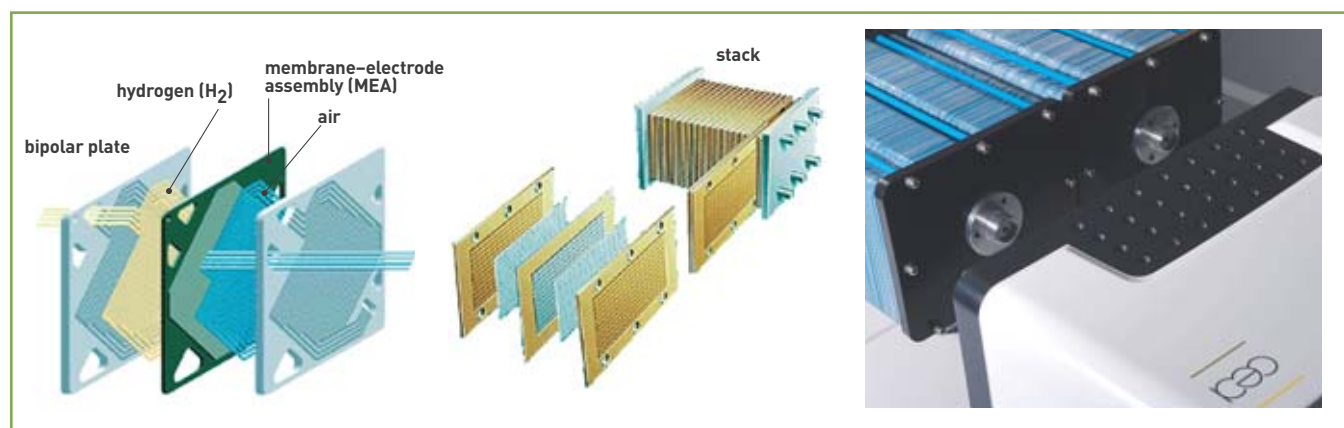


Figure 2.
Construction of a PEM-type fuel cell involves building up a stack of basic cells (left panel). Each cell comprises two bipolar plates (serving to effect gas distribution, along the channels they feature, and the collection of electric current), and one component known as the membrane-electrode assembly (MEA), corresponding, in this case, to the anode/membrane/cathode stack. CEA, working with PSA Peugeot Citroën, under the aegis of the GENEPAC (Générateur électrique à pile à combustible: Fuel-Cell Electric Generator) program, has developed an 80-kW fuel cell for an automotive application (right panel).

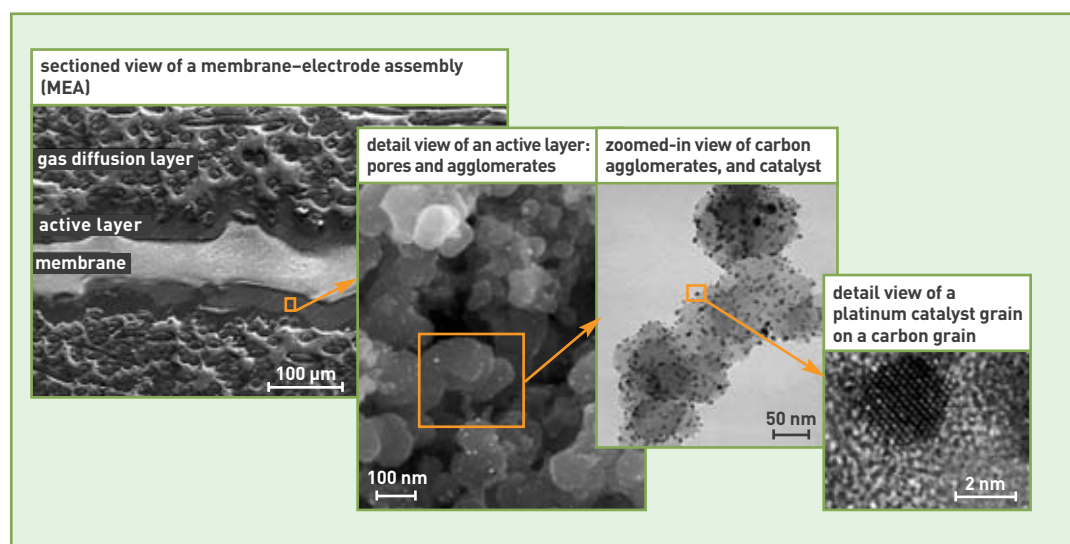
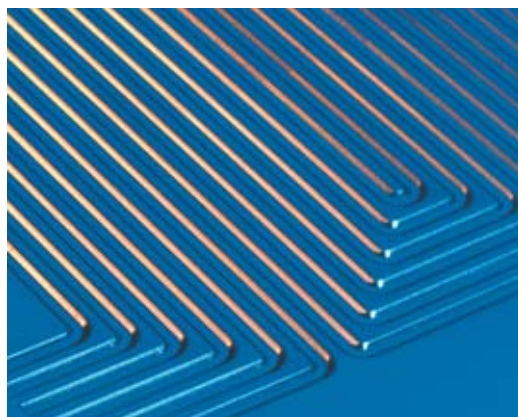


Figure 3.
A membrane-electrode assembly (MEA), as seen under electron microscopy, and detail view of an active layer, showing the various physical scales involved.



D. Michon/Artechnique/CEA

A stamped-metal bipolar plate. The surface corrugation (channels) allows hydrogen, or oxygen (or air) to be supplied, on the other side of the plate. A cooling fluid is circulated between the two back-to-back stamped-metal manifolds. By comparison with conventional machined graphite plates, stamped-metal bipolar plates result in considerable savings, in terms of mass, and volume, improved homogeneity, in terms of temperature, and costs lowered by a factor of 100, allowing their use to be contemplated for automotive purposes.

If they are to be deployed, fuel cells of the PEMFC type needs must first meet a number of constraints. Indeed, it should be borne in mind that the various materials employed to fabricate the components of such a fuel cell involve a number of multiscale, multi-physics couplings: for instance, the transfer of gaseous species (through [convection](#), and [diffusion](#)), in single- and/or two-phase mode (capillarity effects), heat transfers (diffusion, evaporation/[condensation](#)), charge transfers (be they electron, or proton charges, or electrochemical...). It is thus a requisite, that the various materials employed for the fuel cell components afford the ability to effect these diverse transfers. The fuel cell's proper operation is thus dependent on the properties, and stability over time exhibited by the various components, and

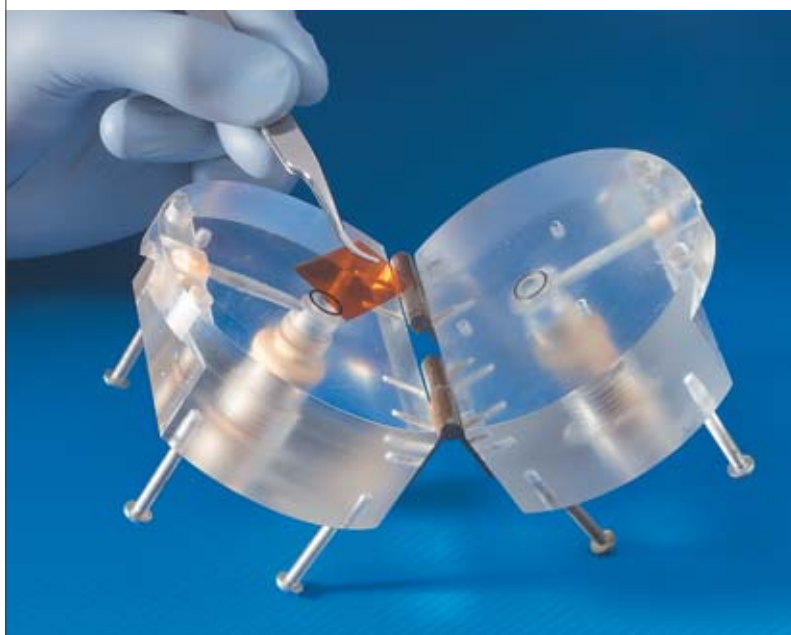
equally on the methods used for their assembly (distribution of the constituents involved, contact resistances arising at the various interfaces). CEA, working in partnership with [PSA Peugeot Citroën](#), under the aegis of the GENEPAC (Générateur électrique à pile à combustible: Fuel-Cell Electric Generator) and FiSyPAC (Fiabilisation système pile à combustible: Fuel Cell Systems Reliability) programs, constructed a fuel cell which ranks, to date, as a world leader, with regard to mass (kW/kg), and bulk (kW/liter) criteria – key criteria, with respect to automotive applications (see Figure 2). The challenges following on from this, set to researchers, and engineers, presently involve bringing down costs, and extending PEMFC lifetime, bearing in mind that the specifications, as regards this automotive application, rank among those entailing the most stringent constraints (numerous transients, cyclings, stop/go, pollution...).

The electrolyte membrane: a component not easily stabilized, in chemical or mechanical terms

In a PEM fuel cell, the electrolyte membrane fulfills the twofold purpose of effecting proton transport, from the anode to the cathode, while partitioning off electrons, and gases, between the anode, and cathode compartments.

Currently, the membranes used, in virtually all fuel cells of this type, involve polymers featuring a similar chemical structure: a [hydrophobic perfluorocarbon](#) polymer skeleton (of the [Teflon®](#) type), along which are positioned, in statistical fashion, pendant chains, terminating in a highly [hydrophilic](#) sulfonic acid (SO_3H) group, ensuring proton conductivity. [Nafion®](#), a compound coming under this family of polymers, has already made it possible to fabricate an initial type of strong, flexible electrolyte, exhibiting fairly high performance, and good stability (see Figure 4). Developed in the early 1960s by [Dupont de Nemours](#) Corporation, this material allowed a significant advance to be achieved in PEMFC technology, in particular through improved performance levels, due to enhanced proton conductivity, but equally owing to its superior chemical stability, ensuring increased lifetimes. This compound's chemical composition results in a peculiar physical structure, characterized by a phase separation, at the nanometer scale, between the hydrophobic domains, comprising the polymer chains, and the hydrophilic domains, holding the proton-donor groups, and absorbed water (see Figure 4). Although its development goes back some 50 years now, Nafion® nonetheless still stands as an inescapable reference, notwithstanding the many research efforts conducted, over the past 20 years, for the purposes of finding an alternative, affording an ability to overcome its drawbacks.

At the present time, continued membrane development entails that a series of barriers first be overcome. First, the high production costs involved, owing to the [fluorine](#) chemistry called for ([corrosion](#), safety). Second, the fact that these membranes must be kept moist, by means of the gases used, if they are to exhibit satisfactory proton [conductivity](#). However, an issue arises at temperatures exceeding 80 °C – i.e.,



D. Michon/Artechnique/CEA

A fuel-cell membrane. Shown here, a mercury-electrode fuel cell, used for the determination of ion conductivity in polymer membranes, by impedance spectrometry.

in the temperature range required, if such fuel cells are to be used for transportation purposes: at that temperature level, all of the mechanical properties exhibited by the membrane fall off sharply, owing to decreased interactions between the polymer chains. The other issue that must be resolved arises as a result of fuel cell operating conditions, these proving at the same time strongly oxidizing at the cathode, and strongly reducing at the anode, this resulting in alterations in chemical composition. Further, owing to its hydrophilic character, the membrane is able to absorb water by as much as 40% of its own volume: as a result, as there is an alternation of drying, and hydration phases over the fuel cell's operation, the membrane is subjected to cyclical variations in its dimensions, liable to cause it to rupture. Finally, it should be emphasized that, while performance degradation does in some cases result from alterations in all of the components, fuel cell stoppage is invariably due to piercing of the membrane, causing the reactants to mix, along with the concomitant hazards (heating up, explosion, in particular). Membrane degradation thus stands as a critical point, as regards PEM fuel cell operation.

Many advances therefore have yet to be made, if the membranes' performance, along with their chemical, and mechanical stability are to be improved, with a view to an application for transportation purposes. New avenues for research are directed to achieving improved control of the membrane's structure, this involving separating its mechanical, and transport properties. This process is already implemented, as regards the organic-inorganic composites developed by CEA's Military Applications Divisions (DAM), or the interpenetrating polymer networks (IPNs) developed at LITEN. This results in restricting membrane swelling, while ensuring adequate water retention at high temperature, making for enhanced proton conductivity. The new composite membranes obtained by the former route stand apart, in terms of their composition: functionalized inorganic particles, dispersed within a neutral polymer matrix, that is more widely available, cheaper, and more easily prepared for use. The advantage they bring is their lower fabrication cost. One difficulty has yet to be resolved, however, namely that of controlling charge dispersion within the organic matrix, with which charges undergo little interaction: the aim being to ensure charge percolation, while precluding their elution, in the presence of water.



A small-angle X-ray scattering camera, used for the investigation of fuel-cell membrane structures, at the nanometer scale.

The other avenue for development concerns IPN membranes, the principle for which involves bringing together two interlaced, but independent polymer networks. The first of these networks, a fluoro-carbon, endows the membrane with its chemical, and mechanical stability, while the second network promotes proton conductivity. The interpenetration of the two networks ensures outstanding mechanical, and chemical stability, since, even in the event of a possible degradation of the proton-conducting polymer, no rupture ensues in the membrane. The difficulty of designing such membranes is that of achieving both monomer synthesis, and control of the polymerization parameters, to ensure phase separation at the nanometer scale.

How are active layers, and catalysts to be structured?

At the core of the fuel cell, another region of strategic importance is to be found in the active layers, these being host to the electrochemical reactions that are indispensable, if the system's power requirements are to be met. These active layers consist of catalytic mate-

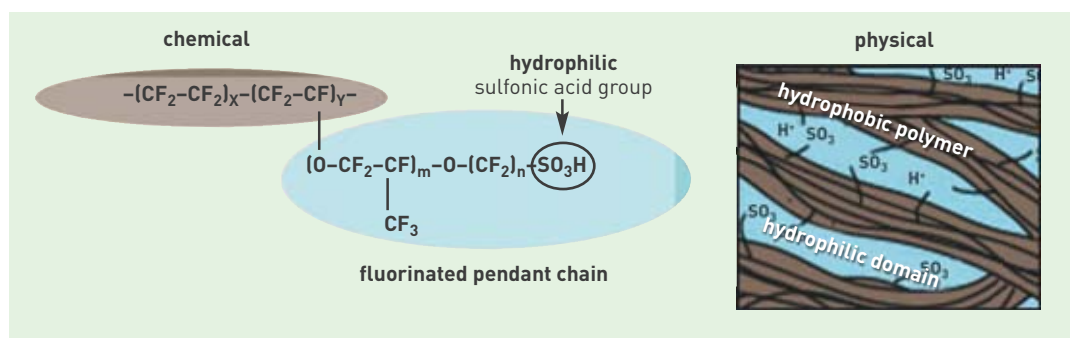


Figure 4.
The physical, and chemical structure of Nafion®.

rials, positioned on either side of the proton-exchange membrane. Now, lying in the immediate vicinity of the membrane entails extreme operating conditions, in terms of acidity, resulting in rapid **corrosion** of the materials involved. These electrodes must thus be made of materials that remain stable, in an acidic environment. This requisite rules out transition metals (**Fe, Co, Ni, Cr**), as catalysts for the electrochemical reactions. In practice, only platinum provides sufficient catalytic ability to achieve appreciable performance, however this is an expensive element, owing to its scarcity. Current fuel cells contain, as a rule, nearly 1 gram platinum per kilowatt (kW) electric power generated. Platinum alone accounts, nowadays, for half of the fuel cell's cost. It is thus crucial that a reduction be achieved, in the amounts of this material required, while ensuring its performance is optimized. In order to arrive at an economic break-even point for fuel cells, CEA is seeking to bring down the quantity of platinum required to 0.1 g_{Pt}/kW. The solution involves structuring the active layer, and/or the materials it is made of. Bearing in mind that electrochemical reactions occur at the surface of the catalytic materials, the first step involves bringing down the platinum particles' size, to increase the surface area/volume ratio, and restrict the amount of inactive platinum, at the core of these particles: the optimum diameter, for spherical **nanoparticles**, to ensure oxygen reduction, stands at 3–5 nm. Second, the platinum particles lying at the surface of the carbon grains – serving to ensure electron transfers – are to be supplemented with a proton-conducting **ionomer**. For what purpose? To ensure there is no break in proton conduction, between the two electrodes. Other investigations, currently ongoing at LITEN, are endeavoring to stimulate all manner of species transport, to and from the active sites. For this type of catalytic material, the positioning of platinum/carbon components, and of the ionomer electrolyte is effected by a printing technique: a mixture of powders is suspended in a liquid, acting as an ink. The most recent advances, in this respect, and the potential for optimization they afford, chiefly concern improvements to deposition



Coating bench for PEM fuel-cell active layers. A membrane is being coated with an ink consisting of platinum/carbon, and electrolyte particles.

D. Michon / Artechnique / CEA

processes for such inks. Large-scale production entails mastering such printing techniques as ink-jet, screen, or microspray... The aim is to improve the materials' relative distribution, or even to achieve controlled gradients, across the bulk of the material, to ensure **functionalization** of the layer, at various scales.

Concurrently with their work on structuring the active layer, researchers at CEA are also looking into structuring the catalyst itself – in particular, by modifying the shape of the particles positioned at the surface of the carbon grains, or by exploring novel structural concepts, integrating all of the functions required (see Figure 5).

In coming years, multimetallic materials involving transition metals may provide substitutes, in part, for platinum. Thus, the electrocatalytic performance of particles of bimetallic catalysts, involving platinum alloyed with other, less expensive metals, e.g. cobalt, nickel, or **palladium**, make it possible to substantially reduce the amount of platinum required, while affording increased stability, and improved performance. The other, highly promising avenue being explored involves the use of catalysts analogous to those active in certain living organisms – for instance, iron-based catalysts to ensure oxygen reduction, or nickel-based catalysts for hydrogen oxidation. Highly promising results have been achieved recently by CEA teams, working at the Radiation-Matter Institute, Saclay (IRAMIS: Institut rayonnement-matière de Saclay), at the Research Institute for Life Sciences and Technologies (iRTSV: Institut de recherche en technologies et sciences pour le vivant), at the Innovation Laboratory for New Energy Technologies and Nanomaterials (LITEN: Laboratoire d'innovation pour les technologies des énergies nouvelles et les nanomatériaux), and at the **Collège de France**.

A number of intersecting avenues are thus opening up, with regard to seeking to reduce the load carried by electrodes, in PEM-type fuel cells, in terms of noble metals: these include achieving a better distribution of metallic particles within the active layer, ensuring nano-organization, and a nanoarchitecture for the electrodes, substituting noble metals with **transition metals**, and, finally, the development of catalysts taking their cue from biological processes. Each one of these avenues leads on to improved performance, and combined development, along these lines, makes it possible to anticipate significant advances, with regard to bringing down the cost of fuel cells.



A screen-printing bench, being used for the application of a ceramic ink.

F. Rhodes / CEA

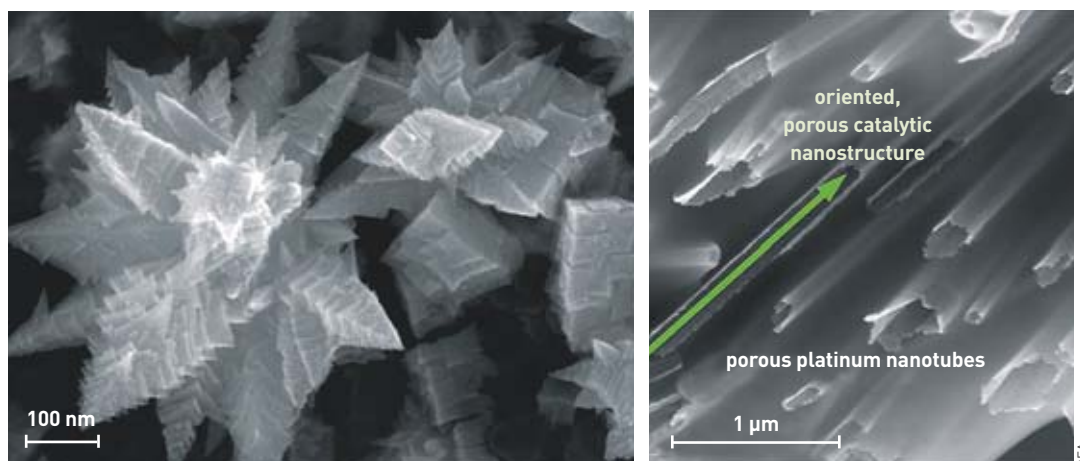


Figure 5. Nanostructuring of platinum, in the form of nanoparticles (left), and (right) porous nanotubes (carried out as part of a research project funded under CEA's *Challenge Innovation* program, aimed at promoting the emergence of ambitious projects, and helping them to take off: LITEN-INAC collaboration).

Fabrication of gas diffusion layers exhibiting controlled properties

The gas diffusion layer has the purpose of ensuring the transfer of reactant gases, from the distribution channels to the active layer (see Figure 1). It fulfills three functions: removal of the heat, and water generated at the cathode, electron transfer, between the active layers and the current collector ribs located in the gas distribution manifolds, and, finally, distributing the mechanical stresses arising from assembly, across the membrane, and active layers.

Formed of a porous material, the gas diffusion layer consists of a carbon-fiber substrate, to which a binder is added, in the form of a fabric (or felt, or paper), involving porosities of about 0.7–0.8, and pore widths of some 1–10 µm. This is complemented, in many cases, by a microporous deposit. This consists of carbon grains, and a binder, exhibiting porosities of about 0.4–0.5, and pore sizes of the order of 10 nm–1 µm.

This gas diffusion layer, the substrate of which proves highly **anisotropic** (see Figure 6), has the purpose of ensuring homogenous operation for the active layer, by setting up a gradient of pore sizes, from, at one end, the centimeter-scale gas supply point, at the cell inlet, to, at the other end, a nanodispersed catalyst. This layer contributes to the solution of a double tradeoff. On the one hand, exhibiting sufficiently high porosity to facilitate access for the gases, not so high, however, as to impair electron conductivity (which would result in increased **ohmic** loss, in particular across the plane, with regard to electron transport to the collector ribs), or thermal conductivity (resulting in larger temperature differentials, thus limiting the risk of condensation, and hence of component flooding).

And, on the other hand, the gas diffusion layer is called upon to play a major part in management of the water present in the fuel cell core (the membrane-electrode assembly [MEA]), in steam, and/or liquid form – depending on operating conditions, and on the properties of the components (condensation is a possibility, since the active layer is at a higher temperature). And, as the electrolyte must be kept sufficiently hydrated to retain its proton-conductor role, this entails that water be retained in sufficient quantity, around the membrane and active layer, not in so large amounts, however, as to

hamper gas transfers, owing to the presence of liquid water. Such liquid water must thus be removed to the gas distribution manifolds, so that it does not obstruct the pores. This tradeoff, commonly referred to as “water management,” involves maintaining hydration levels that are “sufficiently high, but not excessively so.” This is achieved by means of the diffusion transfer properties and capillarity of the fiber substrate, and microporous deposit. These properties are controlled by way of the porous structure of the layers involved, in particular through the distribution of pore sizes, and tortuosity, but equally through the wettability exhibited by this structure. In order to improve the removal of liquid water, these layers are subjected to a hydrophobic treatment, classically carried out by **coating**, or impregnating them with a hydrophobic polymer. This treatment has to be applied as homogeneously as feasible, over the entire surface of the fibers, without obstructing the pores. Finally, as is the case with the other components, a number of degradation mechanisms, affecting the gas diffusion layers (carbon corrosion, loss of hydrophobic character...), are strongly suspected of curtailing fuel cell lifetimes. These effects are exacerbated in the presence of liquid water, owing to the mechanical stresses arising during assembly (tightening), and as a result of fuel cell operations (electrolyte swelling/shrinking). The many investigations currently ongoing at CEA, at LITEN in particular, are evidencing the crucial role played by the gas diffusion layer, in relation to all of the key points, with regard to the industrial development of PEMFCs: performance, lifetime, cost reduction.

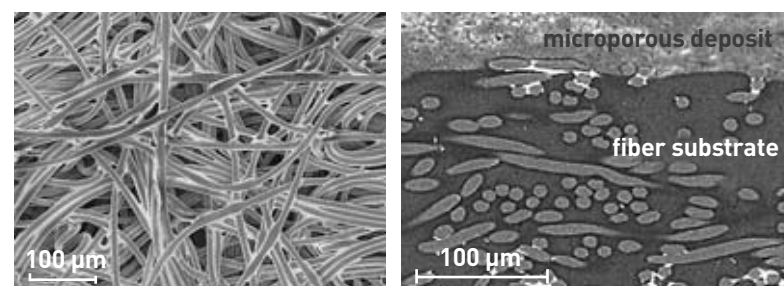


Figure 6. Views, taken under **scanning electron microscopy** (SEM), of a gas diffusion layer, showing the carbon fibers, and the hydrophobic agents around the fibers (white). Viewed from above (left), and in a sectioned view (right).

At the present time, commercially available gas diffusion layers are derived, in most cases, from components developed for other industrial applications. They are, consequently, not specifically optimized for the purposes of PEM-type fuel cells. Recent studies, carried out at LITEN, have shown that improvements may yet be achieved, through modifications to the structure, and functionalization of such layers. For researchers, this entails taking up a number of challenges. First, a way must be found, of fabricating porous (i.e. ensuring porosity, wettability...), multi-layer, multiregion structures, with the ability to be adapted to cater for the inhomogeneities, inherent in the presence of ribs, and channels (see Figure 1). Second, this means being able to cater for the variations in operating regime, arising between fuel cell inlet, and outlet. As conventional processes do not allow this, alternative processes are being investigated at LITEN, in particular as regards microporous deposits. As regards the fibrous substrates serving to ensure diffusion, these processes are intended to organize the spatial distribution of carbon fibers, or to form a controlled conducting structure.

Finally, the crucial role must be emphasized, that the gas diffusion layer plays, as regards distributing stresses across the fuel cell. This impacts both on performance (contact resistances, interfacial decohesion), and lifetime (differential stresses exerted on the other components) – hence it is imperative that the gas diffusion layer's mechanical properties be taken on board.

Curbing bipolar plate corrosion

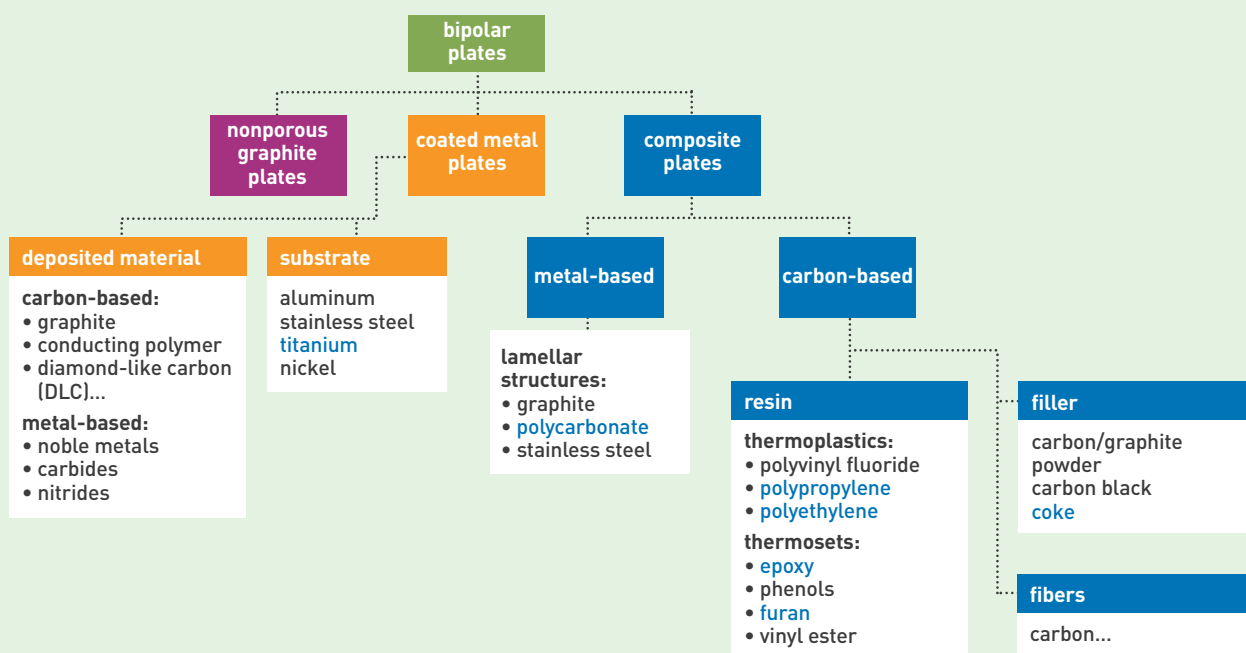
The development, and commercialization of PEM fuel cells entails substituting the **graphite** used in bipolar plates (see Figure 2) with metals, metal **alloys**, or **composite** materials. Indeed, notwithstanding the low operating temperatures involved, the cell's liquid, acidic environment proves corrosive, with respect to conventional bipolar plates. A

number of solutions are thus being investigated, to remedy this drawback (see Figure 7). As graphite composite materials (see Figure 8) still involve large amounts of graphite filler, entailing constraining⁽¹⁾, uneconomic fabrication conditions, the technique most commonly used is **hot pressing**. To allow for large-scale bipolar plate production, the initial mold features the negative imprint of the channels, on its upper, and lower faces: this makes for a minimized need for subsequent finishing machining, or even allows doing away with this. Ensuring channel reproduction, however, while conforming to a *design* optimized to promote fluid flow, raises design, and transformation issues. One alternative route involves going for metal bipolar plates. Unfortunately, the use of metal raises other issues, first and foremost the risk of corrosion. Indeed, should corrosion resistance prove inadequate, there is a risk of poisoning the other fuel cell components, with metal cations originating in the plate. *On the other hand*, in the event of the protective **oxide** layer formed becoming too thick, this will cause increased contact resistances. In either case, the outcome is a falloff in performance, incompatible with the characteristics required for a fuel cell of the PEMFC type.

A satisfactory tradeoff, between corrosion, and electrical conduction, thus, has yet to be arrived at. Uncoated **passivable** materials, e.g. **stainless steels**, could be seen as one possible solution, however they yield results that often prove contradictory, in terms of performance, and durability, precluding any final conclusion from being reached. Thus, for the purposes of curbing the effects related to metal alloy corrosion, the preferred option is to go for added

(1) Indeed, the base material – consisting of a mixture of graphite, and polymer – has to be prepared; this mixture needs to be adequately controlled, and the stages required to heat this material must be complied with, if it is to become sufficiently viscous to undergo forming, while occasioning no flash, and form crosslinks during the subsequent pressing, and annealing.

Figure 7.
Classification of bipolar
plate materials.



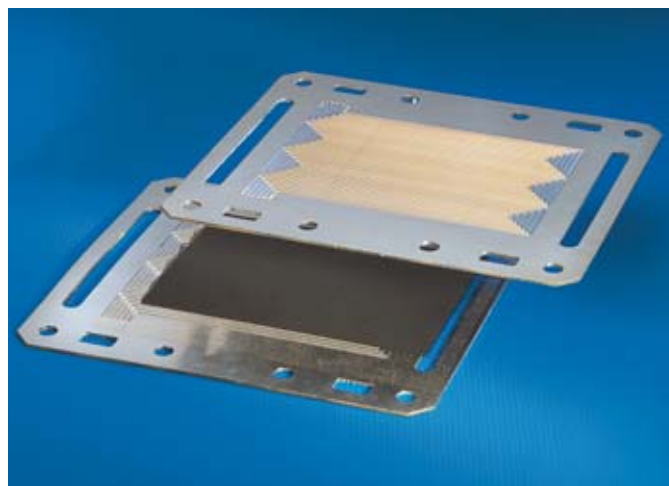


Figure 8.
Composite (left),
and stainless-steel (right)
bipolar plates.

deposits, exhibiting **physicochemical** properties such as to ensure, at the same time:

- satisfactory electrical conductivity, remaining stable in the environment considered;
- adequate chemical stability (corrosion resistance);
- compatibility with the substrate (in terms of the respective thermal expansion coefficients, and electrochemical potentials), as with the other materials in the fuel cell (chemical inertness).

Currently, three types of deposit take pride of place: noble metals, **nitrides**, and conducting polymers, along with carbon deposits. The challenge, at present, is to discover the deposit, or deposits, that will ensure such physicochemical properties at least cost, in the context of an industrial treatment, and as close to the front end as feasible, in the bipolar plate fabrication process. Thus, the number of fabrication steps is to be kept low, and hence plate costs likewise. Further, in the event of a defect arising in the coating, the cost of discarding a blank metal plate will invariably prove lower than that of rejecting a bipolar plate.

Component structuring and functionalization: the route to innovation

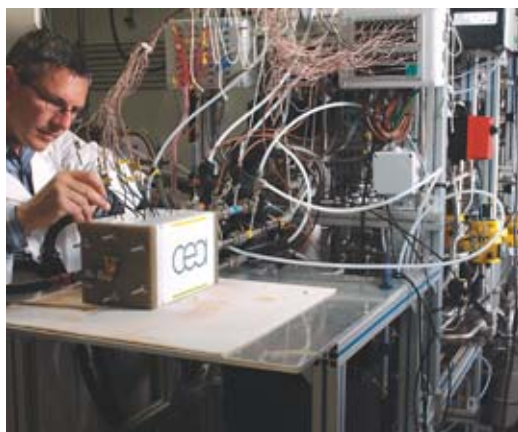
PEM fuel cells do not involve a homogenous operating regime, in particular across the cell, from inlet to outlet, or along the gas distribution channels. As the reactant gases are consumed in the reaction, their concentration becomes lower at the cell outlet

than at the inlet. Conversely, the water yielded by the reaction results in the presence of higher quantities of water (liquid, or steam) at the cell outlet than at the inlet. On the other hand, since the materials and components currently employed are, by contrast, homogenous across the plane they occupy, they are unable to cater for such differentials. The optimization of PEM-type fuel cell components thus entails numerous tradeoffs, between the various physical mechanisms involved, at the various scales arising across the cell. Improved performance levels, increased durability, and lower costs, for such fuel cells, thus necessarily entail achieving better control of the properties exhibited by components, and materials, at various scales (both nano-, and **micro**-scopic), whether it be with respect to structuring, or functionalization.

The scientific, and technical challenge at hand is thus a major one; be that as it may, a number of investigations, addressing materials, and component fabrication processes, are currently ongoing, for that purpose, involving a number of teams at CEA. These studies cover, in particular, the development of bimetallic catalysts, to bring down platinum quantities, or improve tolerance to certain atmospheric pollutants; the structuring of active layers, and gas diffusion layers, so as to position just the right quantities of material at the location required, to improve performance; bringing down materials requirements (as regards platinum, in particular); deposits effected on bipolar plates, to limit corrosion... All of these efforts are focusing on the key points, currently, with regard to the industrial development of PEMFCs: to wit, improved performance, extended lifetimes, and lower costs.

> **Joël Pauchet, Arnaud Morin, Sylvie Escribano, Nicolas Guillet and Laurent Antoni**
LITEN Institute (Innovation Laboratory for New Energy Technologies and Nanomaterials)
Technological Research Division
CEA Grenoble Center

> **Gérard Gebel**
Nanosciences and Cryogenics Institute (INAC)
Physical Sciences Division
CEA Grenoble Center



Test-benching a PEM fuel cell.

HTE: a highly promising hydrogen production process

Hydrogen production by high-temperature electrolysis (HTE) of steam stands as a sustainable solution, provided it is driven by carbon-free energy. At the same time, this technology also affords higher theoretical efficiency than is the case for low-temperature water electrolysis. For all of which reasons, **HTE may be seen as a highly promising hydrogen production process, which could meet a rising demand for hydrogen, in response to the current energy situation.**



Electrochemical test being carried out on an HTE electrolyzer cell operating at 800 °C: cell performance measurements, in terms of voltage, and current intensity, and evaluation of the quantities of hydrogen produced.

From 2005 on, CEA has been engaged in a research program addressing the technological, and economic feasibility of the mass production of hydrogen⁽¹⁾ by high-temperature steam electrolysis (HTE). It should be said that the increasing scarcity of fossil energy reserves, along with ever-rising energy consumption in the developed countries, and strong demand in the emerging countries called for a switch to an energy mix, and the development of new, clean, sustainable technologies, free of greenhouse-gas emissions. In this new context, hydrogen was seen as one energy carrier affording the ability to be directly competitive with electricity, and heat. Provided, that is, it could be mass-produced – hydrogen being of rare natural occurrence. Of the various means available, CEA elected to give the preference to the high-temperature electrolysis (HTE) of steam.⁽²⁾ The process involves splitting the water molecule into hydrogen, and oxygen, at very high temperatures, ranging from 700 °C to 900 °C –

hence the name given to the process. Two considerations militated for this option: first, heat (which is less expensive than electricity) can provide part of the energy required for the reaction; second, the reaction's efficiency is found to be higher at high temperature. For the purposes of demonstrating the advantages afforded by this pathway, CEA is develop-

(1) Hydrogen is a term coined by French chemist Antoine Lavoisier (1743–94), from two Greek words: *hudôr* (“water”), and *gennan* (“to beget, engender, produce”); hydrogen was thus supposed to be that which “produces water.” Originally, this term served to refer to the “inflammable air” discovered by British scientist Henry Cavendish (1731–1810): to wit, a gas of chemical formula H_2 , nowadays referred to as dihydrogen.

(2) There are a number of processes that allow water electrolysis ($H_2O \rightarrow H_2 + 1/2O_2$) to be effected, chiefly differing in terms of the operating temperatures involved. Alkaline electrolysis operates at low temperature (< 100 °C), and uses solely electrical energy, whereas, in the case of high-temperature electrolysis (HTE) of steam, part of the energy required to effect the splitting of the water molecule is provided in the form of heat.

ing prototype electrolyzers, intended to be coupled either to nuclear, or renewable (geothermal, solar) energy sources. To achieve this goal, two CEA units pooled their expertise, to investigate the materials being considered for the fabrication of various components, for systems of this type (i.e. interconnects, cells, but equally seals), and develop the possibilities they afford. The entities involved being the Institute for Innovation in New Energy Technologies and Nanomaterials (LITEN: *Laboratoire d'innovation pour les technologies des énergies nouvelles et les nanomatériaux*), and the Materials Department (DMAT).

HTE production of hydrogen: a technological challenge, an economic option

The design of the HTE electrolyzer involves a stack of several single repeat units (SRU) (see Figure 1). The **electrochemical cell**, i.e. one of the electrolyzer's components, comprises three ceramic layers: anode, **electrolyte**, and cathode – the latter being the site where the water-molecule splitting reaction takes place. The stack further features interconnects, having the purpose of carrying the electric current along, ensuring fluid distribution for every cell, and acting as separators between the anode, and cathode compartments, in pairs of adjacent cells. The HTE electrolyzer operates in the 700–900 °C temperature range. The gaseous atmospheres consist of a water–hydrogen ($\text{H}_2\text{O}/\text{H}_2$) mixture, on the cathode side, and oxygen (O_2), on the anode side. Consequently, the stresses acting on the constituent materials of such an HTE electrolyzer are not very different from those involved in solid-oxide fuel cells (SOFCs) – except with respect to some few characteristics.

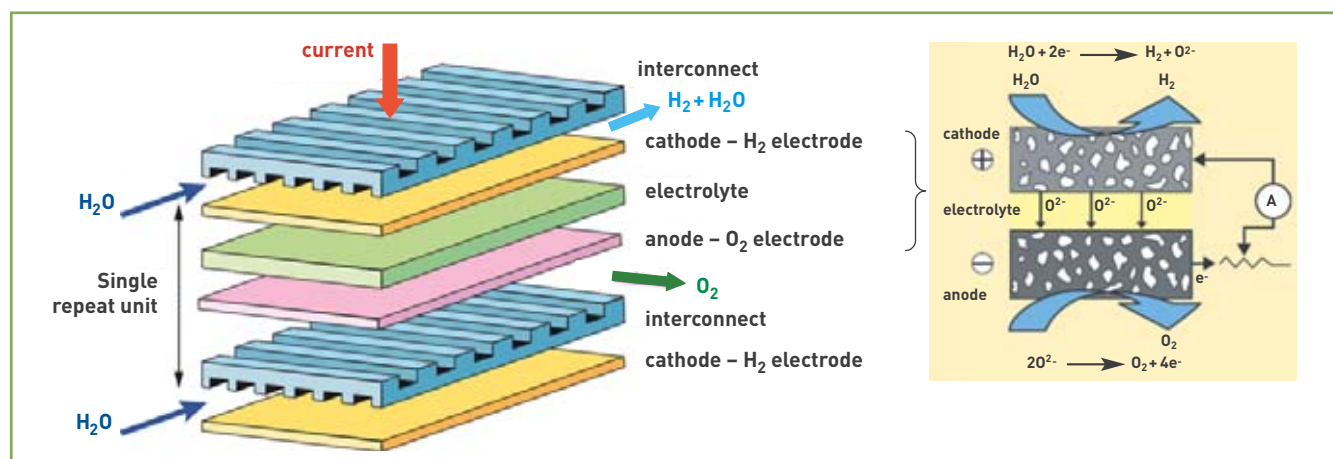
- Thus, the material employed for the interconnects, in the HTE electrolyzer (a metal alloy), must, first of all, exhibit good electrical conductivity, high **oxidation** resistance, in the specific conditions prevailing in HTE (in terms of temperature, and environment), and, second, not impair the electrochemical cells' proper operation. A twofold constraint thus applies to the interconnect: in mechanical terms, the challenge is to avoid any rupture of the **ceramic** cells the interconnect is attached to – and consequently to select a material exhibiting comparable thermal expansion characteristics; in chemical terms, the aim of the design studies is to suppress any risk of emitting compounds that would be detrimental to the electrodes. These technical imperatives are compounded by a further requirement, of an

economic nature: the HTE system must remain inexpensive. For that purpose, the material used in the interconnect must be readily “workable,” i.e. lend itself to cutting, machining, and/or stamping.

- As to the characteristics desired with respect to cell materials, these differ, according to the component considered: ceramic materials for the electrolyte, as for the anode (i.e. the site where oxygen is released); and a “ceramic–metal” composite – generally referred to as a **cermet** – for the cathode (the hydrogen production site). The electrolyte consists of a material exhibiting adequate gas tightness (density > 95%, zero open porosity), good **ion** conductivity ($10^{-2} \text{ S}\cdot\text{cm}^{-1}$ at operating temperature), a thermal expansion coefficient close to that of the electrodes (in order to limit mechanical stresses), further proving chemically inert with respect to the electrode materials, stable in both oxidizing, and reducing environments, and, finally, mechanically stable in HTE operating conditions. As regards the electrodes, the materials selected must exhibit high electron conductivity ($> 100 \text{ S}\cdot\text{cm}^{-1}$), together with – if possible – a degree of ion conductivity, in order to limit **ohmic** losses, and delocalize the electrochemical reaction, across the bulk of the electrode. These electrodes are characterized by their high **porosity**, this property being indispensable, to permit steam diffusion, but equally to allow the removal of hydrogen, at the cathode, of oxygen at the anode. This porosity must be optimized, to avoid any local overpressure, such as would tend to **delaminate** the electrodes' constituent layers. More specifically, the hydrogen electrode calls for both **catalytic** properties, indispensable for the purposes of water reduction, and an ability to remain stable in a reducing environment. As for the oxygen electrode, this must exhibit suitable catalytic properties, to effect the oxidation of O^{2-} ions, while remaining stable in an oxidizing environment. In mechanical terms, the cell must also exhibit adequate strength, in particular with regard to the ceramic layer called upon to serve as a mechanical support (this applying either to the electrolyte, or one of the electrodes, depending on the type of cell selected). Finally, again with regard to developing a process that is economically viable, it is imperative that the constituent materials for the electrochemical cells be available in quantity, at low cost.

- With regard to the coming energy challenges, researchers are striving to endow such HTE catalysers with steadily enhanced performance levels. Achieving this entails, of course, that the various components be optimized, be they metal (interconnects), or ceramic parts (cells), but equally optimizing the interfaces between these components. Indeed, within an HTE

Figure 1. Schematic of a single repeat unit in a planar-technology HTE electrolyzer, showing details of the electrochemical reactions involved. In blue, the interconnect plates, followed by the three ceramic layers, host to the chemical reaction (yellow, green, pink).



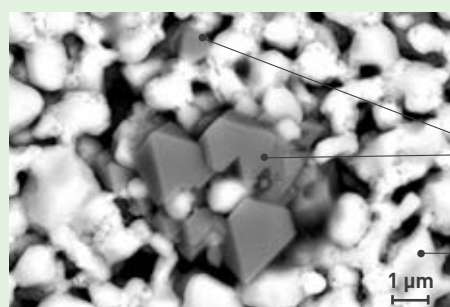


A high-temperature electrolyzer (HTE) cell being mounted in a test bench, serving to determine cell performance, and durability.

electrolyzer, the constituent materials of the cells, and interconnects come into contact with one another. Further, the way these components are stacked within the electrolyzer calls for the use of seals, most commonly made of glass, to ensure tightness between the anode, and cathode compartments, but equally with respect to the outside environment. This entails that the constituent materials of these various components be mutually compatible – chemically, and even mechanically. In chemical terms, it is imperative that materials intended for employment in the electrodes exhibit little sensitivity to contaminants released by interconnects (e.g. **chromium**), and glass seals (**silicon**, in particular). In turn, interconnect, and seal materials must be selected with a view to limiting emissions of contaminant species. A further constraint – not the least taxing one, either – is the need to guarantee the good quality of the interfaces between the various components – the aim being to promote **ion-electron**, and electron-electron charge transfers, while limiting ohmic losses during operation. Finally, in mechanical terms, current studies are looking to ensure compatibility between the various materials, with regard to thermal expansion coefficients.

As HTE electrolyzers are meant to operate for several tens of thousand hours, the properties they exhibit must prove sufficiently long-lasting, to ensure that degradation of the stack stays close to 0.5% per 1,000 hours operation. Of the routes open to exploration, for the purposes of enhancing the durability of such systems, the favored options, for researchers at CEA, are those that would result in lower operating temperatures, while occasioning no drop in performance. Currently, the performance/durability tradeoff, with regard to the electrolyzer core, thus stands as the major challenge – decisive with respect to demonstrating the economic relevance of this pathway, and thus to securing its future development.

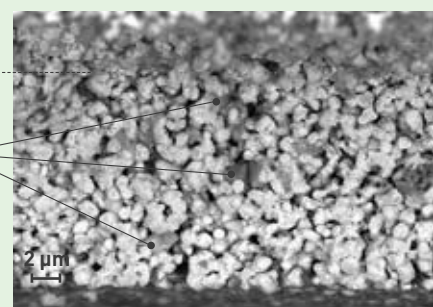
Figure 2. An anode, as viewed under **scanning electron microscopy**, subsequent to a test involving high-temperature electrolysis in the presence of a chromium-rich alloy. Surface (at left), and sectioned (right) views.



anode-electrolyte interface

crystals yielded by trapped vapors: mixed chromium-manganese spinel oxide ($Mn_xCr_{3-x}O_4$)

anode material



Constraints, and solutions

High temperature, aggressive gaseous environments, chemical, and mechanical interactions between the materials involved... Bearing in mind the peculiarly severe operating conditions prevailing in an HTE electrolyzer, the mass production of hydrogen will first entail overcoming a number of technological barriers, with regard to the materials selected for the various components in the electrolyzer.

● As regards interconnects, the chief difficulty calling for resolution is due to a well-known phenomenon: chromium poisoning. Indeed, most of the alloys affording oxidation resistance at high temperature (stainless steels, **nickel**-based alloys) form chromium-rich oxide layers, acting as fairly good electrical conductors; on the other hand, however, such layers also emit volatile chromium compounds, liable to contaminate the cell. This further difficulty arises owing to the trapping of such vapors at the triple-phase boundaries, where anode, electrolyte, and gas meet, i.e. at the site of the electrochemical reaction, as well as within the anode itself (see Figure 2), this resulting in degradation of the cell's electrochemical properties.

Other **alloys** are available, that would afford oxidation resistance, however they do involve a variety of drawbacks (see Figure 3). For instance, silicon- and/or **aluminum**-rich alloys yield non-poisoning oxides, however such oxides prove to be very poorly conducting, even for very thin oxide layers. Other alloys, while forming fairly adequately conducting, non-poisoning oxide layers, exhibit poor oxidation resistance. The solution might entail using noble metals (platinum, gold), such metals alone having the ability to overcome these constraints, however their cost remains altogether prohibitive, with regard to industrial production. As regards the interconnect, the choice of material involves a tradeoff. Among the alloys currently under consideration are **ferritic stainless steels**. Inexpensive as they are, these steels further exhibit advantageous properties, in terms of volume. Among other benefits, they prove particularly suitable for shaping, and welding purposes, exhibit expansion behaviors (as measured by **dilatometry**) compatible with that found for the cell, and are not excessively embrittled by prolonged exposure to high temperatures. On the other hand, their surface properties are not altogether satisfactory, with regard to the heavy stresses encountered in an HTE electrolyzer. Their oxidation resistance in steam, in particular, remains poor, while the oxide layers formed prove to be electrode-poisoning. Research organizations, and manufacturers are currently striving to optimize the composition of such steels, in particular by seeking to control the nature of the naturally forming oxide layers. For instance, as regards the Crofer(®)22APU grade (an iron-chro-

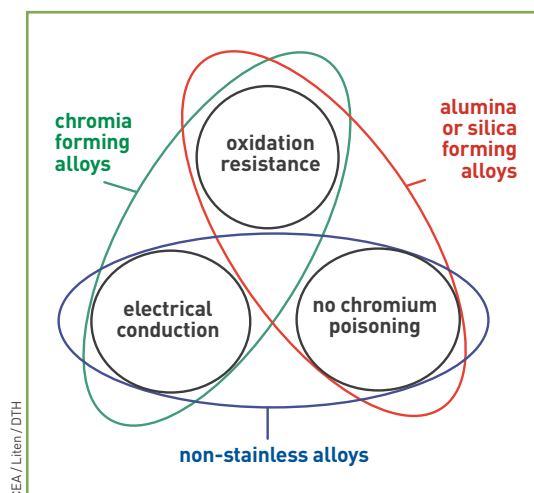


Figure 3.
The limitations involved, for the various metallic materials available for consideration as HTE interconnect materials.

mium alloy containing 22% chromium), developed by ThyssenKrupp, a manganese addition to the alloy promotes the formation, at the very surface, of a mixed manganese–chromium oxide. This oxide affords the twofold benefit of emitting lower quantities of chromium-compound vapors, and of proving to be a far better conductor than chromium oxide by itself – even though the latter oxide does still form, beneath this mixed oxide. Hence, additions of rare earths (of lanthanum, for instance) are made, to bring down oxide growth rate: the ensuing thinner layer exhibits better adhesion, and hence better conduction properties. Finally, titanium is added, to bring down the chromium oxide’s resistivity.

Unfortunately, the effectiveness of such solutions proves altogether limited, with regard to ensuring HTE electrolyzer operation over extended timescales. A research effort is consequently being conducted, at CEA, to obtain improved surface properties, for these components, by means of coatings, in particular. Investigations are focusing more particularly on chromium-free oxides, exhibiting low electrical resistivity, while affording the ability, nonetheless, to prevent, or markedly slow down, oxidation of the underlying alloy. The chief compound investigated in this respect is a mixed manganese–cobalt oxide, exhibiting a spinel structure, with the composition $(\text{Co}, \text{Mn})_3\text{O}_4$. The benefit it affords is its high conductivity: about a thousand times higher than that exhibited by chromium oxide, at 800 °C. Other compounds, however, e.g. lanthanum perovskites, derived from electrode compositions, are equally proving of interest to researchers. Numerous deposition techniques are also being considered. Most of these involve combining the coating operation itself with a post-treatment, for the purposes of achieving the proper stoichiometry, and/or deposit densification. For instance, Sandvik, a metal alloy manufacturer, is currently offering a ferritic stainless steel, featuring a cobalt coating obtained by vacuum deposition. As high-temperature oxidation takes place, spinel-type oxides form, this resulting in lower chromium evaporation, and improved conductivity.

Among these various investigation paths, as regards coatings, CEA has opted to pursue, in particular, the route involving metallic cobalt–manganese deposits, obtained by vacuum spraying, on stainless steels, or

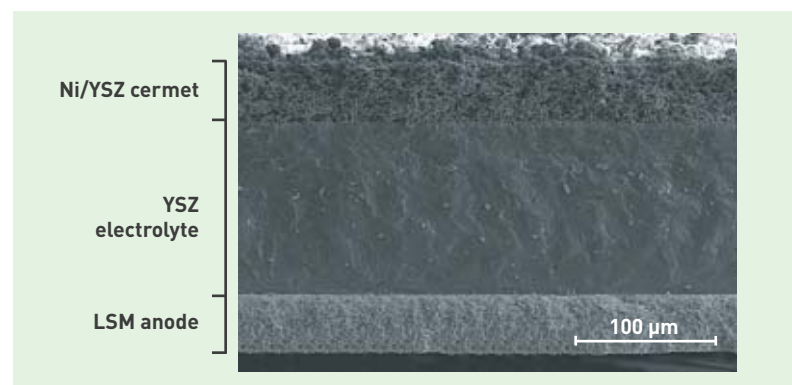
nickel alloys. This technique makes it possible to obtain dense, low-thickness layers, exhibiting good adhesion, through use of a process readily lending itself to industrialization. Hence, researchers are currently looking into the mechanisms that effect the conversion of such deposits into spinel oxides, with the aim of optimizing the structure, and the properties exhibited by the layers so obtained. Concurrently, research workers are evaluating the behavior of the alloy–deposit combination, when subjected to prolonged exposure to high temperatures, in terms of chemical resistance, and mechanical strength. These studies have already made it possible to pinpoint the limitations of the vacuum spraying route, along with identifying possible avenues for improvement, by way of controlling alloy–deposit reactivity, through the interposition of intermediate layers.

Concurrently with these two major avenues, another one is opening up, concerning deposition processes involving powder suspensions. In this case, coating is deposited by screen printing. This is a printing technique which involves depositing a suspension (i.e. a powder mixed with a – possibly aqueous – solvent, and additives: inks, in the present case) onto the surface undergoing the coating treatment, by passing the suspension through a screen. Researchers are addressing the issue of controlling the critical parameters, e.g. viscosity, or the fraction of dry matter, required to obtain the appropriate density, once the layer has been consolidated.

● As regards the HTE electrolysis cells, a variety of reference materials are involved. For the hydrogen electrode, the material is a nickel/yttria-stabilized-zirconia (Ni/YSZ) cermet, containing as a rule 8% yttrium; for the electrolyte, researchers employ yttria-stabilized zirconia [YSZ]; while, for the oxygen electrode, a strontium-doped lanthanum manganite, of the $\text{La}_{1-x}\text{Sr}_x\text{MnO}_{3-\delta}$ type – a compound referred to as LSM⁽³⁾ – is used (see Figure 4). These materials prove particularly well suited to operations at 800 °C. On the other hand, with regard to operating temperatures such as would allow degradation mechanisms to be minimized (i.e. 650–750 °C), optimized solutions are being investigated, in order to achieve satisfactory electrochemical performance at such intermediate tempe-

(3) Widely referred to as lanthanum strontium manganite (LSM). This features a perovskite structure, of the ABO_3 type, in which formula, in the present case, manganese occurs at the B sites, lanthanum and strontium at the A sites. Indeed, a number of substitutions may arise at the A and B sites, as in this case, where lanthanum, occurring at A sites, may be substituted for with strontium, to increase the material’s electrical conductivity.

Figure 4.
Sectioned view of an electrolyte-supported cell, comprising a nickel/yttria-stabilized-zirconia (Ni/YSZ) cermet cathode, an yttria-stabilized-zirconia (YSZ) electrolyte, and an LSM anode (see note 3).



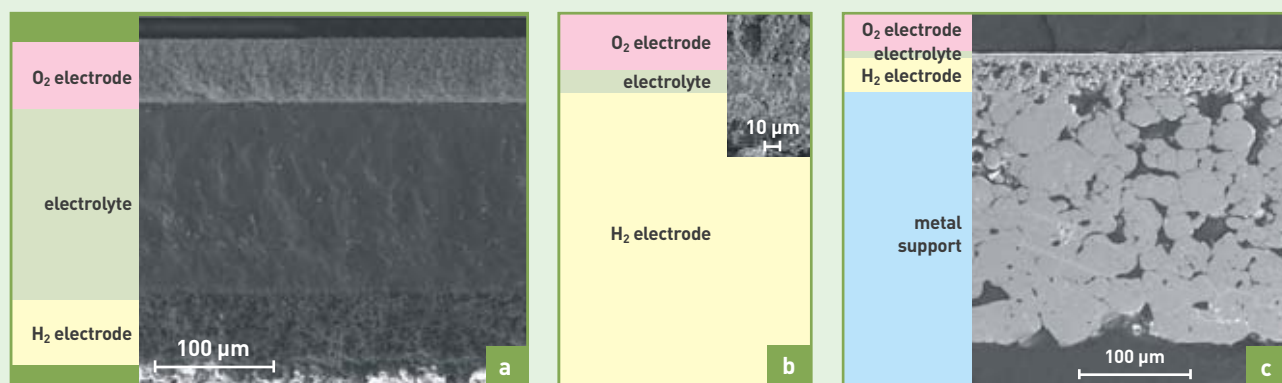


Figure 5. Electrolyte-supported cell (a), electrode-supported cell (b), metal-supported cell (c).

ratures. The aim, for researchers, is to counteract, at the same time, a falloff in ionic conductivity, in the electrolyte, and a slowing down of the kinetics of the electrochemical reaction. Novel materials are thus anticipated, for the electrolyte as for the electrodes, along with novel configurations – for instance, electrode-supported, or metal-supported cells (see Figure 5).

With regard to new electrolyte materials, suitable for intermediate temperatures, *scandia*-stabilized zirconia (ScSZ) is seen as a better candidate than yttria-stabilized zirconia (YSZ), owing to its higher ionic conductivity. On the other hand, researchers are still verifying its capabilities, in terms of stability, and aging resistance – all the more as this is a relatively costly compound. As regards the oxygen electrode, investigations are chiefly concerned with finding a substitute for LSM perovskite, by way of a mixed electron/ion-conducting material. Achieving this would allow a

reduction of the polarization overvoltages arising at temperatures of less than 800 °C, for such an electrode. The mixed oxides considered again belong to the perovskite family⁽⁴⁾ – such being the case, in particular, for strontium-doped lanthanum cobaltite,⁽⁵⁾ or lanthanum cobalt ferrite.⁽⁶⁾ The reasons for taking up this option stem from the properties afforded by this material, which exhibits high ionic, and electronic conductivities at low temperature. Such perovskites, as they undergo a rapid reaction with zirconia, yielding insulating phases, require the interposition of a barrier layer between the electrolyte, and electrode. This, as a rule, consists of *gadolinia*-, or *yttria-doped ceria*,⁽⁷⁾ as it then proves chemically compatible both with the zirconia-based electrolyte, and the electrode material. Thus, many electrode-supported cells, developed to operate at temperatures around 700–750 °C, feature an LSCF⁽⁶⁾ anode, together with a ceria-based barrier layer. Finally – looking more to the future – materials from the *nickelate* family are presently undergoing development, and qualification, for the purposes of HTE electrolyzer operation. Such materials, being developed by the Institute for Solid State Chemistry at Bordeaux (France) (ICMCB/CNRS: Institut de chimie de la matière condensée de Bordeaux), in collaboration with French national utility EDF, and CEA, are seen as being particularly promising, especially those from the $A_2NiO_{4+\delta}$ ⁽⁸⁾ family. Indeed, initial results show that a cell in which $Nd_2NiO_{4+\delta}$ nickelate is used, as a substitute for LSM, exhibits enhanced electrolysis performance, this being improved by a factor 2 at 850 °C, and by a factor 4 at 750 °C (see Figure 6).

As regards the hydrogen electrode, nickel stands as the most effective electrocatalyst discovered to date. Materials of the nickel/gadolinia-doped ceria (Ni/GDC), or nickel/*samarium*-doped ceria (Ni/SDC) type substitute for the conventional nickel/yttria-stabilized zirconia cermets, to achieve higher conductivity

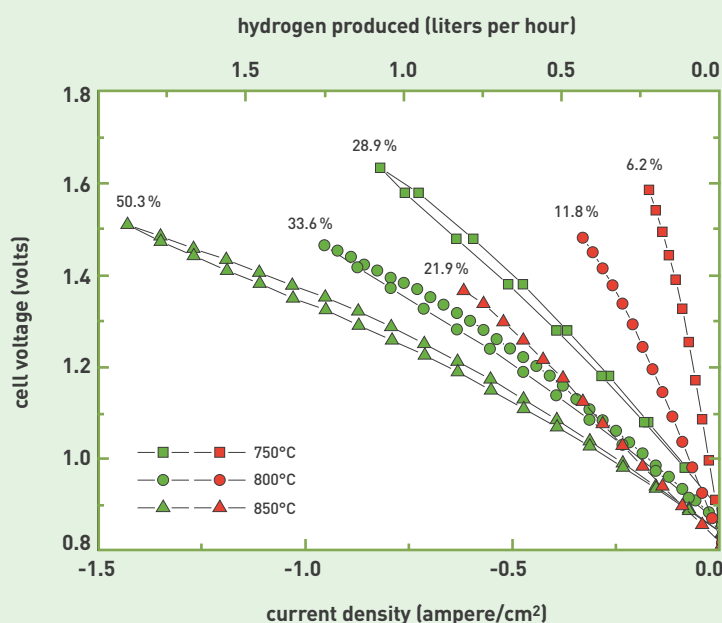


Figure 6. Intensity/potential curves (intensity: current density, in amperes per square centimeter; potential: volts), obtained in HTE mode in electrolyte-supported cells, of the Ni/GDC/YSZ//anode type; the anode being either LSM perovskite (red symbols), or $Nd_2NiO_{4+\delta}$ nickelate (green symbols), at three different operating temperatures; the flow rate of hydrogen produced (in liters per hour) is also indicated, on the secondary x-axis scale; the figures appearing above the lines show the fraction of steam converted into hydrogen, in the test conditions.

(4) Of the type $Ln_{1-x}Sr_xA_{1-y}B_yO_{3-\delta}$ (where Ln = La, Pr, Nd, Sm, Gd, while A and B stand for transition metals, and δ serves to indicate hypo-stoichiometric oxygen).

(5) Or lanthanum strontium cobaltite (LSC): $La_{1-x}Sr_xCoO_{3-\delta}$.

(6) Or lanthanum strontium cobalt ferrite (LSCF): $La_{1-x}Sr_xCo_{1-y}Fe_yO_{3-\delta}$.

(7) Gadolinia- (gadolinium oxide, Gd_2O_3) or yttria- (yttrium oxide, Y_2O_3) doped ceria (CeO_2), respectively noted as GDC, YDC.

(8) In this formula, A stands for lanthanum, neodymium, or praseodymium, Ni for nickel, O for oxygen, the latter element being hyper-stoichiometric in the structure (as indicated by the δ in the formula).

at low temperature. Investigations are likewise being conducted, at CEA, on cermets of the nickel/scandia-stabilized zirconia type, these being peculiarly relevant, with the prospect of using scandia-stabilized zirconia electrolytes. CEA is also looking into all-oxide materials for the hydrogen electrode, acting as mixed conductors, i.e. materials conducting both ions, and electrons – with regard, in particular, to the **titanate** family.⁽⁹⁾ The benefit afforded by these compounds is the satisfactory electron conductivity they exhibit, along with good stability, in reducing conditions. Microstructural optimization is currently being undertaken, to obtain, from such materials, durable, high-performance cathodes.

Cells employing the various materials mentioned in the above paragraphs may be constructed either as planar, or tubular cells, depending on the stacking architecture into which they are to be integrated. CEA is investigating both types of architecture. As regards planar cells, with a view to the mass production of large cells, conventional, low-cost processes are used, e.g. screen printing, or tape casting. The latter technique involves forming a green (i.e. nonsintered) tape, through deposition of a suspension (i.e. powders mixed with a – possibly aqueous – solvent, and additives of the dispersant, binder, or plasticizer – also known as slurry – types) over a casting bench, while controlling tape thickness by way of blade speed, and position. Once the tape has dried (the solvent having been removed), the heat treatment, for consolidation purposes, involves two stages: debinding, this being carried out over a temperature range extending from 300 °C to 600 °C, for the purposes of removing organic additives, followed by **sintering** (1,550 °C for YSZ), to ensure mechanical strength for the cell support. This technique makes it possible to obtain layers having a thickness above 80 µm. It is eminently suitable for the preparation of planar cell supports (be they electrolytes, or electrodes). On the other hand, the fabrication of tubular cells entails going for specific processes, compatible with such a geometry. Thus, for tubular cells, the electrolyte is fabricated by means of a **plasma** forming technique, while the hydrogen electrode, deposited over the tube's inner wall, is obtained by dipcoating, or **coating**. Finally, the oxygen electrode, covering the outer wall, is deposited by screen printing, or coating.

Beyond they can look to the actual deployment of HTE

(9) $(\text{La}_{1-x}\text{Sr}_x\text{TiO}_{3+\delta})$.



Planar HTE components: electrolytes, electrolyte-supported cells, and electrode-supported cells.



P. Stroppa / CEA

Tubular HTE cells. Development work on 600-cm² cells, for an innovative coaxial architecture. Electrode deposition by coating.

electrolyzers, enabling the mass production of hydrogen, researchers thus have to find solutions to a range of issues, raised by these systems' operating conditions – involving extreme environments as they do: high temperatures, aggressive gas environments, chemical, and mechanical interactions between the materials involved. The key to overcoming this technological barrier entails arriving at a satisfactory tradeoff between electrolyzer performance, and lifetime, and the cost of the various components. For that purpose, CEA is pursuing R&D efforts, involving a multidisciplinary, multimaterial, multiphysics approach, supported by modeling campaigns, with regard to the mechanisms involved.

➤ **Julie Mougin** and **Emmanuel Rigal**
LITEN Institute (Institute for Innovation
in New Energy Technologies and Nanomaterials)
Technological Research Division
CEA Grenoble Center

➤ **Julien Vulliet** and **Thierry Piquero**
Materials Department
Military Applications Division
CEA Le Ripault Center

FOR FURTHER INFORMATION

F. LEFEBVRE-JOUD, J. MOUGIN, L. ANTONI, E. BOUYER, G. GEBEL, "Matériaux de la filière hydrogène – 1: Production et conversion", *Techniques de l'ingénieur*, No. 1205 (April 2010).

P. STEVENS, C. LALANNE, J.-M. BASSAT, F. MAUVY and J.-C. GRENIER, CNRS-EDF patent (F), "Procédé et dispositif d'électrolyse de l'eau comprenant un matériau oxyde d'électrode particulier", FR 2872174 2005-12-30 ["Method and device for water electrolysis comprising a special oxide electrode material", international patent application No. PCT/FR2005/001556].

F. CHAUVEAU, J. MOUGIN, J.-M. BASSAT, F. MAUVY, J.-C. GRENIER, "A new anode material for solid oxide electrolyser: The neodymium nickelate Nd₂NiO_{4+δ}", *Journal of Power Sources*, vol. 195, No. 3 (2010), pp. 744–749.

G. GAUTHIER, T. DELAHAYE, "Titanates de structure pérovskite ou dérivée et ses applications", French patent No. 08 02032 (2008) ["Titanates with perovskite or derivative structure and applications thereof", European patent No. EP2110873A1 (2009)].

T. PIQUERO, B. VERGNE, J. VULLIET, K. WITTMANN-TENEZE, N. CARON, and F. BLEIN, "Solid oxide electrolyte tubular cells for hydrogen production", *4th International Conference on Shaping of Advanced Ceramics (Shaping-4)*, Madrid (Spain), 15–18 November 2009.

Li-ion: a cutting-edge technology for novel high-performance, innovative storage batteries

Small mobile devices (cell phones, laptop computers...), but equally automobiles, and photovoltaic solar cells... applications calling for the storage of electrical energy are growing, and becoming ever more diverse, while involving widely different cost, and performance criteria. **CEA is banking strongly on Li-ion technology, in view of the high electrochemical potential it affords – the highest indeed, compared to competing solutions – for the purposes of developing new, high-performance, innovative storage batteries.** A challenge that entails exploring novel approaches, to optimize innovative electrode active materials.



Artechnique / CEA

Electrode active materials in powdered form, for Li-ion storage batteries.

Of all rechargeable energy storage systems, **lithium-ion** (Li-ion) **electrochemical** batteries afford the best performance levels: 400–500 Wh/l, and 140–200 Wh/kg, for a nominal voltage of around 3.7 V, low self-discharge characteristics

(5–10% per month), and a broad range of operating temperatures (from -20°C to $+65^{\circ}\text{C}$). The principle underpinning this technology involves triggering the reversible electrochemical **intercalation** of lithium ions into two distinct materials, for different potential values: at the positive **electrode**, into a **cobalt**-based (in close to 90% of cases) mixed **oxide**, and, at the negative electrode, into **carbon/graphite**. Currently, these performance levels stand as the best compromise achievable, proven, and steadily improved as they have been, since 1991. Figure 1 shows the chief materials being investigated for this technology, for both the positive, and negative electrodes, ranged according to operating **voltage**, and specific capacity. However, meeting the requirements now emerging entailed developing electrochemical couples (positive electrode/negative electrode) better suited for that purpose. Hence the challenge, with regard to innovation, set to researchers, of optimizing the active materials for the electrodes – truly a challenge for our times.



P.-F. Grosjean / CEA

Electrode undergoing slitting (cutting).



P.-F. Grosjean / CEA

Spooling of electrodes (both positive, and negative), and separators.

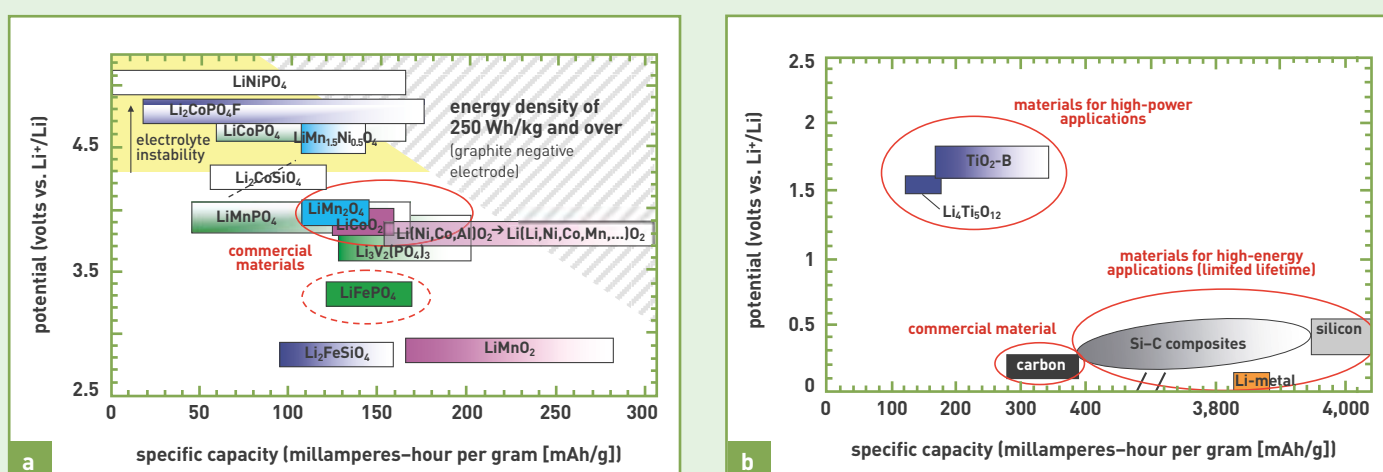


Figure 1.

a. Examples of positive electrode materials (specific capacity vs. operating potential). The colors indicate the various families of compounds (highlighted in pink: lamellar oxides; in turquoise blue: spinel oxides; green: phosphates; dark blue: fluorophosphates, silicates). It will be noted that the LiNiPO_4 compound (lithium nickel phosphate) involves no practical capacity. The area colored yellow corresponds to the instability domain for conventional electrolytes (at voltages around 4.3 V vs. Li^+/Li). The hatched region indicates, in simplified manner, the voltage/capacity domain for positive electrode materials that make it possible to achieve, or exceed a specific energy density of 250 Wh/kg, at the scale of an entire Li-ion storage battery of a few amperes-hour capacity (with a graphite negative electrode).

b. Examples of negative electrode materials (specific capacity vs. operating potential). Shown in blue, two instances of titanium oxides for high-power, extended-lifetime, high-safety applications are indicated; in black, and orange: carbon (in various forms, including graphite), and lithium metal; shown in gray, the capacities, and voltages delivered by silicon, and silicon-carbon (Si-C) compounds.

The red ellipses ring three categories of compounds: current/commercial, new high-power materials, new high-energy (extended-discharge-time) materials.

What materials for high-energy Li-ion storage batteries?

These materials differ, depending on the electrode for which they are intended.

For the negative electrode

Since the emergence of Li-ion technology, in the early 1990s, the **electrochemical** performance levels exhibited by batteries have undergone constant advances, whether in terms of capacity, or energy. Thus, the carbon negative electrode has presently reached a stage

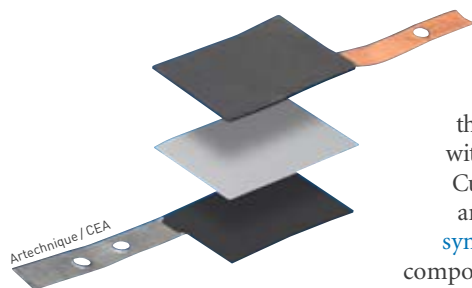
of maturity, with a theoretical capacity⁽¹⁾ of 372 mAh/g. Increased energy requirements thus called for new materials, for the negative electrode. Involving as it does a theoretical capacity estimated at 3,578 mAh/g, **silicon** was seen as providing, at first blush, a plausible alternative to carbon. Were it not for the one drawback, however: the expansion it undergoes, in terms of particle volume, by up to close to 300%, as the electrode is charged, causing it to crack, and suffer de adhesion from the current collector – an unacceptable characteristic, precluding the use of silicon. Researchers thus had no option but to direct their endeavors to seeking a material such as would preserve electrode integrity, after repeated charge/discharge cycles. Silicon/**carbon composites** were seen as outstanding candidates. Indeed, various studies, carried out on **thin films**, with **nanostructured** materials forming alloys with **lithium** (silicon, **tin**, **aluminum**...), demonstrated the feasibility of obtaining satisfactory reversibility, after extensive cycling. Provided, that is, that one condition be complied with: particles should not exceed the decay limit, this standing, as a rule, at about 100 nm. Having achieved this breakthrough, another issue now had to



Electrode undergoing coating in a small pilot bench.

P.-F. Grosjean / CEA

(1) The term "theoretical specific capacity" is used, in the present context, to refer to the specific capacity, expressed in milliamperes-hour per gram (mAh/g), as calculated according to the following theoretical formula: number of moles of Li^+ ions theoretically exchanged between the positive, and negative electrodes (i.e. number of moles of Li^+ ions theoretically extracted, in reversible manner, from the active compound at the positive electrode [or likewise inserted at the negative electrode]), times 1 faraday (96,500 C), divided by 3,600 seconds – divided by the compound's molar mass, expressed in grams per mole (g/mol). The term "practical specific capacity" refers to the actual specific capacity, as measured in milliamperes-hour per gram, exhibited by the compound. Conventional practical values stand at 280–330 mAh/g for the negative electrode material, 130–180 mAh/g for the positive electrode material. Enhancing the electrodes' practical capacities results in extending runtime, for the end application.



A single set of components, comprising a positive electrode, membrane, and negative electrode, prior to being integrated into its housing. A stack comprising several such single sets is built up, as a rule, to increase the system's capacity (i.e. discharge time).

be resolved, namely that of maintaining adequate contact for electrons, through the use of nanoscopic powders, with a high electrode density.

Currently, a number of avenues are opening up, as regards the **synthesis** of silicon/carbon composites suitable for use in commercial Li-ion storage batteries. These involve deposition of silicon onto carbon, by **fluidized-bed chemical vapor deposition (CVD)**; incorporation of silicon-carbon (Si-C) chemical bonds by grafting; or developing optimized composite electrode formulations... All of these experiments have the purpose of enhancing the electrode's mechanical strength, over repeated charge/discharge cycles, and hence extending overall battery lifetime. It would now seem that a practical capacity estimated at 1,000–1,200 mAh/g, at the scale of the composite, corresponding to an estimated area capacity of 4 mAh/cm², may reasonably be anticipated – these data matching the requirements coming from the marketplace. Such a capacity, while remaining less than the theoretical capacity of silicon, would nonetheless allow a trebling of the practical capacity commonly achieved with graphite.

For the positive electrode

As the energy densities achievable for Li-ion storage batteries are more limited with respect to the positive electrode (in particular in terms of **specific energy**), the investigations carried out by the Institute for Innovation in New Energy Technologies and Nanomaterials (LITEN: *Laboratoire d'innovation pour les technologies des énergies nouvelles et les nanomatériaux*) are primarily concerned with the three main families of active materials used for this electrode. Among the various compounds affording the ability to act as substitutes for **cobalt** oxide, and its derivatives, are high-potential insertion materials, viz. oxides exhibiting a **spinel** structure (nickel **manganese** oxides),

materials featuring a **polyanionic** framework (cobalt phosphates, and fluorophosphates), and the newly developed lithium- and manganese-rich **lamellar oxides**, affording high capacities, particularly advantageous when charge cutoff voltage is sufficiently high (4.5–5 V vs. Li⁺/Li). Use of these oxides should result in notably improved stored energy densities.

● Oxides exhibiting a spinel structure, especially those able to operate at high potentials, afford the benefits of a structure suited to fast kinetics, high stored energy density, and relatively low cost, compared to conventional lamellar oxides. Electrochemical activity, standing at 4.7 V vs. Li⁺/Li, i.e. 1 volt higher than for conventional materials, is the factor that allows a high energy density to be achieved (see Figure 2). In such nickel manganese oxides, high voltage is induced by way of the **oxidation-reduction** of nickel (via the Ni⁴⁺/Ni³⁺, and Ni³⁺/Ni²⁺ **redox** couples). When it is active, manganese (i.e. the Mn⁴⁺/Mn³⁺ couple) exhibits an electrochemical activity standing at about 4 V vs. Li⁺/Li. It is thus crucial that the material's composition be optimized, if high voltage is to be obtained. Researchers at LITEN have been investigating this family of high-voltage materials since 2003–2004. The generic material⁽²⁾ exhibiting the electrical performance currently seen as the most advantageous is actually found to feature a notably different composition: a fraction of the manganese occurs in oxidation state +III (with a majority of Mn⁴⁺ ions, and a minority fraction of Mn³⁺ ions), owing to the presence of cation vacancies, and/or small quantities of impurities,⁽³⁾ arising at the synthesis stage. This is accounted for by the fact that the pure, **stoichiometric** compound exhibits a less advantageous electrochemical behavior than does its disordered, nonstoichiometric (in terms of oxygen) counterpart.⁽⁴⁾ The presence of small quantities of Mn³⁺ ions would thus appear to be beneficial, in terms of electrochemical performance. There is an alternative path that allows compounds to be obtained, containing Mn³⁺ ions. This involves substituting small amounts of **nickel** with manganese. Thus, by allowing the various unknowns to vary, the materials affording the best tradeoffs between practical specific energy density (making for high potential, and practical capacity), and **cycling** stability (i.e. minimizing loss of capacity per cycle) were isolated.

At the outcome of this research effort, aimed at ascertaining the level of reversibility, and practical performance (specific capacity, insertion kinetics...) achievable with such materials, it is thus apparent that a material of composition LiNi_{0.4}Mn_{1.6}O₄ exhibits excellent characteristics, even in the event of a few oxygen vacancies occurring.⁽⁵⁾ Putting this breakthrough to advantage, current investigations are focusing on the **electrolyte**, the resistance of which to oxidation, at voltages higher than 4.2 V vs. Li⁺/Li, remains limited, resulting, in particular, in very high self-discharge for the system.

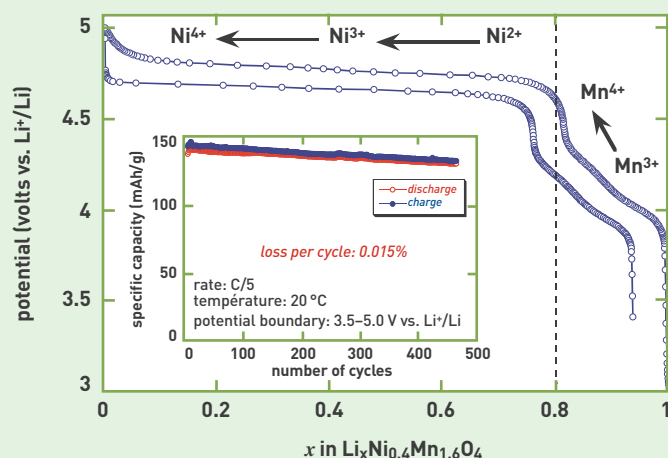


Figure 2. Charge/discharge curve. Potential vs. composition of the (LiNi_{0.4}Mn_{1.6}O₄) spinel oxide, evidencing the reversible oxidation of Mn³⁺, and Ni²⁺ ions, at 4 V, and 4.7 V vs. Li⁺/Li, respectively. The curve should be read from the extreme point, lower right. Inset: specific capacity as a function of discharge rate, evidencing the excellent cycling behavior of the compound investigated. C/5 (inset) corresponds to the charge (or discharge) rate, when completed in 5 hours.

(2) Involving only Mn⁴⁺ and Ni²⁺ ions: LiNi_{0.5}²⁺Mn_{1.5}⁴⁺O₄.

(3) Impurities of the Li_xNi_{1-x}O type, in particular.

(4) I.e. it exhibits lower conductivity (and consequently affords poorer performance with regard to power applications), and a shorter lifetime (and thus makes for fewer charge/discharge cycles).

(5) LiNi_{0.4}Mn_{1.6}O₄: a lithium nickel manganese oxide, featuring a spinel structure, involving a Li/(Ni + Mn) molar ratio of 1/2, a Mn/Ni molar ratio of 4.

● As regards the various materials featuring a polyanionic framework,⁽⁶⁾ the development of innovative synthesis methods, for lithium cobalt **phosphate**, and fluorophosphate, has made it possible to achieve enhanced electrochemical performance levels, compared to the previous state of the art. Indeed, these two materials exhibit an operating voltage of 4.8 V vs. Li^+/Li , together with a theoretical capacity that is higher than that afforded by spinel oxides.⁽⁷⁾ Such performance levels give grounds for believing they could yield outstanding candidates, once cycling behavior, and practical capacity are improved, with regard to the fluorophosphate.

● As is the case with conventional cobalt oxide, lamellar oxides⁽⁸⁾ thus afford some of the highest theoretical capacities of all materials known to research workers: from 270 mAh/g to more than 300 mAh/g. As regards practical capacities, values lie, as a rule, in the 150–180 mAh/g range. Obtaining higher values yet is feasible, however this is invariably achieved at the cost of impaired cycling behavior, involving in particular a downfall in capacity during charge/discharge cycles – hence the imperative requirement that advances be made, with respect to this issue, over the coming years. On the other hand, in contrast to conventional lamellar oxides, lithium-rich manganese lamellar oxides⁽⁹⁾ do allow high specific capacities to be obtained, such as prove indispensable for the purposes of high-energy-density Li-ion storage batteries. Such complex oxides⁽¹⁰⁾ occur in the **crystallographic** sites of **transition element** crystals. Their specific characteristic is due to the complex electrochemical processes that arise, owing to the altered oxidation states of the various constituent transition elements, or through gradual structural transformations (see Figure 3). All of which qualities mean that particularly attractive compositions may be anticipated, with energy densities expected to lie in the range 800–900 Wh/kg material. Moreover, the presence of manganese brings down, by a considerable extent, the cost of this material, while indirectly resulting in enhanced intrinsic safety, relative to nickel-, and cobalt-rich compounds. It has been found that, the less high the nickel, and cobalt content, and correspondingly the higher the manganese content, the more stable the material proves to be, in thermal terms, in particular in the event of inappropriate usage of a storage battery fabricated from such materials. These new lamellar oxides should make it possible to optimize energy density for Li-ion storage batteries



Cycling benches for lithium systems, ranging from a button cell to a mini-battery. Button cells are used for materials testing; the flat units are prototype lithium-polymer mini-batteries, intended for integration into smart cards.

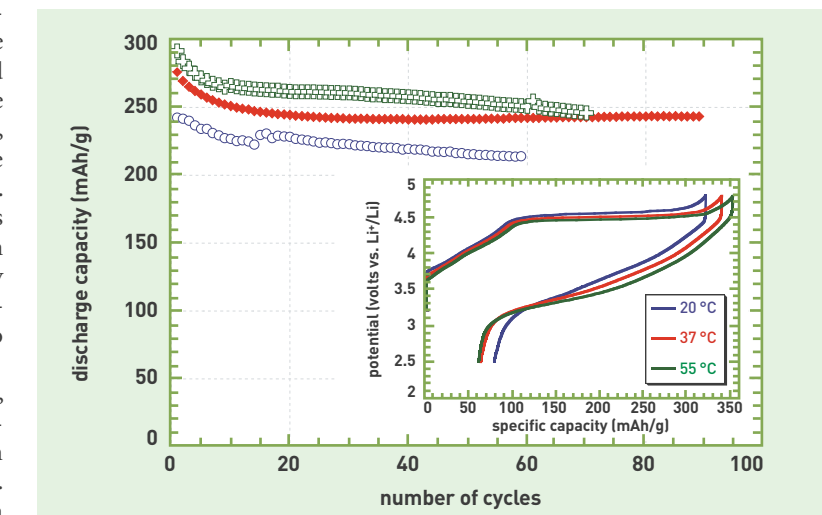


Figure 3.

Specific discharge capacities, at various temperatures, as a function of the number of cycles (10-hour discharge rate), for Li-metal button cells using a lithium- and manganese-rich lamellar oxide. Inset: potential/capacity curves for the first cycle.

intended for mass markets, in particular for the electric car market – hence the numerous academic, and industrial research efforts currently targeting these compounds. For that purpose, researchers yet have to achieve stabilization of specific capacity, under cycling conditions, and improve specific capacity at usual operating temperatures (the most useful reported values as a rule being obtained at 55 °C, for slow charge/discharge rates).

Researchers, and manufacturers anticipate that, with these innovative materials, significant gains will be achieved, in terms of energy, for the Li-ion storage batteries of the future.⁽¹¹⁾

Power electronics materials, and nanomaterials

Next to extended-runtime mobile devices, power electronics should provide major openings for Li-ion storage batteries affording the ability to go through rapid charge/discharge cycles. Such a breakthrough entails, imperatively, optimizing the performance of these storage batteries, in terms of power, and thus switching to innovative electrode, and membrane materials, better suited to this type of application. Among the candidates at hand, lithium **titanium** oxide ($\text{Li}_4\text{Ti}_5\text{O}_{12}$) provides an outstanding alternative to the graphite negative electrode. Owing to a higher potential than that ensured by carbon,⁽¹²⁾ this oxide, featuring as it does a spinel structure, allows very rapid battery charging, even over many cycles, with no risk of lithium dendrites⁽¹³⁾ forming (see Figure 4).

(6) The term “polyanionic framework” refers to compounds of the SiO_4 , PO_4 , P_2O_7 , P_3O_9 , GeO_4 ... type, in contrast to single oxides, e.g. spinel, or lamellar oxides.

(7) 165 mAh/g, and 287 mAh/g, respectively, for the two phosphates mentioned here, as against 147 mAh/g for spinel oxides.

(8) Of the LiMO_2 type (where M stands for one or more transition elements).

(9) In particular oxides of the $\text{Li}(\text{Li},\text{Mn},\text{M})\text{O}_2$ type.

(10) They may be described in terms of a two-component notation, of the type $y\text{Li}_2\text{MnO}_3 \cdot (1-y)\text{LiMO}_2$, where y ranges from 0 to 1, M stands for an element such as Mn, Ni, Co.

(11) From 90 Wh/kg in 1990 to more than 200 Wh/kg in 2009 in commercial systems, on to 250 Wh/kg in 2010, through to more than 300 Wh/kg in 2013.

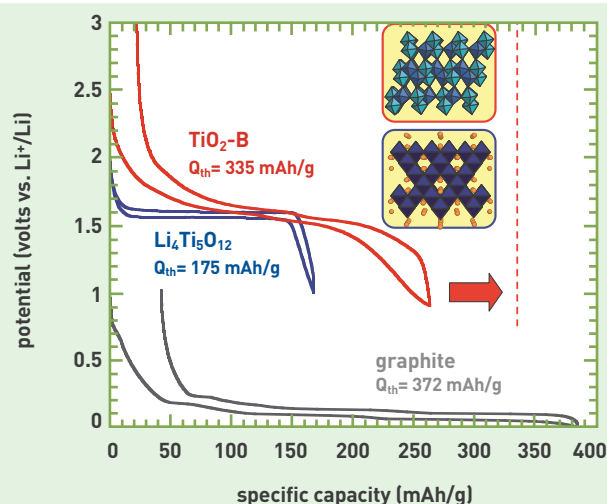


Figure 4. Potential/capacity curves for a graphite, and $\text{Li}_4\text{Ti}_5\text{O}_{12}$ and $\text{TiO}_2\text{-B}$ titanium oxides. The two insets (on top, on the right) are schematics of the atomic arrangements for the two titanium oxides, the cycling curves for which are also plotted in the graph. The red arrow (bottom right) indicates the theoretical value for TiO_2 ; there is a margin for advances, in contrast to lithium titanium oxide ($\text{Li}_4\text{Ti}_5\text{O}_{12}$). As for the $\text{TiO}_2\text{-B}$ (bronze) formula, this identifies the specific structural variety, of which 7 or 8 are known for TiO_2 .

Titanium dioxide (TiO_2) stands as the other solution seen as an alternative to the graphite negative electrode. This compound, in the **bronze** form, was highlighted, in the early 1980s, by Professor René Marchand, at the Nantes (France) Solid-State Chemistry Laboratory (**Laboratoire de chimie des solides de Nantes [CNRS]**). The compound exhibits a theoretical capacity of 335 mAh/g,⁽¹⁴⁾ corresponding to the complete reduction of all Ti^{4+} ions to Ti^{3+} . The compound's open structure, favorable as it is to Li^+ ion insertion, accounts for the growing number of scientific publications on this structural form, from 2005 on. Currently, two main synthesis routes are available, each involving three steps: the solid-state route, or the hydrothermal route – by way of ion exchanges – both of these involving dehydration (see Figure 5). In the laboratory, the synthesis route involving, as its chief step, a solid-state reaction was found to be more advantageous than hydrothermal synthesis – as the route chosen influences grain size, and morphology.

(12) 1.55 V vs. Li^+/Li , as against 0.1 V vs. Li^+/Li for graphite.

(13) A lithium dendrite results from the gradual growth of a lithium-metal outcrop/filament from the negative electrode, this being liable to pierce the separator, thus short-circuiting the system: the two electrodes being connected by this lithium dendrite, which acts as a conductor for the current.

(14) 175 mAh/g for $\text{Li}_4\text{Ti}_5\text{O}_{12}$.

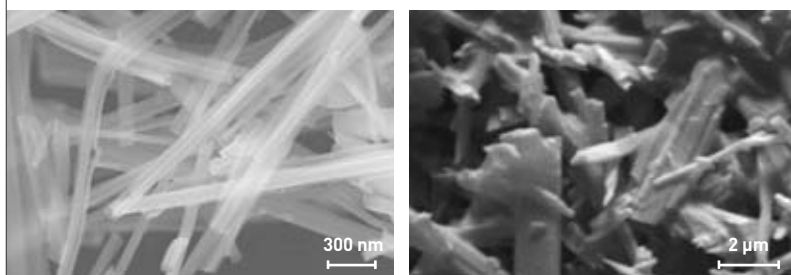


Figure 5. Images, obtained under scanning electron microscopy, of $\text{TiO}_2\text{-B}$ powders, obtained by the hydrothermal route (left), and solid-state route (right).

Powders featuring particles of controlled, varying sizes, and morphologies have been prepared at LITEN, with results on a par with the best research studies in the scientific literature. With a capacity higher than 220 mAh/g at slow charge/discharge rates, the electrochemical results obtained with this form of titanium dioxide are proving highly encouraging. On the other hand, behavior at higher rates is still found to be inferior to that of lithium titanium oxide: 60% of nominal capacity being recovered at 10 C, i.e. in 6 minutes, as against 80%.

High-safety, low-cost materials

If it is to meet the requirements of high-consumption markets, such as the automotive market, or **photovoltaic** solar energy, conventional Li-ion technology, relying on cobalt oxide, and graphite, must adapt. As regards Li-ion batteries, a range of considerations militate in favor of switching away from the active compound currently used for the positive electrode (cost, volume production constraints, power performance, safety...), to go for another material, **lithium iron phosphate** (LiFePO_4), featuring an **olivine** structure (see Figure 6). This is a credible alternative to cobalt oxide, as indeed to the other lamellar oxides, as it has already been commercially available, for use in mobile devices, for some years now, and is in an advanced stage of testing for electric vehicle purposes. The theoretical capacity exhibited by this iron phosphate stands at 170 mAh/g, and the advances achieved over the past few years have made it possible to come close to that figure, in experimental conditions. Be that as it may, operating potential (3.45 V vs. Li^+/Li), and density (3.5 kg/L) remain lower than those found for cobalt oxide (around 4.0 V vs. Li^+/Li , 5.1 kg/L). On the other hand, lithium iron phosphate does afford very low cost, considerable cycling lifetime, and a safety aspect markedly better than is the case for lamellar oxides, particularly in the charged state. This is accounted for by the high thermal, and chemical reactivity exhibited by lamellar oxides in the charged state, when they come into contact with the electrolyte.

However, notwithstanding the benefits it affords, owing to its low cost, and safety qualities, the electrochemical performance exhibited by lithium iron phosphate does still call for optimization – as this compound is an insulator (this making for low practical capacity, compared to theoretical values, the more so the higher the charge/discharge rate). Consequently, ever since it was discovered, in 1996, at the **University of Texas at Austin** (USA), the compound has been targeted by numerous studies, conducted by many research teams. Since 2001, LITEN has been investigating a number of synthesis methods, resulting in several patents being registered:

- hydrothermal synthesis (yielding particles of controlled morphology, homogeneous as a rule);
- synthesis involving use of a growth inhibitor (to restrict crystal growth, and promote lithium diffusion);
- boron “**doping**” (to enhance conductivity);
- synthesis by the “citrate” route (using citric acid, combined with nitric acid, and other nitrates, resulting in the *in-situ* formation, during synthesis, of a conducting carbon film, at the surface of the LiFePO_4 grains).

The most successful material, LFPB, has been the subject of a technology transfer agreement. After going on to the pilot scale, industrial production is presently being contemplated, with a view to supplying battery manufacturers.

At the present time, given the state of our knowledge, for the purposes of constructing a 1 mAh–100-Ah Li-ion storage battery, researchers use lithium iron phosphate together with graphite (about 140–160 Wh/kg), lithium titanium oxide,⁽¹⁵⁾ or silicon/carbon composites (170–180 Wh/kg), depending on the application, and relevant specifications.

Prospects

The heady growth in demand from industry, as regards the storage of electrical energy, nowadays concerns virtually all application sectors (mobile electronic devices, automobiles, homes...), their requirements directing the thrust of research. As regards, more specifically, dedicated materials for Li-ion technology purposes, the stabilization of high-voltage systems, or the development of lamellar oxides exhibiting reversible capacities higher than 200 mAh/g will soon make it possible to arrive at the 250 Wh/kg mark, indispensable if the new, ever more energy-hungry applications are to be catered for. Used together with stabilized silicon/carbon composites, these materials herald storage battery designs that will come close to 300 Wh/kg. Such systems may then be integrated into the high-energy-consumption mobile systems of the future (3G telephony, scale models, video, space applications...). For automotive applications, new investigations, concerning the various families of polyanionic compounds, should result in the development, over the longer term, of a compound exhibiting higher energy density than that of lithium iron phosphate: an improvement by more than 20–30% is anticipated over the next three years, with ever-longer discharge times as the prize. As regards power electronics, for use in hybrid vehicles, or various types of tools (e.g. power drills), the current research effort is focusing on titanium-based compounds, to be used in association with a high-voltage material, affording the ability to counterbalance the falloff registered at the

(15) 60–80 Wh/kg, with less than 5% loss of capacity over 1,000 cycles.



Prototype go-kart, powered by a lithium storage battery.

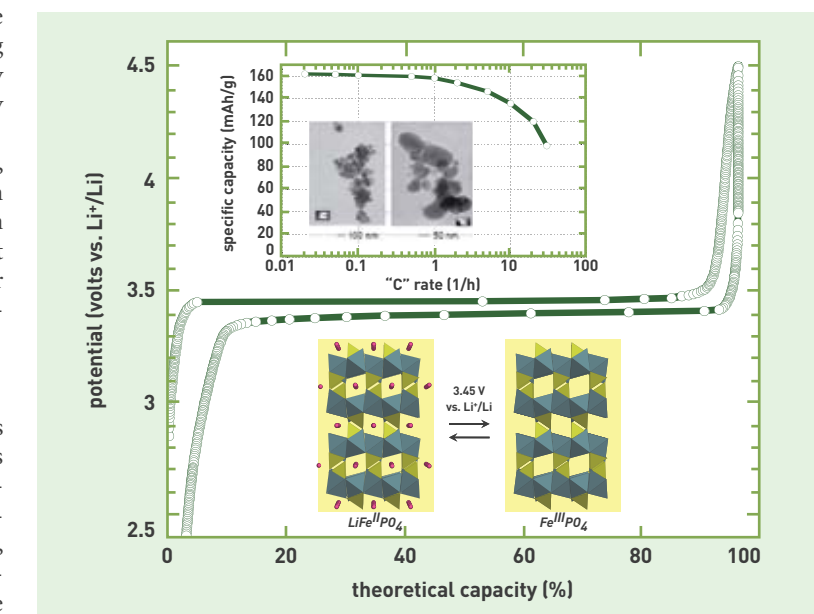


Figure 6.

Practical charge/discharge curve for a LiFePO₄/carbon composite. Lower inset: structural arrangements of the LiFePO₄ (initial/discharged state), and FePO₄ (charged state) phases. The pink spheres show the positions of lithium atoms in the structure. The upper inset shows, first, two images, obtained under transmission electron microscopy, illustrating the morphology, and size of LiFePO₄ grains; and, second, a curve plotting practical specific discharge capacity, as a function of the charge/discharge rate (C indicates that charging is completed in 1 hour). This latter curve highlights the satisfactory performance, in terms of power, exhibited by this compound (more than 60% nominal capacity being recovered at 30 C, i.e. for a discharge completed in less than 2 minutes).

negative electrode. In all of these cases, the electrolyte remains the privileged path for development, with regard to most of the technological solutions for high-voltage systems.

Looking further out than these short-to-medium-term goals, researchers are already looking to the development of alternative solutions to that of Li-ion technology, which as first blush remains restricted to 300–350 Wh/kg. For that purpose, LITEN is already investigating Li–air, and Li–sulfur systems, for which the negative electrode consists of lithium metal, while the positive electrode involves oxygen, and sulfur, respectively. In either type of system, the issue will be, first of all, to control the lithium electrode, which as a rule exhibits poor stability under extended cycling, at high charge/discharge rates; and, on the other hand, it will be necessary to develop an unconventional positive electrode, together with a compatible electrolyte – the technological issue that will have to be resolved concerns the air cathode in one case, the dissolution of sulfur, and of the polysulfides yielded by the cathode, in the other case. As for power electronics, this will call for innovative supercapacitor systems, involving high energies for supercapacitors (less than 20 Wh/kg), or hybrid systems, coupling a supercapacitor with a storage battery. Such systems are already under consideration.

➤ **Sébastien Martinet and Sébastien Patoux**
LITEN Institute (Institute for Innovation
in New Energy Technologies
and Nanomaterials)
Technological Research Division
CEA Grenoble Center

Rugged, safe hydrogen storage systems

Ensuring that hydrogen becomes the energy carrier of tomorrow entails not only that it be mass-produced, but equally that its distribution be guaranteed at all times, at every location throughout the land. A requisite that in turn entails that the issue first be resolved, of storing this energy carrier.

A polyurethane liner being extracted from its mold, at the end of a reactive rotational molding cycle. A typical fabrication cycle is carried out at 40 °C, and lasts 15–45 minutes, depending on component size, and formulation.



P. Stropia / CEA

The increasing scarcity of fossil energy resources, and the drive to curb greenhouse-gas emissions militate in favor of promoting an evolution, with regard to our energy supply system. Standing as it does in a range of possible alternative solutions, the hydrogen pathway is seen as one candidate worthy of very serious consideration, over the medium term. Indeed, a number of studies have confirmed that the prompt introduction of hydrogen into the energy production system could contribute to a considerable reduction in CO₂ emissions. For instance, in the road transportation sector, which would account for 85% of the reductions involved, the development of hydrogen technologies would make it possible to bring down CO₂ emissions by 50%, and oil consumption by 40% by 2050.⁽¹⁾ If energy resources, and demand are to be uncoupled, with a view to promoting the deployment of a true “hydrogen economy,” the ability to store this new energy carrier takes on a crucial importance, since this is found to be “a requisite, if an adequate match is to be ensured, between availability, and demand, this itself varying over time.”⁽²⁾

Hydrogen storage: the options under consideration

Achieving the capability to store hydrogen, to ensure its availability throughout the land, will be an arduous undertaking, and a costly one. This is due to hydrogen's very low molar mass, and equally very low liquefaction temperature, particularly with regard to mobile storage conditions. On the other hand, hydrogen exhibits a highly advantageous gravimetric (or specific) energy

density (33 kWh/kg, as against some 12 kWh/kg for gasoline, or diesel fuel), together with a very low volumetric energy density (3 kWh/Nm³ – i.e. under normal temperature and pressure conditions – as against 8.8 kWh/L, and 10 kWh/L, respectively, for gasoline, and diesel fuel). All of which characteristics warrant going for the design of storage systems intended for a low mass of hydrogen, compared to the masses of hydrocarbons carried, on board road vehicles in particular. On the other hand, such systems do require a large volume. For instance, for a vehicle having a range of some 500 km, the technical targets set involve the design of a tank for 5 kg hydrogen, corresponding to a vessel weight of about 90 kg, with a capacity of 125 liters at 700 bars, i.e. 70 MPa.

At the same time, the inherent characteristics exhibited by hydrogen, in particular in terms of flammability, and explosivity under certain confinement, and stoichiometry conditions, but equally its end applications entail a rugged, safe design for dedicated hydrogen storage systems. To that end, it will be useful to bear in mind the extensive use made of natural gas (methane, or butane/propane), and take our cue from this, for both fixed, and mobile industrial applications. Other models to be borne in mind are that of hydrogen, on an industrial scale: a grid of close to 1,600 km transport pipelines for pure hydrogen, operated at 10 MPa, mainly by Air Liquide, across northern France,

(1) HyWays, The European Hydrogen Roadmap, European Commission, 2008: <http://www.hyways.de/> or: http://ec.europa.eu/research/energy/eu/publications/index_en.cfm.

(2) Thierry ALLEAU, L'Hydrogène, énergie du futur? EDP Sciences, 2007.



P. Stroppa / CEA

Inner liners for type-IV high-pressure tanks, obtained by reactive rotational molding of polyurethane. This technology, involving thermoset-polymer liners, has been developed, and patented in collaboration with **Société Raigi** (France).

Belgium, and Germany; or that of street lighting in Paris, as carried out from 1815 and down to 1971, using a gas mixture consisting, for one half, of hydrogen (coal gas).

Classically, hydrogen may be stored in one of three forms: either in the liquid state (at 20 K, i.e. -253°C), in leaktight tanks, provided with enhanced thermal insulation; or in the gaseous state, at high pressure; or in the solid state, trapped within matrices having the ability to release it subsequently, as and when required. For transportation purposes, as for fixed applications, storage in the liquid, or **cryogenic** state is the favored solution, whenever the capacities involved are as high as several hundred kilograms, or more. On the other hand, for more usual volumes, or quantities, this form of storage becomes far less competitive, in techno-economic terms. For that reason, researchers at CEA have been pursuing two major development directions, to wit:

- compressed hydrogen storage, this being the most promising path, with regard to the results already achieved, and short- and medium-term requirements, and markets;
- solid-state **hydride** storage, for more specific applications, e.g. portable, and ultraportable devices (cell phones, computers...).

Currently, storage in the compressed gas form yet stands as the most mature solution, be it from a scientific standpoint, or industrially. There are good reasons for this: for a long time now, compressed-gas cylinders have formed part and parcel of our social fabric (for scuba diving, breathing apparatus for firefighters, butane/propane cylinders for domestic appliances, industrial and medical gas supplies...). The ruggedness, and safety of such devices have been proven by experience.

For compressed-gas storage purposes, four types of tank are used, at the present time, depending on the application, and desired operating pressure:

- type-I tanks, of wholly metallic construction, designed as a rule in low-alloy steel, to exhibit resistance to hydrogen embrittlement (e.g. 35 CD 4 steel, a low-alloy **chromium-molybdenum** steel subjected to a heat treatment⁽³⁾);
- type-II tanks, featuring the same architecture as the previous type, further featuring, however, a local reinforcement (hoop wrapping) applied to the cylindrical portion, typically involving **glass fibers**; such reinforcement allows cylinders to be made substantially lighter, or operating pressure to be increased;
- type-III tanks, designed to be constructed in **aluminum**, low-alloy steel, or **stainless steel**, feature a metal inner liner,⁽⁴⁾ reinforced by a full **composite** wrap,

or shell; when high-pressure operation is contemplated, such composite wraps are made of long **carbon fibers**, impregnated with **polyepoxy** matrices;

- type-IV tanks, also known as “all-composite” tanks, feature the same architecture as type-III tanks, involving however a **plastic material** (polymer) liner.⁽⁵⁾

Type-III and type-IV tanks gained acceptance early on as development standards, for high-pressure hydrogen storage purposes (at pressures ≥ 35 MPa, and typically up to 70 MPa). Indeed, they are the only designs affording the ability to meet the constraints set, in terms of compactness, and mass, by the requirements of supply logistics, and equally those entailed by integration into automotive vehicle platforms. Of these two models, CEA favors a high-pressure hydrogen storage technology involving all-composite tanks, hence type-IV tanks. It should be pointed out that such tanks, in contrast to their metal-lined counterparts (type-III tanks, in particular), afford the advantage of outstanding resistance to **thermomechanical** fatigue, i.e. to successions of filling/draining cycles. The chief quality they exhibit is thus their outstanding lifetime. Moreover, type-IV tanks further make it possible to achieve gravimetric storage densities 20–30% higher than is feasible with type-III, steel-lined tanks.

Fabrication technologies

Four main technologies come to the fore, for tank fabrication purposes:

- As regards fabrication of the gas-tight **polymer** inner liner, CEA is developing, in collaboration with partners in industry, and academe, innovative materials, and processes, in order to meet the specifications entailed by hydrogen storage. In particular, CEA is pursuing development of the so-called “reac-

(3) For this alloy: 0.37% C, 0.79% Mn, 1% Cr, 0.18% Mo, 0.30% Si.

(4) This type of tank is based on the “Russian-doll” principle, i.e. it involves two nested envelopes. The first, inner envelope, known as the liner, fulfills the prime function of ensuring hydrogen tightness. The outer envelope, i.e. the composite shell, acts as the tank’s structural component, enabling it to withstand the various mechanical, and thermomechanical stresses it is subjected to (pressure, aggressions...).

(5) With regard to storage in compressed form, the overpressure aspect is common to all compressed-gas tanks (i.e. operating at pressures higher than atmospheric pressure).



P. Stroppa / CEA

Rotational molding equipment, serving to rotate the mold about two perpendicular axes, to ensure optimum distribution of the material, during the reactive forming process. The mold features a network of channels, carrying a cooling fluid, allowing outstanding temperature homogeneity to be obtained over the entire mold surface.

A thermoplastic polymer liner – shown here with its metal connectors inserted – obtained in a single step, by reactive rotational molding. Inner volume stands close to 34 liters, while the constituent material is polyamide-6.



P. Stroppa / CEA

tive rotational molding” process, involving the *in-situ* synthesis, and forming of **thermoplastic** polymers, and **thermoset**⁽⁶⁾ networks, in a single step, at low temperature. This process is found to be particularly suitable for the fabrication of large ($> 10 \text{ m}^3$), hollow objects. Of the materials developed in this context, the **polyamide** has already been the subject of an industrial licensing agreement, while the **polyurethane** is presently undergoing evaluation, under the aegis of a project receiving funding support from OSEO. Going over to the industrial stage is on hold, pending confirmation of performance.

(6) Thermoplastic polymers are fusible (i.e. they melt when heated to a temperature higher than their melting point), whereas thermosetting polymers form nonfusible, insoluble 3D networks



P. Stroppa / CEA

Typical composite architecture for a hydrogen tank, seen here in a tank fabricated by filament winding. This technology allows a succession of resin-impregnated carbon-fiber plies to be laid, at varying angles, determined so as to ensure optimum thermomechanical behavior for the structure.

- As regards the composite shell, i.e. the composite component wound around the liner, the point is to ensure its ability to withstand both internal pressure, and outside aggressions (impacts, chemical agents...). To that end, it is fabricated from continuous reinforcement fibers, impregnated with an organic binder, by the filament winding process. The polymer liner acts as a mandrel, over which the resin-impregnated (e.g. with epoxy resin) fiber is laid, at an angle that is determined beforehand by the dimensioning calculations. Bearing in mind the operating stresses involved, the aim is to optimize the resulting structure, in order to minimize the quantity of materials employed, and thus achieve savings in terms of cost, volume, and mass. In most cases, the outcome is a so-called “multiangle” structure, i.e. a structure built up from stacked plies, successively laid at angles varying from one ply to the next. To achieve the performance expected of it, the shell must further undergo **polymerization**, while rotating in a thermal chamber.

- Filament winding affords the benefit of resulting in composite architectures exhibiting twin qualities: a high volume fraction of reinforcing fibers (typically 65%), and structures exhibiting high gravimetric performance (i.e. a high performance/mass ratio), compatible with very high pressures. The continuous fibers used for that purpose chiefly come under the high-strength fiber category. In this respect, while carbon fiber remains the inescapable solution, for onboard applications, owing to the compactness of the storage volume, **glass**, or **basalt fibers** afford satisfactory potential, with regard to less constraining applications, e.g. fixed storage facilities. However, owing to the fiber mass involved, and



P. Stroppa / CEA

Fabrication of a composite structure by filament winding, from continuous carbon fibers.



P. Stroppa / CEA

The stacking of hoop, and spiral plies, resulting in the fabrication of the tank's structural composite shell.



P. Stroppa / CEA

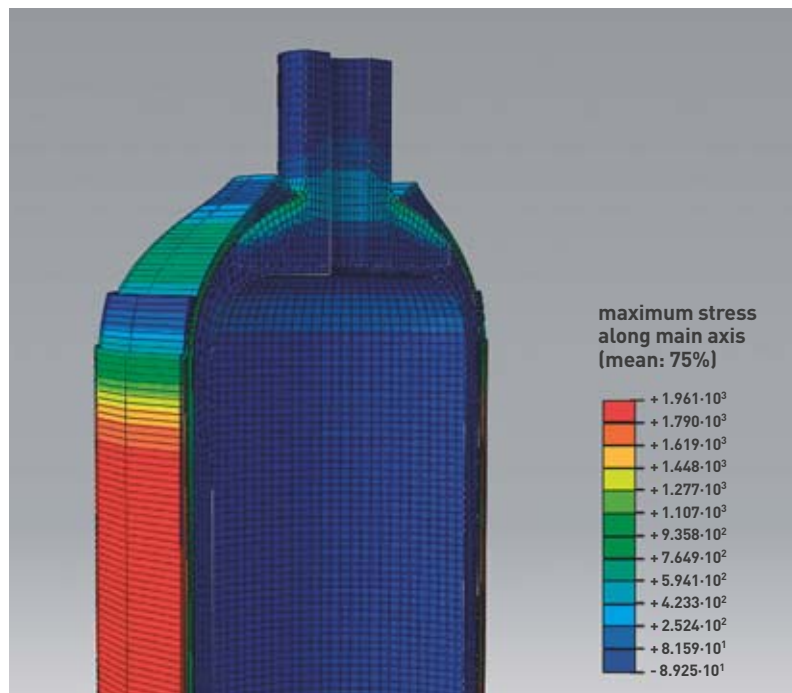
Development work for a tank instrumentation technology involving the integration of optical fibers at the core of the composite structure, during fabrication. These investigations have the purpose of arriving at a better evaluation of the stresses multilayer composite architectures are subjected to, in order to enable their optimization, in the longer term, and – if required – allow such structures to be monitored under operating conditions.

corresponding cost considerations, the option selected is seen to be peculiarly critical, depending on the application. Indeed, while such materials are found to be particularly advantageous, the quantities of fibers used, to fabricate the composite shell, must be managed as sparingly as feasible, to avoid arriving at a prohibitive cost, with regard to the application, or market conditions. Thus, in practice, for 70-MPa onboard applications, the cost of the fiber reinforcement may account for 50–75% of the vessel's final cost. Concurrently with the selection of the appropriate fiber/matrix couple, for the target application, the numerical design, and dimensioning steps also prove decisive, in the fabrication of safe, durable, and competitive tanks.

- For the purposes of providing data for [computation codes](#), ensuring structure validation, or monitoring the tank's in-service integrity, researchers are looking into the feasibility of inserting [optical-fiber](#) sensors directly within the thickness of the composite structure. Achieving this would make it possible to detect initial signs of tank damage, at the microscopic scale. Information that would prove invaluable, for the purposes of addressing the optimization of shell fabrication, at the design stage; or evaluating composite sensitivity, and behavior, when subjected to specific stresses; or adjusting inspection periodicity, and operating lifetime for these objects. Two teams are working on this, at CEA: one at the Materials Department, at the Le Ripault Research Center (central France), the second at the Systems and Technology Integration Laboratory (LIST: Laboratoire d'intégration des systèmes et des technologies), at Saclay (near Paris).

Challenges, and prospects

As of now, the performance exhibited by such tanks has already reached levels compatible with a number of emerging applications. Researchers at CEA are carrying through the development of novel materials,



CEA

Result of modeling maximum stress in the structure of a tank pressurized to 2.25 times operating pressure (in MPa units).

and processes, with a view to optimizing the performance/cost tradeoff, improving the techno-economic compatibility of these systems, and thus speeding their industrial deployment. They are further addressing tank instrumentation, and the [modeling](#) of tank behavior, with regard to the stresses they are anticipated to be subjected to in service – the aim being to arrive at improved composite architectures, while minimizing the quantities of fiber employed. At the same time, CEA is participating in a number of European projects, in particular with regard to pre-standardization research (Standardization Committee), and is thus contributing to bringing about changes in existing regulations, governing the design, and qualification/requalification of high-pressure composite tanks. The safety of compressed-hydrogen tanks is likewise seen as a prime challenge. The aim is to demonstrate that their behavior can be controlled over the long term, whether under normal operating conditions, or in accident conditions. The proportion of composite materials being introduced in everyday, or industrial applications is steadily increasing (airplane components in the aerospace industry, butane/propane cylinders, or sports equipment for private consumers). It should be pointed out that such composite materials allow, in many cases, distinctive, and [anisotropic](#) properties to be combined, while keeping to a highly attractive mass budget.

At the present time, the margin for advances afforded by composite materials, with regard to hydrogen storage, remains quite considerable. In coming years, these materials should make it possible to integrate new functions, and provide novel solutions, as regards the storage of other industrial, or medical gases, while bringing about significant improvements, in terms of systems compactness, and transportability.

➤ **Fabien Nony**

Materials Department
Military Applications Division
CEA Le Ripault Center

Photovoltaic energy ramps up

Standing as it does as an unending, immediate, instant source of energy, and a low greenhouse-gas emitter at that, the Sun is still inadequately exploited. **And yet, using this solar energy, it is possible to generate either heat, by making use of various physical phenomena – e.g. from thermodynamics, or thermics – or electricity, by way of photovoltaic conversion.** This provides the most promising path, for the purposes of generating “clean” electricity. In this respect, CEA, strongly involved as it is in research on low-carbon energies, currently stands as one of the major players in this photovoltaic pathway.



Roof-integrated photovoltaic panels (INES).

Photovoltaic technology makes it possible to recover energy from the Sun's light, directly converting it into electricity, by way of solar cells, which in turn are assembled to form modules (see Figure 1). A number of materials are opening up, as of now, highly advantageous prospects, as regards effecting such conversion. Some of these materials are well known, already quite widespread, and are to be seen on rooftops: such is the case of multicrystalline silicon wafers; others, still at the laboratory investigation stage, stand two, or five years, or maybe ten years or more away from being taken to the production stage: one example being copper compounds in thin film form. These materials are selected with regard to two criteria: photovoltaic conversion efficiency, and cost of the material.

Silicon still ahead of the field

The conversion of solar energy to a form suitable for use in present-day sites, and buildings may be effected along one of two paths: solar-thermal, or solar-electric. The electric mode is realized by way of photovoltaic (PV) conversion within a material of the semiconductor type – whether organic, or inorganic. A variety of photovoltaic energy conversion mechanisms may currently be encountered, depending on the active materials involved, to wit:

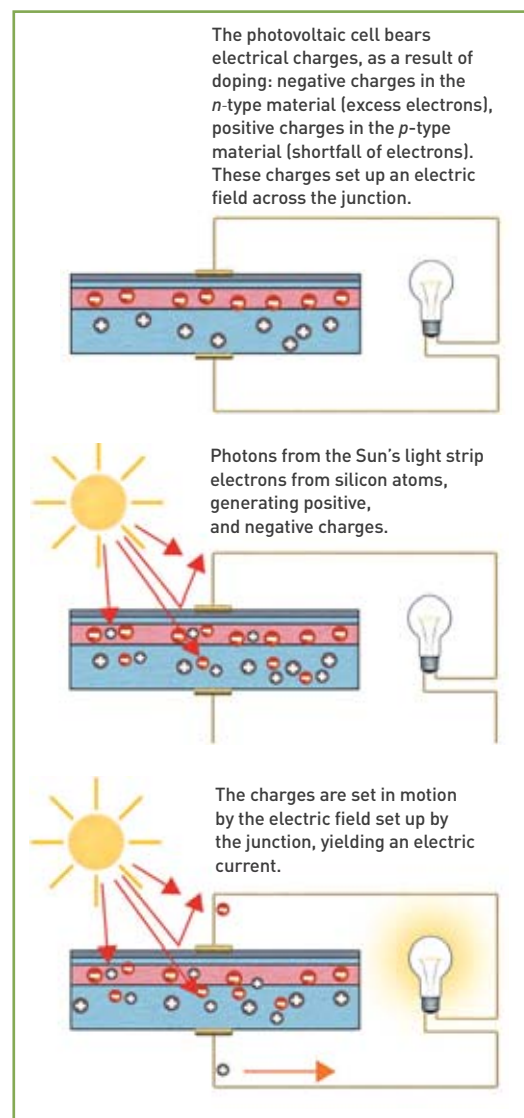


Figure 1
Operating principle of a photovoltaic cell.

- **pi-conjugated** organic materials, e.g. semiconducting **polymers** (used in combination with **fullerene** derivatives), or dyes used in **biomimetic** structures, or in hybrid structures also containing inorganic **nano**-structures;

- semiconductor materials, grouped into various families (III–V, or II–VI compounds),⁽¹⁾ or other, more specific compounds, whether copper- (CuO), iron- (FeS₂), or zinc-based (Zn₃P₂);

- silicon, which stands apart, owing to its abundance in the Earth's crust, and extensive employment in metallurgy, or **microelectronics**.

Employment of these materials may call for finer-scale differentiation – this involving forming, and structuring them, to obtain a device having the ability to meet a number of optical, and electronic criteria. The resulting product is a **photovoltaic solar cell**, which may be used as part of an energy generation system, most commonly by being integrated into a solar panel.

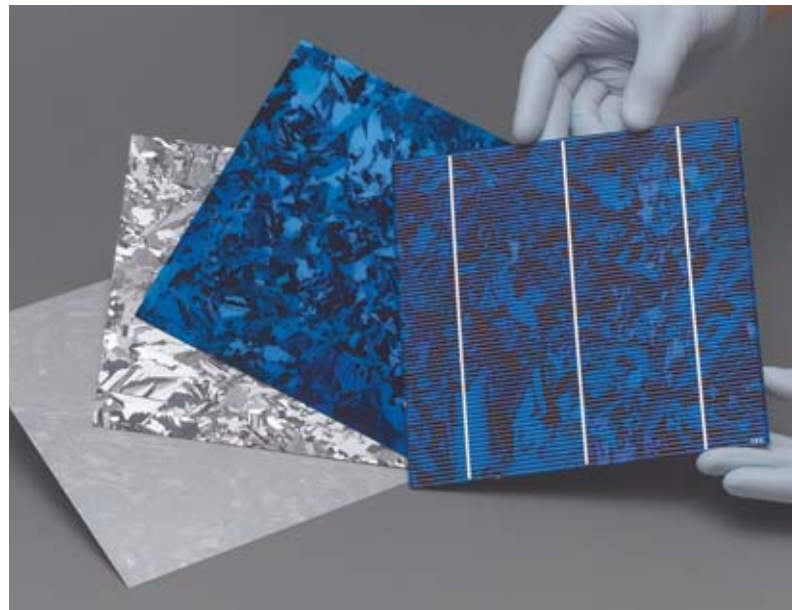
The electro-optical performance exhibited by such materials is proportional to the product of several factors: the fraction of incident light that penetrates into the material; the fraction of this light that is then absorbed within the material; the efficiency with which these **photons** are converted into electron charges; and the resulting electrical potential arising at the terminals of the said material. Ideally, therefore, the material at the core of such a cell should exhibit twin qualities:

- a high sunlight **absorption** capability, for as small a volume of material as feasible;

- satisfactory separation, and transport of photo-generated charges to the cell's terminals – while incurring as little loss as feasible at defects liable to recombine **electrons**, and holes – in such a manner as to allow an electrical structure to be set up, that allows these charges to be recovered outside the material.

Silicon is one of a family of semiconductors exhibiting properties that are well known to scientists, and

(1) The III–V family of semiconductor compounds covers, in particular, gallium- (Ga), arsenic- (As), aluminum- (Al), indium- (In), and phosphorus- (P) based alloys: i.e. materials involving elements from columns III, and V in the periodic table of elements, e.g. GaAs, InP, GaAlAs, GaInP; the II–VI family of semiconductor compounds covers lead- (Pb), sulfur- (S), cadmium- (Cd), tellurium- (Te), manganese- (Mn), and zinc- (Zn) based alloys: i.e. materials involving elements from columns II, and VI in the periodic table of elements, e.g. PbS, CdTe, CdMnTe...



CEA/D. Michon/Artechnique

200 × 200 mm² silicon wafers, at various stages in the fabrication of a cell: from left to right, after slicing by wire sawing; after the emitter has been textured, and formed; after deposition of the blue antireflection coating; and after forming of the contact grids (finished cell, ready for assembly into a module).

manufacturers: electrical, and optical properties that are fully controlled, as are the fabrication technologies involved (in some cases coming from technologies used in microelectronics). Nowadays, this material is employed, in particular, for the purposes of photovoltaic conversion, in wafer form, and is further to be found in most current electronic products, in this case in the form of **integrated circuits**, also known as microchips (in cell phones, microcomputers), but equally in metallurgy, for metal **alloys**... In the monocrystalline (single-crystal) form, silicon is obtained by way of crystal-pulling methods: for instance, by the Czochralski process (whereby an ingot is pulled by a seed rod from a bath of silicon melt in a furnace), or the float-zone (or zone-melting) process (whereby a solid polycrystalline ingot is melted, and crystallized, by passing a heating device along the ingot, held in



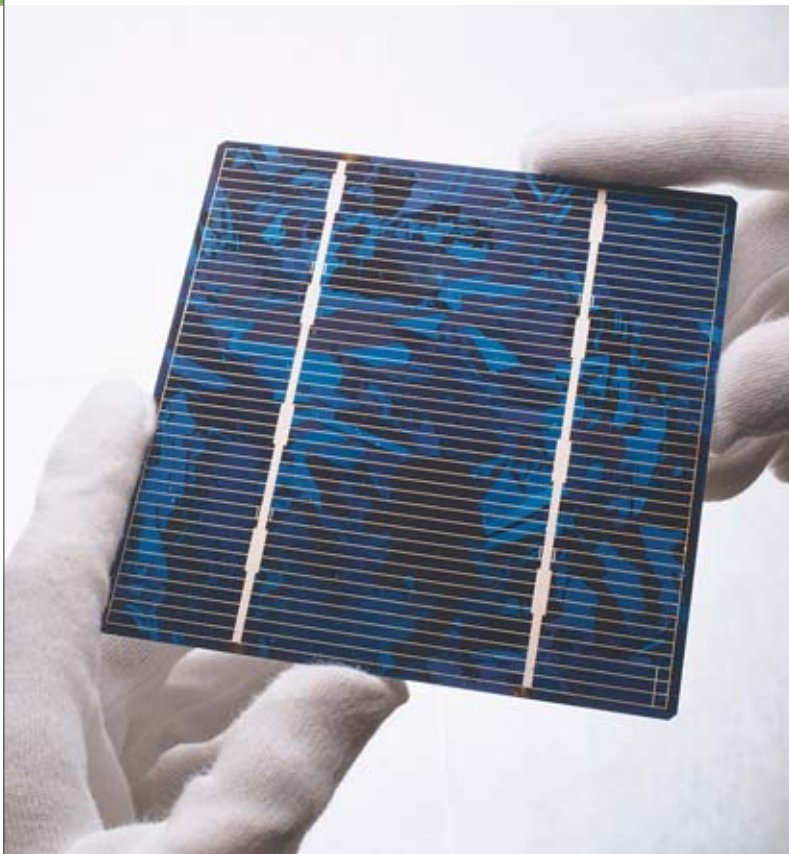
P. Dumas / CEA

A silicon ingot, used for a development study [of laboratory size: 4 kg].



CEA/D. Michon/Artechnique

Laser grooving of silicon wafers. Separation of the front diode from the rear diode. Treatments are carried out in white rooms, using equipment close to industrial standards, which facilitates process transfers.



Multicrystalline-silicon photovoltaic cells by Photowatt. A view of the front face, showing the contact grid, and the antireflection coating (blue).

contact with a seed crystal). Both processes are fully mastered, subsequent to development over many years by the microelectronics industry. For photovoltaic conversion purposes, employment of multicrystalline silicon is favored, owing to its low cost, due to high process outputs (several hundred kilograms), readily obtained, simply by cooling the melting crucible. Rather than a monocrystal, the material obtained consists of a number of fully adjusted crystals – referred to as “grains” – much in the manner of a three-dimensional puzzle. Of

varying shapes, and sizes, these grains are separated by grain boundaries. During solidification, grain nucleation, and crystallization are controlled, in order to obtain large, columnar grains. As a result, once the ingot is sliced into wafers a few hundred microns thick, the grain structure carries through from one side of the wafer to the other – minimizing the number of grain boundaries present, liable to occasion electrical losses.

Once silicon has been obtained in the form of a crystalline rod, some 10–30 cm in diameter, and 1 meter long, a crucial step follows, namely crystal sawing: the rod is cut into slices (wafers), used for the fabrication of photovoltaic cells. This is a highly delicate operation, an indispensable one however, if extremely thin wafers are to be obtained. In order to cut down material wastage, while a low thickness is indeed desired, a minimum thickness is nonetheless required, to ensure adequate mechanical strength for the wafers, thus allowing them to be handled. Currently, that thickness stands at 150 microns, this being set to come further down over the next few years.

Cell fabrication entails that the material be doped, usually by introducing impurities such as phosphorus, or boron. As the doping impurities do not possess the same number of electrons as the silicon atoms in the crystals, these excess charges modify the electrical properties exhibited by the silicon. This doping step makes it possible to control the manner in which the silicon obtained conducts an electric current. This operation is carried out by thermal diffusion, either during crystallization, or subsequently, by way of a surface treatment of the wafers. This allows a p–n junction to be set up, i.e. it sets up an electric field across the semiconductor material: it thus becomes possible to segregate the electrons, and holes arising as result of light absorption. These electrical charges can then be carried along to the electrical contacts, through to the wafer’s terminals (see Figure 2). The charges thus make up the electric current delivered by the solar cell.

While boron, and phosphorus stand as useful, controlled impurities, with regard to electronic properties, such is not the case as regards many other

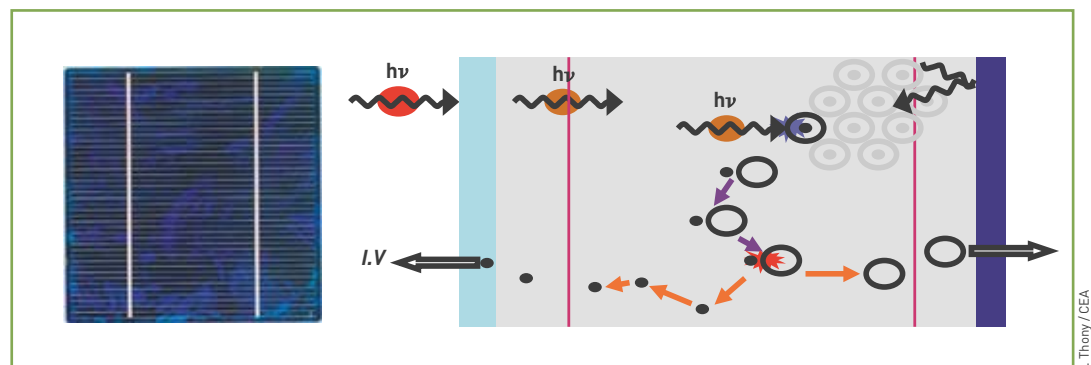


Figure 2.

A standard silicon-wafer-based solar cell (left panel). Operating principle of a silicon solar cell (right panel), showing the front face (in light blue), the rear face (dark blue), and the p–n junction electrical structure (purple line). Photons are indicated as $h\nu$ (this standing for the quantity giving the photon’s energy, viz. the product of Planck’s constant by the light frequency, as a wave). Absorption of a photon is indicated by the blue zigzag line, the separation of an electron, and a hole by the red star flash.

The electrical power delivered is the product of current intensity by voltage ($I \cdot V$). The circles stand for atoms that have absorbed a photon; an electron is then released (shown as a black dot). Subsequent to absorption of a photon, diffusion of the electric charges takes place, to the electrodes (blue); the electron setting off to the left, the other, complementary charge being known as a “hole,” i.e. an absence of electron. The orange arrows show the diffusion of charges across the silicon.



P. Dumas / CEA

Boron and phosphorus diffusion furnace, used for doping purposes (Restaure platform-INES).

elements – e.g. iron, **carbon**, or oxygen. Indeed, certain elements, and some crystal defects are found to impair charge transport to the **electrodes**: they act as traps, and recombination centers. Further, such elements, and defects may come together, forming complexes – stable, or unstable – the effects of which on carrier photogeneration, and recombination are as yet imperfectly understood. An adequate level of material quality thus has to be determined – sufficiently pure, not too much however, since high purity entails high cost: such being the case, in particular, for the silicon produced by the microelectronics industry. This is one of the research directions currently being pursued at CEA.

In wafer form, silicon still stands, at the present time, as a truly peerless material, with regard to photovoltaic applications. Alloys are sometimes put forward in this respect, with **germanium**, carbon, or even **tin**; however, this is still very much in the realm of forward-looking research.

Emerging materials

Standing as the favored material, owing to the simplicity of design it allows, and its low cost, wafer silicon does nevertheless call for improved performance. This entails enhancing the “coupling” arising between sunlight, and the silicon film. The issue of the coupling between incident optical-wavelength radiation (sunlight), and semiconductor was addressed as early



P.-F. Grosjean / CEA

A white room used for energy microsources.

as the mid-1990s. At the present time, however, recent advances have made it a serious proposition to achieve improved performance, provided two issues are resolved:

- a fraction of incoming light undergoes reflection, and thus does not penetrate the material – this affecting only 10–20% of light, for the most commonly used technologies;
- a major fraction of light penetrating into the semiconductor film, to undergo absorption inside it, involves wavelengths that are poorly matched to the material (some 15–30%); this results in a shortfall, arising from the difference between the energy exhibited by incident photons, and that of the electron charges yielded by the silicon.

For the purposes of finding solutions to these two issues, and enhance the efficiency of present-day solar cells, from 20–25% to 40–60%, teams coming under the Physical Sciences Division (DSM), and the Technological Research Division (DRT) at CEA are working on the fabrication of nanostructured silicon. This comes in the form, in particular, of silicon nanoparticles, or nanowires (see Figure 3), in such shapes, and sizes as to make it possible to trap light within the cell, but equally allow absorption **quantum** efficiency to be raised. The explanation: effects, accounted for by quantum-mechanical theory, make it possible to tune the absorption spectrum (or, more accurately,

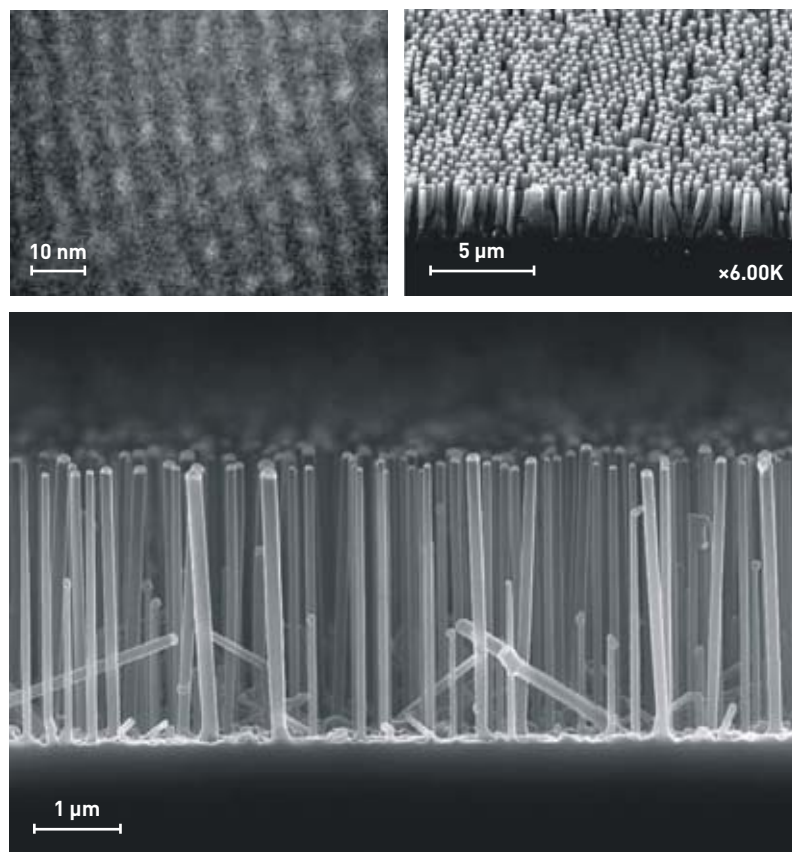


Figure 3. Nanocrystals fabricated at the Ions, Materials, and Photonics Research Center (CIMAP: Centre de recherche sur les ions, les matériaux et la photonique), run under CEA oversight (top left); microwires etched at the Institute for Innovation in New Energy Technologies and Nanomaterials (LITEN: Laboratoire d'innovation pour les technologies des énergies nouvelles et les nanomatériaux), using a chemical route involving catalysts (top right); crystalline silicon nanowires, fabricated at the Nanosciences and Cryogenics Institute (INAC: Institut nanosciences et cryogénie), a few microns long, and with a average diameter of 100 nm, obtained by chemical vapor growth (bottom).

The D2M platform, an item of equipment serving to effect the ordered deposition of micro-, or nanoparticles, onto small-, or large-area substrates (from a few square centimeters to several hundred cm²).



P. Auvion / CEA

the width of the semiconductor's forbidden band), to match the solar spectrum, this resulting in a markedly increased electrical energy yield for the cell, since, in this manner, the energy of the electron charges generated matches the incident photon energy. Were such an adjustment not to be made, the energy difference, between incident photons, and charges generated within the silicon would be dissipated (and therefore lost), in the form of heat.

In order to bring down material costs, manufacturers, and research laboratories are bringing forward thin-film photovoltaic cells. Films of active material are deposited onto inexpensive substrates, e.g. window glass, or sheet steel, but equally onto more innovative substrates, such as polymers, paper, fabrics... With material thicknesses now reaching barely a few microns, it becomes feasible to reduce

the quantity of material employed by a factor of 100. This entails taking care that the amount of electricity generated does not come down too far, since low thickness also means low sunlight absorption. This type of large-area cell is currently emerging on the market – such cells being referred to as second-generation cells. Their advent may well displace silicon from its dominant position, as the absorption coefficient of silicon makes it ill-suited for such a geometry. Indeed, as deposited in thin-film form onto glass, silicon is most commonly found as an **amorphous** material, exhibiting performance, in terms of electrical **conductivity**, that is likewise found to be markedly lower. In order to obtain crystallized silicon thin films, and recover more advantageous performance levels, high-temperature processes must therefore be resorted to, meeting stringent specifications in terms of grain size, and purity. This, on the other hand, does not resolve the issue of interaction with the substrate, owing to the diffusion of defects, and unwanted elements, from the glass into the layer of photovoltaic material.

With regard to thin films, a technique is now available, that makes it possible to improve the collection of charges generated within the photovoltaic material. This involves carrying out further deposits of transparent conducting **oxides**, e.g. tin oxide (SnO₂), or an alloy of this oxide with **indium** oxide (indium tin oxide [ITO]), or zinc oxide (ZnO). Currently, novel candidates (e.g. **carbon nanotubes**, **graphene**) are being evaluated in laboratories. Such extra layers are found to be particularly effective, with regard to enhancing conversion efficiencies for a number of photovoltaic structures: heterojunctions involving amorphous silicon and crystalline silicon; and organic cells.

Further materials are beginning to emerge on the market, highly promising in terms of costs, e.g. **cadmium** telluride (CdTe), a semiconductor material coming under the II–VI family of compounds. This



C. Dupont / CEA

Carbon nanotubes being laid out to form stacked mats, a technique lending itself to many applications, from industry (flat screens, fuel-cell membranes) to defense.

material, used as an intrinsic semiconductor, in conjunction with cadmium sulfide (CdS), already exhibits a conversion efficiency higher than 10% in modules. Notwithstanding issues experienced with tellurium (Te) supplies, and the risks involved in handling cadmium (Cd), modules are now being put onto the market. As the deposition technique involved is quite straightforward (a continuous process, over large-area glass panels), manufacturers are holding out, within a very short time, the prospects of energy production costs falling below the symbolic €1 per watt threshold.

A host of new startups are presently being set up, pushing a novel material, copper indium gallium selenide (CIGS). This is a compound of copper, indium, and selenium (i.e. a copper chalcogenide), to which gallium is added, to obtain an enhanced response to the solar spectrum. However, controlling a quaternary alloy invariably proves difficult. Consequently, a number of manufacturers are developing a variety of processes, involving physical (evaporation), or chemical routes (electrodeposition, or printing using an ink holding nanoparticles). As CIGS composition, in particular the indium/gallium ratio, has a direct impact on the bandgap of this semiconductor, this makes it possible to tune the material's absorption characteristics to match the solar spectrum, and to contemplate complex cell architectures, involving layers of varying compositions, to achieve very high conversion efficiencies (higher than 20%).

Aside from production-cost-related aspects, photovoltaic thin films afford further benefits, for the users of such systems. First, the substrate may be flexible, and the cell may be given any desired shape, facilitating its integration into all kinds of systems, and devices. Second, the design of photovoltaic modules exhibiting varying electric characteristics, to match a variety of applications, involves no major difficulty.

Semiconductor alloys for space applications

Photovoltaic conversion also provides a crucial source of energy for many satellites, and objects put into space. In the field of astrophysics, semiconductor materials from the III–V family have been adopted by all practitioners. The cells used are fabricated from epitaxially-grown crystalline layers, deposited one on top of the other by vacuum processes, of the molecular beam epitaxy type, or involving chemical vapor deposition of metallic precursor-based layers. Stacks of several tens of layers result in very-high-performance devices, comprising several basic cells stacked one above the other. Presently, it is thus becoming feasible to design lattice-matched stacks – i.e. stacked materials having an identical lattice constant, while exhibiting a range of bandgaps – and thus maximize photovoltaic conversion across the entire solar spectrum. A result that is made possible by the wide variety of compositions involved: a gallium arsenide (GaAs) substrate, with indium phosphide (InP), or germanium (Ge) in the epilayers. A number of organizations, e.g. the Fraunhofer Institute (Germany), or Boeing (USA), have achieved efficiencies exceeding 40%.

Owing to the very high cost of such structures, their use remains restricted to space applications, or centralized energy production arrays. In the latter case, cells are cut up into tiny components (of centimeter, or millimeter size), positioned at the focus of large optical systems, concentrating sunlight onto the cells. Such arrays call for mobile mechanical supports, having the ability to track the Sun's diurnal motion across the sky.

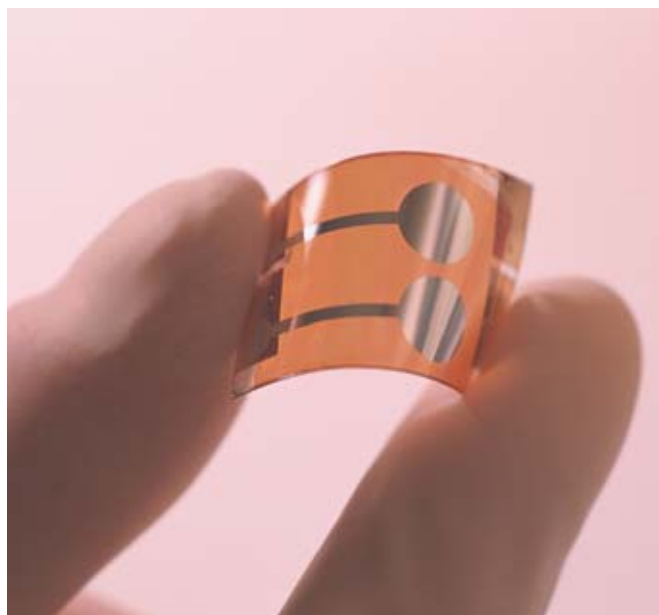
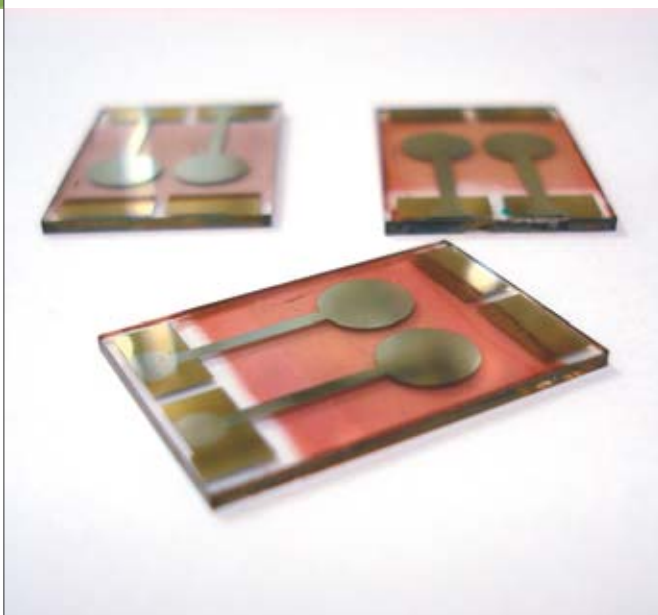
Organic, and hybrid materials

Photovoltaic conversion involving organic materials is a field of research that has emerged relatively recently. Major scientific breakthroughs were not achieved until the early 1990s, these including the construction of the first dye-sensitized solar cells to exhibit high efficiencies, or the discovery of the photo-induced charge transfer occurring between a pi-conjugated polymer, and a fullerene derivative. These discoveries opened the way to a new energy production pathway.

Organic materials afford a number of advantages: their optical and electronic properties are readily modulated, and their preparation is not costly, in energy terms. Moreover, they make for easy fabrication: they may be deposited, in particular, by way of printing techniques, or onto lightweight, highly flexible plastic substrates. Finally, as the thickness of the active layer involved is, as a rule, quite small (of the order of 100 nanometers), these materials may be used to impregnate large areas, while employing quite small quantities of material. On the other hand, the performance exhibited by such materials is limited, owing to lower charge mobilities than in inorganic semiconductor materials, and poorer stability.



Screen-printing the metal contacts onto a silicon photovoltaic cell.



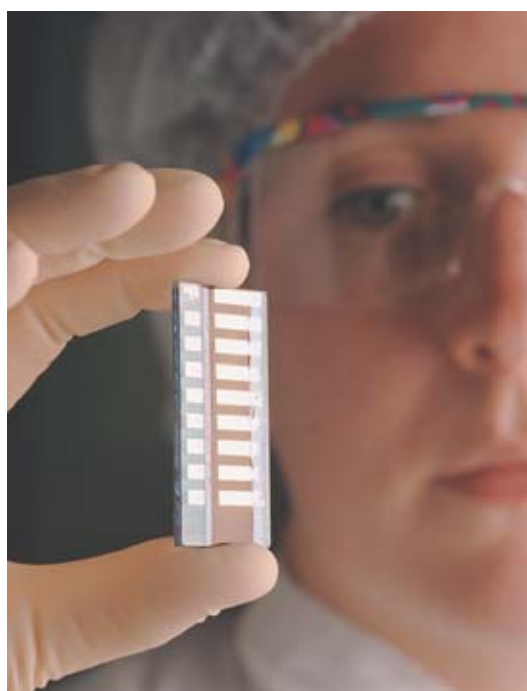
CEA/R. Demadrille (left) and CEAP/ Stroppa (right)

Organic, polymer- and fullerene-based photovoltaic cells, as fabricated on a glass substrate (left), and a flexible plastic substrate (right).

As is the case in so-called “conventional” solar cells, current generation in organic systems occurs as a result of the dissociation of **excitons** – arising owing to the absorption of photons by the material – at the interface between the *p*-type material (usually a *p*-conjugated polymer), and the *n*-type material (a fullerene derivative, or a II–VI semiconductor nanocrystal, in the hybrid structure case). Currently, the best results in this respect (lying in the 6–8% range) are achieved by using low-bandgap polymer materials, combined with a fullerene derivative, to form a so-called bulk heterojunction configuration. This is a junction set up between one, *p*-type semiconductor material, and another semiconductor material, this time of type *n*. A bulk heterojunction may

thus be thought of as a junction extending across three dimensions, with the two materials extensively interpenetrating.

In this configuration, the optimum phase segregation between the two materials should be kept to 5–10 nm. This corresponds to the exciton diffusion length, in organic media. If the efficiency of organic systems is to be improved, it thus proves crucial that high-absorption polymer materials be developed. Such materials must exhibit both high **molar absorption** coefficients, and very broad absorption domains, extending across the visible portion of the solar spectrum (since fullerene derivatives are found to exhibit low absorption, as a rule). The polymer's energy levels (i.e. the positions of frontier orbitals) must be



A. Gonin / CEA

A new type of photovoltaic cell is being developed, using conducting organic polymers, deposited onto glass substrates.

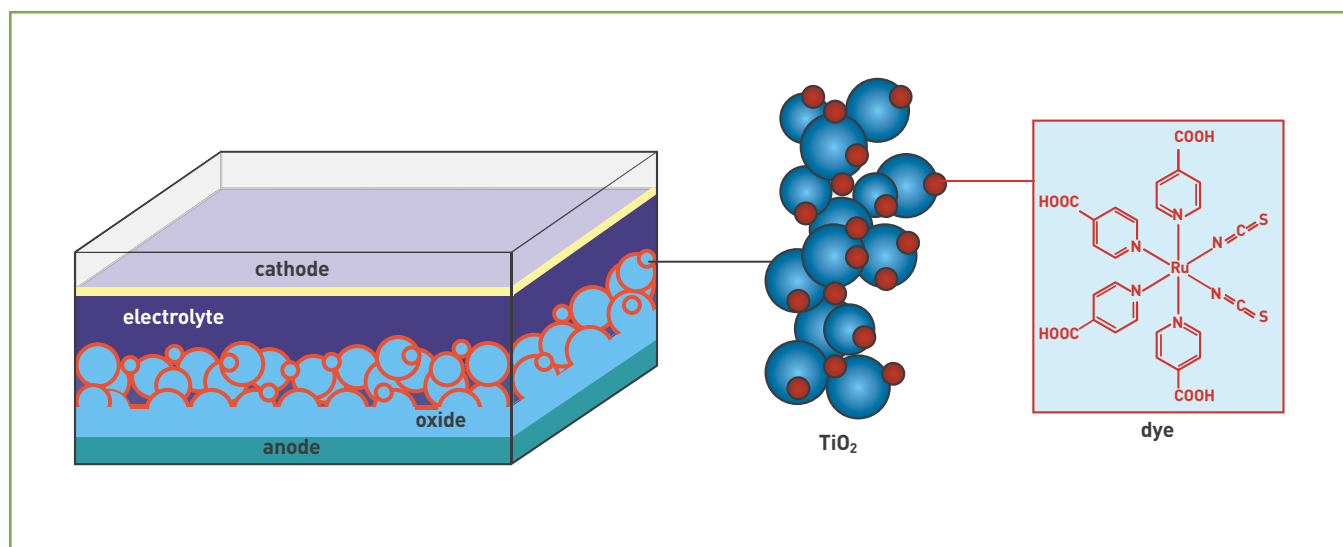


Figure 4. Principle scheme of a Grätzel-type cell, using organic dyes. Scheme of a dye-sensitized solar cell (left): a transparent conducting oxide (in this case, titania, i.e. titanium dioxide) is deposited onto the anode, while the thin red layer stands for the dye monolayer. A titanium dioxide (TiO_2) nanoparticle, bearing dye molecules, shown as red spheres (center). Chemical structure of the dye (right), in this case a ruthenium (Ru) complex, featuring ligands involving carboxylic acid (COOH) groups, which allow the molecule to anchor itself on the oxide.

accurately positioned with respect to those of the acceptor compound, in order to ensure efficient exciton dissociation. The best way to achieve this involves combining, within the polymer chains, chemically different heterocyclic aromatic units. Indeed, organic chemistry offers virtually boundless possibilities, as regards the creation of novel materials, exhibiting optical, and electronic properties that may be tuned, depending on the chemical units selected. Finally, the polymer thus developed must exhibit satisfactory charge transport properties, to allow the transfer of photogenerated charges (arising from the dissociation of the excitons set up, subsequent to photon absorption by the material) to the electrodes. As regards transport properties, any significant improvement must involve self-organization of the material, within the active layer.

In the hybrid cell case, where the polymer occurs in a blend with semiconductor nanocrystals, the inorganic nanoparticles do ensure a fraction of the absorption carried out in the active layer. The absorption spectra of these materials may be very precisely adjusted, by acting on particle size, or on their chemical composition, while transport properties may be tuned by acting on the nanocrystals' shape.

Dye-based photovoltaic materials

Organic dyes are used in another class of cells, known as dye-sensitized solar cells (DSSCs), or Grätzel cells, from the name of their inventor⁽²⁾ (see Figure 4). DSSCs are fabricated from bulk nanostructured materials. Most commonly, the material involved is a transparent titania (titanium dioxide [TiO_2]),

serving to transport the photogenerated electrons to the electrode, featuring a surface onto which are grafted organic, or organometallic photosensitive (sensitizer) dyes. An electrolyte, held between two transparent electrodes, completes the system.

This type of cell is used to construct semi-transparent panels, the color of which varies, according to the dye selected. The separation of the charges photogenerated within the dye occurs at the interface between the dye, the semiconductor, and the electrolyte. Exhibiting efficiencies in the 11–12% range, the most efficient dyes belong to a class of ruthenium-containing organometallic complexes, in which the ligands provide anchoring functions, enabling them to form a monolayer over the oxide's surface. More recently, however, researchers have developed wholly organic molecules, yielding conversion efficiencies lying in the 8–10% range. These dyes contain both functional chemical groups, e.g. carboxylic acids, providing the anchoring function, and pi-conjugated aromatic units, ensuring the absorption of photons emitted in the ultraviolet and visible radiation of the solar spectrum.

Photovoltaic energy conversion stands as an issue of paramount importance, for the years to come. CEA is mobilizing all its resources to maintain its watch, to ensure as exhaustive an overview as feasible of new materials.

> Philippe Thony

National Solar Energy Institute (INES)
Technological Research Division
Le Bourget-du-Lac
(attached to CEA Grenoble Center)

> Renaud Demadrille and Emmanuel Hadji

Nanosciences and Cryogenics Institute (INAC)
Physical Sciences Division
CEA Grenoble Center

⁽²⁾ Michael Grätzel (born 1944), a professor of chemistry at the Federal Polytechnic Institute at Lausanne (École polytechnique fédérale de Lausanne) (Switzerland), is the inventor of the dye-sensitized solar cell, serving to effect the conversion of solar energy into electrical energy. Such cells make use of a photoelectrochemical system, taking its cue from plant photosynthesis.

NANOMATERIALS AND RISK CONTROL

An “integrated” approach

The growth in the demand, from industry, for materials is accelerating. This growth is already benefiting mature markets, e.g. for mass-produced automotive components, but equally markets for dedicated, high-value-added materials, for aerospace applications. At the present time, emerging markets concern environmentally compliant products, and new energy technologies, e.g. fuel cells, batteries, **photovoltaic** technology, new-generation nuclear energy... Which sets a novel challenge, for **nanotechnologies**: that of controlling risk, over the entire lifecycle of materials, and products.

A safety culture fostered by the nuclear experience

Engineering advanced materials frequently entails designing, fabricating, and incorporating high-value-added **nano**-objects, “custom”-designed for each application. A relevant solution, with regard to generating the innovation that is seen to be a requisite, if existing products are to be improved, and new functions or products created, involves bringing nanotechnologies into the design, and fabrication of the multifunctional materials of the future. This results in what is referred to either as incremental innovation (gradual improvement), or disruptive innovation (break-through technology). For nanotechnologies, gaining acceptability entails ensuring risk control is achieved across the entire lifecycle of materials, and products: from fabrication, or construction to end of life. This must meet,

and allay the societal concerns, and queries, inherent in any introduction of a new technology. With regard to implementing a global, integrated approach to such risks, CEA stands as a leader in the field, and a pioneer – as the initiator of *NanoSafe*, the European research project on the safe production of nanomaterials. This is the first global approach to the issue to achieve visibility on the international scene, and one which, as of now, stands as a reference. CEA has been active, for more than 50 years, in securing constant improvements in safety, with regard to its own workforce, and the environment, with respect to the nuclear risk. In this context, CEA has developed a culture, and innovative techniques, concerned with taking risks on board. It is but a natural development that the level of safety achieved, in what stands as CEA's historic core domain, should be likewise carried over, and ensured in its new areas of activity, as regards nanomaterials in particular. Thus it was that, as early as 2005, studies were carried out at CEA's Grenoble Center, to ensure the safety of staff working in the area of nanomaterials, and preserve the environment.

Developing a risk control policy entails that two parameters be taken on board: first, the hazard (in metaphorical terms, the height of the cliff); and, second, exposure (the distance from the cliff's edge one walks to), the two being related by way of a simple equation: $\text{risk} = \text{hazard} \times \text{exposure}$. Bearing in mind that the potential hazard from **nanoparticles** relates, essentially, to their toxicity,⁽¹⁾ one initial approach involves identifying nontoxic nano-



Simulation of an intervention in an accident situation, at CEA's Grenoble Center.

particles, and using only these. The difficulty this involves stems from the very large number of parameters that must be investigated: the material, but equally particle **crystallinity**, shape, size, surface charges, **hydrophilic/hydrophobic** character, degree of agglomeration... The **nanotoxicology** studies currently undertaken, for the purposes of identifying hazardous nanoparticles, will take years to complete; and it will take longer still to ascertain which nanoparticles are harmless to humans, and the environment. Hence, in the absence of ascertained data, as to the actual toxicity of such nanoparticles, the aforementioned equation tells us that, to bring the “risk” factor down to zero, it will be sufficient to reduce the “exposure” term, making it tend to zero (i.e. keep well away from the cliff).

As this argument retains its validity, irrespective of the hazard involved from nanoparti-



Equipment, kept in a white room, serving for the deposition of nanoaggregates intended for use in energy projects.

(1) At very high concentrations, nanoparticles may also cause explosions, in certain conditions.



F. Rhodes / CEA

Plant cultures used to detect the toxicity of nanoparticles in the environment (bacterial, vegetal, animal, human models): shown here, roots from wheat shoots being examined.

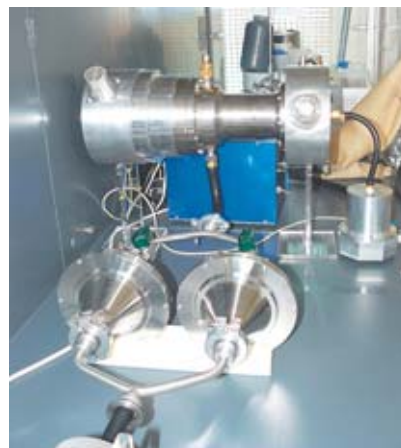
cles, CEA's Grenoble Center therefore focused its endeavors on achieving a reduction in, and control of, exposure, for the purposes of immediate implementation in its own laboratories. A number of points were investigated, to cover the issue as a whole, at the workstation level: safety engineering with regard to equipment, to suppress any risk of leakage (double barrier concept); characterization, with respect to nanoparticles, of protection equipment, whether collective

(filters), or personal (gloves, masks, protective clothing); and monitoring techniques, to cover the work environment. Concurrently, training courses were organized for the workforce, by the Grenoble-based National Institute for Nuclear Sciences and Technologies (INSTN: *Institut national des sciences et technologies nucléaires*), to implement best practices, and current thinking regarding medical monitoring, and interventions in accident situations.

All of these investigations are being conducted as part of a voluntary standardization approach, as recommended by the French Association for Standardization (AFNOR: *Association française de normalisation*), the European Committee for Standardization (CEN), and the International Organization for Standardization (ISO). All results from the studies carried out by CEA may be accessed – in French, and in English – at the website: <http://www.nanosmile.org>.

Collective, and personal protections: investigations, and findings

According to a study published by **Lux Research**, by 2014, some 14% of all manufactured goods, around the world, could incorporate nanomaterials. Such a dissemination calls for a reflection, and studies to be initiated, as to the potential risks involved by these novel products, whether for researchers, or for the consumer public. CEA, as part of a responsible approach, is participating in the identification of the risks involved, and in the implementation of solutions, so that the exposure incurred by people, as by the environment, may approximate to zero.



CEA

Prototype particle counters, allowing the 1 nm limit to be reached.

Top: prototype differential mobility analyzer (DMA), with its associated electrometer, from Yale University (1 nm; detection threshold: 100 particles/ml).

Bottom: DMA and electrometer from German firm Grimm Aerosol Technik (0.8 nm; detection threshold: about 20 particles/ml).

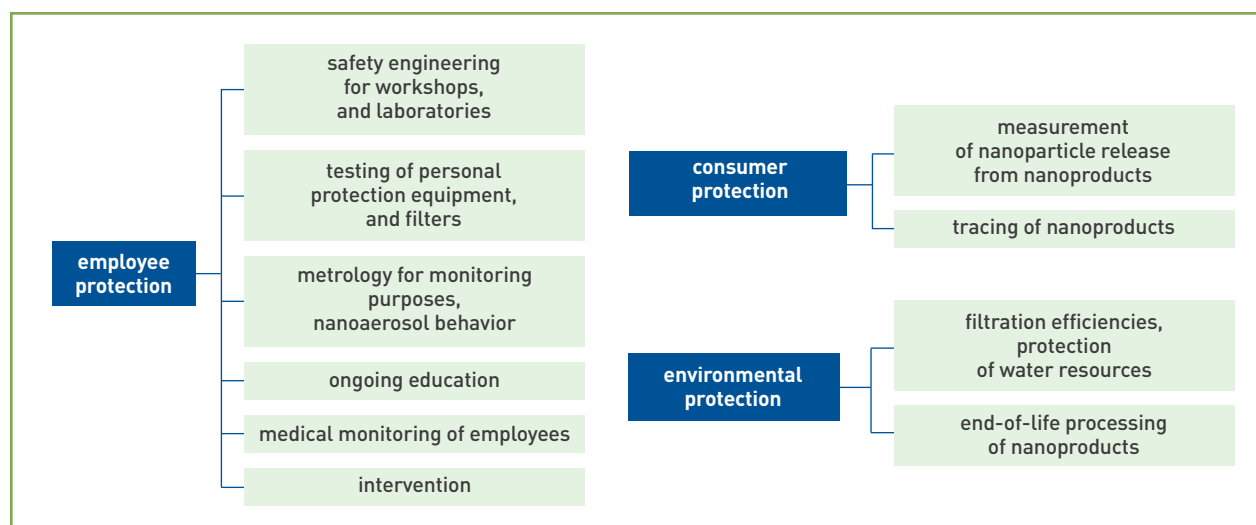


Table 1. Issues addressed at CEA's Grenoble Center to bring down exposure to nanoparticles.

NANOMATERIALS AND RISK CONTROL

Nanoparticle detection

For the purposes of characterizing the air breathed by workers exposed to nanoparticles, the marketplace offers a wide variety of laboratory equipment. These devices rely on detection principles which may differ widely (measurement of electric charges, of scattered light, of mass...), resulting in likewise widely diverse metrics. Reference equipment includes the scanning mobility particle sizer, which makes it possible to bring down the lower detection limit, to cater for particles 5 nm in diameter. Covering the full range of nanoparticles, however, does entail that this limit be brought down to 1 nm. CEA is working on this, under the aegis, in particular, of a collaboration with Yale University (USA), and an industrial partnership with German firm Grimm Aerosol Technik.

CEA is also active with regard to continuous measurement at workstation level, to ensure its workforce is not exposed to nanoparticles. The difficulty involved in getting a measurement of particles produced in the laboratories, and workshops stems from the presence of very high concentrations of "natural" particles, of diverse provenance: some 10,000 natural particles per cubic centimeter of air, of a size larger than 10 nm, generated by chemical reactions in the atmosphere, plants, volcanic eruptions... but equally highly variable concentrations of particles originating in anthropic sources, e.g. road traffic, domestic heating... Measurements carried out as part of the NanoSafe project show that the threshold of 10,000 particles per cm³ air may be heavily exceeded, in an urban environment (10⁵ particles/cm³ close to a motorway, 10⁶ on an airport tarmac...), or in an industrial context (plasma cutting: 10⁶ particles/cm³, welding: 10⁷...). Further, such concentrations can undergo very significant fluctuations, from one time of day to another (for instance, by one decade over half an hour). As regards the ambient atmosphere, as may be seen in Figure 1, the smaller the particles measured, the higher the concentrations that are found (dashed line).

These values should be referred to the acceptable limit proposed by the US National Institute for Occupational Safety and Health (NIOSH) for nano-titanium dioxide (TiO₂).⁽²⁾ 0.1 mg/m³, this corresponding to some 4·10⁵ particles/cm³ (50-nm particles), or 5·10⁴ particles/cm³ for 100-nm particles. Thus, for what is after all deemed to be a low-toxicity compound, the recommended mass-

concentration limit, when converted into concentration in terms of particle number, can turn out to be of an order of magnitude comparable to that of the natural particle background. It may reasonably be anticipated that more stringent limits will be set for particles of higher toxicity than TiO₂.

The measurement of deliberately engineered particles – i.e. those of interest, in this context – is thus liable to be extensively masked by, and subjected to heavy perturbation from, existing particle concentrations. CEA is

working on two methods affording the ability to effect specific nanoparticle measurements: the first method involves adding a tracer (e.g. fluorescein) to the nanoparticles, while the second involves analyzing their constituent material by ultratrace detection methods (see Figure 2). Thus, for the purposes of measuring titanium dioxide nanoparticles, nanoparticles are collected on filters, the chemical presence of titanium being subsequently measured by mass spectrometry. This method allows a sensitivity gain by a factor 10–100 to be

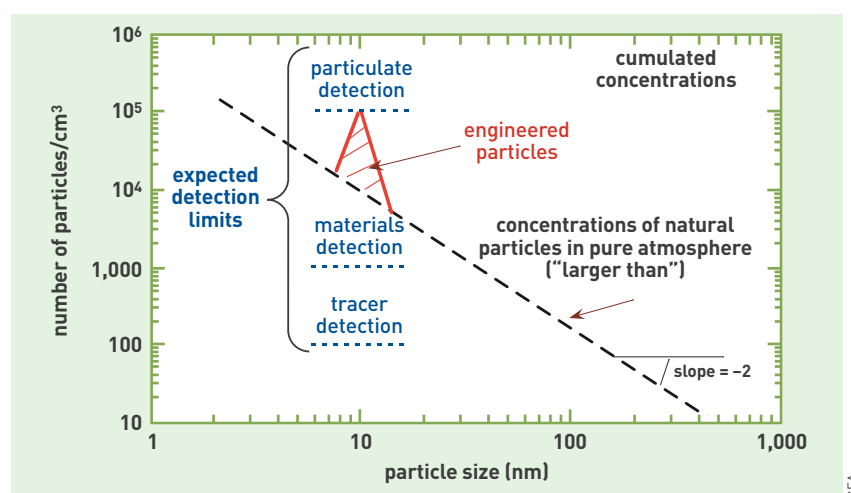


Figure 1. Evolution of nanoparticle concentration, as a function of nanoparticle size ("larger than"), and alternative detection strategies, relying on the measurement of a specific characteristic of the nanoparticles of interest.

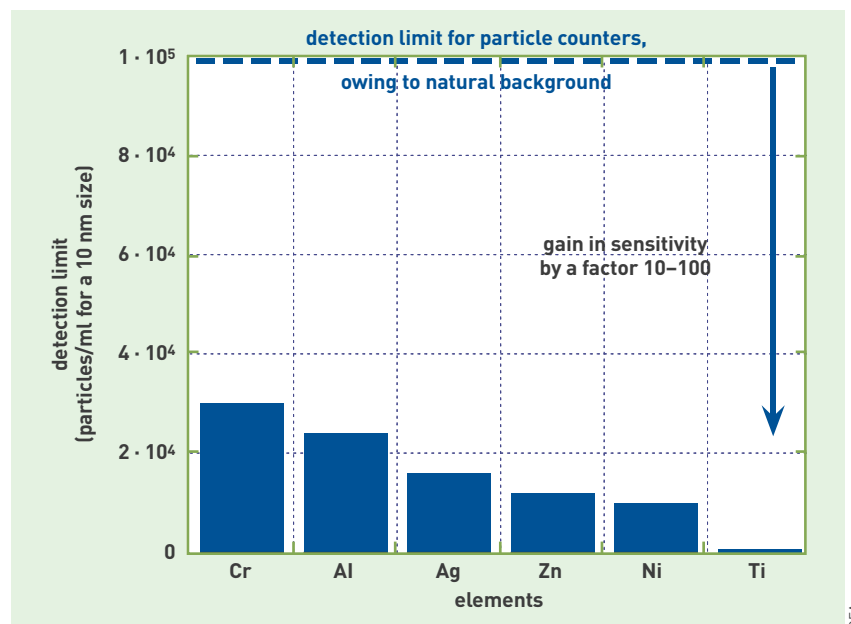


Figure 2. Detection limits for 10-nm nanoparticles, as measured in terms of their constituent elements, by inductively-coupled plasma mass spectrometry (ICP-MS), a method widely used by the chemical industry for ultratrace detection purposes.

(2) Figures calculated for an average TiO₂ density of 4, with particles assumed to be spherical.



A small soil column, used for the investigation of nanoparticle migration, by means of fluorescent nanotracers.

achieved, as regards nanoparticle detection, and may be implemented by way of a badge worn by operators.

Filters of proven efficiency

Conventional industrial operations have been able to reduce workforce exposure to toxic particles (paints and varnishes, smoke, dust...): first, by acting on overall workplace air conditioning, by installing filters at workstation level, but equally by taking measures directly affecting the individual workers, by making the use of personal protection equipment mandatory (masks, protective clothing, gloves).

To be effective, such measures entail, as a prerequisite, that the various filtration mechanisms be properly taken into account.



Setting up an experiment serving to test the imperviousness to nanoparticles of personal protective equipment (masks, gloves), as part of the European NanoSafe project.

The idea should be abandoned – once and for all – that a paper filter, or the woven fabric of a protection suit, acts as a “sieve,” or a “skimmer,” arresting just those particles that are larger than its own holes. A simple observation under scanning electron microscopy shows, in contrast, that such filtration media consist of a tangled crisscross of fibers (commonly glass fibers, or cellulose fibers), held together, in some instances, by organic linking strands a few micrometers long (see Figure 3). The spaces between two fibers may be as large as several tens of microns, in some cases, and yet the thickness of the filter acts as a highly effective trap, for particles much smaller than this.

Such filters retain particles across their thickness, by way of three distinct mechanisms (see Box), then, as particles come into contact with a fiber, Van der Waals forces – which are largely predominant, compared to other forces, at that scale – trap them, irreversibly as a rule. There is a process which can be used to optimize filtration: this involves adding electrostatic charges – both positive, and negative – to the fibers. Charged particles are then attracted to, and subsequently captured by, fibers bearing charges of opposite sign. This type of filter medium, used for the fabrication of masks, makes, in particular, for greater ease of respiration, as it occasions a lower pressure drop.

To arrive at the overall efficiency of a given filter, the performance of the various elementary capture mechanisms must be summed. Figure 4 shows an example of filtration efficiency, for a fibrous filter, as a function of particle size. For large (larger than 1,000 nm) particles, the overall efficiency of a fibrous filter is high, owing to capture phenomena involving interception, and inertial impaction. For particle sizes smaller than 50 nm, the efficiency of a fibrous filter is likewise found to be high, owing to particle deposition through diffusion. Filters show minimum efficiency for intermediate particulate fractions, the maximum penetrating particle size (MPPS) being deemed to lie in the 150–300 nm range, for standard paper filters.

On the other hand, a theoretical study, published by H.-C. Wang and G. Kasper in 1991,⁽³⁾ predicted that, for particles smaller than 10 nm, particle adhesion energy (which decreases with particle radius) may be lower than the particles’ kinetic energy due to thermal agitation (this remaining constant,

(3) H. C. WANG, G. KASPER, “Filtration efficiency of nanometer-size aerosol particles”, *J. Aerosol Science* 23 (1991), pp. 31–41.

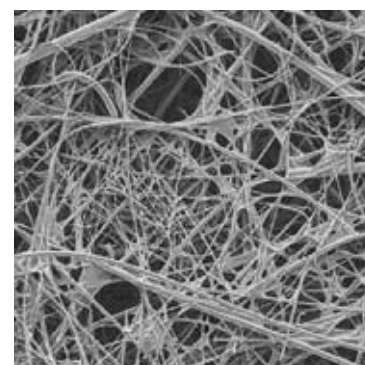
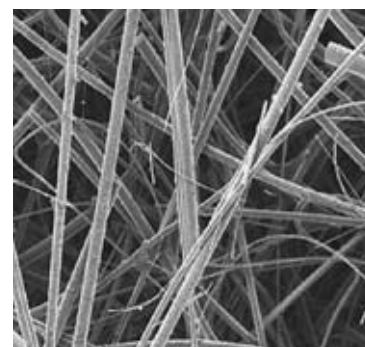


Figure 3. Two types of fibrous filters, as observed under scanning electron microscopy. At this scale, a 10-nm particle would appear with a size of about 1 thousandth of a millimeter.

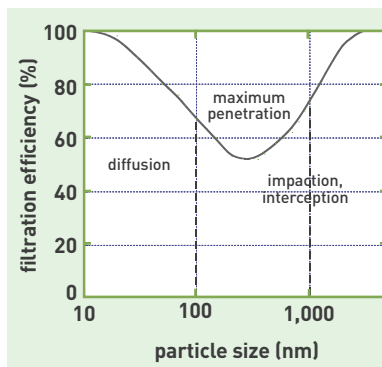


Figure 4. Example of the evolution of filtration efficiency for a fibrous filter, as a function of particle size.

NANOMATERIALS AND RISK CONTROL

Various particle mechanisms involved in particle capture by filtration fibers

a. Deposition by inertial impact

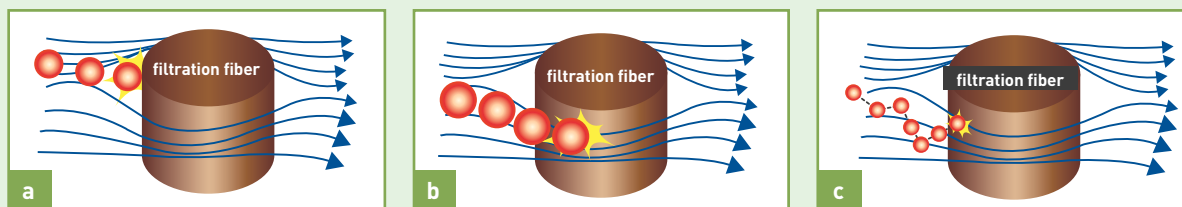
The airstream flows around the filtration fibers, whereas particles, which as a whole are denser than air, are unable to keep in step with the deformation undergone by the fluid stream, owing to their inertia. The efficiency of this deposition mode is enhanced at high entrainment velocities, and for large particle sizes.

b. Deposition by interception

When the path of a particle encounters a fiber, the particle is deposited onto the fiber. The efficiency of this mechanism is not dependent on gas flow velocity, rather it is enhanced for large particle sizes.

c. Deposition by diffusion

Aside from their motion due to entrainment by the gas, smaller particles are subjected to random motions, owing to Brownian motion. These extra motions increase the probability of these particles colliding with a fiber. Diffusion capture efficiency rises as particles become smaller, and also rises with temperature, and slower entrainment velocities.



regardless of particle size, in a given medium). This phenomenon, known as thermal rebound, is dependent on many parameters: particle size, particle-fiber affinity, the particles' ability to undergo deformation, temperature... It has been reported only in a very limited number of publications, some of them indeed being subject to controversy.⁽⁴⁾ In most of the studies carried out to date, no deviation from classical filtration theory was found, for silver, sodium chloride, or graphite particles, down to 2 nm.⁽⁵⁾ Thus, in practice, the efficiency of a fibrous filter rises, in the nanoparticle domain: from 100 nm (a size strictly smaller than MPPS), at least down to a few nanometers. The "skimmer" model is thus found to be inaccurate, for paper filters (see Figure 5).

At CEA, similar results were obtained, in the context of the NanoSafe project,⁽⁶⁾ for protective clothing, when operating both in the presence, or absence of airflow, to get close to the actual conditions prevailing, when protective clothing is worn. Figure 6 shows the results obtained in the absence of airflow,

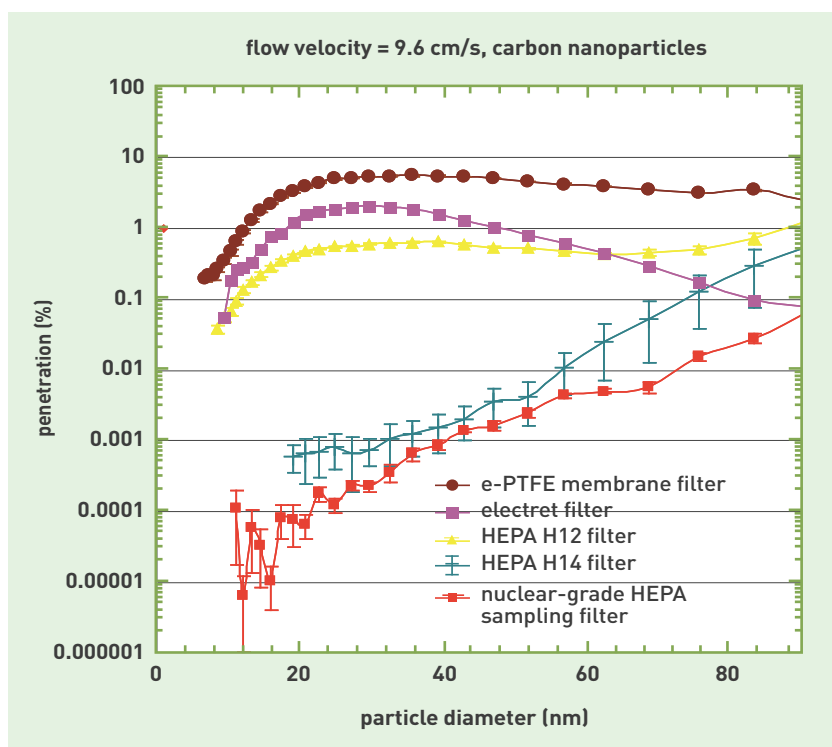


Figure 5. Performance of various commercial filtration media, with respect to graphite nanoparticles. The graph plots the results, in terms of efficiency, for various types of filter: Teflon (e-PTFE) membrane, electrostatic (electret) filter, or fibrous high-efficiency particulate air (HEPA) filters (HEPA H12, HEPA H14), as expressed in terms of the ratio of the number of particles not retained, over the number of incoming particles. In this case, the lower the penetration, the higher the filtration efficiency.

(4) M. HEIM *et al.*, "Filtration efficiency of aerosol particles below 20 nanometers", *Aerosol Science and Technology* 39 (2005), pp. 782–789.

(5) ICHITSUBO *et al.* (1996), ALONSO *et al.* (1997), HEIM *et al.* (2005), KIM *et al.* (2007), GOLANSKI *et al.* (2008).

(6) www.nanosafe.org.

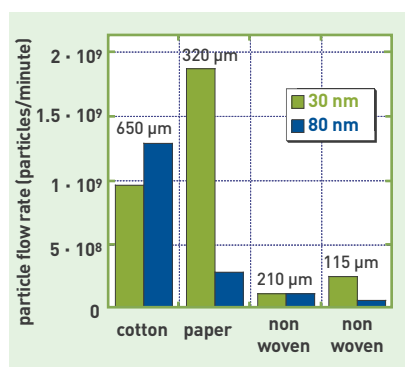


Figure 6. Performance of various types of media, with respect to the diffusion of graphite nanoparticles of sizes centered around 30 nm, and 80 nm. Concentration inside the upstream cavity is kept at about 10⁷ particles/ml, each sample has an area of about 100 cm². Results obtained with air flowing through the media likewise confirm the good performance exhibited by nonwoven materials.

in a diffusion cell the upstream cavity of which is kept at a constant nanoparticle concentration. The flow rates for particles diffusing into the downstream cell make it apparent that the best results are obtained with nonwoven materials, their low thickness notwithstanding. With regard to nanoparticles, one-piece suits made of relatively airtight materials, of the Tyvek® type, afford the best protective performance. Unfortunately, this type of material is found to be less pleasant to the wearer. Tests were likewise carried out, at CEA, using the diffusion method (with no airflow), on a number of glove samples. Although made from porous materials, gloves prove highly effective as regards protecting against nanoaerosols, in this case also owing to the Brownian motion affecting the smallest particles, which adhere to pore surfaces, within the gloves.

To sum up, it proves perfectly feasible to ensure workers are protected from nanoparticles, in the event of some of these particles involving a risk of toxicity. It likewise proves feasible to carry out – with high efficiency – the filtration of nanoparticles produced in workshops, and laboratories, and to ensure environmental protection, through the adoption of:

- so-called paper filters, used for the purposes of workplace air filtration, mask cartridges proving even more effective against nanoparticles, at least down to 2 nm;
- protective clothing made from airtight, nonwoven materials, which yield outstanding results;
- gloves, those tested all proving highly impervious to nanoaerosols.

Ensuring consumer protection through the measurement of nanoparticle reemission from nanoproducts (abrasive release)

In the absence of adequate knowledge as to the possible toxicity of nanoparticles, it is crucial to ensure that no exposure be incurred by consumers of nanoproducts (i.e. manufactured goods containing nanoparticles). As the pulmonary route is deemed to be the most highly sensitive one, with regard to exposure, CEA has developed a control method, to check the absence of dispersion, into the atmosphere (aerosolization), of nanoparticles contained in nanomaterials, when these are stressed in service. Thus, as shown in Figure 7, a measurement bench has been developed, to measure the release of nanoparticles, as nanomaterials are subjected to abrasion. The graph reproduced in the right panel shows the results of a test carried out on polyethylene terephthalate

(PET), and polyvinyl chloride (PVC) nanotextiles, developed at the French Textile and Clothing Institute (IFTH: Institut français du textile et de l'habillement), containing clay nanoparticles, to render them fireproof. The findings show that:

- materials subjected to an abrasion test yield nanoparticles, even when they contain no nanoparticles;
- if nanoparticles are not strongly locked into the matrix, they are liable to be released into the atmosphere.

Results obtained with other nanomaterials (paints, polymers), better optimized with regard to nanoparticle locking-in, show it is feasible to achieve a highly effective locking in of nanofillers. To sum up, it is feasible to ensure that nanoparticles introduced into nanomaterials are not released when these are subjected to abrasive stresses. As developed by CEA, this test is currently under

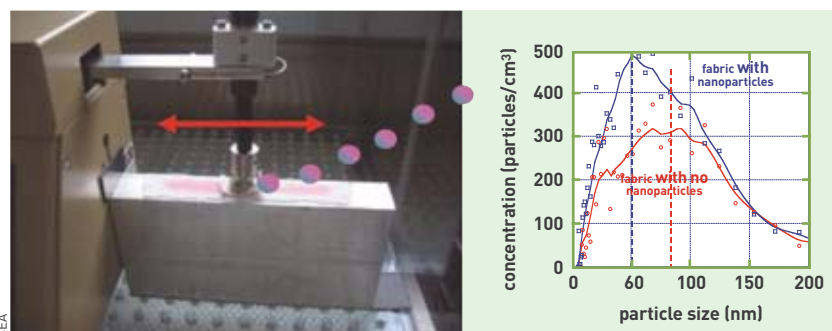


Figure 7. Left panel: measurement bench used to measure the release of nanoparticles from nanomaterials subjected to abrasive stress. Right panel: graph plotting the results obtained for two fabrics: one containing nanoparticles, the other containing no nanoparticles.



A dedicated glovebox, used for nanosafety studies. Shown here, a test on clothing to be worn by operators involved in the production, and handling of nanopowders, and nano-objects.

NANOMATERIALS AND RISK CONTROL



Setting up a nanoparticle release test for nanoproducts in general use (polymers, fabrics...).

discussion at the standardization level, within the International Organization for Standardization (ISO) – the aim being to set up a certification of nanoproducts, prior to their commercialization. Further tests are likewise being developed, to control the absence of nanoparticle release under stresses representative of every stage in the lifecycle of nanoproducts: use, recycling, ultimate destruction.

Indestructible labels for nanoparticle detection purposes

Consumers demand that information be provided, as to the composition of products, so that they may make informed decisions. A recommendation from the [European Parliament](#) emphasizes the need to inform the public as to the presence of nanoparticles in products. However, such nanoparticles may only be detected by means of heavy [microscopy](#) equipment, altogether inaccessible to consumers. For that reason, nanolabels have been developed at CEA, which nanoparticle manufacturers would be able to introduce into their products, at the fabrication stage. With such a process, it would prove impossible to remove the label from nanoparticle-containing products. The presence of nanoparticles in products, and the type of nanoparticle involved, could then be read out by consumers, by means of simple-to-use sensors.

One of the technologies used by CEA, for that purpose, involves producing nanotracers based on 30–100-nm nanoparticles containing fluorescent compounds, making up a veritable optical barcode: a simple handheld detector would then make it possible to read out the information. While it is technically feasible to label nanoparticles in indelible fashion, to ensure consumers are informed, nanoparticle producers have yet to be persuaded to adopt that technology.

Development, and monitoring: the current state of nanotoxicology research at CEA

The specific character exhibited by research efforts in the field of nanotoxicology stems from the need to match up two issues: the imperative requirement to ensure occupational monitoring, and protection; and development strategies for nanotechnologies, seeking to arrive at commercially viable industrial applications.

In this context, researchers needs must take on board the data already at hand, concerning nanoparticles. These data suggest that such particles may prove more toxic than micrometer-scale particles of identical nature, even though it may not be possible to adduce any strict, conclusive demonstration as to the existence of adverse effects, with regard to health. Hence the concerns that arise, regarding the ability of conventional toxicological evaluation methods to yield evidence of a potential risk from nanoparticles. These queries stem from the singular characteristics exhibited by nanoparticles, in terms of behavior, and biological action mechanisms. It is apparent that the qualitative, and quantitative analysis of the health effects of nanoparticles calls for the taking on board of a complex ensemble of parameters, bringing together a number of [physicochemical](#) characteristics: diameter, surface area, number, surface chemical reactivity, shape, charge... Such analysis further entails that these particles' behavior within the organism be ascertained, as a function of their ability to undergo dispersion, aggregation, and interaction with biological [molecules](#), while relating this to their immediate, and delayed effects at the various organizational levels of a living entity. This is a vast area of research, requiring that criteria be identified, such as will make it possible to draw up a classification of nanoparticles – this serving to facilitate the working out of “exposure/biological response” relations – and further determine the relations between these biological responses, and adverse effects on health.

Drawing on the specific expertise of its biologists, chemists, and physicists, CEA is developing an integrated approach to nanoparticle



Small-angle X-ray scattering apparatus, being used to characterize nanoparticle size, shape, and concentration.



A culture of cyanobacteria naturally present in the environment, used for the purposes of nanoparticle ecotoxicology studies.

toxicology. This approach should make it possible to overcome technological barriers with respect to two areas:

- the characterization of exposure, in particular through the production of controlled nanomaterials, and the development of **radio-active marker** techniques; such characterization may also be effected through the use of **chromophores** for visible-light imaging, for the purposes of detecting, and quantifying nanoparticles in biological media, thus yielding improved determinations of their behavior in cells, and tissues, and of their paths, and persistence in the organism;
- the *in-vivo* biokinetics of nanoparticles (**carbon nanotubes**, silicon oxides, metallic particles, **silicon carbide**...), fully controlled in terms of formulation, and characterization. Concurrently, researchers are carrying out *in-vitro* investigations on cell models, representative of target organs. Such investigations should make it possible to pinpoint the interaction mechanisms involved, for nanoparticles. New predictive toxicology approaches are being implemented, with the further aim of arriving at a categorization of nanoparticles in terms of their biological, and toxicological effects. These approaches involve, in particular, looking for profiles inducing, or otherwise, a toxicological effect, by way of a global,



Investigation of nanoparticle migration in soils, to ensure the preservation of potable water resources. The soil column is positioned on a gamma-ray measurement bench, to record soil water content on a continuous basis.

P. Avavian / CEA

transcriptomic and proteomic analysis. This program is being carried out under the aegis of wide-ranging collaborations with the French players in this field. These include: the National Institute for Industrial Environments and Risks (INERIS: **Institut national de l'environnement industriel et des risques**), for the *Nanotrans* project, set up for the purpose of validating cell models, and protocols for the investigation of biological barrier crossing; the National Research Agency (ANR: **Agence nationale de la recherche**), for the *Partox* project, investigating the toxicological effects, or innocuousness, of nanoparticles, and Nanobarrriers; the French Environmental and Occupational Health Safety Agency (AFSSET: **Agence française de sécurité sanitaire de l'environnement et du travail**), to gain a better understanding of the way carbon nanotubes pass through the pleura, and associated effects; and likewise with the National Institute for Health and Medical Research (INSERM: **Institut national de la santé et de la recherche médicale**), the National Center for Scientific Research (CNRS: **Centre national de la recherche scientifique**), and academe. CEA is further involved in the *Nanogenotox* project, a joint initiative, supported by the **European Commission**, bringing together 11 member states in the European Union. This initiative has been set up for the purpose of standardizing **genotoxicity** tests, for the various commercially available productions of titanium oxide, or silicon oxide nanoparticles, or of carbon nanotubes.

The findings from these studies should make a major contribution, in terms of submissions for consideration by the standardization organizations (ISO, European Committee for Standardization [CEN], *Association française de normalisation* [AFNOR]), and public health authorities involved in the specification of quantities serving to characterize exposure to nanoparticles, exposure standards, and recommended exposure values, or exposure limits.

Nano©Smile: an educational, and information tool

The responsible development of nanotechnologies must meet a number of conditions: ensuring public health is guaranteed; environmental compliance, across the entire lifecycle of nanomaterials; and an ongoing dialog with society, to allay its concerns, in a fully transparent manner. This is what led to the setting up of *Nano©Smile*, a bilingual, English/French website: <http://www.nanosmile.org>. The site addresses these issues at three levels:



- education as to, and dissemination of, good practices, aimed at companies, and laboratories;
- information, to facilitate understanding in the public at large;
- setting up a dialog, and promoting democratic debate, by means of attractive, accessible media.

The good practices presented are of interest to employees in this area (operators, managers, medical staff, safety engineers...), and to the public at large, seeking to be informed of the benefits of nanomaterials, and of the associated risks, along with waste management methods. The *Nano©Smile* site addresses each issue by setting out, explicitly, both the certainties, and uncertainties involved, without seeking to force the points home. Rather, it aims to provide resources, to stimulate thinking, and promote dialog. Short animations cover topics as diverse as the definition of nanoparticles and nanomaterials, their applications, and products in which they are to be found, toxicity, current ongoing research work, the precautions that should be taken, or the ethical issues raised...

> Rémy Maximilien

Life Sciences Division
CEA Fontenay-aux-Roses Center

> Frédéric Schuster

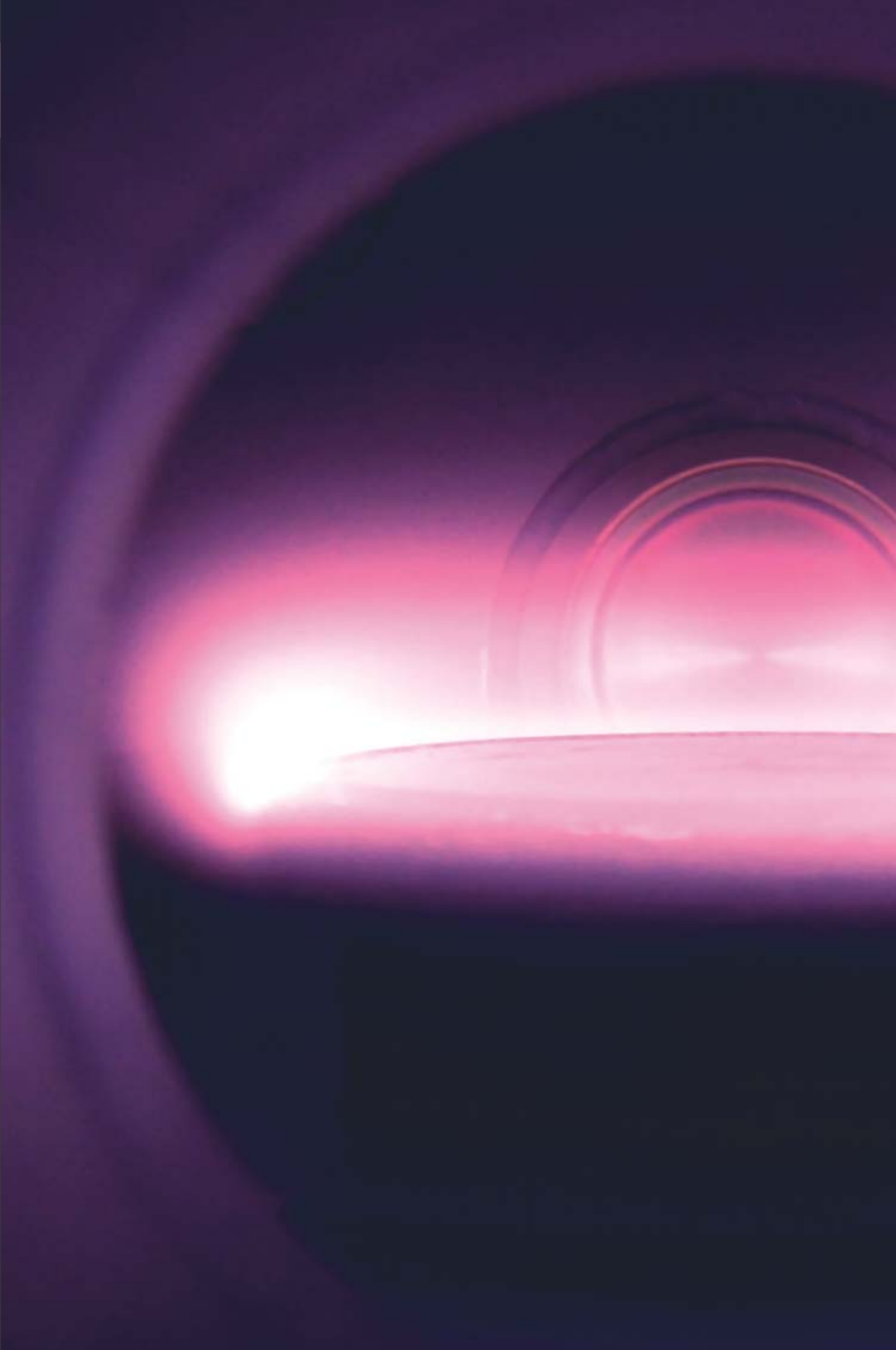
"Advanced Materials"
Crosscutting Program
CEA Saclay Center

> Yves Sicard

Nanochemistry and Materials Safety
Laboratory/Joseph-Fourier University
Technological Research Division
CEA Grenoble Center

> François Tardif

Nanochemistry and
Materials Safety Laboratory
Technological Research Division
CEA Grenoble Center



III. MATERIALS FOR INFORMATION AND BIOMEDICAL TECHNOLOGIES

The knowledge of the physical and chemical properties of materials will determine the functionality of the devices that are produced to meet the needs of industry, and society at large, in the application sectors of information technologies and biomedical technologies. Over the past few years, innovation has been aided by the introduction of many novel materials. The properties of these new materials that are now available for incorporation in nano-scaled devices is due to advances that have been achieved in both manufacturing and integration processes. Also, the effects of scaling, together with the control of interface stability, and surface functionalization are key factors in the emergence of these novel properties.

The papers in this present chapter serve to illustrate the remarkable variety of materials and their applications that have been developed by creative researchers and technologists. Thus, recent advances achieved with the synthesis of wide-band-gap materials, such as diamond, make it possible to construct very-high-performance X-ray detectors. Mastering the deposition of large numbers of dielectric thin films in one stack, allows the engineering of optoelectronic devices with improved performance. Nowadays, researchers are able to confine materials to one or more dimensions at the nano-scale to provide new and interesting electronic properties, as has been recently observed with carbon. Indeed, nanotubes and graphene phases of carbon are currently of great interest and have potential to be incorporated in micro and nano-scale technologies for number of applications. At the same time, the control of the properties of biological molecules, along with their preferential interaction with specific surfaces is opening up exciting prospects in the biomedical sector.

The trend of miniaturization and the rising complexity of electronic devices require the integration of materials that exhibit many complementary properties. These must be optimized for the performance levels of the devices that are desired, in terms of response time, power consumption and heat dissipation. In order to develop these advanced technological processes and to meet the requirements of the current industrial context, significant resources of materials science and ingenuity are now being deployed.

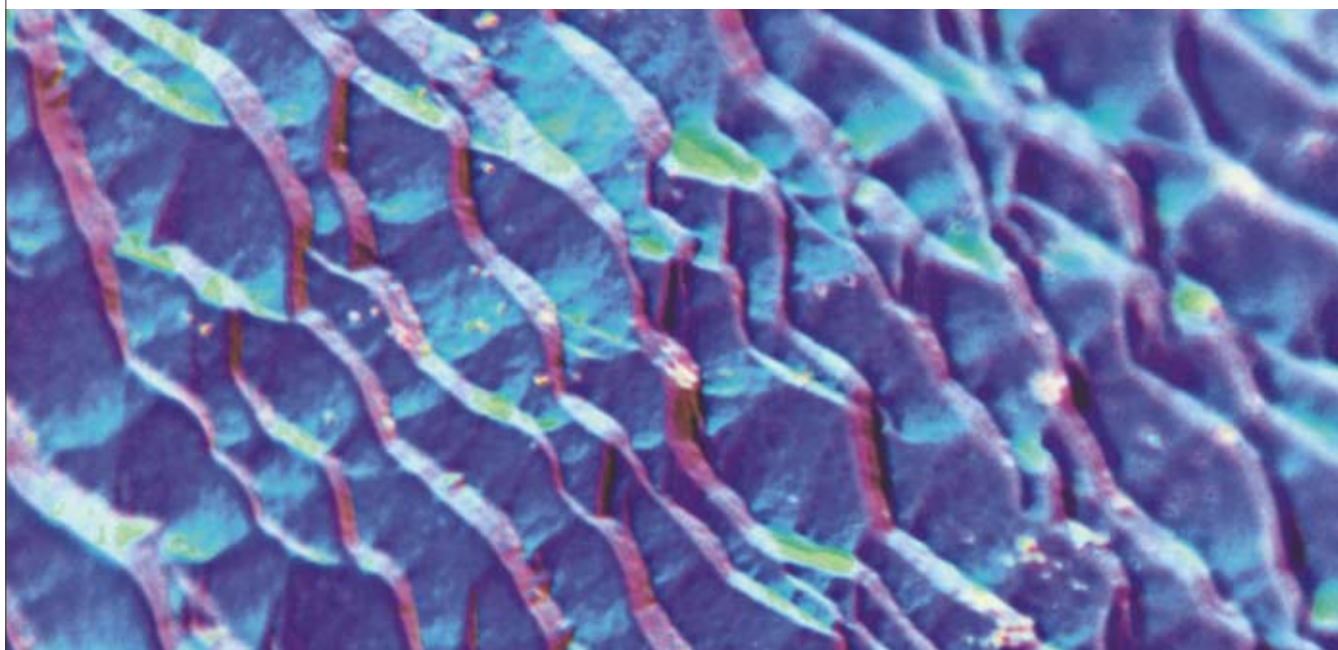
➤ **Amal Chabli**

LETI Institute (Electronics
and Information Technology Laboratory)
Technological Research Division
CEA Grenoble Center

Diamond, the ultimate material for sensor fabrication

Diamond features many remarkable properties. Therefore it may be used in many applications, where its characteristics yield outstanding performance –

e.g., for the fabrication of sensors, and transducers – MEMS-type transducers, SAW sensors – or of electrodes.



The surface of a synthetic polycrystalline diamond, magnified 800-fold.

Compared to materials such as [silicon \(Si\)](#) or silicon carbide (SiC), diamond exhibits an altogether exceptional combination of electronic, thermal, optical, and mechanical properties (see Table). Diamond is an optically transparent [semiconductor](#) material, with a level of [biocompatibility](#) close to that of glass, and exhibiting remarkable mechanical, and

chemical properties. This paper concentrates, more specifically, on the way this material is used in the fabrication of specific sensors, in particular for sensors involving [transduction](#) modes of a mechanical (micro-electromechanical systems [MEMS]), acoustic (surface acoustic waves [SAW] devices), or [electrochemical](#) ([electrodes](#)) character.

property	silicon	silicon carbide	diamond
Young's modulus (Gpa)	150	450	1,050
Poisson's ratio	0.3	0.14	0.1
hardness (kg/mm ²)	1,000	3,200	7,000
fracture toughness (Gpa)	1	5.2	5.3
flexural strength (Mpa)	127.6	670	2,900
coefficient of friction	0.4–0.6	0.2–0.5	0.01–0.04
bandgap width (eV)	1.1	2.9	5.5
electron mobility at 300 K (cm ² /V/s)	1,400	1,000	2,200
hole mobility at 300 K (cm ² /V/s)	600	50	1,600
thermal conductivity at 283 K (W/cm/K)	2	5	20
acoustic velocity (km/s)	8	13	18
density	2.1	3.2	3.5

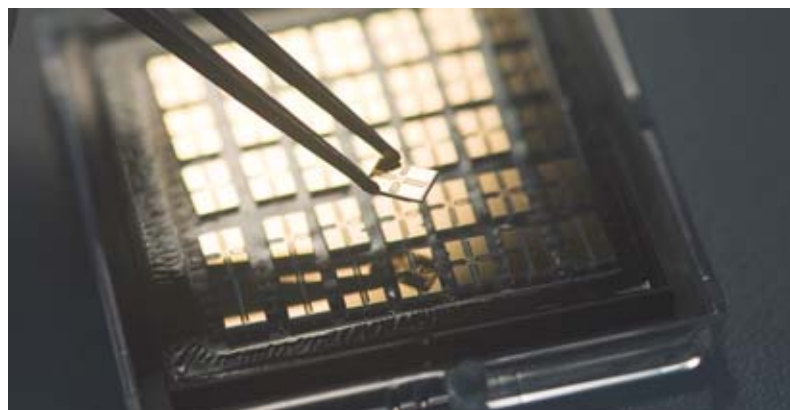
Table
Physical properties of diamond, compared to those of silicon, and silicon carbide.

Diamond owes its performance characteristics, as a whole, to:

- its intrinsic mechanical, optical, thermal, **physico-chemical**, and acoustic properties;
- its composition, as a **carbon**-based substance, allowing **functionalization** to be achieved by way of covalent binding, by attaching specific chemical, or biological groups: enzymes, proteins, or **DNA**, for sensors operating in accordance with a **biomimetic** approach;
- its semiconducting properties, allowing the fabrication of **electronic components**;
- its electrochemical performance: stability, inertness, wide potential window;
- its biocompatibility, with regard to *in-vivo* applications.

Since natural diamond are rare and expensive, the diamond used for research purposes has to be **synthesized** in the laboratory: since 1997, the Diamond Sensors Laboratory (*Laboratoire capteurs diamant*),⁽¹⁾ at CEA, has relied on **chemical vapor deposition (CVD)** for the fabrication of high quality diamond. Originally employed for the fabrication of **radiation** detectors, this process is now more specifically dedicated to the fabrication of devices used in information technology as well as for biomedical technology. The process involves depositing thin films, obtained from gaseous precursors (**methane, hydrogen**), in a microwave-assisted **plasma**, typically at a pressure of 100 mbar, and a temperature of 700 °C, using a variety of substrates, e.g. silicon, glass, quartz... Depending on the synthesis process, the materials obtained may consist of insulators (used for detectors, dosimeters, thermal dissipation layers, optical ports), or conductors, these being employed to fabricate dedicated electrodes for electrochemical, thermoionic, bioenergy... applications. This process, moreover, is particularly suitable for the purposes of sensor fabrication. In this respect, the Diamond Sensors Laboratory team is involved in several converging multiannual European collaborations.

In the following pages, a number of applications are reviewed: the fabrication of microcantilever chemical sensors; the functionalization of SAW resonators; and electrode fabrication:



P. Stroppa / CEA

- the fabrication of MEMS⁽²⁾-type chemical sensors featuring diamond beams (microcantilevers), serving for chemical detection purposes (biology, narcotics...);
- the functionalization of SAW⁽³⁾ resonators, i.e. the deposition, onto the resonator's surface, of a sensitive layer, used for specific detection of a number of chemical or biochemical agents. This technique is used, e.g., to achieve the specific detection of toxic chemical agents, or explosives (in collaboration with teams at CEA/Le Ripault);
- electrode fabrication: this type of diamond electrochemical sensor exhibits high stability, and strong reactivity; such sensors allow chemical compounds being detected electrochemically, in a liquid medium;

SAW devices, to be used for chemical sensors.

(1) One of the components of the Systems and Technology Integration Laboratory (LIST: *Laboratoire d'intégration des systèmes et des technologies*), coming under CEA's Technological Research Division (DRT).

(2) MEMS fabrication involves the use of microtechnologies. These devices feature vibrating beams, the vibrational characteristics of which make it possible to ascertain their mass, and thus the presence of chemical compounds fixed to their surface. Their selectivity with respect to certain compounds means such devices may be used as mechanical transducers.

(3) The construction of SAW devices relies on the setting up of an acoustic wave traveling across a surface. In like manner to a wave at the surface of a fluid, the presence of chemical compounds on that surface disturbs the propagation of this acoustic wave, thus making it possible to detect certain compounds, the device thus serving as an acoustic transducer.

In-situ measurement of the diamond thickness synthesized, during deposition.



P. Gripe/Signatures/CEA

Diamond growth being carried out in a microwave-plasma-assisted chemical vapor deposition (MPCVD) reactor.



P. Gripe/Signatures/CEA

Fabrication
of a diamond
microelectrode array.



P. Siroppe / CEA

the chief applications relate to the areas of environmental **trace** measurements (heavy metals, pollutants...), or biology (measurements of urine samples, neuronal interfaces...).

MEMS: vibrating-beam chemical sensors

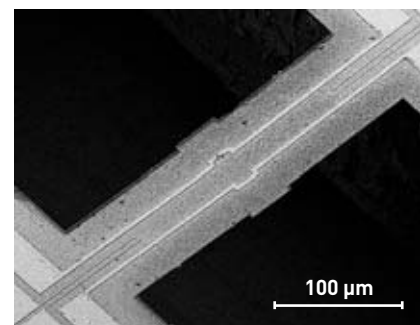
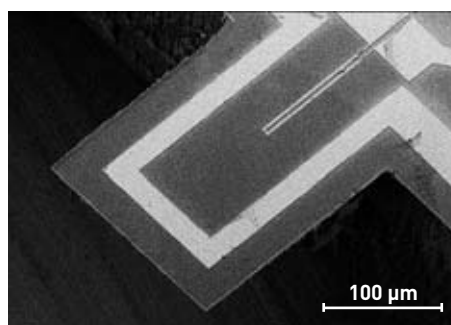
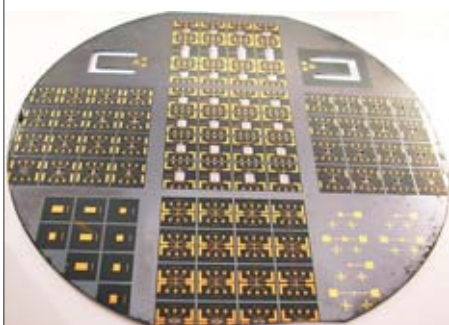
MEMS-based sensors, i.e. sensors involving electro-mechanical transduction, mainly rely on silicon technologies (handling, manufacturing...). However, notwithstanding the advances achieved, in terms of know-how, the mechanical properties featured by this material are not seen as altogether advantageous, for this type of application. Such applications, indeed, would benefit from the availability of a material affording improved performance in terms of mechanical toughness, fatigue resistance, chemical inertness, thermal conductivity, and stability. Hence the approach, taken up by researchers, of fabricating diamond **microstructures**, affording potentials seen as favorable for the purposes of MEMS fabrication. Indeed, diamond cantilevers operate at very high resonance frequencies, and consequently higher sensitivity: two major advantages, with regard to the fabrication of vibrating-beam sensors. At the same time, because of its **carbon** terminated surface, diamond offers a wide range of possible chemical synthesis routes to immobilize organic functional groups onto its surface, providing the ability to make such transducers particularly selective, with a view to applications as chemical, or biological sensors. One

such functionalization is the subject of a collaboration bringing together the Diamond Sensors Laboratory, and the French Higher School of Electronics and Electrotechnical Engineering (**ESIEE: École supérieure d'ingénieurs en électronique et électrotechnique**). The two teams have developed selective diamond nucleation techniques, suitable for all kinds of substrates, allowing the fabrication of vibrating beams (see Figure 1). In contrast to conventional **nanotechnology** approaches, the material is directly synthesized across the regions where the cantilevers are to be fabricated. By way of a mechanical characterization of these devices, it was shown that diamond enables to obtain remarkable mechanical properties, with a **Young's modulus** involving values close to 1,000 GPa: i.e. values more than 7 times higher than when using silicon.

Currently, researchers are looking into the feasibility of using this technology for the fabrication of specific, dedicated detection devices, to be used in the area of biology. Indeed, one of the advantages offered by diamond is the ability to render its surface selective, by immobilizing biological receptors such as DNA, enzyme, or proteins. By way of a biometric approach, the biological function recognizes specifically the target species. It is thus possible to measure that species' mass, and hence its presence. Researchers anticipate that these new-generation sensors will have the ability to detect toxic compounds, such as, e.g., narcotics (this is part of a European project, to effect the detection of cocaine), or pesticides in drinking water. This is a very definite possibility, as recent studies, carried out by the Diamond Sensors Laboratory on prototype detectors, were able to evidence the measurement of the hybridization of DNA chains (i.e. the assembly of each of the sequences involved with its complementary sequence), on the basis of the measured resonance frequency of vibrating diamond beams, onto which a DNA fragment – albeit quite a short one: 32 base pairs – had been grafted.

Functionalization of SAW sensor systems by diamond nanoparticles for selective detection purposes

The operation of chemical, or biochemical sensors of the **gravimetric** type relies on the measurement of a variation in the sensor's resonance frequency. Such sensors are made by coating one side of a **piezoelectric** transducer (also known as an acoustic resonator, or piezoelectric resonator) with a sensitive layer, synthesized



CEA

Figure 1.

4-inch substrate used for MEMS fabrication: the process relies on selective diamond growth, in the nanocrystalline form (left panel). Metal lines, to allow beam actuation by means of Lorentz forces [i.e. **Laplace forces**], can also be seen on the cantilever (middle panel) or bridge structures (right panel).

from a material having the ability to adsorb – more or less selectively – the target chemical, or biochemical species. Since such species interact with the sensitive layer, the mass of that layer rises, causing the transducer's resonance frequency to drop. The mass adsorbed onto the sensitive layer thus induces a change in the transducer's resonance frequency, which can be measured. However, there is a downside to this: any further variation in the sensor's surface acoustic properties contributes – in some cases, to an extent that is far from negligible – to the modification of the transducer's resonance frequency – for instance, a change in the material's intrinsic parameters (*density*, elasticity), or any alteration of its physical dimensions (thickness, in particular). There is thus a risk of perturbations to the measurements obtained by the sensor, or of a falloff in the signal-to-noise ratio.

To address this issue, the Diamond Sensors Laboratory has developed an original technique, relying on the chemical stability exhibited by carbon, and involving the use of diamond *nanoparticles*. This technique serves the purpose of stabilizing the sensitive regions, in the form of a thin – hence not liable to disturb the acoustic resonator – *porous* monolayer. In this configuration, the diamond nanoparticles serve to enhance the active surfaces of the sensitive layers, with a good reproducibility of their distribution across the surface of SAW sensors. This process has been patented by LIST. The stability of the nanoparticles' position, on their support, is the outcome of diamond deposition – carried out in a matter of minutes – over these surfaces. This deposition makes it possible to bind the nanoparticles to one another, while not affecting the coating's porous character.

Such nanoparticles have been used, in particular, on 433-MHz quartz SAW resonators, with a circuit board having the capability to record simultaneously measurement, from 8 readout channels. Figure 2 plots the response to successive cycles of exposure to calibrated concentrations – as generated on the laboratory's test bench – of dinitrotoluene (DNT) vapors. Use of a diamond-nanoparticle functionalization layer enabled the team, in particular, to bring down detection limits to values lower than 1 part per billion (ppb) for dinitrotoluene (DNT), a harmless derivative of the explosive trinitrotoluene (TNT), as well as for a classic – and likewise harmless – simulant of toxic warfare agents, viz. dimethyl methylphosphonate (DMMP), which is similar to sarin nerve gas.

Ongoing investigations are dealing with selective compounds subject to detection, by means of comparative measurements. This type of process also serves for the detection of gas-phase neurotoxic compounds, or chemical pollutants. It is further used for the specific detection of explosive compounds in the gas phase, e.g. of trinitrotoluene (TNT), or ethylene glycol dinitrate (EGDN). These investigations are being carried out in collaboration with CEA's Le Ripault Center (central France).

Electrochemistry for the purposes of chemical detection in liquid media

The electrochemical properties of diamond are well known: a wide potential window, low residual currents, high corrosion resistance, and good fouling

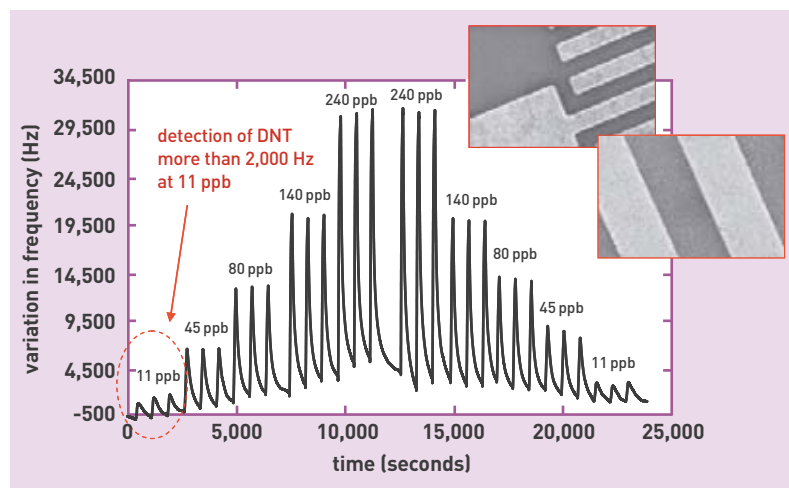


Figure 2. A 433-MHz SAW transducer, featuring a surface enhanced through deposition of diamond nanoparticles (insets). This type of device makes it possible, by means of specific functionalization, to effect the detection e.g. of dinitrotoluene (DNT), in a fast, reproducible, linear manner, with very low detection limits: less than 1 ppb. Similar detection limits are obtained for DMMP.

resistance. Such properties mean that diamond is a material of choice for designing electrochemical sensors (see Figure 3). Such sensors are commonly used to determine analyte concentrations in samples, for security purposes, or for biomedical engineering, measurement engineering, or environmental

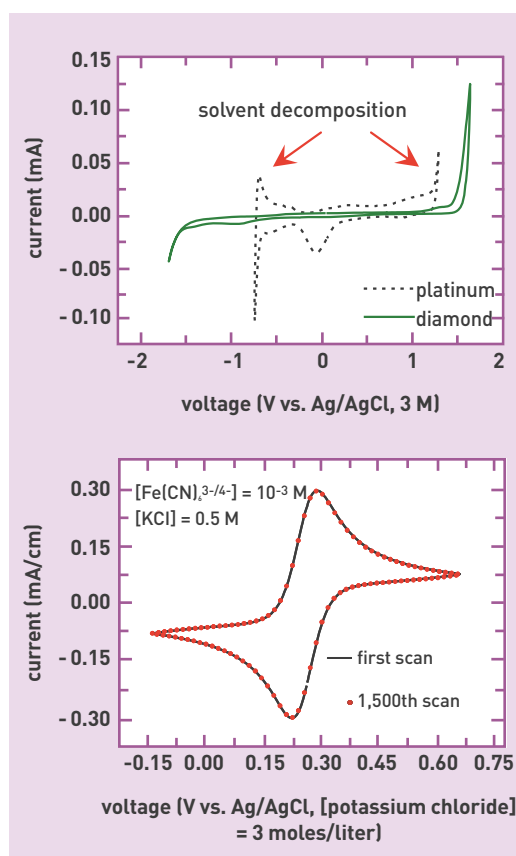


Figure 3. Electrochemical properties of diamond, compared to those of a conventional platinum (Pt) electrode: the potential window, in water, is about twice as wide, and dark currents are weaker (top). Cyclic voltammetry measurement, carried out using diamond electrodes, with the ferri/ferrocyanide couple, demonstrating electrode reactivity, and perfect stability, as measured in this instance after 1,500 cycles (bottom).

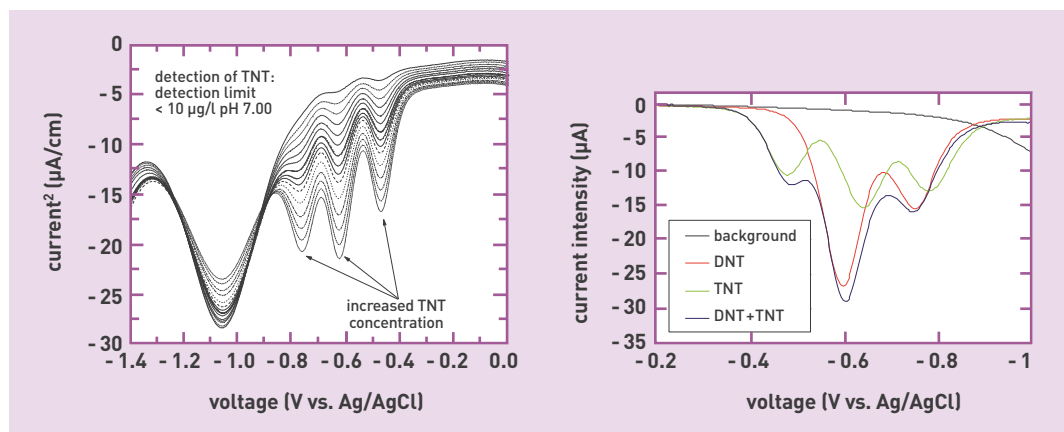


Figure 4. Specific response observed as TNT undergoes reduction, when using diamond electrodes (left panel). Direct discrimination is a possibility, even for DNT, on the basis of the position, and number of reduction spikes (right panel).

analysis... The fabrication of these sensors entails, as a prerequisite, that two challenges be taken up: first, that of enhancing diamond reactivity, to match the levels achieved with commonly-used sensor electrodes (platinum electrodes, in particular), since response quality, for a sensor, is determined by reactivity; second, improving electrode stability, this being a condition of sensor reliability.

On the basis of CVD synthesis, investigations were carried out on boron-doped nanocrystalline⁽⁴⁾ diamond films to enhance their electrochemical performance. The electrodes fabricated for these studies were optimized by cyclic voltammetry, and electrochemical impedance spectrometry. The stability of the electrodes electrochemical behavior was computed by carrying out a systematic characterization of the temporal evolutions of electrode response, both when subjected to intensive electrochemical stimulation, and in quiescent conditions. The results obtained by the Diamond Sensors Laboratory show that electrode stability increases, for an optimum concentration of boron atoms in diamond. A refinement of the electrochemical characterization protocol allowed improved discrimination, and quantification to be achieved, as regards the component of electrode evolution attributed to exposure to air, to the redox solution, or to electrochemical stimulations, according

to the material's terminals, or dopant concentration. This made it possible to obtain extremely stable electrodes (see Figure 3), for which response remains unaltered after more than 1,500 voltammetry cycles (in the presence of the ferri/ferrocyanide couple). These electrodes have been successfully used, in particular for the purposes of TNT detection by square-wave voltammetry in acetonitrile, or aqueous media, or in seawater. Lower detection limits stand at less than 15 µg/l (see Figure 4).

Such electrodes are found to be highly useful for the purposes of trace detection, in drinking water: e.g. for the detection of heavy ions, or of such contaminants as lead, cadmium, arsenic, cyanides, or pesticides. This type of device has further been found helpful for the investigation of high oxidation states in inorganic complexes of biological relevance. Thus, by setting up catalytic receptors on the electrode, it becomes feasible, e.g., to achieve the direct detection of hydrogen peroxide (H₂O₂). As a result, by making use of the possibility of covalent⁽⁵⁾ grafting of specific functions, dedicated sensors may be fabricated, for the purposes of glucose detection by means of the immobilization,

(4) Involving nominal grain diameters close to a few hundred nanometers.

(5) The strongest type of chemical bonding, which may be set up, in the present case, with carbon in diamond form.

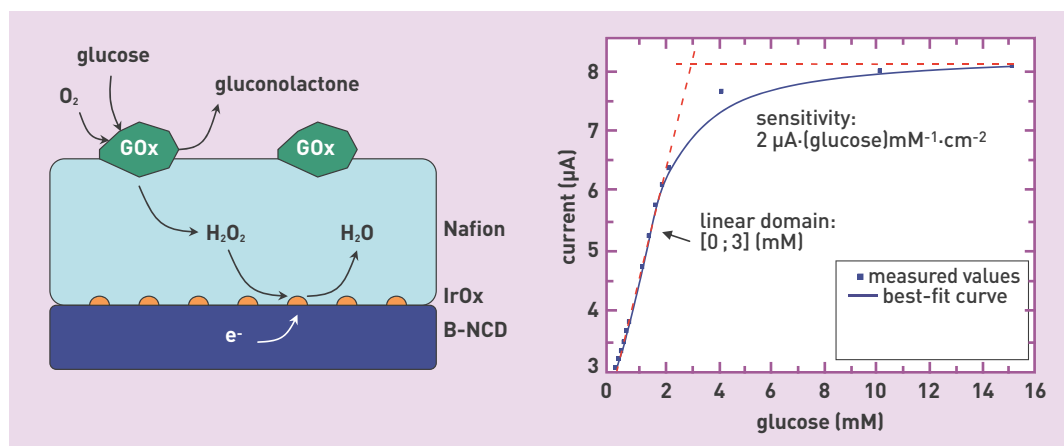


Figure 5. An example of the electrochemical detection of glucose, by means of the immobilization of glucose oxidase, and detection of hydrogen peroxide (H₂O₂) over a diamond electrode. Shown at left: the principle: iridium oxide (IrOx) is the mediator, glucose oxidase (GOx), and boron-doped nanocrystalline diamond (B-NCD). Right panel: the response, showing the linearity region.

on the diamond electrode's surface, of the glucose-specific enzyme glucose oxidase (see Figure 5). The principle may be adapted for many other enzymes, e.g. for the direct detection of neurotransmitters, or of specific compounds in urine (lactate, urea...). This investigation is being conducted by the Diamonds Sensors Laboratory in collaboration with the Nanosciences and Cryogenics Institute (INAC: *Institut nanoscience et cryogénie*), at CEA's Grenoble Center (southeastern France), and the Néel Institute (*Institut Néel, CNRS Grenoble*).

The Diamond Sensors Laboratory is further developing diamond electrode arrays, also known as "multi-electrode arrays," or "microelectrode arrays" (MEAs; see Figure 6). These arrays are fabricated by means of selective diamond growth, conforming to array patterns, over various kinds of substrate – a similar process to that used for MEMS fabrication. This work is being carried out in collaboration with ESIEE. For instance, microelectrode arrays fabricated in this manner were developed to perform neuronal stimulation, as part of projects aimed at the fabrication of

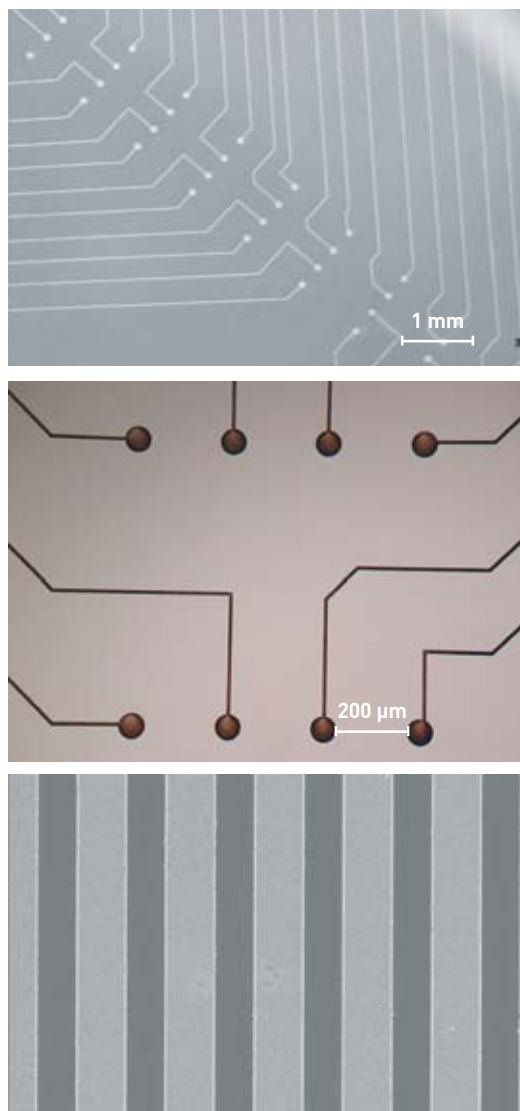


Figure 6. Diamond microelectrode array, fabricated from diamond lines selectively deposited onto glass, used for the recording, and stimulation of cell culture arrays. The three pictures show different sizes of contacts, and lines, which may be varied as desired.

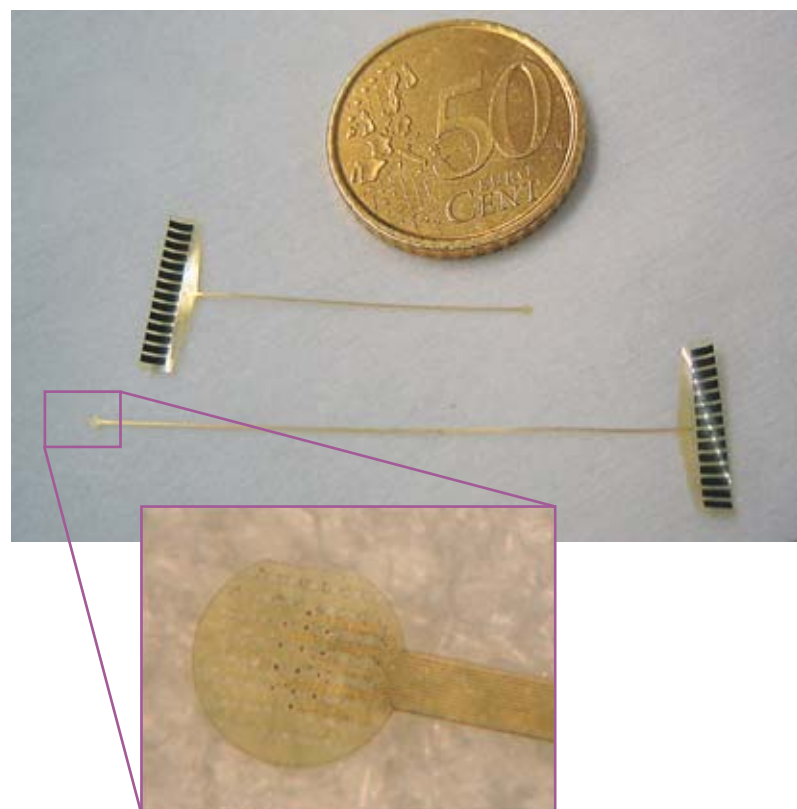


Figure 7. Flexible diamond-on-polyamide implants, developed, in partnership with ESIEE, for the purposes of retinal implant fabrication, under the aegis of the MEDINAS project, sponsored by the French National Research Agency (ANR: *Agence nationale de la recherche*).

retinal implants (see Figure 7). Owing to the use of diamond electrodes, such implants exhibit high stability, and biocompatibility.

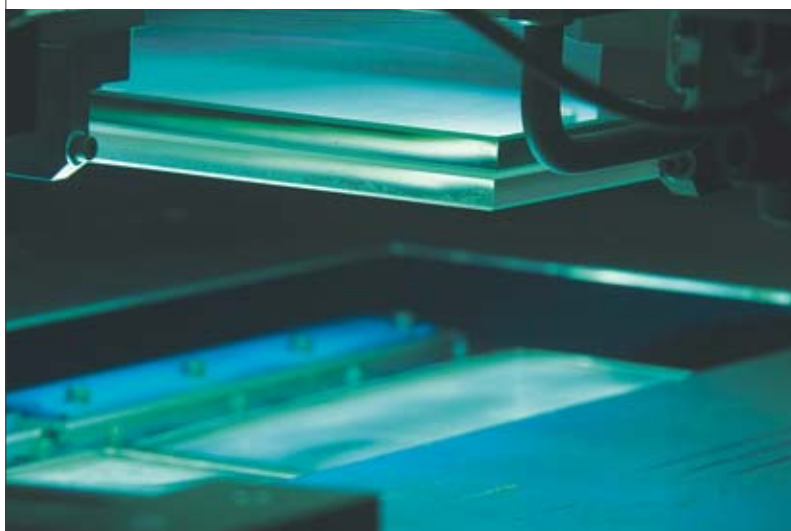
Interfaces of this type are currently being developed with the Vision Institute, in Paris (*Institut de la vision de Paris*), under the frame of retinal implant fabrication projects. Achieving a successful outcome entails that one major issue be resolved: narrowing down the interelectrode gap, to ensure increased resolution, for the image being stimulated over the retina. The difficulty concerns, first of all, the physical positioning of diamond microelectrodes with a separation of about 10 μm ; and, second, the feasibility of reducing the intensity of the stimulation current, at each electrode (pixel) – this involving a risk: that of not being able to locate effectively the stimulation generated. This is where the electrochemical properties of diamond may show their full effectiveness.

The advances achieved, with regard to diamond synthesis, have resulted in the emergence of novel, prototype chemical, and biological sensors. Current developments are focusing on the detection, in the liquid phase, including in biological fluids, or in the gas phase, of toxic, or explosive compounds, narcotics, or biological substances, with applications in security, medical or environmental areas. The part of this effort concerned with biological tissue stimulation stands as a further, highly promising area.

> Philippe Bergonzo and coworkers
LIST Institute (Systems and Technology
Integration Laboratory)
Technological Research Division
CEA Saclay Center

Nanostructured thin films by the sol-gel route

As of now, **sol-gel chemists have the ability to construct materials in “customized” fashion, the variegated wealth of possible combinations opening the way to a multiplicity of applications.** Easily implemented as they are, and readily transferred to an industrial environment, thin-film coating techniques unquestionably afford the most promising potential, in the range of forming techniques available.



P. Stroppa / CEA

Ultraviolet (UV) insolation being carried out on a multilayer sol-gel coating, deposited by laminar-flow coating. This a densification method for inorganic materials, patented by CEA, where it is used as an alternative method to thermal, or chemical treatment. The apparatus subjects the coating to irradiation by UV radiation, the energy of that radiation being absorbed by the materials deposited in thin film form. Inorganic polymerization ensues, the material thus being endowed with enhanced mechanical strength, and chemical resistance. The chief advantage afforded by this method is its rapidity: a few tens of seconds insolation time, as against some 30 minutes for heat treatment at 120 °C.

Beginning as early as 1985, the Materials Department at CEA, based at CEA's Le Ripault Center (central France), has been devising complex multilayer architectures, for the purposes of fabricating a wide range of materials, exhibiting specific properties, indeed, in some cases, altogether novel ones. The laboratory relies on the sol-gel⁽¹⁾ technique, which allows the synthesis of glasses, **ceramics**, or organic-inorganic hybrid or composite materials, and is currently employed – as its main application – for the purposes of fabricating **thin films**, i.e. layers involving a thickness not exceeding a few **nanometers**, or up to some 10 **micrometers**. The advantage afforded by this process stems from the fact that, once deposited onto a substrate, such a thin film provides the ability to modify the latter's properties in “customized” fashion. Of the many possible options, as regards nanoscopic

■ (1) An abbreviation for “solution-gelation.”



P. Stroppa / CEA

Visual inspection of a highly reflective stacked multilayer sol-gel coating.



P. Stroppa / CEA

A substrate bearing a high-reflectivity stacked multilayer sol-gel coating.

organization, the Materials Department has elected to prioritize four possible solutions, in terms of film nanoconstruction, and **nanstructuring**.

Oxide-nanoparticle films

It is now feasible to fabricate sol-gel coatings by the colloidal route⁽²⁾ – to synthesize, that is, coatings solely consisting of nanometer-size particles. The **porosity** obtained, in such coatings, results in their exhibiting peculiarly advantageous functional properties. The process involves effecting the chemical conversion of the material to the **oxide** form. This operation is invariably carried out in solution, this making it possible to operate at ambient pressure, and temperature. The outcome yields a particle assembly of low compactness, forming porous layers. The point should be made that colloidal thin films, aside from exhibiting a low **refractive** index, remain mechanically fragile; on the other hand, they give rise to low levels of internal stresses, this allowing the deposition of micrometer-scale thicknesses. For the properties of the deposited film to be controlled, the solutions containing the nanoscopic particles must remain stable over time, in terms of **rheology**. A variety of methods are available, to achieve this: **electrostatic**, or **steric** methods, or haloing, i.e. the setting up of halos of **nanoparticles** around microparticles, serving to stabilize them.

This colloidal route is found to be particularly suitable for the purposes of optical applications, in particular for optical thin films, owing to its ease of implementation at low temperature, and of the outstanding performance obtained, in terms e.g. of the optical index, or of the ability to withstand intense light fluences. On the other hand, making use of this route entails that two barriers first be overcome, to wit those of mechanical fragility, and sensitivity to the atmosphere. Indeed, since colloidal thin films are porous, and lack cohesion, they are found to exhibit high sensitivity. This has led researchers to endeavor to reconcile optical performance, in films, and satisfactory mechanical properties. A recent study, carried out on a colloidal silica film, has made it possible to arrive at a promising compromise.⁽³⁾ The study shows that, by means of a **catalytic** post-treatment in a gaseous environment (more precisely: a treatment using **ammonia**),



P. Stroppa/CEA

A substrate being positioned for optical coating, deposited by way of a laminar-flow coating treatment.

abrasion resistance, in silica-nanoparticle films – exhibiting as they do a porosity higher than 50% – may be considerably enhanced. This result is readily accounted for. Indeed, post-catalysis promotes the formation of interparticle bonds, by way of a surface reaction, resulting in the setting up of **siloxane**, or **hydrogen** bridging bonds between neighboring colloids (see Figure 1).

(2) Two sol-gel synthesis routes are available: the inorganic, or colloidal route, effected from metal salts in aqueous solution (chlorides, nitrates, oxychlorides...); and the organometallic, or polymer route, obtained from metal alkoxides in organic solutions.

(3) This an original result, demonstrated as part of a doctoral thesis, and subsequently patented by CEA.

(4) Such a film exhibits resistance under moderate test conditions, as per US standard MIL-C-675-C.

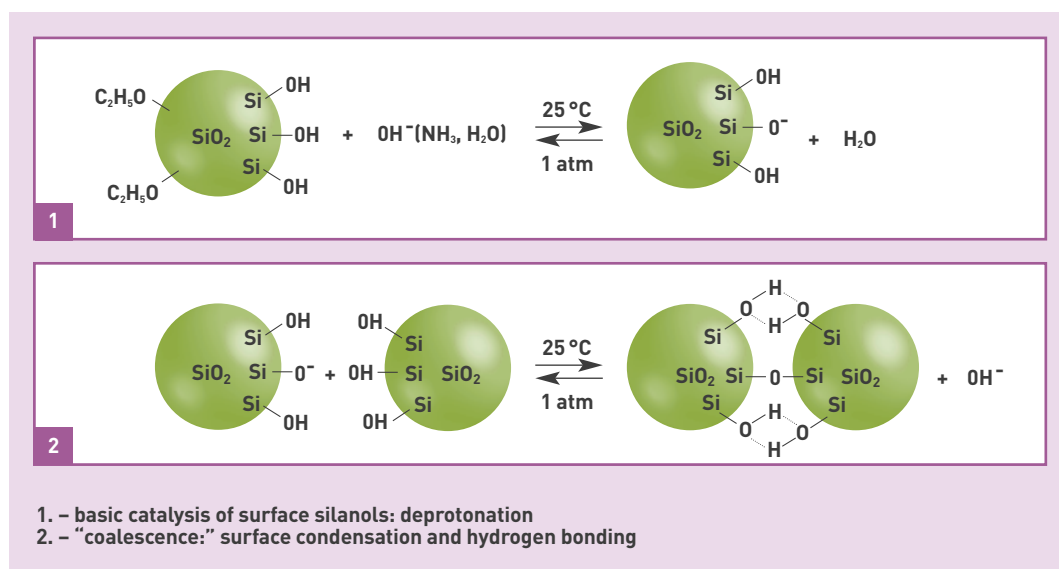


Figure 1.
The ammonia hardening reaction mechanism. 1 atm stands for the unit of atmospheric pressure, C₂H₅O for the ethoxy radical, Si for a silicon atom, OH for the hydroxyl radical, NH₃ for ammonia, and – of course – H₂O for water.

Carried out at ambient temperature, such chemical **sintering** has the effect of enhancing the film's mechanical cohesion, while leaving its index unaltered – thus not altering its optical properties.⁽⁴⁾ This instance of the nanostructuring of an inorganic film is a good illustration of the way deposition of a thin film results in a morphological alteration of the surface (see Figure 2). At the same time, to preclude any degradation, over time, of the optical properties exhibited by such films, there remains the possibility of a **functionalization** of these coatings, by means, in particular, of **nonpolar** groups. This operation results in considerably diminished sensitivity, for the colloidal films involved, to molecular **adsorption**. It makes it possible to obtain a high-porosity (50%) nanoparticle film, exhibiting a transparency as high as 99%, **hydrophobic** in character – with a water contact angle of 125° – affording a high specific surface area, together with mechanical strength. Owing to their properties, such coatings are also used as sensitive layers in dedicated sensors, for the purposes of detecting gas-phase molecules – for the detection e.g. of explosives, or pollutants.

Mesostructured hybrid organic–inorganic membranes

The synthesis of hybrid organic–inorganic materials opens up striking prospects, with regard to the development of functional nanomaterials,⁽⁵⁾ suitable for a vast range of applications, spanning all of the fields of experimental science (chemistry, physics, biology, mechanics...). As there is no way all of these areas could be reviewed, one instance is covered here, concerning the synthesis of a functional nanomaterial, developed for an application as a fuel cell component (an **electrolyte** membrane, for an electrolyte-supported cell). In this synthesis operation, the inorganic fraction brings the functions inherent in inorganic compounds: e.g. mechanical strength, chemical inertness, high-temperature resistance, or

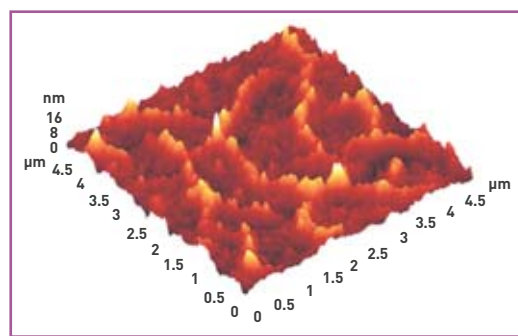
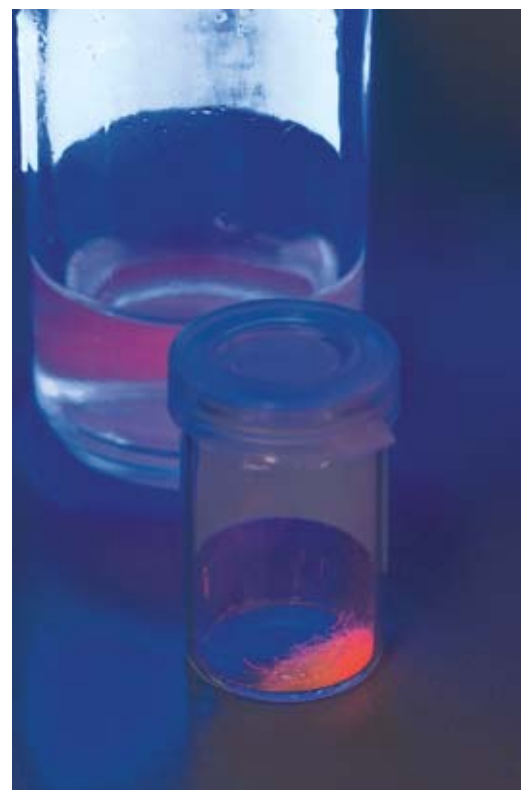


Figure 2.
A nanostructured sol-gel coating, subsequent to chemical sintering, as viewed under atomic-force microscopy [scale: 5 μm (x) × 5 μm (y) × 10 nm (z)].



Figure 3.
Detail micrographs of the (mesoporous) nanostructure of a composite sol-gel matrix.



A hybrid organic–inorganic solution containing nanostructured particles, functionalized by means of chromophores.

optical, and electrical properties... while the organic fraction contributes to mechanical behavior (by way of structuring, as a matrix), plasticity, adhesion, transparency...

By taking up an option that contrasts with recent concepts, as regards nanostructured materials,⁽⁶⁾ it now becomes possible to put forward innovative structures, based on a simple idea: employing a two-phase **composite** structure, in which a nanostructured phase is yielded by in-situ synthesis, within a dense **polymer** (see Figure 3a). In such a configuration, each of the two phases provides the desired physical property. By acting on the nature of the chemical precursors,⁽⁷⁾ it then becomes feasible to influence the nanostructure exhibited by the phase so generated, and thus to vary its optical properties, for instance (see Figure 3b, c).

In such a process, nanostructuring is achieved through the use of **molecules** serving as templates, as the material builds up in solution. These molecules are subsequently removed, thus generating porosity within the material. The porosity thus obtained is characterized by a calibrated pore size, or even by a **crystalline** struc-

(5) C. SANCHEZ, B. JULIAN, P. BELLEVILLE, M. POPALL, "Applications of hybrid organic–inorganic nanocomposites", *J. Mater. Chem.* 15 (2005), pp. 3559–3592.

(6) Recent concepts call for the mere blending of one component of organic character, with one inorganic component. Opting for a method that contrasts with such concepts means that a single material is fabricated, consisting of two interpenetrating networks, owing to the method used for the synthesis of the inorganic phase, this being effected e.g. within the organic phase (*in situ*).

(7) A compound that occurs prior to the emergence of a given intermediate, or end product – into which it is subsequently converted – in a chain of chemical, or biological reactions: dopamine is a precursor of noradrenaline.

ture (see Figure 4, left panel). This concept was successfully implemented, for the development of hybrid **ion-conducting** nanomaterials, involving the fabrication of interpenetrating organic, and inorganic components (see Figure 4, right panel). The porous inorganic phase, generated *in situ*, provides a large exchange surface area – particularly advantageous, with regard to its ion-conduction properties – which may be as high as 1,200 m²/g. Concurrently, the **hydrophilic** character of the inorganic phase (silica)⁽⁸⁾ endows the material with a high water retention capacity, within the membrane itself. There is thus a benefit to be gained in using **mesostructured** hybrid organic–inorganic membranes, in low-temperature proton-exchange membrane fuel cells (PEMFCs), i.e. the type of fuel cell that is being most actively investigated, owing to its many possible applications, in the automotive sector in particular. Compared with conventional **proton-exchange** membranes, fabricated from **Nafion®**, such membranes stand as a real breakthrough, with regard to improving membrane **conductivity**. The other possible option involves a functionalization of the pores in the inorganic network, by means of proton-conducting groups, likewise affording the ability to optimize membrane conductivity.

Nanocomposite films featuring a ceramic composition

For the purposes of developing materials in the form of coatings, it is imperative that control be ensured, of the thickness of the deposits being carried out – a know-how all the more difficult to achieve, should it be desired that a wide range of thicknesses be catered for. For instance, obtaining deposits of supermicron (1–100 µm) thickness by the liquid route raises a number of issues, related to the internal mechanical stresses that arise in films (**tensile**, or compressive stresses), which may yet be bypassed, by making use of a nanocomposite formulation, involving a blend of a polymer material with nanoparticles.

The composite sol–gel process was first described in

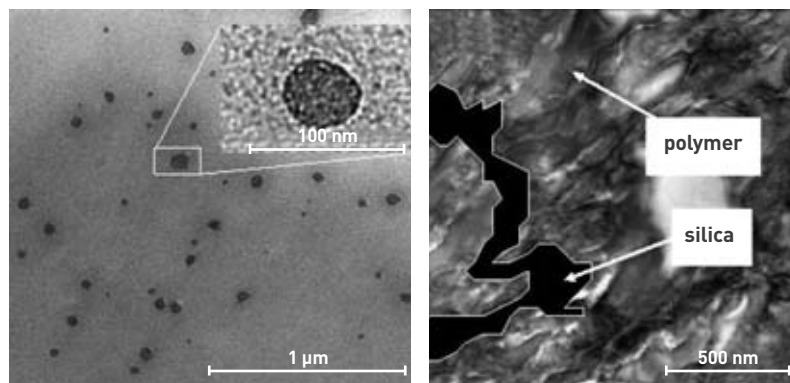


Figure 4. Micrograph of a mesostructured hybrid membrane, held in a proton-conducting polymer. The left panel shows mesoporous silica particles – as viewed under microscopy – synthesized within an organic polymer matrix; the inset (top right) shows a detail view of a magnified silica particle. The right panel shows a micrograph of interpenetrating organic/inorganic networks, resulting in a nanostructured hybrid membrane.

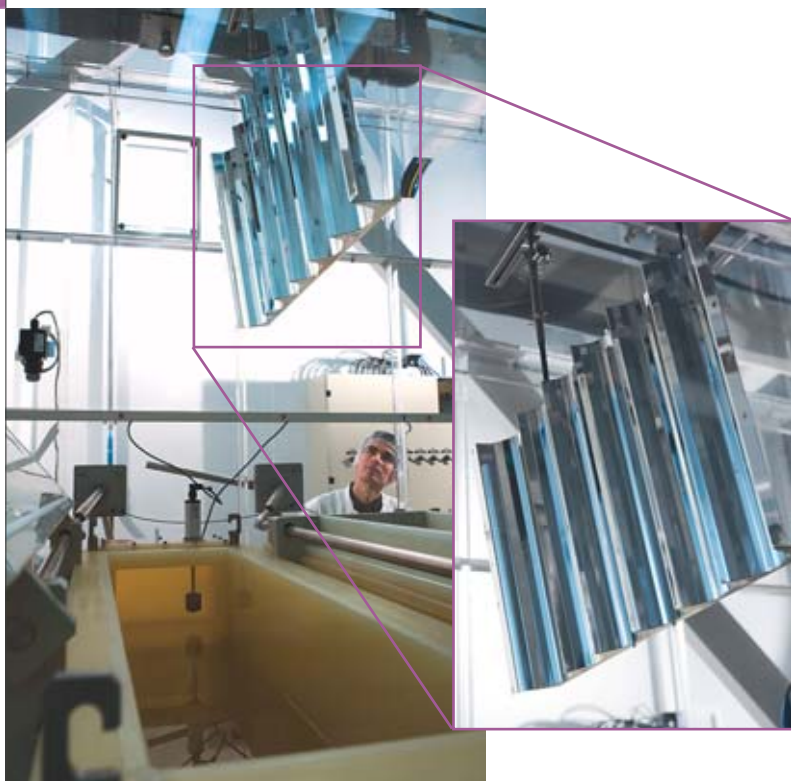
1995, by David Andrew Barrow, then employed as an engineer at **Datec Coating Corporation** (USA). The solution implemented involves a mixture of sol–gel binders (as a rule, a polymer solution), to which small **ceramic** particles – referred to as the “filler” – are added – the binder’s function being that of “cementing” the ceramic grains to one another. Such a composite formulation (i.e. the polymer–particle blend) has the effect of limiting the propagation of mechanical stresses within the deposit. Material chemists use this process for the preparation of inorganic films involving thicknesses ranging from a few micrometers to several tens of micrometers, free from cracking, or **delamination** – a result conventional solutions had proved unable to achieve. The solution is deposited onto the substrate by spin **coating**.⁽⁹⁾

(8) A material of choice, being chemically stable, and inexpensive to synthesize.

(9) A deposition method involving the injection of a liquid onto a support that is then rotated.



An operator setting up a nanoparticle synthesis operation – taking place in a fume hood – by the sol–gel process, in a rotary evaporator.



A metal reflector undergoing dip-coating treatment.

dip-coating,⁽¹⁰⁾ pneumatic spraying,⁽¹¹⁾ or by laying on as a varnish. Once deposited, the solution is subjected to a thermal treatment, at a temperature sufficiently high to remove the organic groups, and induce the formation of the crystal lattice. The outcome of these operations yields a polycrystalline film, featuring a tunable porosity, which is able to absorb such mechanical stresses as may arise, in the event of stacks being built up to a large thickness. This nanocomposite sol-gel process is employed, in particular, for the preparation of **lead zirconate titanate (PZT)** thick films, more specifically used for applications as high-frequency ultrasound **transducers** (for high-frequency echography probes). With regard to the **piezoelectric** properties exhibited by such films, the nanocomposite sol-gel process makes it possible to achieve precise control of the thickness of the layers deposited, but equally to investigate the feasibility of

depositing them onto substrates featuring complex shapes. The process further allows control to be achieved for low-temperature thermal treatments. Moreover, should the filler in the composite be yielded by the polymer solution that serves as a binder, the chemical affinity between the two components is thereby enhanced, this optimizing the composite's properties. High values for the coupling factor – a parameter expressing piezoelectric performance – standing at around 50%, have been achieved, for 50 μm thick films, with a resonance frequency of 50 **MHz** (see Figure 5, left panel). Concurrently, researchers have produced prototype ultrasound transducers (see Figure 5, right panel). A multielement transducer, of the “linear array” type, featuring a resonance frequency of 30 **MHz**, likewise demonstrated outstanding **electroacoustic** properties – a result verified for some 10 elements.

These investigations show the feasibility of, and the benefits to be gained from, the composite sol-gel process, for the purposes of fabricating piezoelectric thick films, and as regards their application as high-frequency ultrasound transducers. Compared with the results reported in papers published to date, the performance levels obtained, with respect to the coupling factor, went up from 34–35% to 50%. As of now, such electroacoustic properties are seen to stand at a sufficiently high level to warrant an industrial application being contemplated, for single- or multielement transducers. Under more specific consideration is the incorporation of such coatings into an ultrasound device, to be used for medical imaging purposes: for skin, or eye echography, or small-animal imaging.

Nanostructured coatings obtained by thermal spraying

Used for the purposes of fabricating refractory coatings on free-form components,⁽¹²⁾ this process involves depositing a material by injecting it, through a dry process, into the jet of a **plasma** torch – serving to effect the melting of the ceramic grains, and to spray them

(10) A deposition method whereby a support is dipped into a bath of liquid solution, and subsequently withdrawn, at a controlled rate.

(11) A deposition method whereby a liquid is pneumatically sprayed onto a support.

(12) I.e. components involving a non-planar geometry.

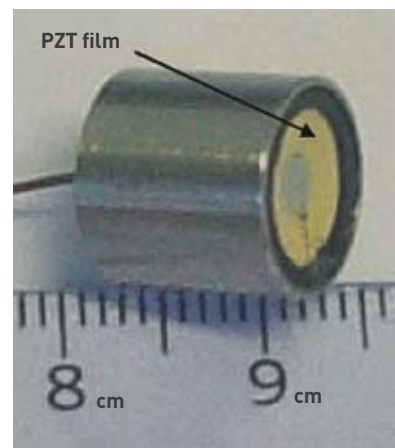
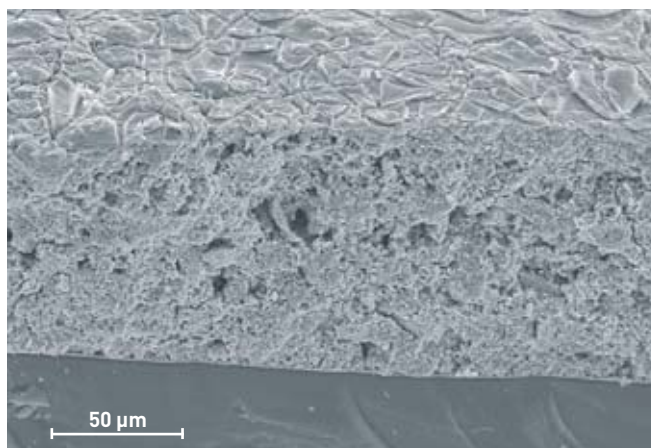


Figure 5.
A piezoelectric lead zirconate titanate (PZT) film, fabricated by the nanocomposite sol-gel route (left panel); and a sol-gel PZT-based focusing ultrasound transducer (right panel).

onto a support, in the form of micrometer-scale (about 50 μm) particles – by means of a carrier gas. This operation yields thick deposits, ranging in thickness from about 100 micrometers to several millimeters, exhibiting a highly **anisotropic**, lamellar structure, determining their **thermomechanical** properties. The drawback, as regards this process, is its inability to ensure the penetration – still as a dry process – of submicron particles into the plasma jet, meaning it is thus of no use, for the purposes of fabricating thin films. This gave rise to the notion, taken up by researchers, of substituting the carrier gas with a liquid, to obtain novel (**isotropic**) coating microstructures, and microthicknesses. This principle was demonstrated with a colloidal suspension of nanometer-scale **zirconia** particles (see Figure 6).

The nanostructuring of the thin films obtained is achieved with a tunable **density**, depending on the nature of the plasma (see Figure 7). As it is injected, the liquid (a **solvent**, into which nanoparticles have been added) breaks up as a result of the pressure – the plasma's **kinetic energy** breaking up the droplets into a multiplicity of microdroplets, while its **thermal energy** vaporizes the liquid. As the liquid undergoes vaporization, the particles held in one and the same droplet agglomerate with one another. The resulting agglomerates are then melted, wholly or in part, by the plasma, and accelerated, before reaching the substrate, and coating it. In the event of the agglomerates being wholly melted, grain sizes range from a few hundred nanometers to several micrometers. On the other hand, should melting be partial only, grain size, in the deposit, remains identical to the size of the particles held in the initial liquid. In the context of thermal spraying, this is an altogether innovative result, yielding as it does the construction of nanostructured deposits. This is accounted for by the fact that, as the coating is synthesized, the characteristics of the initial colloidal sol (**crystallite** size, distribution of crystalline phases) are preserved (see Figure 7).

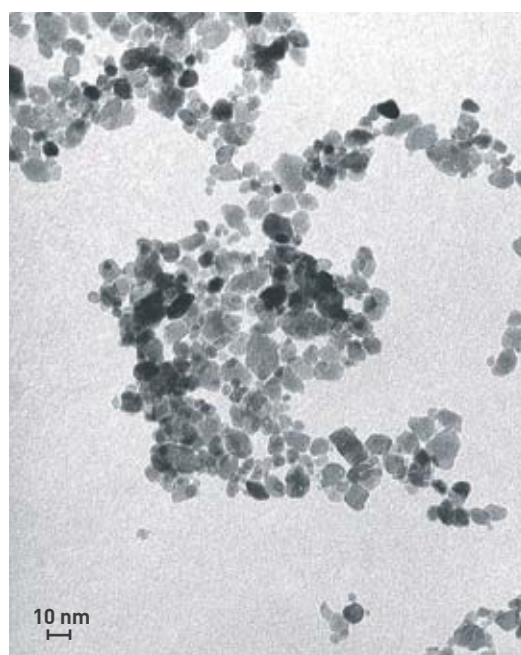


Figure 6.
A nanocrystalline zirconia sol, as viewed under transmission electron microscopy.

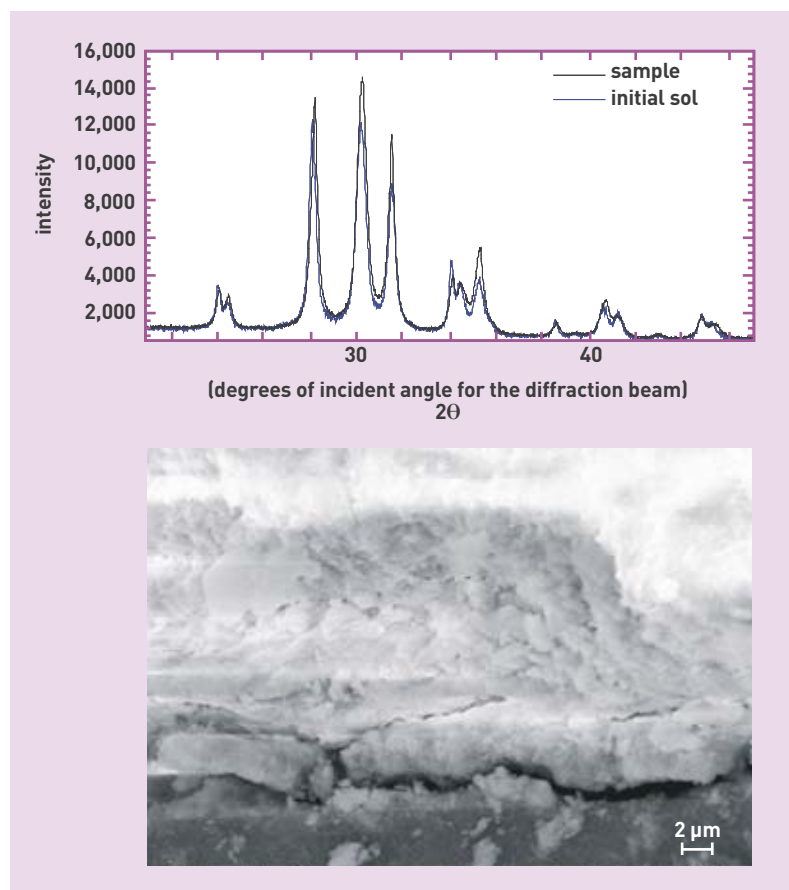


Figure 7.
Top panel: comparison of the initial sol, and the final layer, by X-ray diffraction (XRD);
bottom panel: cross-section of the nanostructured deposit obtained by plasma thermal spraying.

The preceding examples show that the very rich chemistry of nanoparticles in suspension, combined with the feasibility of “nanoconstructing” the desired material, afford unquestionable potentials, with regard to the fabrication of novel materials, making use of innovative processes, involving a breakthrough technology. The possible combinations of precursors are seen to be endless, opening up prospects such as to allow chemists both to satisfy their eagerness to make discoveries, and to gain an understanding of new materials, and their need to have the ability to meet the demands, and requirements of industry. Obviously, preference should be given to a fabrication route in solution, bearing in mind the ability of such a route to limit, or even suppress, the risks associated to nanomaterials, and thus respond to societal concerns relating to the production, and use of nanomaterials.

> **Philippe Belleville**
Materials Department
Military Applications Division
CEA Le Ripault Center

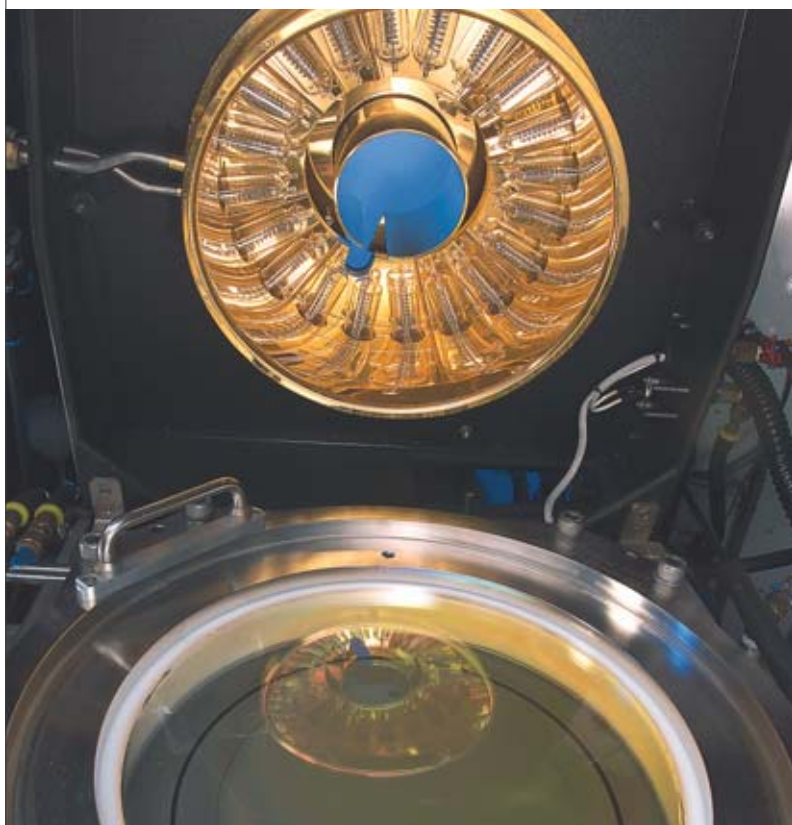
FOR FURTHER INFORMATION

JEAN-PIERRE JOLIVET, MARC HENRY, JACQUES LIVAGE, *De la solution à l'oxyde*, Paris, CNRS Éditions-EDP Sciences (1994).

CLÉMENT SANCHEZ, BEATRIZ JULIAN, PHILIPPE BELLEVILLE, MICHAEL POPALL, “Applications of hybrid organic-inorganic nanocomposites”, *J. Mater. Chem.* 15 (2005), pp. 3559-3592.

Carbon nanotubes and two-dimensional carbon materials for microelectronics

The renewed excitement felt by the scientific community, with respect to carbon, and carbon materials, is not only due to the structural beauty of these materials, rather it owes much to the extraordinary physical properties they exhibit. **CEA has achieved excellence, with regard to the worldwide state of the art, in terms of R&D on carbon nanotubes, and graphene.**



A Centura reactor, opened up to show the support for the silicon wafer onto which carbon nanotubes will be deposited.

The past 20 years have witnessed a major rediscovery – that of a chemical element scientists had believed to be well known to them: **carbon**. Standing as the sixth **element** in the periodic table of elements, and the fourth most abundant element in the Universe, found in every form of life so far known to us, carbon nonetheless had experienced an ebbing away of interest from the research community. Over the past 20 years, however, it has made a comeback to the forefront of the scientific scene, with renewed panache. It all started in 1985, with an original paper that was to earn its authors (Robert F. Curl, Jr., Harold W. Koto, and Richard E. Smalley) the Nobel Prize in Chemistry, awarded to them in 1996. The paper they had coauthored described what they dubbed buckminsterfullerene (C_{60}), a **molecule** belonging to the **fullerene** family, consisting of precisely 60 carbon **atoms**, also known as the “football” molecule (or

“buckyball”), owing to its configuration, which may be likened to that of a soccer ball (see Figure 1).

What really set things on fire, however, was the discovery, in 1990, of the first bulk **synthesis** route for C_{60} , and more widely for the entire fullerene family, by Donald R. Huffman, and Wolfgang Krätschmer, then a postgraduate, and professor, respectively, at the **Max Planck Institute for Nuclear Physics**, in Heidelberg (Germany). On the basis of their work, it became feasible, almost overnight, to achieve the simple, reproducible synthesis of a molecule, the scientific importance of which, and the potential for applications, in physics as in chemistry, were seen as ranking on a par with those of **benzene**. All the ingredients had come together, therefore, that were to enable Japanese physicist Sumio Iijima to observe, in 1991, **carbon nanotubes** (see Figure 1), under **electron microscopy**, in the products yielded by C_{60} synthesis – and that would result in his findings being received with particular attention, even though, historically speaking, that observation was not the first one of its kind. The final bombshell came in 2004, when Andre K. Geim, a research scientist and professor at the School of Physics and Astronomy, at the **University of Manchester** (UK), published the results of his investigation of carbon atoms arranged in a single sheet: a

(1) It should be noted that, owing to a prevalent misuse of the term, the word “graphene” tends to be used to refer to graphite materials comprising a very limited number of sheets, whereas this designation was strictly reserved, originally, for the single-sheet material.

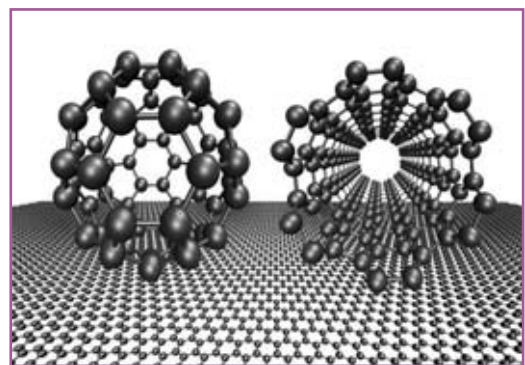


Figure 1. Atomic models of the buckminsterfullerene [i.e. $[60]$ fullerene, C_{60}] molecule, of a carbon nanotube, and of a graphene sheet.

material known as **graphene** – a stack of several graphene planes constitutes **graphite** (see Figure 1).⁽¹⁾ This was to earn him, together with his colleague at Manchester Konstantin S. Novoselov, the Nobel Prize in Physics, in 2010.

Structural beauty, allied to extraordinary physical properties

These twin characteristics, standing as they do as the hallmark of these substances, account for the excitement generated by such carbon-based materials in the scientific community – nanotubes, and graphene, in particular.

Carbon nanotubes: an iconic industrial product, yielded by nanotechnologies

Classically, carbon nanotubes are described as the outcome of the folding, into a tubular shape, of one of more graphite planes. However – a subtle point, with major consequences – the tube's **chirality** varies, depending on the direction of the axis about which the sheet is rolled up, relative to the hexagonal lattice of carbon atoms in the plane. This results in an infinity of possible chiralities, for carbon nanotubes. Each of these determines a distinct, specific band structure, with correspondingly distinctive electrical characteristics. Statistically, nanotubes fall into the category of metallic materials for one third of chirality values, other values inducing the character of a **semiconductor** material, with bandgaps varying according to chirality. The advantage afforded by metallic nanotubes is their ability to withstand current **densities** of $4 \cdot 10^9 \text{ A/cm}^2$, i.e. double the density achieved in copper. Exhibiting as they do a **thermal conductivity** of $3,500 \text{ W/(m}\cdot\text{K)}$ at ambient temperature, as against $\sim 400 \text{ W/(m}\cdot\text{K)}$ for copper, nanotubes are further found to act as outstanding **heat conductors**. Finally, carbon nanotubes exhibit remarkable mechanical properties, including the highest known elastic moduli – and hence the highest tensile yield strengths – for any material.

Graphene: a crystal confined to a two-dimensional space

Owing to the band structure that characterizes it, graphene comes under the class of semi-metals. Its specific characteristic is a considerable charge mobility (i.e. both hole, and **electron** mobility) at ambient temperature, with measured values of more than $15,000 \text{ cm}^2 \cdot \text{V}^{-1} \cdot \text{s}^{-1}$ (i.e. more than 10 times the value found for **silicon**), and a maximum theoretical value of $40,000 \text{ cm}^2 \cdot \text{V}^{-1} \cdot \text{s}^{-1}$. Further, graphene's magnetic properties mean it has the potential to stand as a major material in the field of **spintronics**: spin relaxation lengths of more than 1 **micrometer** have thus been reported (at low temperature). As for its optical properties, it has been shown that the absorbance of a single sheet of graphene stands at about 2.5%, inducing a drop in transparency, for the substrate onto which it is deposited, visible to the naked eye – a rare occurrence, for an atomic monolayer.

Miracle materials, with a stiffness 10 times higher than steel

Three methods currently predominate, for the purposes of fabricating carbon nanotubes, and graphene.



C. Dupont / CEA

Laid out here in superposed mats, carbon nanotubes afford a wealth of applications for industry: for flat screens, fuel-cell membranes, or as chemical pollutant sensors, when molecules are grafted onto them.

Synthesis

The initial technique employed, for the purposes of carbon nanotube synthesis, involved using an electric arc, set up between two graphite **electrodes**, in a reduced atmosphere of inert gas, in the presence of a metal **catalyst**/promoter, serving to promote nanotube growth. This fabrication method was abandoned, owing to its many drawbacks: low efficiency, high energy demands, the presence of large amounts of impurities once synthesis is completed (e.g. amorphous carbon, fullerenes, metal particles) – this leading to the development of new synthesis methods, affording higher performance.

At the present time, the favored method makes use of the so-called vapor growth technique. This involves effecting the decomposition, in a furnace, of a gaseous carbon source (e.g. **methane**), in the presence of a growth promoter. While new variations may arise, the process usually relies on the same principle: a carbon source serving to saturate, at high temperature, a metal **nanoparticle**, as a rule kept in the liquid state, so as to enhance, and speed up, carbon dissolution. If all external conditions are met, this carbon-saturated nanoparticle keeps on dissolving carbon, subsequently “releasing” some of it, in nanotube form. These nanotubes may feature a single wall, or several walls, depending on the – tunable – synthesis parameters, and on the particle's chemical nature, and diameter. Owing to the large number of parameters involved, the nature of the nanotubes produced varies from one source to the next, or even from one synthesis to the next. The final goal does remain, nevertheless, that of controlling the number of walls such nanotubes feature, and their diameter, and equally the number of topological defects arising in the carbon atom lattice, and, most crucially, nanotube chirality. Now, this chirality is what determines the physical properties of nanotubes, in particular the electrical properties they exhibit. In a matter of 10 years, tremendous advances have been made in this respect, and very high efficiencies are obtained, with single or double-walled nanotubes exhibiting truly monodisperse diameters, but equally a relatively limited chirality distribution, and consequently more uniform electrical properties (rather than the conventional distribution, with 33% metallic materials against 67% semiconductors: a 90% fraction, for one or the other class of material, may thus be achieved). In this respect, CEA has achieved excellence, with regard to the worldwide state of the art, as a result, in particular, of:

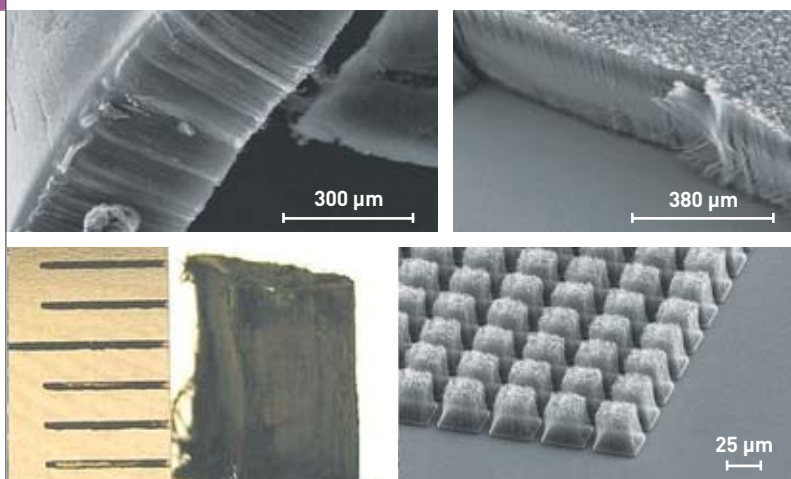


Figure 2.
Carbon nanotube forests. Top left: a monolayer forest; top right: a multilayer forest;
bottom left: forest of ultralong (longer than 5 mm) nanotubes; bottom right: a forest
featuring controlled localized growth.

- its achievement, as regards effecting nanotube synthesis in the form of very dense nanotube forests, or lawns (see Figure 2). In such structures, nanotubes grow perpendicular to the substrate, and parallel to one another, much as trees in a forest, or blades of grass in a lawn. In this context, nanotubes may be grown to lengths of several millimeters. These structures are found to be particularly useful for the purposes of fabricating high-performance electric wires (at nano-, micro-, or macroscopic scales), or – once impregnated with polymers – for water filtration purposes: the tubes (having been opened by the fabrication process) act as the pores in a conventional membrane. This work involves a collaboration bringing together the Nanosciences and Cryogenics Institute (INAC: Institut nanoscience et cryogénie), the Radiation-Matter Institute, Saclay (IRAMIS: Institut rayonnement-matière de Saclay), and the Innovation Laboratory for New Energy Technologies and Nanomaterials (LITEN: Laboratoire d'innovation pour les technologies des énergies nouvelles et les nanomatériaux);
- its ability to grow nanotubes in isolated, localized manner, for application purposes: e.g., to form dedicated emission tips, for field-effect devices, such as those used in portable X-ray generators.

With regard to graphene, research is at a less advanced stage. In this context, the initial preparation technique involved the use of a simple adhesive tape, to peel off

graphene planes from a graphite crystal, and transfer some of the material onto a plane surface – a silicon wafer, for instance. Selection of the best sample would then be carried out under transmission electron microscopy, or near-field microscopy. Currently, three new methods are seen as contenders, for the purposes of obtaining a graphene plane that is well crystallized (as the number of defects directly impacts the mobility of charge carriers), and that features as large a spatial extension as feasible:

- heat treatment of silicon carbide, at very high temperature (higher than 1,200 °C), in vacuum, to effect the sublimation of silicon: this technique affords the advantage of leaving carbon in graphene form on the surface of the substrate, thus making it possible to subject it, subsequently, to the processes conventionally used in microelectronics (lithography, doping...);
- insertion of alkali metals, or organic molecules, intercalated between the sheets of a graphite block, this allowing graphene to be exfoliated into an organic solution, and subsequently deposited, in controlled fashion, onto a surface, from the graphene sheets held in suspension;
- decomposition of a carbon source at the surface of a metal catalyst: the best results achieved involve the use of nickel, or even of copper tapes, yielding graphene sheets of several square centimeters. Expertise, in this respect, has been developed at the Electronics and Information Technology Laboratory (LETI: Laboratoire d'électronique et des technologies de l'information), working in collaboration with INAC, with regard to graphene growth on silicon carbide (SiC) substrates, and a low-temperature catalytic method on nickel (Ni), and copper (Cu), making it possible to obtain graphene in conditions that are compatible with the processes of conventional microelectronics (see Figure 3). This is complemented by a chemical approach, implemented by the Surface and Interface Chemistry Laboratory (LCSI: Laboratoire de chimie des surfaces et interfaces). This approach makes it possible to graft, in a straightforward, effective manner, graphene sheets onto monomolecular layers, thus fabricating multilayer-type graphene/molecular plane/metallic substrate junctions; this is a promising architecture, for molecular electronics.

Purification

This is a step that has already been addressed by many papers in the published literature. Its purpose is to remove the residues yielded by carbon nanotube synthesis: amorphous carbon, metal particles, fullerenes... In most cases, this involves extracting the



Experimental synthesis of carbon nanotubes by chemical vapor deposition (CVD).

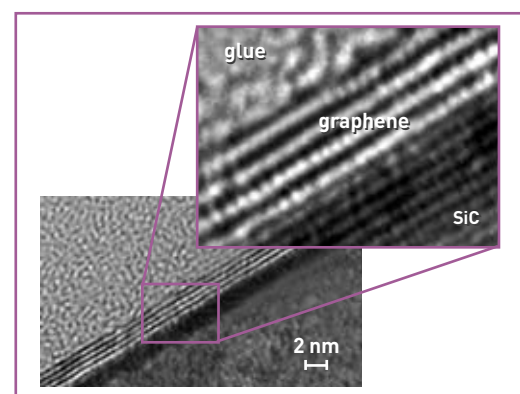


Figure 3.
Views from an investigation, under transmission electron microscopy, of graphene planes fabricated by silicon sublimation (from SiC).

fullerenes through the use of an organic solvent, and subsequently alternating acid treatments, and **oxidation** steps, to remove the metals, and amorphous carbon. Researchers are thus able to achieve high levels of purity, involving contaminant contents sufficiently low to remain compatible with utilization by the semiconductor industry.

Sorting

None of the synthesis methods currently used makes it possible to obtain a monochiral nanotube production – hence the practice of sorting nanotubes in solution. This technique involves carrying out the selective **complexation** of nanotubes, by means of an organic molecule, and subsequently effecting separation by **centrifugation**, or **chromatography**. A recent result, in this area, involves the use of a set of **DNA** sequences: each sequence exhibiting a specific affinity for a given chirality. The end result this allows is the separation of carbon nanotubes according to chirality. At CEA, the Biology and Technology Institute (iBiTec: Institut de biologie et de technologie) has developed a technique involving the covalent grafting of dedicated selective groups, with respect to semiconducting nanotubes, allowing a chemical differentiation to be achieved between metallic (not **functionalized**), and semiconductor (functionalized) nanotubes. These advances make it possible to look to the commercialization of nanotubes sorted by chirality, in the fairly near future, although neither in large quantities nor cheap. This will be tantamount to overcoming a major barrier, with regard to the applications domains for nanotubes, in electronics, which mostly rely either on metallic, or semiconducting tubes, or on tubes exhibiting one and the same chirality (e.g. for **transistors**), in order to ensure good reproducibility, for end components.

Given access to purified nanotubes of this type, a joint CEA-CNRS team, at the Radiation-Matter Institute, Saclay (IRAMIS), working in association with the Electronics, Microelectronics and Microtechnology Institute (IEMN: Institut d'électronique, de micro-électronique et de microtechnologies), at Villeneuve-d'Ascq (northern France), was able to fabricate nanotube-based electronic devices, exhibiting the highest performance achieved worldwide (at the time), in terms of cutoff frequency (see below). This result was obtained under the aegis of an international collaboration with **Northwestern University** (USA).

From research to industry

Simple electronic circuits, involving graphene-based, or carbon-nanotube-based **field-effect transistors**, are being produced, as of now, in the laboratory. These are seen, consequently, as emerging materials/components by the semiconductor industry, with a potential for integration into the structures of future electronic systems. Their manifold properties mean their possible use may be contemplated, at various levels in the architecture of such systems:

- To form the semiconductor channel in a transistor, as a substitute for silicon: such an application entails that the issues be resolved, of effecting the deposition of this material with nanometer precision; of ensuring reproducibility for the electronic properties of such a channel; and of setting up reliable contacts. Indeed, carbon nanotubes may occur with any one of many

possible chiralities, each involving electrical properties that prove slightly, or markedly different. Likewise, with regard to graphene, it must be made to exhibit the properties of a semiconductor (since this is not its intrinsic nature), and formed into a strip having a width of less than a few nanometers (to match the size of the semiconductor channels, in transistors for the coming decade), and featuring an edge definition of atomic precision (since electronic properties are dependent on this structure). Conductance ratios higher than 10^5 (for the on/off states) have thus been achieved, with transistors incorporating nanotubes, or nanostrips featuring widths of less than 10 nm – which is highly promising, albeit insufficient with regard to possible electronics applications.⁽²⁾ Finally, a reproducible process has yet to be developed, to carry out the “*n*,” and “*p*” doping of such channels.⁽³⁾ Now, theoretical simulations, carried out at INAC, and LETI, show that, in the case where a graphene strip is doped with an alkali metal, transistor properties vary widely, depending of the position of the alkali metal in the channel – to within 0.1 nm. Atomic-level precision, with regard to deposition, is thus called for, if the required reproducibility levels, from one transistor to another, are to be achieved.

- An application for this type of device, possibly in the shorter term, may arise in the area of radiofrequency applications, in particular as high-performance analog components, as found in dedicated low-noise amplifiers for wireless transmission systems. Indeed, owing to the properties they exhibit, it is anticipated that such components will be able to operate at very high

(2) It should be noted that, for graphene nanostrips, the bandgap opened up may be empirically determined as a function of strip width (*W*), using the relation:
 $E_g \text{ (eV)} = 0.8/W \text{ (nm)}$.

(3) Doping makes it possible to modify the conduction exhibited by semiconductor materials. This involves, as a rule, introducing, into the crystal lattice, a minute quantity of “perturbing” atoms. As regards silicon, “*n*”-type doping is effected by means of atoms featuring 5 valence electrons (phosphorus), i.e. one extra free electron per atom, having the ability to move about – resulting in a surplus of electrons. “*p*”-type doping is effected by means of atoms featuring 3 valence electrons (boron). In that case, there is a shortfall of 1 electron per boron atom – and consequently a surplus of “holes.” This technique is widely used for the fabrication of electronic components. In effect, the overall structure remains neutral: strictly speaking, neither “charges,” nor ions are involved.

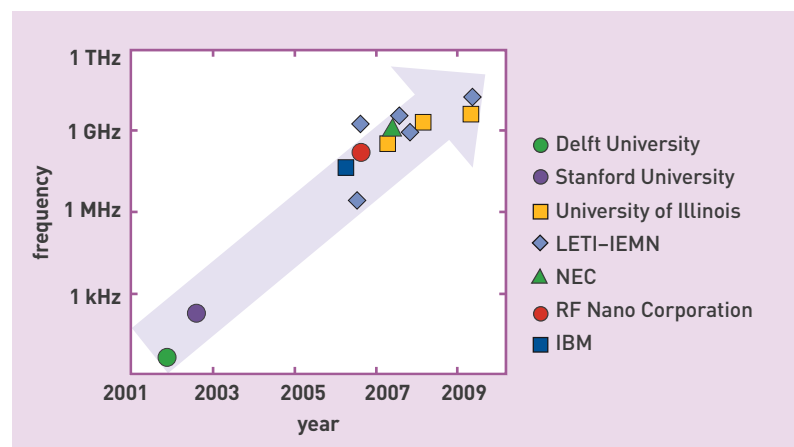


Figure 4.
 Maximum operating frequencies (on a logarithmic scale), ranged by publication date, for carbon-nanotube-based field-effect transistors. Various symbols are used, according to the organizations publishing these results.



C. Morel / CEA

Designing RFID tags, i.e. smart labels, involving electronic chips and transponders, along with radio equipment, serving to effect the rapid identification of items by means of radiofrequency signals.



Artechnique

Fabrication of organic electronic component-based devices: deposition of the various semiconducting, conducting, and insulating layers by the liquid route.

frequencies. In this respect, the results from research carried out at IRAMIS, in collaboration with IEMN, are on a par with leading efforts, worldwide (see Figure 4). Further, the ability to fabricate such transistors on flexible substrates will make it possible to incorporate these **electronic components** into organic, large-area electronic devices.

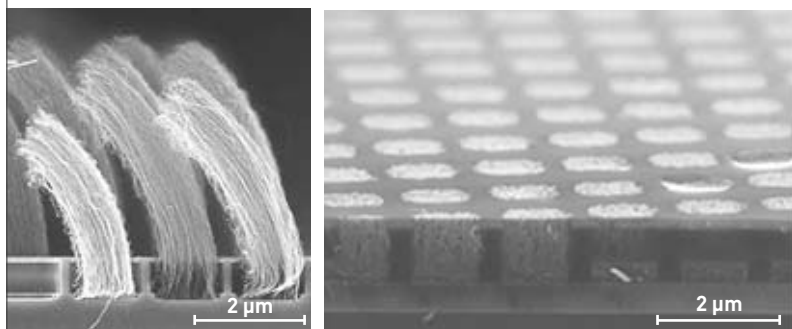
• LETI, together with the Innovation Laboratory for New Energy Technologies and Nanomaterials (LITEN) is also investigating the possibility of using such materials for interconnects, or for heat removal purposes,

under the aegis of programs set up at national level, in France, or within the European Union, in particular in collaboration with **INTEL**. With regard to interconnects, the challenge is that of promoting the growth of a forest of metallic nanotubes, aligned perpendicularly to the substrate, with a nanotube density higher than 10^{13} carbon nanotubes/cm² (in the single-wall nanotube case), held in cylindrical holes let into the substrate (vias) featuring diameters of less than a few tens of nanometers. Such a geometry results in current densities higher than 10^7 A/cm², i.e. values comparable, or even higher than those obtained with carbon nanowires of the same size. It should be noted that CEA holds the world record, as regards nanotube density, in the forests it fabricates, at $5 \cdot 10^{12}$ carbon nanotubes/cm², inserted in 1- μ m vias (see Figure 5). With regard to heat removal, the use of nanotube forests, integrated into the packaging of electronic processors, is being heralded, as of now, by the industry, as a prospect within some 3–5 years. An improvement of 20% is anticipated, as regards dissipation performance.

• Graphene, and carbon nanotubes are also being considered as substitute materials, for the transparent conducting **oxides** currently used in flat screens (whether tactile, or otherwise). For this to be feasible, a prerequisite is to obtain a film resistance sufficiently low to allow maximum light transmission. LITEN has put into operation a technology line for the deposition of such materials, allowing deposits to be made in accordance with a variety of processes, onto many, diverse types of large-area substrates. This technology is aiming for **resistivity** values lower than those achieved with the oxide currently used ($< 100 \Omega/\text{square}$, for $> 90\%$ light transmission).

A number of teams, at CEA, are also working on the employment of carbon nanotubes, or graphene, in the design of mechanical, or electronic **transducers**, to be used in the construction of dedicated chemical, or biochemical sensors (in the gas phase, or in solution) for medical applications, for diagnostic purposes in particular. These materials are used, in such a context, for the conduction channel in a simple electrical resistor, or in a field-effect transistor. The low dimensionality featured by these materials endows them with extreme potential sensitivity to any variation in their environment. For instance, the sensitivity level involved is lower than 1 part per billion (ppb) for atmospheric **nitrogen dioxide** (NO₂). On the other hand, such an advantage can turn into a drawback. Indeed, the sensitivity such components exhibit, to a wide range of stimuli (temperature, moisture, other gases...), calls for the development of specific countermeasures for each target application, depending on specifications. Researchers at IRAMIS, and LITEN are looking into ways of bypassing these barriers, with regard to the construction of gas-phase sensors, in the area of trace detection of toxic, or explosive gases.

Other advances achieved at LETI, and LITEN further include the incorporation of nanotube forests into two kinds of device. First, in the field of **liquid chromatography**, in which context this material has made it possible to enhance, by several orders of magnitude, the separation power of a microfluidic system. This is a major advance, in the area of laboratories-on-a-chip (see Figure 6). The **biocompatibility** of carbon nanotubes made it possible to design a second device.



M. Fayolle, J. Dijon / CEA

Figure 5. Carbon nanotubes held in 1- μ m-diameter vias, involving a record density, of about $5 \cdot 10^{12}$ carbon nanotubes/cm². Carbon nanotube packing density: 64%; shown after synthesis (left panel), and once the process is completed (right panel).

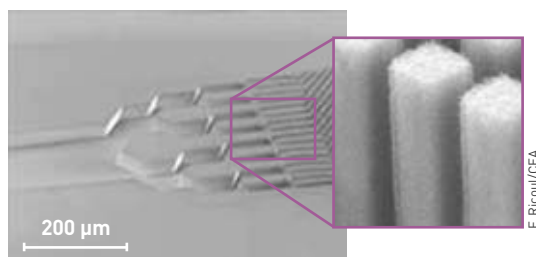
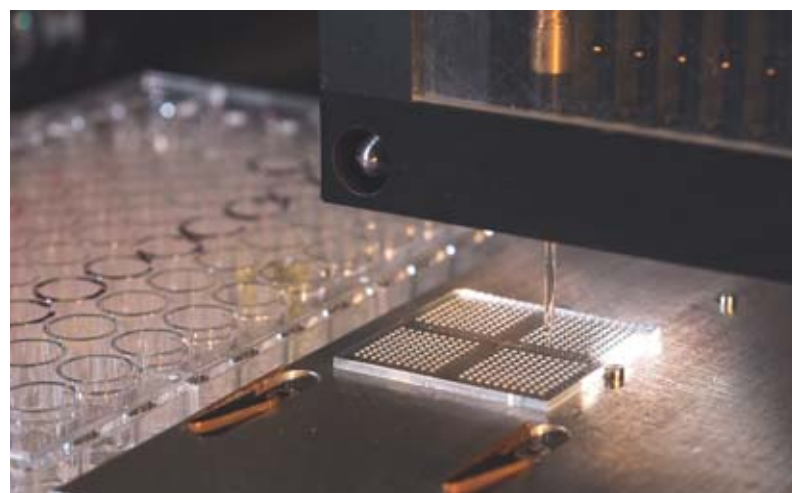


Figure 6.
A chromatography microcolumn. Shown at left, an input channel is subdivided into increasingly narrow subchannels, which run into a set of columns (right panel), functionalized by means of nanotube forests.



A technician, operating in a white room, at work on a dedicated chemical reactor, used for the collective silanization of silicon wafers, or glass plates used for the preparation of DNA chips, or laboratories-on-a-chip.

Nanotubes were thus incorporated into **electrodes**, to enhance the interface between neurons, and biosignal acquisition systems. This is a key component in the device used for the treatment of Parkinson's disease, by the deep cerebral stimulation technique. Such relationships between carbon nanotubes, and cells are being investigated by CEA in partnership with the Grenoble Neurosciences Institute (**Institut des neurosciences de Grenoble**) (see Figure 7)



Biochips for the Canérodop project. Phenochips allow for the development of chips featuring cells, on which many cell phenotypes may be recorded, by way of reactions carried out in parallel on the chip. The nature of the substrates, together with the treatments they are subjected to, make it possible to position precisely the nanodroplets, and analyze their content under microscopy (50-nl droplets on a 4-cm² glass plate).

Prospects

The various examples reviewed in the above paragraphs serve to illustrate the potential afforded by one- and two-dimensional carbon materials, and CEA's expertise, with regard to mastering the incorporation of such materials. Obviously, this is far from being an exhaustive roll call of applications – for instance, materials making use of their mechanical properties are not considered. As of now, the development of graphene-based products is at a less advanced stage than is the case for carbon nanotubes, for which research was initiated some 10 years earlier. Be that as it may, less than 4 years after the first published papers on graphene, a technology developed in the group led by Alex Zettl, a professor at the **University of California, Berkeley** (USA), was already in a position to be transferred to industry. This concerns sample-holder grids, making use of a graphene membrane, for the purposes of electron microscopy, with which atomic-scale resolution, of a quality unrivalled to date, has been achieved.

These examples show how, drawing on their creativity, research scientists are able to smooth over the frontiers setting apart basic science from applied research, by constructively quizzing one another.

> Jean-Christophe P. Gabriel

Associate Director, Cross-divisions
Nanoscience Program
CEA Grenoble Center

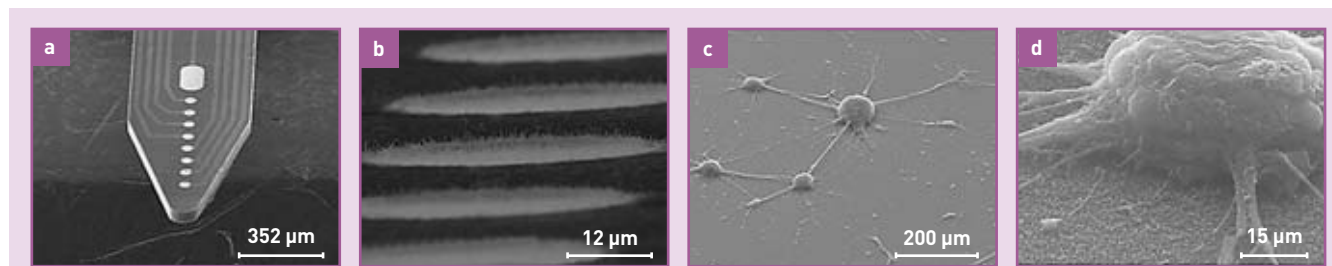


Figure 7.
Illustration, as viewed under scanning electron microscopy, of a tapered nanostructured silicon micropin, featuring 10 circular electrical contact regions (a); detail view of the carbon-nanotube-based electrical contact regions (b); *in-vitro* culture of hippocampus neurons, seen under various magnifications (c, d).

SURFACE ANALYSIS

XPEEM: a surface analysis technique eminently suited to innovative materials

When a material is exposed to **electromagnetic radiation** of sufficiently high frequency, it emits **electrons** (known as *photoelectrons*), by the *photoelectric effect*. This process involves the interaction of an incident **photon**, with an energy higher than the *photoelectric threshold*, with the electron cloud surrounding an **atom**, resulting in an electron being ejected from its orbital (*photoemission*). The photon's excess energy, corresponding to the difference between the photon's incident energy and the photoelectron's *binding energy*, is then transferred to the latter, in the form of *kinetic energy*. The deeper the shell the photoelectron comes from, the higher its binding energy, and consequently the less kinetic energy it will exhibit, as it escapes from the material. The analytical technique based on measuring the kinetic energy of photoelectrons is known as photoelectron **spectroscopy** (PES). Depending on the kind of excitation source

used – i.e. whether it involves **X-ray**, or **ultra-violet** (UV) photons – this technique is more commonly referred to either as X-ray photoelectron spectroscopy (XPS), or ultra-violet photoelectron spectroscopy (UPS). Photoelectron spectroscopy techniques make it possible to ascertain the **elemental** composition of the material being investigated, together with the electronic state and chemical nature of its various constituents. These analytical capabilities have led to the name “electron spectroscopy for chemical analysis” (ESCA) being used for XPS. Combined use of the PES spectroscopy technique with electron-emission microscopy – based as this is on the spatial variations in photoelectric emission – led to the inception of energy-filtered PEEM (photoelectron-emission microscopy) spectro-microscopy, or spectroscopic PEEM. If X-ray photons are used as the excitation source, the method is referred to as energy-filtered XPEEM spectromicroscopy, or spectroscopic XPEEM. Thus, XPEEM yields information on the electronic and chemical structure of surfaces, with a **spatial resolution** ranging from several hundred to a few tens of **nanometers**. It thus stands as a complete surface analysis technique, and one perfectly suited to the investigation of nano-objects, or heterogeneous materials studied at **mesoscopic** scales and beyond.

The binding energy of a **core-level** electron is specific to the emitting atom, providing sensitivity to that atom's local chemical environment (i.e. the nature of its first-neighbor atoms) and local atomic environment (bond lengths and angles). The **valence electrons** determine the material's electronic structure, as reflected by its **metallic, semi-conducting**, or **insulating** character. The valence electrons – particularly those lying close to the **Fermi level** – are likewise responsible for the physical properties of greatest interest with regard to nanoscience and nanotechnology applications, e.g. transport, and effective mass⁽¹⁾ properties as regards semiconductors, or those physical properties reflecting strong electron correlations, as in the case of **superconductivity**. The unique characteristics exhibited by **synchrotron radiation** mean it is a photon source that is peculiarly well suited for high-

resolution (< 100 nm) spectroscopic XPEEM purposes. However, bright laboratory sources (UV, **VUV**) may also be used, as indeed, in particular, X-ray sources, to obtain XPS imaging featuring a spatial resolution better than 1 **micron** – a result never previously demonstrated, in the laboratory.

The principle of spectroscopic XPEEM

The principle of photoelectron-emission microscopy is set out in Figure 1a. An incident beam of photons, of energy $h\nu$,⁽²⁾ illuminates a sample. A high voltage – typically 10–20 kV – allows an extractor lens, positioned a few millimeters away from the sample, to collect the photoelectric emission, across a broad range of emission angles. Behind this stands an electron optics system, for focus and image magnification purposes. The detector consists of a multichannel plate, coupled to a fluorescent screen, which is ultimately imaged via a CCD camera.⁽³⁾

The practical lateral resolution, in a PEEM system, is dependent on the counting statistics and mechanical stability. If these points can be optimized, then constraints on resolution stem, on the one hand, from the optical system's spherical⁽⁴⁾ and chromatic⁽⁵⁾ aberrations, and, on the other hand, from the **diffraction** limit for the photoelectrons being analyzed.



P. Stroppa/CEA

The “NanoESCA” microscope, a spectroscopic XPEEM system, set up at CEA/Grenoble. Combining as it does microscopy and spectroscopy capabilities, this innovative surface imaging technique allows a physical characterization to be obtained of the surfaces of materials and nanostructures, from the mesoscopic scale down to 10 nanometers or so. As it strikes the sample's surface, an X-photon beam extracts from it electrons, which are then sorted according to their energy, by means of twin hemispherical analyzers. One of these may be seen in the background.

(1) Effective mass (properties): a notion used in solid-state physics, for the investigation of electron transport. Rather than describe electrons having a fixed mass, moving under a given potential, this involves describing them as free electrons, with an effective mass, which may vary. This mass may be positive, or negative, and higher, or lower than the electron's actual mass.

(2) I.e. the product of frequency ν , by the Planck constant h , this being the universal constant whereby, in **quantum mechanics**, the particle and wave aspects of matter are related: $h = 6.626\,068\,96(33) \cdot 10^{-34}$ J·s.

(3) CCD (charge-coupled device) camera: an imaging system in which a conventional optical system focuses the image onto an array of photosensitive semiconductors.

(4) Spherical aberration (of an optical system): a geometric aberration due to the fact that rays coming from the edge and center of the optical system are not focused onto the same point. The anticipated point image is replaced by a more or less blurred halo.

Using a bandpass electron analyzer, of bandwidth ΔE , allows a spectroscopic PEEM analysis to be carried out, i.e. an analysis involving full energy filtering. It then becomes feasible to image the intensity of a given electronic level – e.g. a core level – with a resolution of the order of a few tens of nanometers, if the counting statistics warrants it. The system is tuned to ensure optimum transmission. In this manner, the entire photoemission spectrum may be investigated using spectroscopic XPEEM (see Figure 1b). The energy-filter symmetry,

involving as it does two hemispheres, suppresses aberrations that would be inherent in using a single hemisphere.

At the present time, the spectroscopic XPEEM technique is applied to a wide variety of research domains: **nanstructures**, **doped semiconductor structures**, **polycrystalline materials**, **ceramics**, electronic structures and electronic band dispersion, magnetic domain⁽⁶⁾ imaging. Two relevant examples, with regard to the characterization of new materials and objects, are reviewed here.

Imaging polarized ferroelectric domains in BaTiO₃

Ferroelectric thin films are attracting considerable interest, owing to their potential applications, for low-energy-consumption electronic devices. Indeed, engineering the **polarized** domains in such films would allow commutation between logic states (i.e. states that may take on either 1, or 0 as value) to be achieved, with no electric current going through. Barium titanate (BTO: BaTiO₃) is a ferroelectric oxide, of the **perovskite** type, of prime importance in this respect. In strained thin film form, on a suitable substrate, e.g. **strontium titanate** (STO: SrTiO₃), BTO remains in the **tetragonal** ferroelectric phase up to 600–700 °C.

Micron-size domains of polarization P^- were written into a 20-nm BTO film, **epitaxially** deposited onto a STO(001) substrate, by **piezoresponse force microscopy** (PFM). The electronic structure was investigated by core level imaging, at the photoemission threshold, for barium (Ba), **titanium** (Ti) and oxygen (O), and valence band imaging. It will be noted, for instance, that barium core levels undergo a shift, which is dependent on the intensity of the polarization applied (see Figure 2). A certain degree of surface **adsorption** was also evidenced, exhibiting polarization-dependent variability. These observations are of the utmost importance, since interaction between the atmosphere and a ferroelectric body's surface is liable to have a strong influence on the latter's electrical properties. These initial studies, carried out at CEA, show that a simple **electrostatic model**, involving a rigid shift affecting *all* electronic levels, due to the effect of the fixed polarization charge, does not account for experimental findings. More thoroughgoing investigations, of the complex physics involved in the electronic structure of ferroelectric thin films, are thus called for.

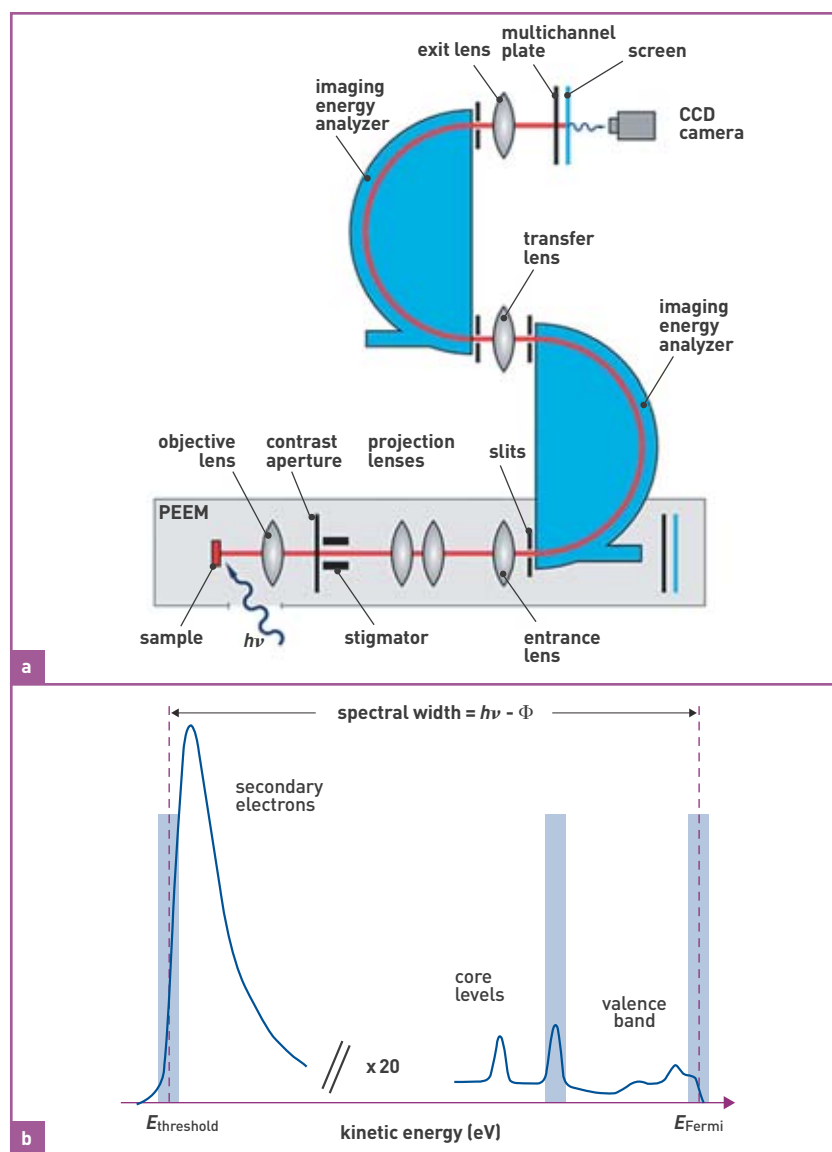


Figure 1. (a) Schematic of the “NanoESCA” microscope, a spectroscopic XPEEM system, showing the electron optics column and the twin hemispherical analyzers, allowing electrons to be imaged at a given kinetic energy. (b) A complete photoemission spectrum, showing the transitions of interest: secondary electrons (yielded as a result of inelastic energy losses undergone by primary electrons within the material), core levels, and valence band. The total spectral width is given by the difference between the energy of the photons serving to excite photoelectrons ($h\nu$) and the work function Φ .⁽⁷⁾

(5) Chromatic aberration (of an optical system): an optical aberration due to the fact that electron rays of different energies, coming from one and the same point in the object, are not focused onto the same point of the optical axis. The anticipated point image is replaced by a more or less blurred halo.

In conventional optics, a similar effect occurs with white light, the various color (i.e. frequency) bands being focused differently from one another.

(6) Magnetic domains: regions within which all **magnetic moments** are aligned in the same direction. These regions are separated by domain walls.

(7) Work function (Φ): the energy a photoemitted electron requires to escape from the material, when it can be detected. This is expressed in **electronvolts**.

SURFACE ANALYSIS

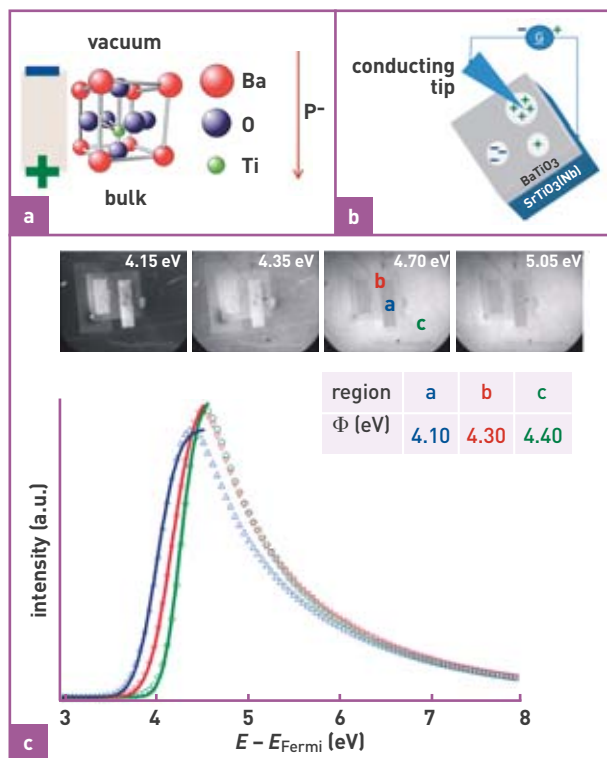


Figure 2. (a) Tetragonal ferroelectric distortion in barium titanate (BaTiO_3). (b) Principle schematic of the writing of a ferroelectric polarization, using a piezoresponse force microscope (PFM). (c) XPEEM images of Ba 3d electrons from a BaTiO_3 surface, featuring polarized domains written by PFM. Local spectra are reconstructed from the set of images for each of the ferroelectric domains.

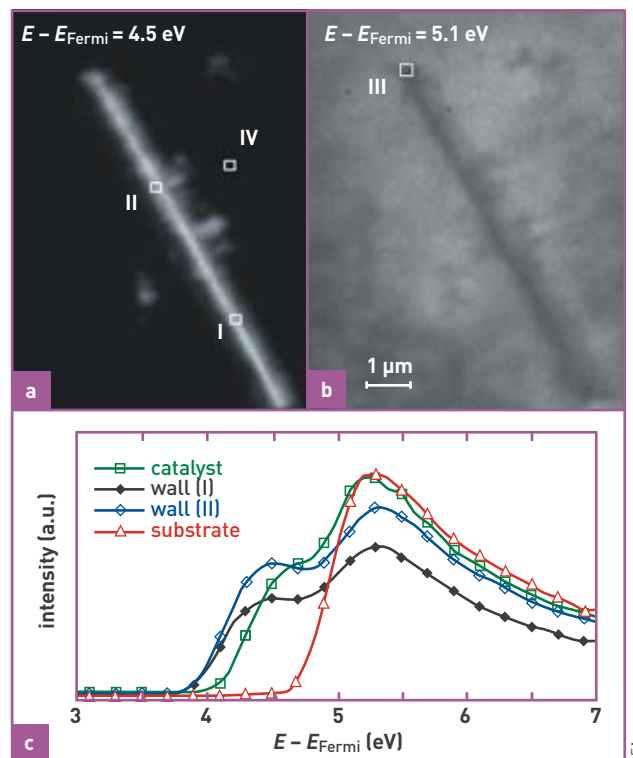


Figure 3. (a) and (b) Images, obtained at the photoemission threshold, of a silicon nanowire. The contrast observed is due to the difference in work function, as between the nanowire – made of silicon – and the substrate, i.e. gold. (c) Local spectra, extracted from this set of images. The presence of a double threshold shows that the gold catalyst, indispensable as it is to promote nanowire growth, has gradually diffused along the nanowire.

Analyzing individual silicon nanowire surfaces

Semiconducting nanowires, i.e. quasi-one-dimensional structures featuring a diameter of the order of 5 nm to 1 μm , and lengths of 1–50 μm , have been prompting numerous investigations, from photovoltaics to nanophotonics. With regard to XPEEM, the smallest size detectable, for isolated objects, ranges from 5 nm to 35 nm, depending on the signal obtained from the electrons used for imaging purposes. Hence, the limiting factor, as regards XPEEM analysis of individual nanowires, is only dependent on the spatial resolution achieved along the nanowire, this typically standing at less than 100 nm, when using a synchrotron source. An initial investigation, carried out at CEA, is illustrated in Figure 3. On this nanowire, “laid out” over a gold (Au) substrate, spectra were obtained, at the photoemission threshold, along the nanowire (for 200-nm regions), from the gold catalyst, serving to promote growth. The remarkable character exhibited by these spectra is the

occurrence of a double threshold – i.e. two distinct values for the work function^[7] – evidencing the existence of two different chemical terminations on the sidewall of the nanowire, in contrast to the spectrum generated over the substrate. These terminations are identified as gold and silicon (Si), on the basis of the work function values obtained by modeling the threshold. The presence of gold, in the form of islands, on the nanowire sidewall, resulting in catalyst consumption arising as poorly controlled growth occurs, along with a consequent narrowing of the nanowire, was confirmed by quantitative analysis of the XPEEM images obtained with Si 2p and Au 4f_{7/2} core electrons, correlated with morphological images obtained under scanning electron microscopy (SEM). These initial results were followed by other findings, involving thinner (< 100 nm) nanowires, opening up the way for quantitative photoemission studies (surface oxidation, doping...) of single semiconducting nanowires.

> Nick Barrett

Radiation-Matter Institute,
Saclay (IRAMIS)
Physical Sciences Division
CEA Saclay Center

> Olivier Renault

LETI Institute
(Electronics and Information
Technology Laboratory)
Technological Research Division
CEA Grenoble Center

FOR FURTHER INFORMATION

N. BARRETT, O. RENAULT, “La spectromicroscopie XPEEM avec le rayonnement synchrotron”, *Matériaux & Techniques* 97 (2009), pp. 101–122. DOI: 10.1051/mattech/2009023.

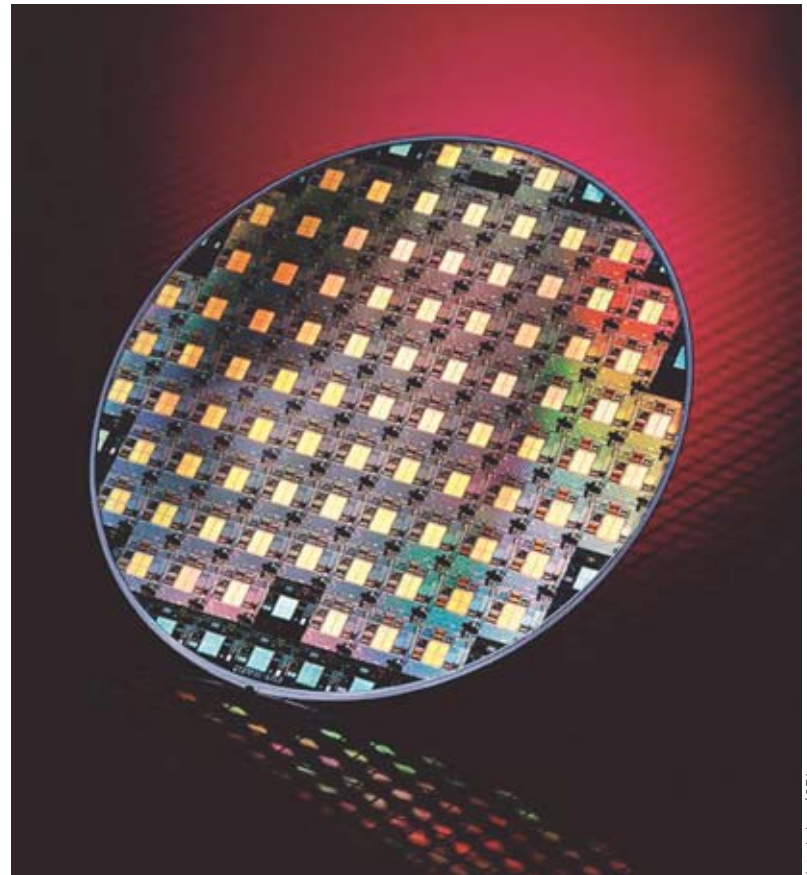
O. RENAULT, M. LAVAYSSIERE, A. BAILLY, D. MARIOLLE, N. BARRETT, “Core level photoelectron spectroscopy with Al K_{α1} excitation at 500 nm spatial resolution”, *J. Electron Spectrosc. Relat. Phenom.* 171 (2009), pp. 68–71. DOI: 10.1016/j.elspec.2009.03.008.

Substrates and materials: the race to miniaturization

So far, every new generation of electronic chips has proved twice as powerful as the preceding one.

At this rate, by 2022, transistor lengths will be no larger than 10 nanometers, and a layer of insulating material no more than a few atoms thick. The physical limits of matter may well soon be reached, and a technological breakthrough would seem to be imperative. Or is it? Indeed, some researchers are already claiming these limits may yet be bypassed.

As early as 1965 – and thus well before the first **microprocessor** was fabricated (this dating from 1971) – US scientist Gordon Moore stated an empirical law, claiming that the performance of **integrated circuits** was set to double every 18 months or so, at constant cost. Moore, who was trained as a chemist, is best known for his role at **INTEL**, of which corporation he was the cofounder, in 1968, together with Robert Noyce, and Andrew Grove, and which soon rose to rank as the world's leading microprocessor manufacturer. This law, which by now bore his name, was to be revised by Moore in 1975: he now stated that the number of **transistors** in microprocessors (rather than in mere integrated circuits) would double every 2 years (see Figure 1). Entailing as it does a steady, drastic reduction in the



Artechnique/CEA

A 200-mm-diameter silicon wafer carrying electronic chips.

size of elementary transistors, this pace has governed the **microelectronics** industry right through the past 40 years.

However, that such a steady enhancement in performance could indeed be achieved, and sustained over such an extended period was due, in particular, to the

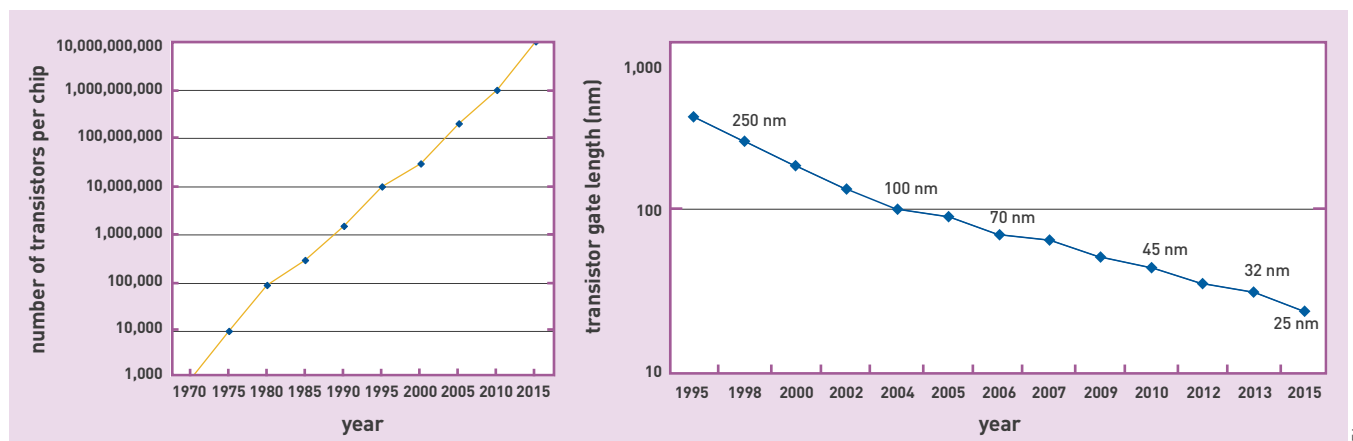


Figure 1.

The curve shown on the left plots the evolution of the number of transistors in a typical silicon-based chip, over the past few decades. What made this increase in the number of transistors – and thus in chip power – possible was the reduction achieved in transistor size. The curve shown on the right plots the evolution of transistor channel length, over the past few years.

Equipment used for substrate engineering purposes.



G rard Cottet/CEA

reduction in geometrical dimensions achieved for transistors, and to the employment of the materials conventionally used in microelectronics: **silicon**, and silica, for the transistor gates, and **aluminum** for the metal interconnects. Looking forward, however, the situation is altogether different. Indeed, if electrical performance is to be maintained, the reduction in lateral dimensions, for transistors, must now go hand in hand with a further reduction, in the thickness of the layers making up the transistor – in particular, the thickness of gate **oxide** (see Box). In such a configuration, starting at the 32 **nanometer** (nm) technological node, the thicknesses involved become so small that conventional materials are unable to sustain operating voltages, without giving rise to major current leakage. Concurrently, the rise in the number of transistors held on one and the same area of silicon entails a concomitant reduction in the cross-section of the conductor lines connecting them, causing increased resistance, and longer time constants in the interconnects. While the detrimental effect of higher resistance (in terms of circuit power consumption) is readily understood, the time constant – resistance times capacitance of the metal interconnects (which product likewise increases, as downscaling proceeds) – is a measure of the delay affecting a signal passing from one transistor to the next, and thus of the degradation incurred, in terms of circuit speed. Consequently, in order to keep to Moore's law, while taking on board the technological issues this raises, researchers are investigating three approaches:

- the development of new materials, and processes, the aim being to keep on bringing down transistor dimensions – this is the approach known as “More Moore:” it involves pursuing the present evolution, pushing it to the ultimate limits of silicon;
- the development of alternative technologies, and assembly technologies that would make it possible to add new functions on the chip, while optimizing system compactness – this is the so-called “More than Moore” approach;
- the development of components based on the so-called “**bottom-up**” approach, based that is on the properties of nanomaterials, or making use of different

principles to ensure charge transfer – e.g. **carbon**-based (**graphene**) components, or **spin** electronics (spintronics) – the idea being they should take over from current technologies, when these reach their physical limits. This approach is referred to as “Beyond **CMOS**” (**complementary metal–oxide–semi-conductor**), as it seeks to go beyond these limits.

Materials as key to a continued validity of Moore's law

The fact that bringing down the geometrical dimensions of transistors was now no longer sufficient to secure the increase in performance described by Moore's law led to novel materials being employed, affording more advantageous properties than conventional materials.

Transistors: from gate oxide to high-k materials

Taking up the “More Moore” approach, the first difficulty that had to be resolved was how to bypass the current leakage issues induced by the extreme thinness of the layers of gate **dielectric** material (see Box). This was the reason for the development of new materials, exhibiting higher **permittivity** – i.e. a higher **dielectric constant** κ – so-called “high-k” materials, having the ability to react strongly to the applied electric field. These materials afford the advantage of having the ability to maintain a satisfactory gate–channel coupling, while retaining greater thickness – and making for a capability to design new stacks, involving such materials, thus ensuring continued compliance with the targets set by the **International Technology Roadmap for Semiconductors (ITRS)**.⁽¹⁾

In this manner, by introducing materials exhibiting a higher dielectric permittivity than silica, it becomes feasible to limit the transistor's leakage current. This

(1) The International Technology Roadmap for Semiconductors (ITRS) is an organization bringing together experts of international standing (including LETI), which has set itself the remit of putting forward quantitative targets, year after year, to help track Moore's law. Its recommendations reflect the thinking of experts from across the corporations, and laboratories affiliated to ITRS. These recommendations may be seen as a kind of worldwide *consensus*.

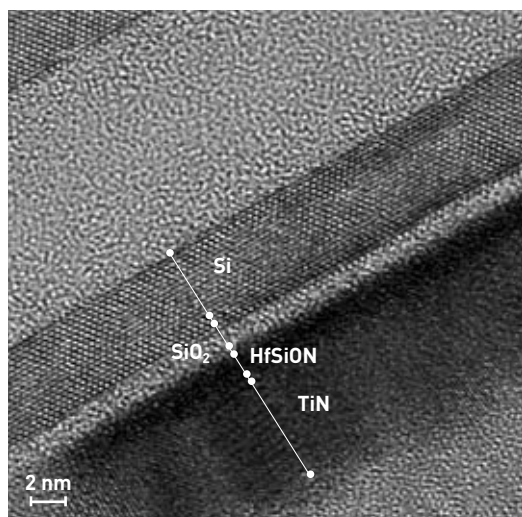


Figure 2.
A stack of dielectric, and metallic layers, making up a transistor gate: silicon (Si), hafnium silicate (HfSiO_x), titanium nitride (TiN).

outcome is achieved by the deposition of a greater thickness of material than would be the case with silicon dioxide (SiO₂), while the same capacitance value is retained. As far as researchers were concerned – including the scientists at CEA's Electronics and Information Technology Laboratory (LETI: Laboratoire d'électronique et des technologies de l'information) – this was a complex undertaking, which took them some 10 years work. They succeeded in developing hafnium oxide- (HfO₂) based materials, and subsequently others involving hafnium alloys, in particular hafnium silicate (HfSiO_x). Under certain conditions, this substance can remain amorphous, and thus exhibit characteristics close to those of silica, in terms of dielectric properties (bandgap, and band overlap with respect to silicon),⁽²⁾ while significantly increasing the material's permittivity.

Further investigations showed it would be necessary to interpose a very thin (a few tenths of a nanometer) layer of silica, between the silicon, and the high-k material, if the transistor's properties, in particular charge carrier mobility in the channel, were to be preserved. These investigations confirmed the irreplaceable character of the Si/SiO₂ interface. The gate insulator must thus be turned into a highly sophisticated SiO₂/high-k bilayer (see Figure 2). To form this bilayer, growth of a few atomic monolayers of silica is effected under an atomic oxygen atmosphere. This is a highly reactive oxygen species, in which the atoms making up the usual oxygen molecule are kept separate from one another. This form of oxygen can only be obtained in a plasma – a specific state of matter, in which atoms, and their electrons are kept apart. The silicate is subsequently deposited, with specific gaseous precursors of silicon, and hafnium, which, as they decompose, yield the various layers of solid material.

Metal for the gates

The substitution of SiO₂ with high-k materials is complemented by a further substitution: that of polysilicon with a conducting metallic material. This is due to the fact that polysilicon gates, even when highly doped, feature, at the interface with the oxide, an electron-depleted region, bringing down the gate's overall

electrical capacitance, and consequently lowering transistor performance. This was the reason for introducing titanium nitride (TiN), which exhibits conduction of the metallic type, and energy levels that show a good alignment to those of the dielectric, as of silicon – for both “N,” and “P” transistors (see Box). Ensuring this metallic material is compatible with the high-k material remains a complex operation. Currently, one solution predominates, for that purpose. This involves treating the surface of the high-k material with nitrogen, to set up stable nitrogen bonds, thus obtaining a material that is compatible with titanium nitride. The important parameters, for this operation, include the amount of nitrogen, and depth of nitrogen penetration. Indeed, an excessive quantity of nitrogen, in the vicinity of the interface, results in a degradation of transistor performance, and reliability. Here again, use of a plasma allows nitrogen confinement to be controlled, within layers of high-k material featuring thicknesses of some 1.5–2 nm.

Investigations carried out by the teams at LETI made it possible to obtain very-low-consumption

(2) All insulating and semiconductor materials exhibit a band structure, representing the ranges of energy states occupied by electrons orbiting an atom. In low energy states, electrons remain localized around their atom, and participate in the chemical bonding between atoms (such states form the valence band). At higher energies, electrons are sufficiently energetic to escape from their atom, and serve to carry an electric current (this is the conduction band). Between these two bands, there lies a range of values electrons are unable to take up (this is the forbidden band, or bandgap). This band has zero width in metals, an intermediate width in semiconductor materials, and a very large width in insulators. For a transistor to operate properly, the insulator's forbidden band must be large compared to that of silicon, but it must also show suitable alignment to it (i.e. they should overlap).

(3) Low-power transistors, using fully depleted SOI technology.



Operators standing in the photolithography zone, in front of the exposure system used for 300-mm wafers.

transistors,⁽³⁾ affording the benefit of considerably lowering circuit power consumption (see Figure 3). These results were achieved through employment of **silicon-on-insulator** (SOI: Si/SiO₂/Si) substrates, featuring a very **thin** silicon **film** (see the section on substrate engineering).

With regard to the technologies exhibiting the highest performance, in terms of speed, the incorporation of high-k/metal gates becomes more complex, owing to the introduction of two distinct metals, noted “N,” and “P,” for the purposes of retaining low threshold voltages – this being required to keep power consumption low, while enhancing performance. While solutions are available, as regards fabrication of the NMOS-type transistor, by contrast, complex **physico-chemical** mechanisms result in making the fabrication of PMOS-type metal gates far more difficult. Indeed, obtaining an electrical thickness of barely 1 nanometer, as required by the most advanced high-perfor-

mance technologies, entails bringing down the thickness of interfacial silica. At this point, the gate's electrical properties become degraded, owing to its interaction with the high-k material, through thermal treatment (oxygen displacement, generation of vacancies...).

In conventional CMOS (complementary metal–oxide–semiconductor) assemblies, the gate, once fabricated, undergoes a heat treatment at high temperature, causing the activation of the junction dopants. This is a process that retains its attractiveness, as it is straightforward, and inexpensive. On the other hand, nowadays, researchers tend to favor the so-called *Damascene* technique – so called as it is akin to the technique employed by the denizens of the Damascus region (Damascenes), in ancient times, to obtain metal incrustations, inlaid in a darker background metal. The technique involves, first of all, etching the insulator layer, then effecting the deposition of critical layers of gate metals, and, finally, polishing these, so that only the useful regions are retained. This operation is carried out at the back end of the process, after the high-temperature annealing steps, to preclude these steps destroying the materials' intrinsic properties.

Materials: the silicon substrate is also changing

While the dedicated materials, and processes employed for the control gate, in transistors, are changing, the same thing is happening as regards **semiconductor** materials, silicon in particular. These changes serve to enhance their properties, carrier mobility especially.

The technique employed, **epitaxy**, involves effecting the deposition of single-crystal films, lattice-matched with the silicon in the substrate. In other words, the aim is to grow a layer of semiconductor material over a substrate, exhibiting a crystal orientation identical to that of the substrate (see Figure 4). The mastery achieved, with regard to this technique, has enabled LETI to develop growth processes, to be used for a variety of silicon, **germanium**, and carbon **alloys**. The

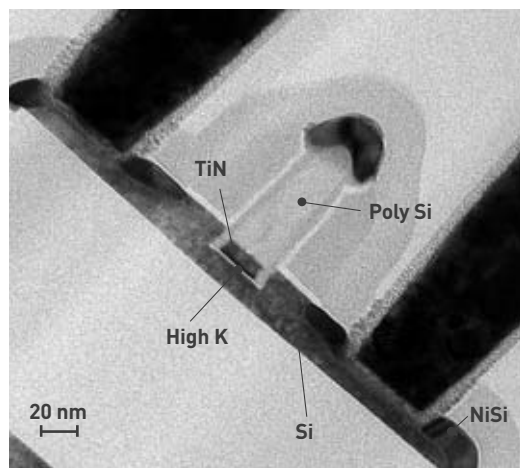


Figure 3.
A MOS (metal–oxide–semiconductor) transistor, featuring a high-k/titanium nitride (TiN) gate, fabricated with silicon (Si) on insulator (SOI) technology. The various stacks of materials may be seen, serving to fabricate transistors for microprocessors: polycrystalline silicon, titanium (TiN), hafnium (HfO₂), nickel (NiSi).



An operator loading the electron-beam exposure system. This equipment allows patterns smaller than 11 nm to be traced onto 300-mm-diameter silicon wafers.

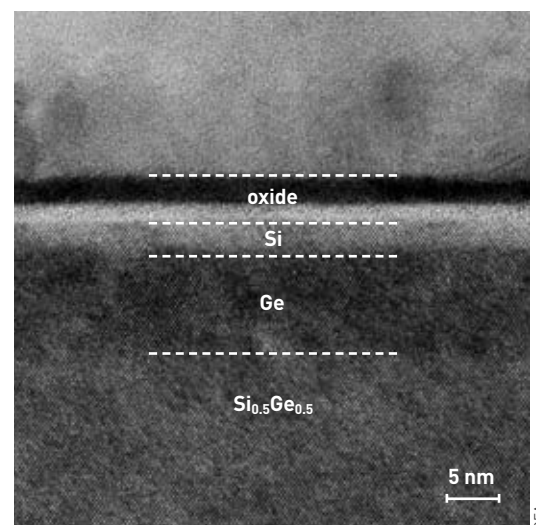


Figure 4.
A bilayer, as imaged under transmission electron microscopy. The view shows germanium (Ge), under compression (8 nm), and silicon (Si), under tensile strain (5 nm), deposited over a very thick layer of silicon–germanium alloy. The oxide forms the gate for the transistor.

operation is carried out – selectively, or otherwise – with reference to the underlying layers, and/or under strained conditions – compressive, or tensile – with respect to the silicon substrate, owing to the different lattice parameters involved, in silicon, germanium, and carbon.

Depending on the nature of the strain involved, and on the chemical composition of the layers, researchers succeeded in enhancing, by a factor ranging from 2 to 10, electron and hole mobility in the conduction channel, in MOS (metal–oxide–semiconductor) transistors (see Box). By putting to advantage the difference in etching rates, for silicon, and for the silicon–germanium alloy, the same researchers were further able to effect the lateral etching of silicon–germanium–alloy layers, selectively with respect to silicon, and to stack conduction channels, one on top of the other. This resulted in a major quantitative gain, in terms of integration.

Billions of transistors requiring to be interconnected

With transistors coming down in size, researchers are now able to design increasingly complex integrated circuits, featuring up to several billion transistors (see Figure 5). For these researchers, the challenge now is to ensure the interconnection of these components. This is anything but a straightforward task, owing to the increased length of metal conductors (the cumulated length, on one chip, thus exceeding 1 kilometer), their ever-slenderer thinness, and their proximity to one another. For that reason, aluminum and SiO₂, which had been employed right down to the mid-1990s, in structures featuring only one, or two connection levels, are now being supplanted by new materials, affording the ability to bring down conductor line resistance, and couplings between neighboring lines. This has resulted in a reduction in signal propagation times, and in *crosstalk* between lines (i.e. the undesired transfer of a signal from one line to another), as in consumption. Achieving this entailed introducing electrical conducting materials affording enhanced quality. Copper was seen as an outstanding candidate, for the purposes of bringing down line resistance. In like manner, dielectrics exhibiting a very low relative permittivity – i.e. a very low dielectric constant – made it possible to reduce couplings between neighboring lines.

Bringing in these materials called for more than 10 years work. The chief difficulty that had to be resolved concerned copper. Indeed, this metal ranks as one of the main “poisons” of silicon, owing to its ability to diffuse very rapidly, and to kill the lifetime of carriers. Consequently, thin, low-resistance metal barriers had to be developed, providing the ability to prevent copper from diffusing into the silicon, and thus to conserve full, unimpaired component performance. Once that issue had been resolved, another one arose: the impossibility of etching copper by means of conventional etching techniques, as had been used for aluminum. To overcome this barrier, researchers developed an original technology, affording the ability to handle copper – the so-called *Damascene* technology, described above, which involves three steps: etching the dielectric, filling the tracks with metal, and then removing the excess metal by mechano–chemical

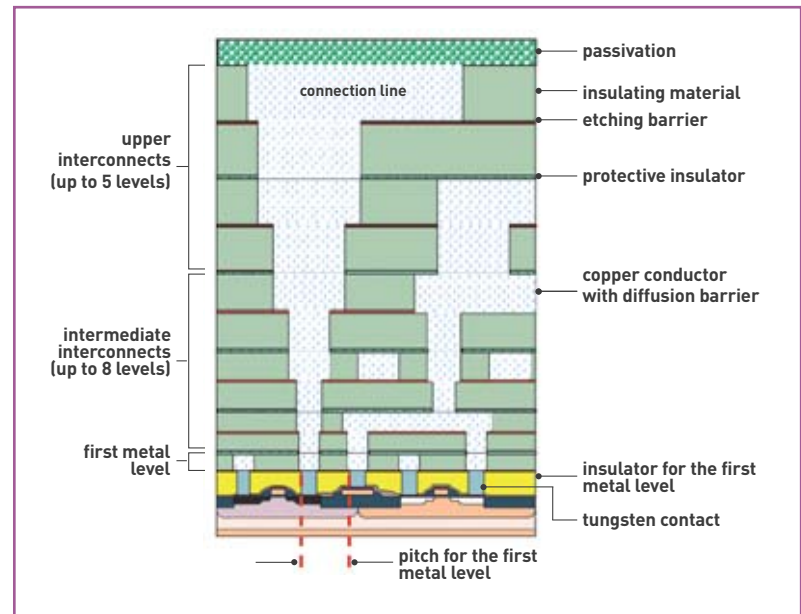


Figure 5. Cross-section of a current-generation integrated circuit, which may feature up to eight interconnection levels.

polishing. As regards dielectrics, the reduction in permittivity was achieved by first incorporating carbon into silica, and thereafter increasing *porosity* in the matrix.

Currently, researchers are looking into new approaches, with regard to integration, seeking either to substitute dielectrics with air, or to connect the various metallization levels by means of *carbon nanotubes*.

Substrate engineering: innovative materials for breakthrough applications

The performance levels exhibited by dedicated nano-electronics materials, and processes are still very highly dependent on the quality of the substrates on which these materials are developed. For a long time, silicon afforded the ability to ensure the required performance levels. As of now, however, researchers are seeking to go further, and no longer wish to limit their investigations to the study of new types of stacks. Their endeavors now concern the substrate itself: by succeeding in structuring the basic materials, combining different materials within one and the same substrate, or even carrying out fabrication processes, for components, on a different substrate from the one on which these components are to be subsequently used. At LETI, substrate engineering is developing around a process dubbed Smart Cut™, operated under license by the French *Soitec* Corporation, a world leader in the field of silicon-on-insulator (SOI) substrate supplies. Combined with thin-film transfer techniques, this process allows ever-higher performance to be achieved, be it by way of the More Moore approach, or More than Moore.

Notwithstanding all of the technological advances reviewed in the preceding paragraphs, the fact remains that, as a transistor is scaled down, gate–channel coupling tends to become ever weaker, compared to source–drain coupling (see Box). The task that has to be addressed is thus one of containing such loss of electrostatic control, by designing, and fabricating



Artechnique / CEA

Germanium-on-insulator (GeOI) wafers. A substrate fabricated using the Smart Cut™ process (bottom), and a wafer carrying chips (top).

CMOS circuits to operate on innovative substrates – for instance, on the SOI substrate. Nowadays, this stands as a product that has reached maturity, featured as it is in the roadmaps of the major integrated circuit manufacturers around the world (IBM, Freescale, AMD...). In metaphorical terms, the SOI substrate may be seen as a sandwich, with a slice of bulk silicon, topped with a thin oxide layer (buried oxide [BOX]), and a further thin layer of silicon, on which the components are fabricated.

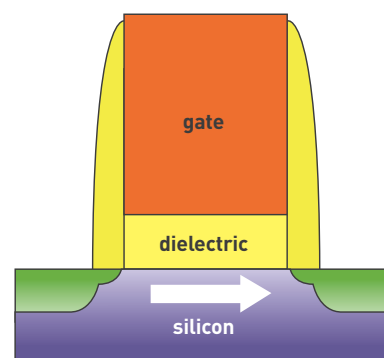
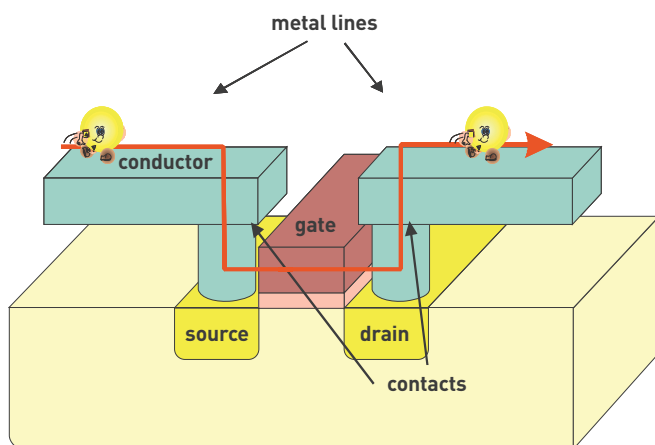
As the inventor of the Smart Cut™ process, LETI, together with its industrial partner Soitec, are in the lead, in the race to performance that is being played out around the various SOI substrates. This dominant position is due to the type of work that is conducted in the laboratory, namely coupled component/substrate investigations, going further still in pursuit of Moore's law. Using the Smart Cut™ process, it proved feasible to devise very-high-performance, very-low-consumption circuits. Pushing the process further still should allow the thickness of the oxide, and silicon layers to be brought down, to retain the performance level ensured by very short channels, while improving the electrostatic control of these channels by using the substrate itself as an **electrode** – hence the name of ultra-thin BOX (UTBOX) substrates for this technology.

Novel sandwiches, comprising other materials than silicon, should emerge, with the Smart Cut™ process. Their purpose will be to enhance carrier mobility, by way of induced strain (strained silicon on insulator [sSOI]), or improve the properties of "P"-type transistors through the use of germanium, an element exhibiting better positive charge-carrier mobility (GeOI). Finally, the Smart Cut™ process – as indeed, more widely, all thin-film transfer processes – promotes the continued validity of Moore's law, by way of the More than Moore approach, in two areas: peripheral functions for the CMOS circuit, and power electronics components. In this respect, this involves either transferring functional materials onto silicon circuits (e.g. transferring single-crystal films of a **piezoelectric**

How does a transistor work?

The MOS (metal-oxide-semiconductor) transistor stands as the basic **component**, for **microelectronics**. Two kinds of transistors of this type are to be found, differing in terms of the type of **doping** used, in the silicon entering in their composition.

- An NMOS (negative-channel metal-oxide-semiconductor) transistor is obtained from a "P"-type **silicon** wafer (see Figure a), on which are added two "N"-type regions, fabricated through implantation of a dopant: these form the drain, and source, through



CEA

Figure a.
Left panel: principle schematic of a MOS (metal-oxide-semiconductor) transistor; right panel: cross-section of a MOS transistor.

material), to fabricate **radiofrequency** filters, or transferring active layers onto transparent substrates (to produce imagers), or onto substrates exhibiting good thermal conductivity (for power components).

What next?

The most advanced processors make use of 45 nm technology, while the next, 32-nm stage, should be coming out in the course of 2010. LETI is already working on the subsequent generations: 22 nm, 16 nm, 11 nm. At these scales, the channel, in a MOS transistor, consists of just around 100 atoms, laid end to end. Bearing in mind that doping levels, for silicon, stand at about 1 atom in 10,000 or so, two questions are currently exerting researchers: Where does the doping atom lie, in the channel? Or is there even one such atom, at least, in the channel? And yet, even for these dimensions, there are good grounds for believing transistor performance will meet the targets set by the ITRS roadmap.

However, once the single-atom limit is reached, what is to be the researchers' line of investigation? They will doubtless have to devise other materials, and discover different physical effects, if they are to stay in the lead, in the race for performance, with regard to the materials of the future. Carbon may well emerge as a strong candidate for the winner's crown – hence the studies already prompted by that element. Thus, in the form of graphene – a sheet of carbon hexagons barely one atom thick – carbon may behave either as a metal, or as a semiconductor material. Indeed, an electron is able to sustain lossless motion across graphene, much

as a body launched out in empty space, which would keep on moving indefinitely: the only cost entailed being the energy required to set it on its course. Rolled up on itself, such a graphene sheet is referred to as a carbon nanotube – a material affording the ability to set up highly efficient interconnections, or even to act as a transistor channel. In diamond form, carbon stands as an outstanding electrical insulator, exhibiting high thermal conductivity, which may be used to fabricate innovative substrates, as an alternative to SOI. Silicon on diamond (SOD) is already heralded as affording the ability to cater for the high heat densities arising from the operation of integrated circuits. Looking out further than materials, other effects will, no doubt, serve to translate the 0s and 1s on which all of information technology is based. Based on **spintronics**, a novel type of computer is set to emerge in the near future.

In the information technology race, researchers have invariably proven their ability to tweak the physical limits of materials, and put them to advantage. It would seem that this race is only bounded by the limits of human imagination. Which is tantamount to saying we are not going to see an end to it anytime yet!

> **Jean-Jacques Aubert, Thierry Billon, Laurent Clavelier, Olivier Demolliens, Jean-Michel Hartmann, Didier Louis and François Martin**

LETI Institute (Electronics and Information Technology Laboratory)
Technological Research Division
CEA Grenoble Center

which **electrons** enter, and exit the transistor. Between these two electrodes, a third region is inserted. Known as the "gate," this defines the transistor's channel. It comprises a layer of insulator (the gate oxide), covered with a metallic conductor. When no voltage is applied to the gate, the "P"-type channel forms two **diodes**, with the drain, and source, one of which prevents any current going through. In that case, as in the case of a negative voltage being applied, the transistor stays "off." On the other hand, should a positive voltage be applied to the gate, it then repels the holes in the "P"-type silicon, thus setting up the channel that will allow current to pass from the source to the drain. The transistor is then "on."

- A PMOS (positive-channel metal-oxide-semiconductor) transistor is fabricated in like manner to the NMOS type, the only difference being that the substrate consists of "N"-type silicon, whereas the drain, and source are "P"-type regions. This kind of transistor is turned on when a negative voltage is applied to the gate.

An NMOS and a PMOS transistor may be combined, to form a **CMOS** (**complementary MOS**) inverter. In this technology, one of the two transistors stays off, while the other one allows the current through. By switching the polarity of the control input A, the polarity of output Q is reversed (see Figure b). Thus, once the inverter

has been switched, no current passes through the system. Current passes through, and thus energy is dissipated, only during the switching phase. This property ensures very low power consumption, and strong noise resistance – hence the widespread adoption of these devices.

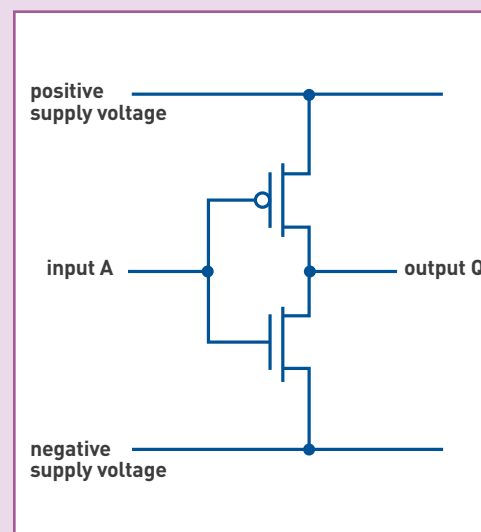
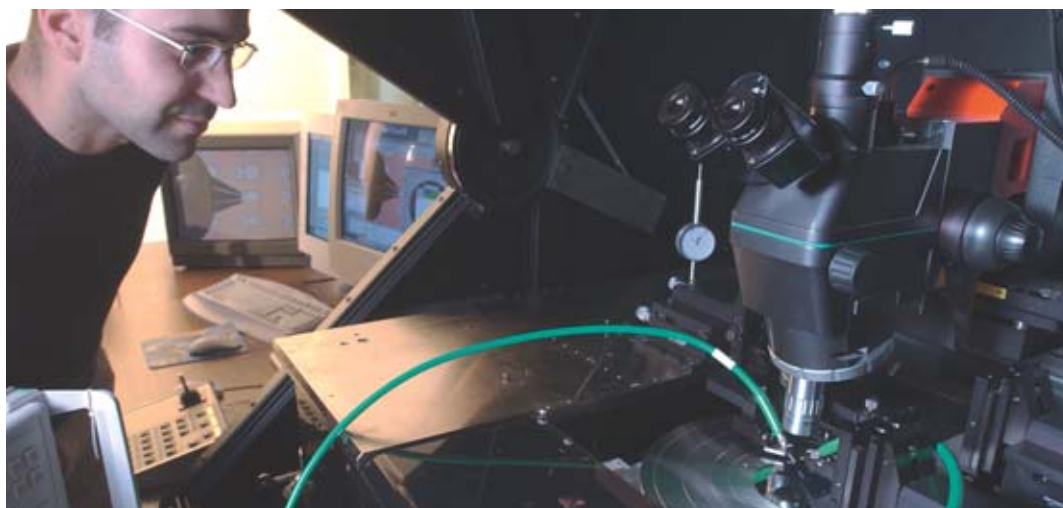


Figure b.
Diagram of a CMOS inverter.

Integrated materials for new radiofrequency functions on silicon

Together with silicon technology, the integration of new magnetic, and dielectric materials to obtain radiofrequency (RF) functionalities has opened up numerous prospects for applications: transmitter/receiver miniaturization, agile communications systems, self-tuning sensors, to meet societal challenges, arising in the biomedical, automotive, domotics... sectors. **The technological challenge that must be met is on a scale to match that of the anticipated scientific, and industrial benefits.**

Radiofrequency measurement hall at LETI, used to ascertain the frequency response of some components. Measurements are carried out by means of tip probes (on-wafer measurement), and may range up to 65 GHz.



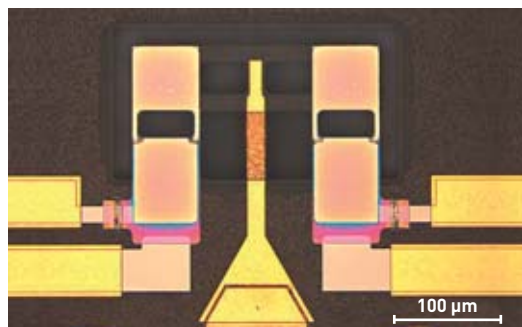
P. Stroppa / CEA

Emerging on the back of the fabrication techniques developed for **microelectronics**, microsystems nowadays account for a growing fraction of electronic systems. This is an outcome of what is now known as the More than Moore approach, which seeks to extend Moore's law – the well-known statement of **semiconductor** materials trends. This evolution is accounted for by improved materials compatibility, in terms, in particular, of semiconductor contamination. This led to the notion of integrating a steadily increasing number of new materials, to enable novel functions. Of the range of opportunities at hand, the Radiofrequency Components Laboratory (LCRF: Laboratoire des composants radiofréquence), a unit in the Electronics and Information Technology Laboratory (LETI: Laboratoire d'électronique et des technologies de l'information) at CEA, has elected to work – for some 15 years already – on the integration of new **magnetic**, and **dielectric** materials.

Nowadays, magnetic **thin films** – issuing from a line that began with magnetic hard disk drive read/write heads – are to be found as part of multiplicity of technologies involving hyperfrequency (i.e. **microwave**) applications – e.g. oscillators making use of **spin** electronics,⁽¹⁾ planar inductors for mobile phones, or anti-

theft tagging systems. Such a wide takeup is due to the fact that magnetic thin film engineering now makes it possible to tune the properties of thin films, to match the target application, by developing new materials – whether homogenous, or heterogeneous – featuring structures that are exactly controlled, at a scale of just a few **nanometers**. Currently, LETI, together with the Nanosciences and Cryogenics Institute (INAC: Institut nanosciences et cryogénie), is able to match the best state of the art, worldwide, in this respect, owing to a strongly multidisciplinary outlook, spanning the entire range from fundamental physics to technological applications, and microwave instrumentation. Having advanced to this stage, in the field of magnetism, researchers yet have to take up a new challenge: that of constructing devices featuring high operating frequencies, and/or “frequency-agile” operation, e.g. variable inductors – a type of component that does not as yet exist. Achieving this entails overcoming constraints related to limited device dimensions, but equally meeting the new requirements set by applications, in terms of

(1) Bernard DIÉNY and Ursula EBELS, “Data storage: achievements and promises of nanomagnetism and spintronics”, *Clefs CEA*, No. 56 (winter 2007–2008), pp. 62–66.



Matthieu Queff/CEA

Figure 1.

A piezoelectric PZT actuator, pictured here with its contacts. At center, the radiofrequency (RF) line transporting the signal may be seen. The contact is the uppermost region of this line. It is this region which comes up against another contact, opposite to it (not shown), to close the electric circuit. Two piezoelectric actuators are located on either side of the RF line. The gold-colored tracks leading away from these are used for the controls serving to actuate them.

frequencies, quality factors, and power consumption. Dielectric thin films have likewise seen major advances being made. They are found to be peculiarly suitable for the purposes of sensors, or actuators, making use of the [piezoelectric effect](#) (see Figure 1), of built-in high-capacitance capacitors, or voltage-controlled agile components, e.g. variable capacitors: for instance, microswitches making it possible for a cell phone to switch from one communications standard to another, or variable-focus lenses used in cameras, or built-in detection capabilities for pacemakers...

The fabrication of dielectric thin films, at LETI, involves two types of materials, viz. [aluminum nitride \(AlN\)](#), and oxides coming under the [perovskite](#) family. For researchers, this sets a twofold challenge. First, the issue they face is one of ensuring enhanced intrinsic qualities, for the material at hand, thus matching the state of the art – a goal that has already been achieved, as regards AlN, and [lead zirconate titanate \(PZT\)](#). Second, they must be able to integrate these films, to make them into devices, while preserving the material's qualities. Whether it be for magnetic, or dielectric thin films, researchers fully understand the requisite of bringing together the various specific materials-, components-, and systems-oriented disciplines – a meeting of minds that entails suppressing the separations, or even the barriers, that still set apart physicists, and applications designers.

Very-high-permeability magnetic materials

As regards the miniaturization of radiofrequency circuits, one strong constraint is the requirement to integrate inductors, resonators, and antennas: these are, indeed, passive components,⁽²⁾ that prove particularly demanding in terms of surface area. The integration of magnetic films on [silicon](#) is seen, as of now, as a promising avenue, provided one condition can be met: being able to achieve a high level of [permeability](#), while keeping losses low.

Iron-, or iron-cobalt-alloy-based nanocrystalline films

Such permeability levels, if they are to involve low losses, entail that novel magnetic materials be

(2) A passive component is a component that involves no transistor.



O. Redon/CEA

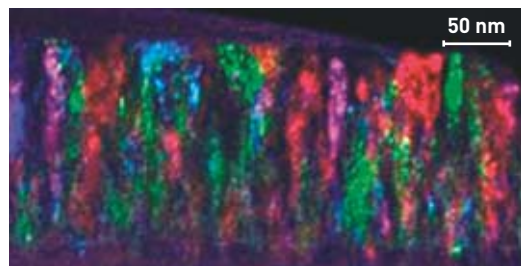
Deposition of magnetic, and dielectric thin films inside an ultrahigh vacuum chamber. This unit is used to transfer substrates to the deposition chambers, and subsequently to extract the finished product, bearing its thin film. This makes it possible to control film thickness to within one atom.

synthesized, featuring a suitable microstructure, such as to ensure very-high-frequency utilization. Iron-, or iron-cobalt-alloy-based nanostructured [ferromagnetic](#) films (i.e. involving grain sizes of just a few nanometers) are seen as leading candidates for that purpose. Indeed, in these materials, microwave permeability is found to be proportional to saturation magnetization, this in turn exhibiting the largest known values.

As early as 2006, it was shown at LCRF that nanostructured films of the FeX(N,O) type, where "X" stands either for [tantalum](#), or [hafnium](#), exhibit remarkable dynamic properties (up to frequencies of more than 2 [gigahertz](#)), including particularly low damping constants (see Figure 2). This result is due to a highly specific [crystal microstructure](#), involving grains of less than 5 nanometers, held in a very fine dispersion within an amorphous, very highly resistive matrix. These nanostructured materials combine high [resistivities](#) at around 100-1,000 $\mu\Omega\cdot\text{cm}$ and high saturation magnetization values, at around 1 [tesla](#). This remarkable combination makes it possible, technologically, to integrate the magnetic material in very close proximity to the inductive component, while minimizing the risk of parasitic capacitances arising, such as would impair high-frequency operation, for planar inductors.

Multilayers featuring antiferromagnetic-ferromagnetic exchange coupling

Interfacial exchange coupling, arising between one, ferromagnetic material, and another, antiferromagnetic material, shows up as a shift in the ferromagnetic material's [hysteresis](#) loop, to a field value which may be very high (see Figure 3). This property has formed the basis



B. Viala/CEA

Figure 2.

Transverse section, as viewed under [transmission electron microscopy](#), of a nanostructured FeHf(N,O) film. The ferromagnetic grains are very small (5-10 nm), resulting in high permeability, and finely dispersed across an amorphous matrix, this endowing the film with high resistivity.

for all modern magnetoresistive devices. In 2007, it was shown at LCRF that such materials, particularly materials consisting in a stack of **manganese-nickel** (NiMn), or manganese-, manganese-**iridium**-, and iron-cobalt- (FeCo) based films likewise exhibited unrivaled dynamic behavior. This may rise to frequencies of some 10 gigahertz, i.e. to a spectral range that had thus far proved unattainable for magnetic materials.

Integration of such materials made it possible to fabricate inductors which may be operated at 5 GHz, featuring much more compact topologies than the planar inductors in general use. Extremely simple filters have also been constructed. These make use of the material's absorption power at resonance, making it possible to dissipate more than 99% of the transmitted signal. This type of filter may be used up to frequencies of more than 10 GHz.

Dielectric, and piezoelectric materials

The integration of a new material into a complex technology calls for a specific investigation, in its own right – indeed, few materials prove able to pass all of the stages leading on to industrialization.

Built-in high-capacity capacitors

Under the aegis of a collaboration set up with **STMicronics**, LETI has just achieved a world first: the synthesis of a **strontium titanate** (SrTiO_3) alloy-based material, deposited above a **CMOS** (**complementary metal-oxide-semiconductor**) amplifier circuit, in order to obtain very-high-**permittivity** (i.e. very-high-dielectric-constant) capacitors, connected to the CMOS circuit. This is a veritable technical feat. Indeed, a quite stringent constraint, if new functions are to be set up above CMOS circuits (by the so-called “above IC” approach), is that a process temperature lower than 450 °C must be complied with. Now, materials in the SrTiO_3 family (referred to as perovskites, this being the name for the crystal structure they exhibit) require, as a rule, synthesis temperatures of some 700 °C. By using a specific deposition technique, developed by LCRF, and the Surface Technology Laboratory (LTS: Laboratoire des technologies de surface) – part of the Innovation Laboratory for New Energy Technologies and Nanomaterials (LITEN: Laboratoire

d'innovation pour les technologies des énergies nouvelles et les nanomatériaux) – researchers were able to **synthesize** SrTiO_3 at a temperature lower than 400 °C, above a CMOS circuit. The functional circuit has allowed the “above IC” approach to be validated, this involving the fabrication of a complete function – rather than just a component – on a single chip.

Variable capacitors for impedance matching

Another material featuring a perovskite structure is being investigated. This is barium strontium titanate (BST: $(\text{Ba},\text{Sr})\text{TiO}_3$). The advantage it affords stems from the variability exhibited by its dielectric constant, as a function of the applied direct voltage. This property opens the way to the fabrication of variable-**impedance** components, controlled by an external voltage. It makes it possible to enhance the impedance ratio by a factor 4, while limiting dielectric losses to less than 1%, at a few gigahertz. The desired function, in this case, is real-time impedance matching. This will enable power amplifier operation, in mobile telecommunications systems, to be achieved always at maximum efficiency, thus bringing down power consumption. Battery lifetime would then be doubled.

Electromechanical actuators

Among dielectric materials, some are found to exhibit piezoelectric properties. Those exhibiting the highest piezoelectric coefficients, when in thin film form, belong to the perovskite family. The materials involved are PZT, and lead magnesium niobate-lead titanate (PMN-PT).⁽³⁾ LETI is actively pursuing PZT integration. Owing to the very strong demand from industry, in the telecommunications sector, one of the goals being followed up concerns the fabrication of piezoelectric actuators, on a technology platform involving the use of 200-mm silicon wafers. The large diameter featured by these wafers makes it possible to increase the number of components fabricated on one and the same wafer, and thus bring down unit component cost. A collaboration has been set up with **Freescall** for that purpose. This has already allowed wafers to be obtained, carrying functional radiofrequency micro-switches, featuring an actuation voltage no higher than 5 V, this being the fundamental limit, for operation in a cell phone. Figure 1 shows one of these integral structures, prior to final assembly, and fitting with its upper protection, known as the cap.

Dedicated radiofrequency filters

Of the range of piezoelectric materials of interest, CEA has further elected to work on aluminum nitride (AlN), which exhibits exceptional acoustic properties. This is the constituent material for the active layer, in radiofrequency acoustic resonators involving extremely low losses (less than 0.1%). Such frequency filters, fabricated from AlN, are featured in most wireless communications systems. As part of its recent R&D effort, LETI has just completed development of a filter obtained by stacking two coupled resonators, one on top of the other, thus affording maximum compactness (see Figure 4). Apart from CEA, few organizations around the world are able to show evidence of expertise, involving a capability to produce such results.

■ (3) $\text{Pb}(\text{Mg},\text{Nb})\text{O}_3\text{-PbTiO}_3$.

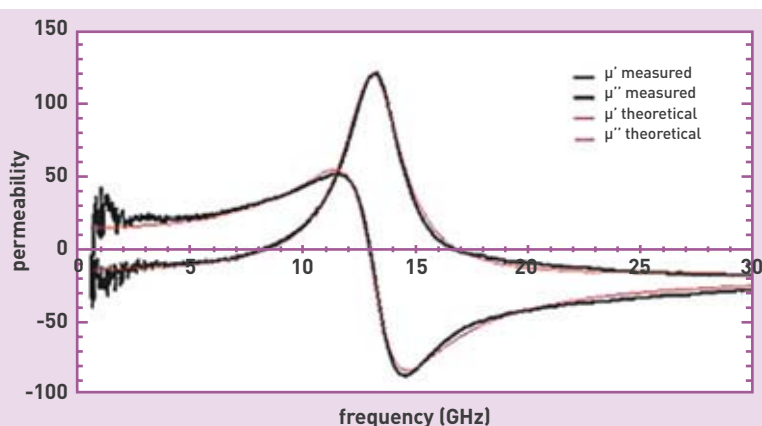


Figure 3. Magnetic **spectrometry** allows the complex permeability of a material to be measured, as a function of frequency. The real part μ' expresses the material's ability to respond to an external **magnetic field**, while the imaginary part μ'' is a measure of the losses through dissipation within the material. The example shown here plots the experimental (black), and theoretical (red) responses of a ferromagnetic FeCo film, coupled to an antiferromagnetic NiMn film (referred to as the polarizing film).

B. Viala / CEA

An ambitious avenue for dielectrics: integrating single crystals

Presently, researchers are endeavoring to go even further, as regards the development of dielectric films. LETI is seeking to integrate piezoelectric single crystals, by way of two approaches: [epitaxy](#) on silicon, and film transfer – the materials being investigated, in this respect, being perovskites, [ilmenites](#),⁽⁴⁾ and AlN.

- Epitaxy involves fabricating single-crystal films, in other words films exhibiting no crystal defects, obtained through evaporation, using the molecular-beam epitaxy (MBE) technique. Highly promising initial results show a considerable enhancement is achieved, in terms of structural quality, in the material thus fabricated. These advances were the outcome of a number of collaborations, set up by LETI with the Research Center on Heteroepitaxy and Its Applications in Sophia-Antipolis (CRHEA/CNRS: [Centre de recherche sur l'hétéroépitaxie et ses applications](#)), the Lyon Nanotechnology Institute (INL: [Institut des nanotechnologies de Lyon](#)), and IBM Zürich (Switzerland).

- Film (or layer) transfer involves bonding, onto a silicon host wafer, a piezoelectric film of submicron thickness, obtained from a single-crystal wafer of that selfsame piezoelectric material. This unique process, developed by LETI and [Soitec](#), allowed the demonstration to be made that the [electromechanical coupling](#) coefficient for [lithium niobate](#) (LiNbO_3) films – featuring an ilmenite structure – can match the value found for the bulk material (about 45%). An important point is that this result, obtained as it was with submicron films, outclasses all of the results found in the literature for polycrystalline thin films – regardless of the piezoelectric material involved. This is a highly encouraging result, and it is being developed in collaboration with [Laboratoire FEMTO-ST](#), in Besançon (eastern France).

Magnetoelectrics revisited: multiferroic multilayers

First and foremost, among the collateral benefits flowing from R&D on multilayer materials, is the bringing down of barriers thus achieved, between a number of scientific disciplines.

Thus, since 2008, LCRF has been contributing to the renewal of interest in magnetoelectrics, worldwide, by opening up a new path for multiferroic materials, for the purposes of facilitating their integration. The aim is to achieve an engineered combination of properties that are of diverse natures, in order, in particular, to reproduce the piezomagnetic effect. Numerous applications are already being contemplated (tunable antennas and filters, switches, memories...), their common feature being that they allow a considerably reduced power consumption to be achieved, owing to magnetization being controlled by the electric field, rather than by the magnetic field, which is highly power consuming. The reverse principle (i.e. generating a voltage by means of a magnetic field source) is likewise being investigated, as it would afford a major advantage, for energy harvesting purposes.

As regards radiofrequency applications, the advent of [opportunistic radio](#) systems marked a historic turning point. This is an area in which the difficulties arising, as regards miniaturization, and multifunctionality, with regard to the transmitter/receiver, and signal

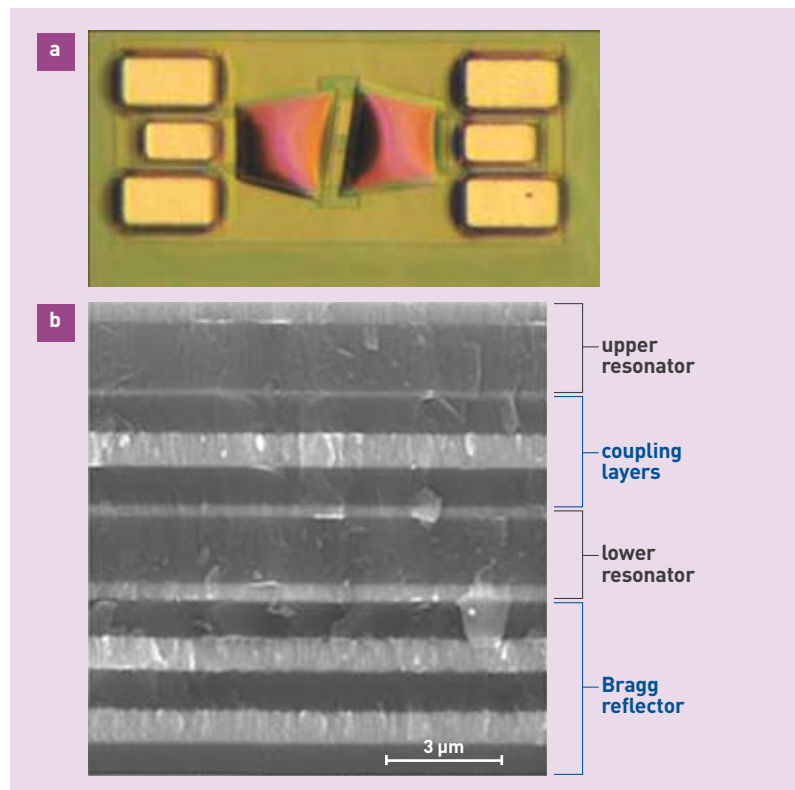


Figure 4.

Acoustically coupled radiofrequency filters, using aluminum-nitride- (AlN) based piezoelectric resonators. Panel a shows a two-section acoustically coupled filter (i.e. featuring a total of 4 resonators), as viewed from above. The six rectangles on either side are the electric contacts, while the two "apodized" forms, which are bulged – as may just be seen – are resonators covered with a protective film developed at LETI.

Panel b shows a sectioned view of the filter (minus protection). The very large number of layers required for the fabrication of the component may be noted (14 layers). The Bragg reflector prevents energy losses to the underlying silicon substrate. The upper, and lower resonators comprise a piezoelectric layer (AlN), and two electrodes ([molybdenum](#)). Between these two resonators, so-called coupling layers are positioned, allowing the exchange of acoustic energy between the two resonators to be managed. It is the combination of these four components that makes it possible to provide the filtration function.

processing units, call for a veritable cultural shift. The applicative departments at LETI⁽⁵⁾ rank among the major players, with regard to this new departure, in the worldwide telecommunications community. However, the technological barriers involved are such that some of the challenge also bears down on the physicists from which novel materials are expected. LCRF is currently investigating magnetodielectric thin films, exhibiting the ability to combine high permeability (μ), and high permittivity (ϵ) (see Figure 5). In the field of electromagnetism, tweaking these two fundamental quantities results in extreme miniaturization for resonator, and/or radiating structures operating in the microwave domain (see Figure 6). Indeed, the size of such structures is equal to a fraction of the wavelength (λ) of the signal illuminating them. Now, λ is inversely proportional to the square root of the product ($\mu \cdot \epsilon$), for the medium the signal passes through. Moreover, if the ratio (μ/ϵ) remains close to unity, the wave propagates through the material without undergoing unmatched, with respect to

(4) LiNbO_3 .

(5) The Architecture, Design, and Embedded Software Department (DACLE: *Département architecture, conception et logiciel embarqué*), and the Systems and Systems Integration Department (DSIS: *Département systèmes et intégration des systèmes*).

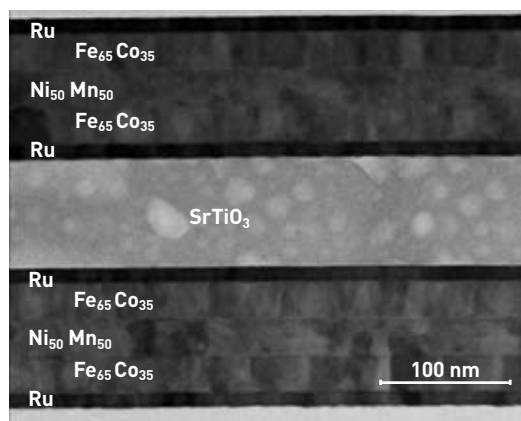


Figure 5. Transverse section, as viewed under transmission electron microscopy, of a composite multiferroic material, consisting of thin films, exhibiting high permeability, and high permittivity. The material consists of an alternating stack of magnetic electrodes, mainly consisting of FeCo, to ensure high permeability, and dielectric layers made of SrTiO₃ perovskite, making for high permittivity. It should be noted that a layer of antiferromagnetic material (in this case, NiMn) is used, within the magnetic electrode, to polarize it, for very-high-frequency utilization purposes.

propagation through air, which precludes any efficiency loss. Nowadays, the advances achieved, with regard to thin films, mean that this kind of tweaking may be contemplated. Thus, for the very first time, LCRF and LTS were able to synthesize such a material, involving an alternating stack of magnetic electrodes, making use of films made of iron–cobalt (FeCo), or nickel–manganese (NiMn) alloys, and dielectric films using strontium titanate (SrTiO₃), for which the crystallization temperature could yet again be brought

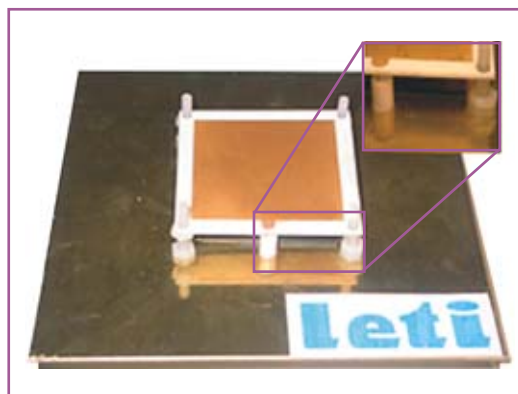


Figure 6. An example prototype 2-GHz patch antenna, making use of the multiferroic material shown in Figure 5. The antenna comprises a ground plane (lower surface), and a metallic patch above it (upper surface). The multiferroic material, positioned in the antenna's cavity (between the ground plane and the patch: see the zoomed-in view, top right), allows the antenna to be operated at lower frequencies, without increasing its dimensions, and also makes for a larger bandwidth [i.e. a larger range of frequencies for which the antenna is an efficient radiating structure, on either side of its central frequency].

(6) The MINATEC micro- and nanotechnology innovation campus was set up at the initiative of the Grenoble INP group – bringing together a number of renowned engineering schools, close to the world of industry, and opening onto the international scene – and CEA's Grenoble Center. It is supported by France's national government, and local authorities. Inaugurated on 2 June 2006, MINATEC draws together the chief players in the Grenoble area, influential with respect to the evolution of micro- and nanotechnologies.

down (in this case, to 260 °C), to ensure full compatibility with the magnetic electrodes. LCRF has further embarked on development of a variable inductor for radiofrequency applications – an altogether novel component, based on alternative processes to piezomagnetism, as outlined above. Expectantly awaited as it is by telecommunications circuit designers, this is a component that should afford frequency-tuning possibilities never before achieved, for a passive integrated component (higher than 100%). This type of component will make it possible, in particular, to make filters that are tunable over a broad frequency range, thus avoiding the – highly costly – requirement to resort to several filter technologies, for each subband covered. Another exciting application concerns a self-tuning antenna, matching the signal being received by way of this controllable component. Achieving this result entails making use of magnetostriction, i.e. the sensitivity to strain exhibited by the magnetic properties of a material. Now, this property is very little used, as of now, aside from a few magnetic switch applications. LCRF is looking into iron–cobalt–boron (FeCoB) alloys, these involving the best tradeoff in terms of microwave performance, and sufficiently high magnetostriction levels (20–60·10⁻⁶). For that material to be controlled, a suitable strain generator must also be available – ideally, an integrated one. LCRF is currently working on a quite original solution, involving the fabrication of piezoelectric PZT membranes, exhibiting strain that can be controlled simply by an electric voltage, onto which the magnetostrictive material is directly deposited.

Thus, the integration of new magnetic, dielectric, and multiferroic materials into microsystems is bringing novel radiofrequency functionalities to existing devices – in particular frequency agility, for multimodal communication systems. This approach, which has been followed by LCRF from the start, is fully consonant, of course, with the historically silicon-related environment at LETI. It stands as an offshoot from the More than Moore approach, strongly branching out, however, into the academic community. The Carnot Institute, likewise coming under LETI, has thus supported a number of collaborations on this topic, set up with CEA (INAC), and the Spintec laboratory at Grenoble (southeastern France), CNRS/XLIM at Limoges (central France), the Rennes (western France) Electronics and Telecommunications Institute (IETR: Institut d'électronique et de télécommunications de Rennes) and the Information, Communications and Knowledge Science and Technology Laboratory (CNRS/LabSTIC: Laboratoire en sciences et technologies de l'information, de la communication et de la connaissance), at Brest (western France).

Such a success is due to one resolve: that of inserting advanced research, on materials exhibiting unequalled properties, at the core of a dedicated infrastructure of world ranking (MINATEC),⁽⁶⁾ intent on the transfer of high technology. It is further due to the shared trust, and confidence of academe, and industry.

➤ **Bernard Viala and Emmanuel Defaj**

LETI Institute (Electronics and Information Technology Laboratory)
CEA Grenoble Center

Surface functionalization: from organic electronics to sensors, and biosensors

From stainless steel to liposomes, through polymer prostheses, and carbon fibers...

all materials interact with their environment, via their surfaces. Adhesion, corrosion, lubrication, electrical contact, biocompatibility, wetting – these are but some in the inventory of commonplace phenomena governed by surface effects. Living organisms are no exception, and also enter that inventory, as giving rise to numerous interface phenomena, localized in lipid bilayers, or on the outside surfaces of proteins.



X-ray photoelectron spectrometry (XPS): positioning a sample holder in the analysis chamber.

Taking benefit from surface effect phenomena entails, as a prerequisite, mastering an ensemble of knowledge spanning both fundamental research, and technological applications – for instance, knowing how to design, and fabricate engineered surfaces having the ability to interact with the outside environment in a predetermined manner; or how to modify the native surfaces – i.e. as yielded by the manufacturing process, or original, natural surfaces – of materials. Surface **functionalization** meets this requirement, by regulating the interaction of a material with its environment, while not altering its structural properties: one and the same material may thus exhibit different surface properties, depending on functionalization.

Polymer film formation

Organic coatings, in particular **polymer** thin films, have pervaded our daily life: for anticorrosion protection in automobiles, specific nontoxic coatings to line

foodstuff cans, lubricating films for electrical contacts, robust **biocompatible** films for medical instruments and implants, **microelectronic** chip packaging... Every one of these applications involves stringent requirements, in particular regarding the stability in utilization conditions, which conditions in turn are heavily dependent on the bond set up between the polymer film, and its substrate, i.e. the material onto which it is deposited. This has led to a classification of the methods used in polymer film formation, according to the type of polymer–substrate bond involved.

Spin coating, and vapor deposition

Both of these methods come under the category of what might be termed “soft” methods, in that no strong bond is set up between the final film, and its substrate. They are commonly used in microelectronics, to form



Covalent chemical grafting by the GraftFast™ process: preparation of the reactive mixture.

sacrificial layers,⁽¹⁾ serving the purpose of ensuring a temporary protection for this or that region of the surface – and affording the advantage of being readily removed, by way of a suitable washing step.

Plasma polymerization and cathodic electrodeposition

These two methods, by contrast, yield grafted films, i.e. films bonded to their substrate by covalent bonds (involving energies higher than 10 kJ/mol). Plasma

(1) To effect the local modification of a surface, a number of operations are required: fabricating a temporary mask, through deposition of a homogeneous photosensitive film, by the spin coating technique; carrying out localized irradiation of that film through a mask, thus locally modifying the solubility of the irradiated regions, with respect to a suitable solvent; durably altering the surface of the “unprotected” regions; removing what remains of the mask by means of a second solvent.



Covalent chemical grafting by the GraftFast™ process: shown here, a gold foil strip, grafted over its lower region.

polymerization yields films that exhibit strong adhesion, and that are highly cross-linked. This is accounted for by the large number of reactive units formed, at the same time, in the plasma. Electrodeposition, in turn, allows a further degree of control to be exerted, as the voltage is readily tuned, and serves to control the formation of reactive species in the immediate vicinity of the conducting surface being modified. Moreover, since each material involves its own specific threshold potential that allows electrodeposition to be initiated, it then becomes possible to turn to advantage certain mixed surfaces, to effect localized functionalizations.

Polymer deposition by chemical initiation, also known as chemical grafting

Based, as plasma polymerization, on the generation of reactive species, in the vicinity of the surface undergoing modification – though in solution, in this case – this deposition method makes it possible to extend most of the benefits afforded by electrodeposition to insulating surfaces, e.g. surfaces of oxides, or plastics.

Electrografting, and chemical grafting: two valuable tools for surface functionalization

Three examples – though others could be cited – will serve to make this point.

Electronics

In this sector, surfaces and interfaces play an altogether major part, since this is where many materials come into contact, each exhibiting different characteristics. For instance, transistors, photovoltaic cells, or light-emitting diodes – mainly based on stacks of organic, and/or inorganic layers – feature extensive interfaces that strongly influence their behavior during utilization, and aging. The same is true of the more basic electronic components, e.g. connectors. In letting electrical current through, temporarily, between two distinct parts in a functional unit, such connectors are subjected to numerous connect/disconnect actions, along with vibrations generating large amounts of friction, affecting the conducting surfaces, as they come into contact. Such friction may damage the metals employed (as a rule, brass, covered with a thin gold film), giving rise to poor contacts. To mitigate this issue, manufacturers have long used liquid lubricants: e.g. perfluoropolyethers (PFPEs), or polyphenyl ethers (PPEs), serving to lubricate contacts, protect against corrosion, and ensure high thermal stability. Unfortunately, these liquid lubricants remain ineffective, with regard to employment in extreme environments (ultrahigh vacuum, very low temperatures), or in miniaturized systems, in which surface forces, e.g. capillarity, become dominant, while coating thickness becomes an important parameter. In such cases, another technique comes to the fore, namely “dry lubrication,” involving the use of solid lubricating films. Several solutions are available, for instance one involving the use of self-assembled monolayers (SAMs) – a path which has been deemed unconvincing by the electronics industry, since it affords neither thermal stability, nor compatibility with the metals commonly used (brass, or tin, in particular). By contrast, polymer organic films, as obtained by cathodic electrografting, meet all the relevant specifications. Indeed, since they

are grafted, and cross-linked, these films exhibit a characteristically high stability. Further, their chemical composition may yet be tuned, according to requirements. As for grafting, this may be applied to any metallic surface, in straightforward, inexpensive conditions. The best results are achieved with the electrografting of **diazonium salts**. These **molecules** are already well known to chemists, as intermediate products in the synthesis of diazo dyes (**methyl orange**, **amaranth**...). Electroreduction of these substances yields **aryl radicals** (see Figure 1), having the ability to graft themselves onto the negative electrode (i.e. the cathode), and subsequently onto any previously grafted aryl groups (by the **aromatic radical substitution reaction**). As such grafting occurs in random fashion, reduction may carry through, beyond the first thickness of grafted aryl groups. This operation readily yields grafted, partially cross-linked polyaryl films (see Figure 1). Researchers working at the Surface and Interface Chemistry Laboratory (LCSI: Laboratoire de chimie des surfaces et interfaces) have shown that such ultrathin films (less than 10 **nm** thick) exhibit both very low contact resistance, and an extremely low coefficient of friction, which remains constant under mechanical stress. Such grafted films may thus be seen as outstanding candidates, for the purposes of acting as dry lubricants for microconnectors.

Carbon nanotubes, and graphene

In no more than 10 years or so, carbon **nanotubes** (CNTs), first, then **graphene** – more recently – have become the be all and end all of organic electronics. Indeed, these two **allotropic** forms of **carbon** exhibit remarkable electronic properties: very high charge mobility, in the case of graphene, metallic **conductivity** for certain nanotubes. These properties are complemented by the advantage afforded by dimensions that are both nanoscopic (thickness, as regards graphene, diameter for CNTs), and **macroscopic** (several millimeters, in the case of some CNTs, several **microns** for graphene single sheets). Finally, the exceptional mechanical qualities exhibited by CNTs mean they stand as a choice material, as regards providing a substitute for **carbon fibers**, and acting as a conducting reinforcement for **polymer composite** materials.



Covalent grafting of ultrathin lubricating films sometimes calls for operations to be carried out in glovebox conditions, to analyze the effects of atmospheric pollutants.

However, if such carbon nanotubes are to be handled, formed, and positioned, they must first be amenable to be placed in suspension. This is a difficult operation to carry out, with native CNTs, owing to their strong natural tendency to aggregate into bundles, due to the **Van der Waals interactions** arising between the aromatic nuclei making up their surfaces. Functionalizing their surfaces will resolve this issue. Thus, by coating multiwall CNTs⁽²⁾ with a thin polymer film, it becomes possible to modify their interaction with the outside environment. This polymer film is obtained either by an **electrochemical** route, on nanotube mats connected to an **electrode**, or by chemical grafting, on dispersed nanotubes. The

(2) I.e. nanotubes consisting of a number of concentrically nested single-wall nanotubes.

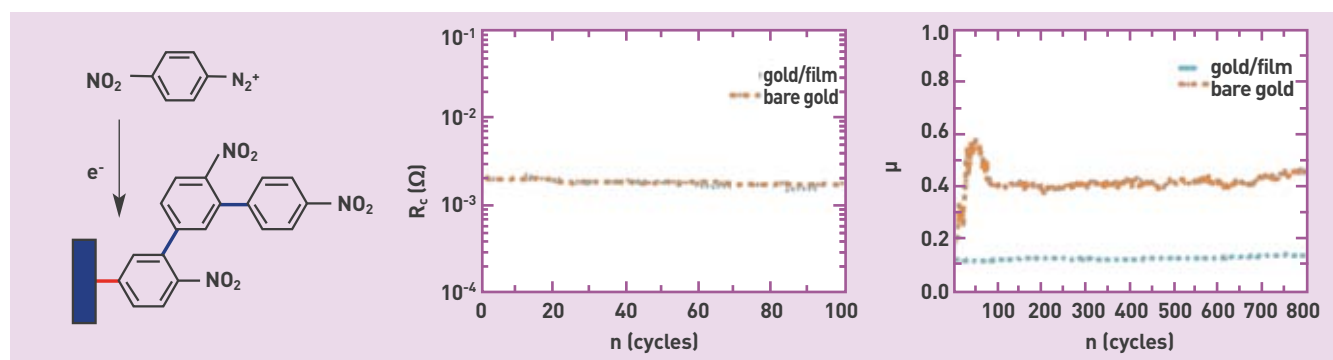


Figure 1.
Left panel: principle schematic of the electrografting of diazonium salts, and formation of grafted polyaryl films. Shown in red, the covalent molecule-substrate bond; in blue, the covalent molecule-molecule bond, within the grafted polyaryl film; e^- indicates an added electron: this stands for the reduction of the diazonium salt to an aryl radical, at the negative electrode.
Center panel: comparison of contact resistance (R_c), expressed in ohms (Ω), for bare gold, and gold grafted with a polyaryl film, during repeated connect/disconnect cycles.
Right panel: comparison of the friction coefficient (μ), for bare gold, and gold grafted with a polyaryl film, during repeated connect/disconnect cycles; n (cycles) is the number of measurement cycles, serving to mimic actual utilization of a connector, involving numerous connect/disconnect actions.

thickness of these films varies, from a few nanometers to several tens of nanometers. The chemical functionality of such coatings depends on the planned utilization of these nanotubes. For instance, by coating CNTs with a polymer rich in **amine** functions, such CNTs can be readily dissolved in an aqueous medium, while their sensitivity is enhanced, with respect to electron-poor gases, e.g. **chlorine** (see Figure 2). Such functionalized nanotubes form the sensitive layer in gas sensors using electrical detection processes, achieving sensitivities as high as 20 **ppb** at ambient temperature. This is a performance level fully on a par with that of the best inorganic sensors – which call for high operating temperatures. By contrast, functionalization carried out by means of acid groups (e.g. **polyacrylic acid** [PAA]) promotes detection of **ammonia**.

Surface functionalization is thus found to be a highly versatile tool,⁽³⁾ for the purposes of tuning the electronic response of carbon-nanotube-based chemical sensors. Likewise, functionalization of the outside wall of nanotubes makes it possible to stabilize suspensions of such nanotubes in all kinds of media: be it a **solvent**, or a precursor polymer for a composite material (see Figure 2).

Decontamination of water tracts featuring high heavy-ion contents

The conventional industrial decontamination process is based, essentially, on the bulk **precipitation** of **heavy ions**, in the form of solid **hydroxides** – an operation that relies on the action of lime. However, even when the operation is nearing completion, filtrates may be found still to contain unacceptable heavy-ion concentrations, which must therefore be removed. With the trapping technique, as carried out in exchange resins, polymers featuring many charged sites serve to trap heavy ions, replacing them, in most cases, with **protons**, or **sodium ions**. The drawbacks this method involves are the high cost of resin regeneration, and the use of reactants that prove, in many cases, hazardous. This was the reason behind the notion of substituting such resins with **carbon felts**, exhibiting high specific surface areas,⁽⁴⁾



P. Stroppa / CEA

Decontamination of water exhibiting high heavy-ion contents: investigation of the electrically triggered acid washing step, on a dedicated pilot setup.



P. Stroppa / CEA

Detail view of the pilot decontamination setup, for water exhibiting high heavy-ion contents: on the right, the stack of active felts (serving to trap heavy ions), and counter-electrodes (serving to effect electrically triggered acid washing, to regenerate the felts); at left, the tank holding water with high heavy-ion content.

- (3) Starting from one and the same base material (CNTs), different surface functionalizations induce diverse sensitivities, with respect to a variety of chemical agents subject to detection.
- (4) Specific surface area is a measure of surface area per unit mass. The higher its value, the more highly divided the material is (very-fine-grained powders, very thin wires...), by contrast to a dense bulk material.

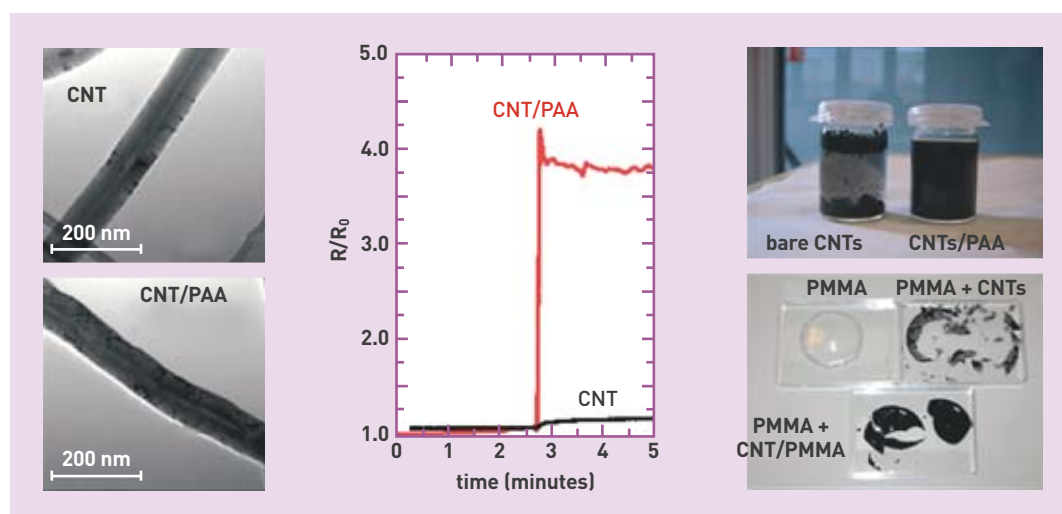


Figure 2. Functionalized carbon nanotubes. At left: a fresh carbon nanotube (CNT) (top), and a CNT functionalized by means of grafted polyacrylic acid (PAA) (bottom), as viewed under scanning electron microscopy (SEM). Center: differential resistance exhibited for ammonia by a CNT sensor, as plotted for a bare nanotube (in black), and a nanotube functionalized by PAA (red). R/R_0 stands for the differential resistance measurement, corresponding to the readings yielded by the sensor. Right: CNTs held in solution in water (top), and in polymethyl methacrylate (PMMA) (bottom).

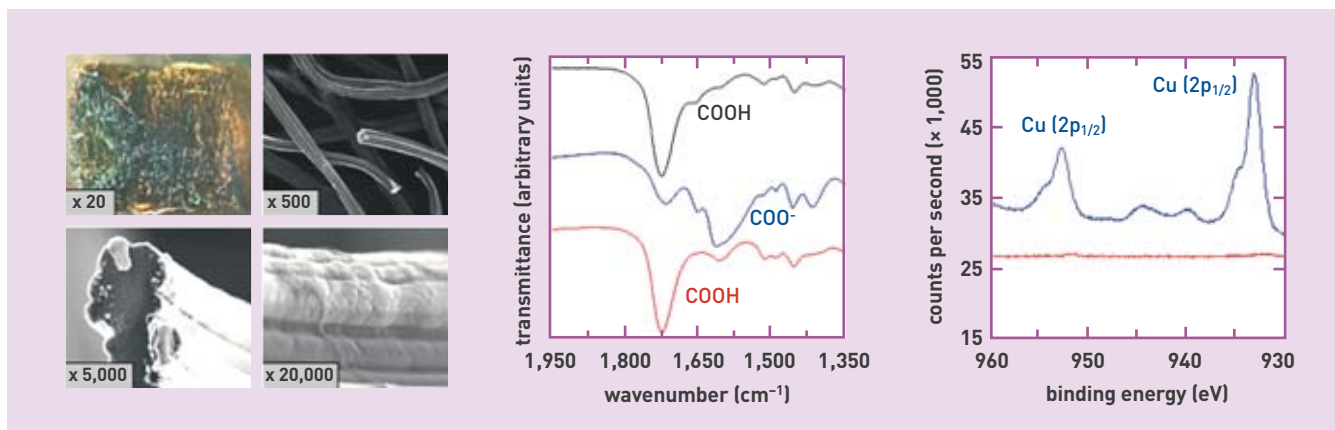


Figure 3. Functionalized carbon felts, used for decontamination purposes. At left: views of felts functionalized by means of grafted polyacrylic acid (PAA), under various magnifications. Center: infrared spectra, as obtained before (black), and after (blue) the trapping of cupric ions, and subsequent to their electrically controlled release (red). Transmittance is the ratio of initial, over final intensity, after the infrared beam has passed over the sample. (The absence of a unit scale indicates, in this case, that any unit used only remains valid so long as these three spectra are being compared with one another.) Transmittance is the inverse of absorption. COOH stands for the carboxylic acid function (carried by the PAA polymer): when in this form, no ion is trapped within the film. COO stands for the carboxylate function, for which cupric ions are trapped inside the film. Right: X-ray photoelectron spectroscopy (XPS) spectra, as obtained before (blue), and after (red) release of the ions, at two energy levels for copper (Cu).



X-ray photoelectron spectroscopy (XPS): finescale analysis of a modified surface.



X-ray photoelectron spectroscopy (XPS): positioning a sample holder in the entrance bay of the spectrometer.

and featuring suitable surface functionalization (see Figure 3). This may be achieved, for instance, by using a carbon felt grafted with PAA, which has the ability to immobilize cupric ions readily. As the grafted film is a thin film (less than 300 nm), the entire film is involved, and saturation swiftly ensues.

Moreover, in contrast to resins, regeneration calls for no hazardous additive, since the conductivity exhibited by carbon felt makes it possible to electrochemically trigger the expulsion of previously trapped ions. Applying an oxidizing potential to the felt sets off the **electrolysis** of any water present within the film, in accordance with the reaction: $\text{H}_2\text{O} + 2\text{e}^- \rightarrow \frac{1}{2} \text{O}_2 + 2\text{H}^+$, which thus releases protons. These protons, once released within the carbon felt, are expelled to the outside of the felt, under the action of the applied electric field. They are thus in a position to “scavenge” the PAA film, releasing cupric ions as they go. This operation is known as “electrically triggered acid washing.” This is limited to the time during which the potential is applied, and to the film’s interior. It is sufficient that this release occurs in an aqueous medium, for achieving the removal of the ions that were trapped inside the film – which is then ready to carry out a new trapping operation. This procedure may be automated, of course, in treatment pilot systems, designed to control washing fluid streams, and electrolysis times; and felt functionalization may be tuned, to cater for the target ions.

The three examples outlined in the above paragraphs provide a good illustration of the major role played by surface functionalization, as regards tuning a native material (brass, carbon nanotubes, carbon felts) to match the function intended for it. Surface functionalization may thus be seen as a simple, elegant way of achieving savings in energy, since it allows one and the same material to be tuned, to fulfill a variety of functions. For researchers, it further stands as an inexhaustible source of scientific, and technological innovation.

➤ **Serge Palacin**

Radiation-Matter Institute, Saclay (IRAMIS)
Physical Sciences Division
CEA Saclay Center

New high-value-added biomaterials

The development of biomaterials, i.e. materials based on biological molecules, has been experiencing heavy growth. Improved knowledge, as regards the self-assembly, and structuring properties exhibited by polypeptides, now makes it feasible to use such macromolecules for the purposes of fabricating a wide variety of high-value-added materials, at scales that may range from the nano- to the macroscopic. **Major industrial outlets are foreseen, in sectors as diverse as papermaking, textiles, or green chemistry.**

For a long time, the term “biomaterials” was only used to refer to materials that are **biocompatible** with human, or animal organisms, as produced by combining the expertise of several separate disciplines, such as medicine, biology, chemistry, and materials science. Placed in contact as they are – in temporary fashion, or permanently – with a variety of tissues, organs, or fluids in living organisms, these

biomaterials serve diagnostic, preventative, or therapeutic purposes. For some years now, this term has further covered materials, yielded by a number of **biotechnologies**, consisting of **polymers**, of natural provenance or otherwise. Their utilization is thus no longer restricted to the sole medical domain, rather it now encompasses the areas of agricultural and food technologies, life sciences, textiles, paper-making, or even cosmetics.

Biological macromolecules in the service of biomaterials

At the present time, the natural **molecules** commonly used for the purposes of fabricating biomaterials fall under the category of sugars.

- For instance, chitosan is a product derived from chitin, a constituent of the **exoskeleton** featured by **arthropods**, e.g. crustaceans, or of the **endoskeleton** found in **cephalopods** – a family of which squids are members. Already used as it is in the fabrication of contact lenses, cosmetics, or dietary products, chitosan may well find new applications, for the purposes of tissue regeneration, **osteogenesis**, or even as a carrier of biologically active molecules.

Another sugar, hyaluronic acid, is one of the chief constituents of the **extracellular matrix**, and is peculiarly suitable for the purposes of biomedical applications concerning those bodily tissues in which it is naturally found, e.g. skin, or cartilage. It is extracted, industrially, from cocks' combs, or produced by genetically engineered bacteria. Over the past few years, it has been employed in cosmetic medical procedures, as a filling product for wrinkle reduction, or for breast augmentation.

Alginates, which are **polysaccharides** obtained from a group of brown algae, known as laminaria (kelps), are widely used as thickeners, gelling agents, emulsifiers, and stabilizers, in numerous industrial products. They are thus found in edible jellies, cosmetics, paints and printing inks, but equally in more specific products, e.g. molds used to take dental impressions, or for cinematic special effects, where they are used to reproduce certain human body parts..

- Polypeptides** are found as constituents in materials already found in nature, e.g. mother-of-pearl, silk, or wool. They form another major class of biological **macromolecules**, also used for the fabrication of some biomaterials. In particular, gelatin – which is already



Working out the experimental conditions that will serve to optimize the characteristics of a biomaterial fabricated from proteins.

P. Avastian/CEA

widely used by the food industry – is obtained by the partial **hydrolysis** of a polypeptide that has been in use for some 8,000 years as an adhesive: to wit, collagen. Nowadays, collagen is also employed for applications in the pharmaceutical industry, for cosmetics, and in photography.

In molecular terms, polypeptides are amino acid polymers. An amino acid is a **carbon** chain featuring one amine (NH_2) function, and one **carboxylic acid** (COOH) function, carried by the same carbon atom. The final two positions, around this carbon atom, are taken up by one **hydrogen** atom, and a variable group, known as the side chain. The properties exhibited by these side chains allow amino acids to be classified under four groups: acidic, basic, **hydrophilic**, and **hydrophobic**. In polypeptides, amino acids are linked to one another by peptide bonds. These are **covalent bonds**, set up between the carbon atom in the carboxyl group of one amino acid, and the **nitrogen** atom in the amine group of the next amino acid. The number of amino acids involved, and the order in which they appear within the chain determine the structural, and functional characteristics of the polypeptide thus constituted. More than one hundred amino acids occur in nature, however only 20 or so are found as components of natural polypeptides. As a rule, a molecule is referred to as a **peptide**, or a polypeptide, when the size of the chain involved is no larger than about 50 amino acids; larger chains being known as **proteins** – which may consist of more than a thousand amino acids.

Proteins account for half the dry weight of living organisms, and serve to carry out a multiplicity of functions: **catalysis** of the chemical reactions involved in **metabolism**, metabolite transport, communication within the organism (by way of certain hormones, in particular), the ability of the immune system to recognize, and discriminate between, the self (i.e. those molecules that specifically belong to an individual), and the non-self (foreign molecules), cell motility (**flagellae**, muscle contraction), or tissue, and cell structure (collagen, the **cytoskeleton**). If they are to carry out their biological functions, proteins must fold upon themselves, to achieve a stable three-dimensional structure (see Figure 1). This structuring action, known as the “protein folding reaction,” is a spontaneous phenomenon. The mechanisms involved in this reaction are still, in the main, far from being understood, and are the subject of intensive investigations, straddling biology, chemistry, and physics.

Whereas peptides tend to be obtained by chemical synthesis, proteins can be extracted – in large quantities – from natural produce (plants, meat, milk...), or be manufactured by **biotechnologies**, making use of genetically engineered organisms (e.g. bacteria, yeasts...). The latter approach has opened up, for researchers, the path of protein engineering, which involves modifying a natural amino acid sequence. This makes it possible to produce a novel protein, featuring a different function, or distinctive interfacial properties, compared to the initial protein. At an

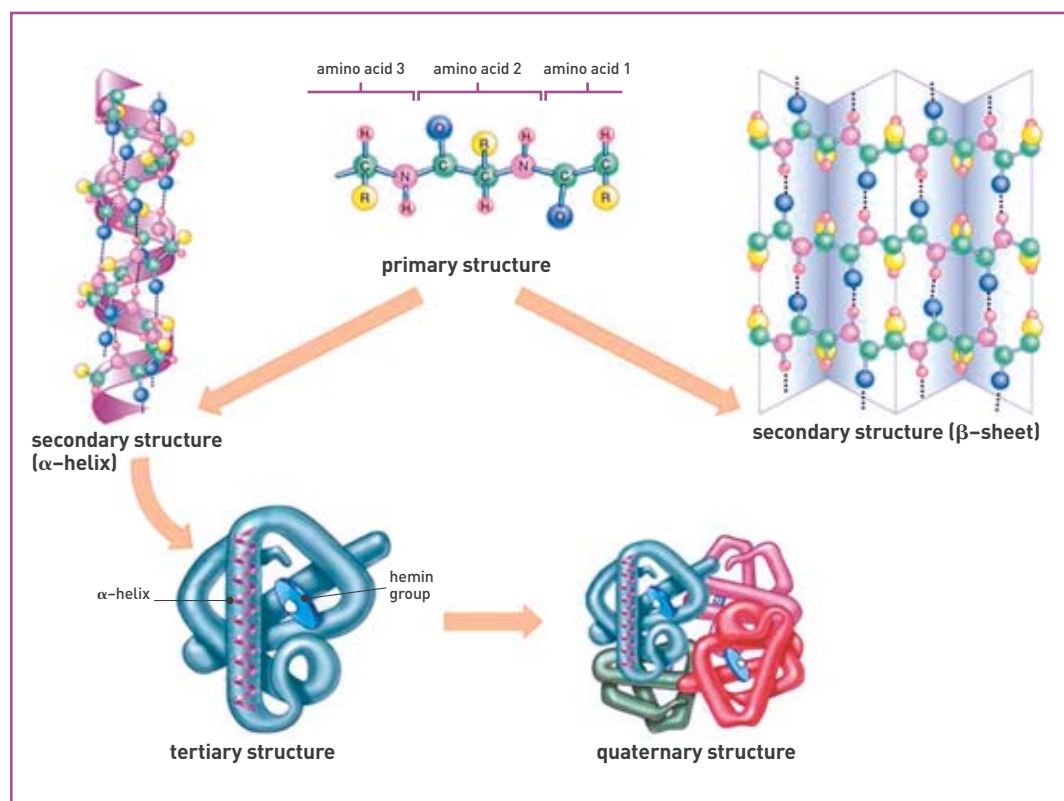


Figure 1.

The structure of proteins. The primary structure is the polypeptide's amino acid sequence. This may range from a few amino acids, in peptides, to more than one thousand, in a protein. The amino acids are linked by peptide bonds, and are differentiated by their side chains (noted R). A first structuring level arises with the formation of secondary structures, set up by way of a network of hydrogen bonds, between the peptide bonds. The positions of these hydrogen bonds allow the structure to become stabilized, into an α -helix, or a β -sheet. The tertiary structure is the protein's three-dimensional structure; this is the functional state for the vast majority of proteins. The manner in which secondary structures are arranged within the tertiary structure is stabilized by a network of close interactions arising between the side chains in the amino acids. Proteins, once folded, may further assemble themselves to form a quaternary structure.

The McGraw-Hill Companies, Inc

industrial scale, such biotechnology techniques are chiefly employed by the pharmaceutical industry, to meet its own demand for proteins of therapeutic interest, e.g. **insulin** – used for the treatment of diabetes – or **monoclonal antibodies**, serving for the production of vaccines. At the present time, people engaged in research, as in industry are looking to use these techniques to obtain proteins entering in the fabrication of high-value-added materials – one of the best-known examples being the attempts to manufacture the proteins found in spider silk.

Biopolymers: highly organized molecules

For several years now, polypeptide-based materials have been targeted by major research efforts. The self-assembly properties exhibited by such biopolymers, at scales ranging from the **nano-** to the macroscopic, mean they are seen as peculiarly promising, with regard to the “**bottom-up**” approach, which is adhered to, as a rule, when it comes to designing materials. Indeed, the interactions involved, within polypeptides, as also between such molecules, are all low-energy interactions (hydrogen bonds, ionic bonds, hydrophobic interactions, **Van der Waals forces**), though their cumulated effect, within ordered structures, can result in highly stable objects. Currently, numerous investigations are looking into the employment of **synthetic** peptides, exhibiting specific properties, promoting supramolecular self-assembly. Of the issues

raised by this technology, first and foremost is the impossibility of synthesizing many sequences, owing to their physicochemical properties. Other issues concern production processes, which undergo a fall in efficiency, while costs rise considerably, as the length of the amino acid sequence increases. Notwithstanding these difficulties, a number of materials, involving small peptides, and structured at the nanometer scale, have already come out – e.g. in the form of **hydrogels**, to be used in three-dimensional cell cultures, or for the transport of active molecules, or in printing inks.

For the purposes of forming materials, molecular self-assembly may also be undertaken with proteins. The diversity, and stability of the structures proteins may form mean it is possible to contemplate a broad range of materials. The proteins used, in this respect, may also be yielded by biotechnologies involving the production of **heterologous** proteins by genetically engineered organisms, as outlined above. While the Metals Chemistry and Biology Laboratory (LCBM: Laboratoire de chimie et biologie des métaux) has indeed mastered this protein production method, another strategy, relying on the isolation of natural proteins, available in large quantities, is also being implemented, for the purposes of developing new materials – e.g. the proteins found in **whey**, which had long been seen as a mere waste product, yielded by the cheese industry.

The advantage afforded by whey is related to its composition: it is a heterogeneous mixture of proteins, exhibiting a wide range of functional properties, of interest to the food industry, as to the chemical, pharmaceutical, and cosmetics industries. The chief proteins in this mixture are β -lactoglobulin, α -lactalbumin, **immunoglobulins**, bovine serum albumin, and lactoferrin. The rising number of fractionation, and isolation techniques available, with respect to these proteins, has resulted in many forms of enriched whey being produced, featuring varied, albeit outstanding nutritional qualities. Such diversification has thus made it possible to extend the use of such wheys as food supplements, from cattle rearing to ameliorating the health of individuals presenting specific nutritional needs. Moreover, recent discoveries, regarding a number of biological activities attributed to these proteins found in whey, have further led to the isolation of such proteins being seen as affording particularly high benefits. In the future, utilization of individual whey proteins should make it possible to broaden the range of possible outlets for that produce, resulting in its increased commercial value, for the dairy industry.

Depending on conditions, certain whey proteins may undergo self-assembly, to form a variety of objects, of sizes ranging from 10 nanometers or so to several micrometers. α -Lactalbumin may serve to illustrate the diversity of the objects so obtained (see Figure 2). For instance, at high temperature, this protein is able to interact with lysozyme – a protein found, in particular, in the egg white of hens' eggs – to form micrometer-scale supramolecular assemblies. The structures formed are **porous** microspheres, which could be used, for instance, to deliver bioactive molecules (Figure 2, top right). Under different conditions, α -lactalbumin molecules are also able to self-assemble, resulting in the formation of fibers several hundred **nanometers**-



P. Avignon / CEA

Preparing a sample for the purposes of carrying out the preliminary characterization of a material fabricated from proteins.



P. Avavian / CEA

A suspension of proteins being used for the fabrication of a biomaterial.

long (Figure 2, top left). Other assemblies, in the form of **nanotubes**, are obtained, at high temperature, by treating the protein with a specific **protease** (Figure 2, bottom right). The advantage such nanotubes afford stems from the truly highly diverse possibilities they provide, of which the inventory keeps growing, month by month.

The various objects so obtained may further interact, and organize themselves into larger-scale structures. For instance, in the presence of **liposomes**, α -lactalbumin fibers grow, and may reach a diameter of 1 μm , over lengths of several tens of micrometers (see Figure 2, bottom left). Likewise, nanotubes obtained by partial **proteolysis** can interact, and organize, yielding hydrogels.

Biomaterials of the future

The advantage afforded by natural-protein-based materials chiefly concerns their biodegradability, but equally fabrication processes carried out under moderate solvent, temperature, and **pH** conditions – i.e. processes compatible with green chemistry. While whey utilization is growing in the agrifood, and cosmetics sectors, other commercialization outlets have yet to be found. For instance, the special papers manufacturing sector has been voicing a strong demand, as regards new biodegradable poly-

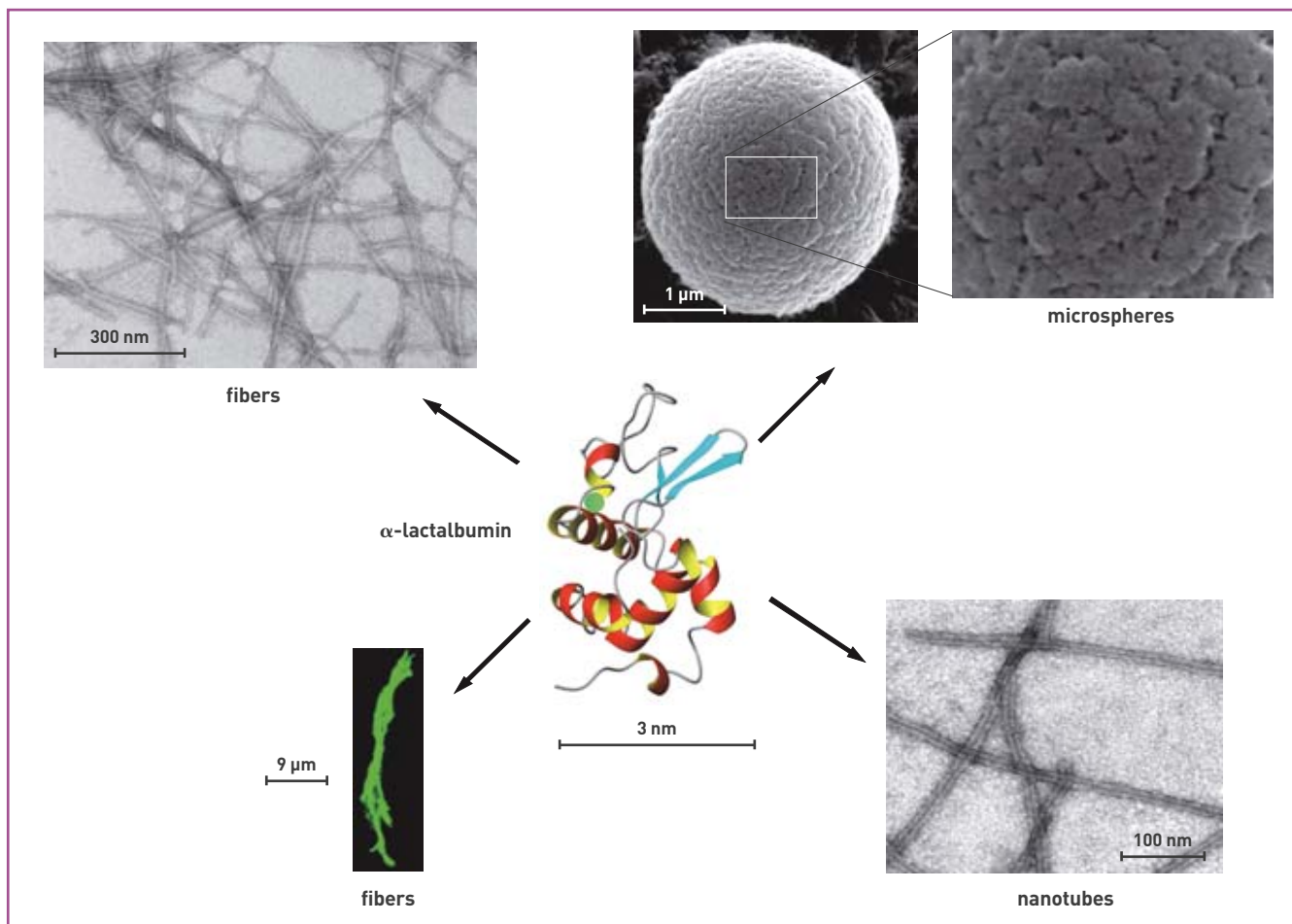


Figure 2.
The variety of materials obtained, by way of self-assembly, from one protein. The topology of the polypeptide chain featured by α -lactalbumin is shown at center. The side chains are not represented. The α -helices are colored red/yellow, the β -sheet blue. The green sphere stands for a calcium ion, attached to the molecule. The various materials obtained through the self-assembly of this protein are described in the body of the text [adapted from Figure 6 in Nigen *et al.*, *FEBS J.* 274(23): 6085–6093 (2007); adapted from Figure 2 in Graveland-Bikker *et al.*, *Langmuir* 20(16): 6841–6846 (2004); adapted from Figure 3 in Zhao *et al.*, *Biochemistry* 43(32): 10302–10307 (2004)].

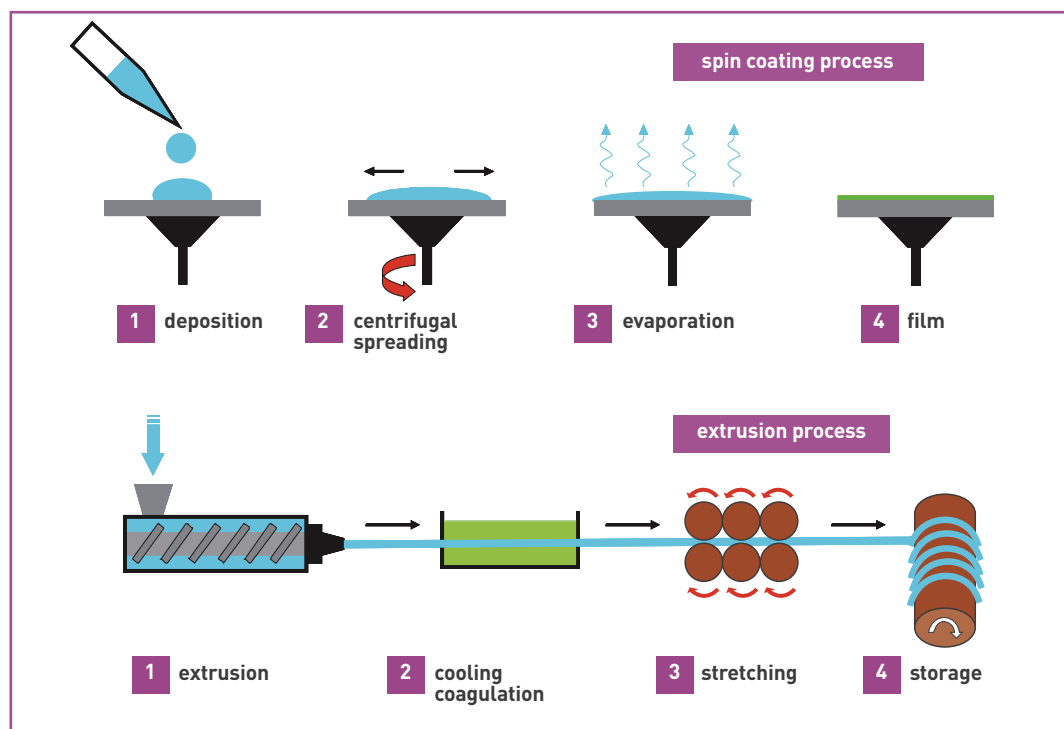


Figure 3.

Materials fabrication processes. For the purposes of spin coating, the suspension of objects is deposited at the center of a plate, and subsequently spread out by controlled spinning of that plate. After evaporation, a film is obtained, with a thickness of the order of 100 nanometers. The process may be reiterated a number of times, to fabricate a multilayer film. For extrusion, a high-concentration suspension is forced through a small-diameter (down to a few micrometers) orifice, or die, at controlled pressure, resulting in the formation of a yarn. The yarn may then be passed through a cooling bath, or a bath involving a different solvent, prior to being stretched. This step is required, in some cases, to induce a change in polypeptide configuration, within the yarn; this is the case for silk, in particular. The yarn obtained is then stored by spooling it.

mers. Consequently, the Metals Chemistry and Biology Laboratory is investigating the feasibility of substituting, in the longer term, plastic materials currently used in the luxury goods industry (e.g. for champagne bottle labels), or those used for public security purposes (for the fabrication of identity documents, in particular), or for food safety appli-

cations (for the purposes of ensuring goods, and foodstuff traceability). One of the solutions being considered involves the spin coating technique (see Figure 3), which makes it possible to obtain films featuring thicknesses of 100–200 nm. This method is used, in particular, to obtain stacks of layers, involving different films so produced, serving to fabricate **composite materials**.

At the same time, with the rise of textile techniques, current trends in the textiles market act as an incentive to investigate novel kinds of fibers, of materials, and coating processes. With the developments achieved with regard to the extrusion technique, it has now become feasible to produce yarns no more than a few microns thick (see Figure 3).

Finally, aside from the papermaking and textiles sectors, the biomaterials being developed at the Metals Chemistry and Biology Laboratory will also be finding outlets for applications in areas as diverse as green chemistry, or biomedical devices.

> Carole Mathevon and Vincent Forge

Metals Chemistry
and Biology Laboratory (LCBM)
(UMR 5249 CEA-CNRS-UJF)
Research Institute for Life Sciences
and Technologies (IRTSV)
Life Sciences Division
CEA Grenoble Center



A biomaterial obtained from proteins being observed under a binocular microscope.

Institutions and organizations: who does what?

Advanced Micro Devices, Inc. (AMD): US corporation, headquartered in Sunnyvale (California), founded in 1969 by a group of engineers and executives from Fairchild Semiconductor, for the purposes of fabricating semiconductor materials and devices.

Agence française de sécurité sanitaire de l'environnement et du travail (AFSSET): the French Environmental and Occupational Health Safety Agency (merged in 2010 into the National Food, Environmental, and Occupational Health Safety Agency [ANSES: Agence nationale de sécurité sanitaire de l'alimentation, de l'environnement et du travail]) has had the remit of working for the protection of human health, by contributing to health safety with regard to environmental, and occupational contexts, by assessing the risks these may involve, and providing government with full information as to health risks, and the advice required for the purposes of drafting legal, and regulatory provisions.

Agence nationale de la recherche (ANR): France's National Research Agency is a public-sector establishment of administrative character, acting as a funding agency for research projects. Its purpose is to ensure a greater number of research projects, put forward by the scientific community as a whole (i.e. from both the public, and corporate sectors), are granted funding, subsequent to competitive evaluation, and peer assessment.

Agence nationale pour la gestion des déchets radioactifs (ANDRA): set up in 1991, France's National Agency for Radioactive Waste Management is a public-sector establishment of industrial and commercial character, set under the joint oversight of the Ministries charged with Energy, Research, and the Environment. ANDRA is charged with the long-term management of radioactive waste arising in France. Its remit includes: the management, on an industrial basis, of short-lived waste; research on very-long-term management solutions, for long-lived waste (it was charged with directly steering work on Direction 2, for research on radioactive waste management, as set out by the French Act of 30 December 1991); and maintaining the national inventory of all such waste extant on French soil. These remits were amplified by the Act of 28 June 2006 setting out the program for the sustainable management of radioactive waste and materials.

Air Liquide: standing as the world leader in the field of industrial, medical, and environmental control gases, the corporation is present in more than 75 countries, with a workforce of 43,000.

Areva: a French industrial group, set up in 2001 through the merger of CEA-Industrie, COGEMA, and FRAMATOME; the group is charged with the management of any industrial, and commercial activities, arising particularly in the areas of nuclear power, renewable energy, and electricity transport, and distribution. Subsidiaries include **Areva NP** (Nuclear Power) – formerly FRAMATOME ANP – a world leader in the field of nuclear power, as regards reactor design, and construction, fuel supplies, and the provision of maintenance, and upgrade services; **Areva TA** – formerly TechnicAtome – specializing in the construction of research reactors, and nuclear propulsion systems; and **Areva NC** (Nuclear Cycle) – formerly COGEMA – which covers the full gamut of fuel-cycle-related services.

Association française de normalisation (AFNOR): the French Association for Standardization is an international group, acting as a service provider, structured around four main areas of expertise: standardization, certification, specialist publishing, and training; its specific feature is that it acts in the public interest, with regard to its standardization remit, while operating, as regards part of its activities, in the competitive sector. Its range of expertise stands as an ensemble of assets, made available to more than 75,000 customers, in 90 countries.

Boeing (the Boeing Company): US corporation, one of the largest aerospace manufacturers worldwide, headquartered in Chicago (Illinois), specializing in the production of civilian airliners, military aircraft, helicopters, satellites, and launchers.

Centre de recherche sur l'hétéroépitaxie et ses applications (CRHEA): the Research Center on Heteroepitaxy and Its Applications is an organization set up, in 1998, within **CNRS**, specializing in the epitaxy of semiconductor materials, e.g. nitrides, zinc oxide, silicon carbide, arsenides; it is set up with the full range of equipment required for structural characterization, together with a technology hall, enabling it to carry out all the steps involved in microelectronics-type technology (lithography, metal and dielectric deposition, chemical etching, plasmas).

Centre de recherche sur les ions, les matériaux et la photonique (CIMAP): the Ions, Materials, and Photonics Research Center is a joint research unit (UMR 6252) – involving CEA, **CNRS**, the Caen (western France) National Higher School of Engineering (ENSICAEN: École nationale supérieure d'ingénieurs de Caen), and Caen University – charged with a threefold remit: research (in the areas of ion-matter interaction, and the relaxation of excited materials; materials defects; materials for lasers, photonics, and electronics; the theoretical foundations of, and applications for, such investigations); acting as the host organization for interdisciplinary investigations carried out on the beamlines of the National Large Heavy-Ion Accelerator (**GANIL: Grand Accélérateur national d'ions lourds**); and teaching (Caen University, ENSICAEN).

Centre de spectrométrie nucléaire et de spectrométrie de masse (CSNSM): the Center for Nuclear Spectrometry and Mass Spectrometry, sited at Orsay (Essone *département*, near Paris), is a multidisciplinary joint research unit, under joint **IN2P3 (CNRS)** and Paris-Sud (Paris-XI) University oversight. It is able to draw on numerous collaborations, both in France (CEA, CNES...), and internationally, as well as with industry.

Centre national de la recherche scientifique (CNRS): France's National Center for Scientific Research is a public-sector establishment of scientific and technological character, carrying out its activity in all fields of research.

CEZUS: an **Areva NP** subsidiary, CEZUS stands as the market leader, worldwide, for zirconium products. Its activities are distributed over six sites – five in France, one in Germany. The Paimbœuf (Loire-Atlantique *département*, western France) site manufactures zirconium-alloy cladding tubes, and guide tubes for fuel assemblies. CEZUS runs its own research center, sited at Ugine (Savoie *département*, southeastern France).

Collège de France: a unique French institution, founded in 1530, having no counterpart in any other country, and occupying a singular position in fundamental research, and higher education, since it is neither a university, nor a school of engineering – nor does it deliver any degrees; dispensing courses of lectures that are open to all, it is endowed with 52 chairs of education, for professors covering a vast range of disciplines – from mathematics to the study of great civilizations, through physics, chemistry, biology and medicine, philosophy, sociology and economics, prehistory, archeology and history, linguistics... and it makes specific provisions to host visiting foreign scholars.

Datco Coating Corporation: US corporation, set up in 1995 to meet the requirements arising in specialized markets (compact, tough ceramics for home cookers, heating elements for cooking hobs, safe, reliable resistors for portable heaters, antiadhesive finishes for plastic material fabrication equipment), and to set up key relationships with the market leaders in industry, for such products.

DuPont de Nemours and Company: US corporation, founded in July 1802 in Wilmington (Delaware) by Eleuthère Irénée du Pont de Nemours; initially set up as a gunpowder factory, it has now become a multinational corporation, ranking among the chemicals majors, and the originator of such plastic materials as Nylon, and subsequently of a number of polymer materials (Neoprene, Teflon, Kevlar, Lycra).



École polytechnique fédérale de Lausanne: the Federal Polytechnic Institute at Lausanne (Switzerland), one of the Swiss Federation's two such institutions; in association with a number of research institutes, its remit covers education, research, and the development of commercial applications, at the highest level worldwide; with more than 10,000 people working together at its site, the institute fosters interchange between students, faculty members, researchers, and entrepreneurs, to promote the emergence of new scientific, technological, and architectural projects.

École supérieure d'ingénieurs en électronique et électrotechnique (ESIEE): the Higher School of Electronic and Electrotechnical Engineering is a public-sector establishment, set up by the Paris Chamber of Commerce and Industry; the group dispenses scientific education, training engineers, and technologists for careers in electronics, information technology, and embedded systems; aside from ESIEE, the group further consists of the Higher School of Electronic Technology (ESTE: École supérieure de technologie électronique), and the Higher Institute of Technology and Management (ISTM: Institut supérieur de technologie et de management).

EDF: as the power utility leader, in France, EDF Group is present in all segments of the electric power industry, from production to trading and distribution grids, as well as in the natural gas supply line; as the chief player in the French, and UK power markets, and with a strong foothold in Germany, and Italy, the Group is able to rely on a 38.1-million-strong customer base in Europe, and on the largest nuclear power reactor fleet the world over.

EFD Induction: set up as the result of successive mergers involving three German, Norwegian, and French firms, EFD's standing is recognized the world over, in the field of induction heating.

European Commission: one of the major institutions of the European Union (EU), its chief function being to put forward, and implement EU policies; it is further charged with enforcing the due application of treaties.

European Committee for Standardization (CEN): a Brussels- (Belgium) based organization, set up for the purposes of ensuring the harmonization of standards drawn up in Europe.

European Parliament: the sole parliamentary organ of the European Union (EU), elected by direct universal suffrage; together with the Council of the European Union (bringing together ministers from the governments of every member state), and the European Commission (appointed), the European Parliament forms the legislative power, in the EU's institutions.

European Synchrotron Radiation Facility (ESRF): 19 countries contribute to the funding, and operation of this X-ray source, one of the most intense in the world, set up in Grenoble (southeastern France). The extremely bright synchrotron radiation emitted by ESRF opens up unrivaled possibilities, with regard to the exploration of biomolecules, nanomaterials, catalysts in action, fossils, or valuable artifacts of historic heritage status. Some 6,000 scientists are hosted at the facility every year.

Ferro: Ferro France, based in Saint-Dizier (eastern France), has been operating, since 1960, as a subsidiary of US Ferro Corporation, headquartered in Cleveland (Ohio). The group, founded in 1919, employs a workforce of some 6,800, across 20 countries, with 75 production sites. A leading specialist, worldwide, in enamel metal glazes, Ferro has worked for more than 30 years for the nuclear sector, supplying it with glass frits.

Franche-Comté électronique, mécanique, thermique et optique, science et technologie (FEMTO-ST): a joint research unit associated with CNRS (UMR 6174), simultaneously coming under Franche-Comté University (UFC), the National Higher School of Mechanical Engineering and Microtechnology (ENSMM: École nationale supérieure de mécanique et de micro-

techniques), and Belfort-Montbéliard Technology University (UTBM), FEMTO-ST was set up, in 2004, through the merger of five laboratories in the Franche-Comté Region (eastern France), working in the areas of mechanics, optics and telecommunications, electronics, time frequency, energetics, and fluidics.

Fraunhofer-Gesellschaft zur Förderung der angewandten Forschung: named after German physicist Joseph von Fraunhofer, the Fraunhofer Society for the Advancement of Applied Research brings together 57 institutes, at 40 sites across Germany, each specializing in a particular area of applied scientific research; with a workforce of 13,000, the Society draws its funding from the German federal state (and regional states), and through research contracts drawn up with industry.

Freemove: a world leader as regards the design, and fabrication of semiconductor materials, and embedded processors for the automotive, and consumer electronics markets, and for the wireless networking and communications industry; this US corporation, based in Austin (Texas), operates its own design, research and development, fabrication, and commercial units around the world.

Grand Accélérateur national d'ions lourds (GANIL): France's National Large Heavy-Ion Accelerator facility, set up by two research organizations which came together to fund, on an equal footing, its construction, and operating costs – CEA/Physical Sciences Division, and CNRS/IN2P3 – GANIL stands as one of the four largest laboratories, worldwide, carrying out research using ion beams. This is a very large facility, serving French, and European research. The experimental domains catered for range from radiation therapy to atomic, and nuclear physics, and from condensed-matter physics to astrophysics. In the field of nuclear physics, GANIL has allowed many discoveries to be made.

Grimm Aerosol Technik: a German corporation, specializing in providing high-performance, cost-effective solutions in the area of dust, and aerosol analysis, and detection.

IBM Research Zürich: as the Switzerland-based European branch of IBM Research, specializing in leading-edge research for tomorrow's information technologies, this unit entertains close relationships with partners in industry, and academe.

Institut Carnot: a research network set up to assist firms in industry, for the purposes of anticipating the innovations of tomorrow, in the fields of information and communications micro-, and nano-technologies, materials, mechanical engineering and processes, Earth sciences and natural resources, energy and the environment, propulsion, chemistry, life sciences, biomedical technologies, civil engineering, and regional public works and infrastructure.

Institut d'électronique et de télécommunications de Rennes (IETR): the Rennes Electronics and Telecommunications Institute, bringing together 250 researcher/teachers, engineers, PhD students, and administrative workers, is endowed with an extensive range of technical equipment, enabling it to carry out full scale experiments; based in Rennes (western France), it pursues a strong research role, both nationally in France, and internationally, along with conducting many investigations under contract to industry, on issues standing at the core of the information and communications society.

Institut d'électronique, de microélectronique et de nanotechnologie (IEMN): the Electronics, Microelectronics and Nanotechnology Institute is a joint research unit (UMR 8520), set up, in 1992, by CNRS, Lille-I Science and Technology University (USTL), Valenciennes and Hainaut-Cambrésis University (UVHC), and the Higher Institute for Electronics and Digital Technology (ISEN: Institut supérieur de l'électronique et du numérique); its research activity covers the areas of physics, electronics, and micro- and nanotechnologies; its main laboratory is sited at Villeneuve-d'Ascq (northern France).

Institut de chimie de la matière condensée de Bordeaux (ICMCB): the Bordeaux Condensed-Matter Chemistry Institute was set up as a **CNRS** unit in 1995; associated with Bordeaux-I Science and Technology University (southwestern France), it specializes in solid-state chemistry, materials science, and molecular science.

Institut de la vision de Paris: the Paris-based Vision Institute is the first integrated research center, in France, working on diseases of the eye; set up in 2008, it hosts 12 public-sector research teams, specializing in visual information processing, developmental biology, genetics, and therapeutics. These teams work in close collaboration with partners in industry, e.g. Essilor, Fovea Pharmaceuticals, Iris Pharma, Visiotact, Ardoysset, Horus Pharma, IMI, Laboratoires Théa... for the purposes of developing technologies to assist visually impaired patients, novel imaging processes, innovative molecules...

Institut des nanotechnologies de Lyon (INL): the Lyon (southeastern France) Nanotechnology Institute carries out research, ranging from materials to systems, seen as promoting the emergence of original technology lines; areas of application cover the major economic sectors, e.g. the semiconductor, microelectronics, and photonics industries, telecommunications, power, health and biomedical, biology, industrial monitoring, defense, the environment...

Institut des neurosciences de Grenoble: the Grenoble Neurosciences Institute, set up in 2007, brings together 10 research teams (**INSERM**, CEA, Grenoble University Hospital, Joseph-Fourier University), with a view to fostering a multidisciplinary approach to the neurosciences, with regard to cancer, Parkinson's disease, epilepsies, neurovascular diseases, Alzheimer's disease, and schizophrenia.

Institut français du textile et de l'habillement (IFTH): the French Textile and Clothing Institute is a technology center serving the industry, by offering an ensemble of solutions for the development of new products, or novel processes, directed at such diverse markets as transportation, clothing, the biomedical sector, or construction.

Institut national de l'environnement industriel et des risques (INERIS): France's National Institute for Industrial Environments and Risks is a public-sector establishment of industrial and commercial character, having the remit to carry out studies, and investigations for the purposes of risk prevention, with regard to the risks, arising from economic activities, bearing on the safety of persons, and property.

Institut national de la santé et de la recherche médicale (INSERM): the National Institute for Health and Medical Research is the sole public research organization, in France, that is wholly dedicated to human health; its role is to ensure the strategic, scientific, and operational coordination of biomedical research.

Institut national de physique nucléaire et de physique des particules (IN2P3): the National Institute of Nuclear Physics and Particle Physics, set up within **CNRS**.

Institut Néel: named after French physicist Louis Néel (1904–2000), 1970 Nobel laureate in Physics, the Néel Institute provides unrivaled working conditions for young scientists wishing to be involved in research, and to fulfill their potential at a level equaling the best, worldwide, by bringing together physics, chemistry, and engineering in three departments operating in strong synergy; sited in the **CNRS** campus in Grenoble (southeastern France), this fundamental research laboratory has set up major partnerships with industry.

INTEL: US corporation, set up in 1968, headquartered in Santa Clara (California), specializing in electronics, and microelectronics; it employs a workforce of some 85,000.

International Organization for Standardization (ISO): an international standardization organization, bringing together representatives from national standardization organizations in 158 countries; ISO's purpose is to produce international standards – known as ISO standards – covering scientific, industrial, and commercial activities.

International Technology Roadmap for Semiconductors (ITRS): an organization set up to promote semiconductor development, and to publish reference documents, in the field of microelectronics, highlighting the chief barriers to development for new generations of components, to help pace an evolution cycle complying with Moore's law.

International Union of Pure and Applied Chemistry (IUPAC): an international nongovernmental organization, concerned with advances in the field of chemistry; its members are national chemistry societies. It is the recognized authority, with respect to the development of rules for nomenclature, and symbols and terminology to be used for chemical elements, and their compounds.

Japan Atomic Energy Agency (JAEA): this agency was established in 2005, through the merger of the erstwhile Japan Atomic Energy Research Institute (JAERI), and Japan Nuclear Cycle Development Institute (JNC). It stands as the leading nuclear development organization, in Japan.

Laboratoire de chimie des solides de l'Université de Nantes: the Nantes- (western France) based Solid-State Chemistry Laboratory carries out research activities concerned, at the same time, with the synthesis of novel materials, the investigation of their properties, and their optimization, and utilization of such materials for applications – further covering the development of new analytical techniques, in particular with regard to what presently comes under the extensive domain of nanotechnologies.

Laboratoire des composites thermostrostructuraux (LCTS): the Thermostrostructural Composites Laboratory is a joint research unit (UMR), coming under joint **CNRS**, Bordeaux-I University, **SNECMA Propulsion solide** (SPS: Safran Group), and CEA oversight. Set up in 1988, it is sited in the Pessac-Talence-Gradignan (Gironde *département*, southwestern France) university campus. It stands as a major player in the field of ceramic-matrix composite materials, for applications involving extreme conditions.

Laboratoire en sciences et technologies de l'information, de la communication et de la connaissance (Lab-STICC): the Brest- (western France) based Information, Communications and Knowledge Science and Technology Laboratory, chiefly active on issues spanning the range from sensors to knowledge; it brings together 350 researchers, and has become a reference center for research on communicating systems, with regard to their hardware, and software, architecture.

Laboratoire Science des procédés céramiques et de traitements de surface (SPCTS): the Science of Ceramic Processes and Surface Treatment Processes Laboratory is a joint research unit, bringing together staff from Limoges University (central France), the National Higher School of Industrial Ceramics (ENSCI: École nationale supérieure de céramique industrielle), and **CNRS** (UMR 6638). The research work conducted at SPCTS concerns, as whole, the investigation of the transformations undergone by matter, as ceramic processes, and surface treatment processes are implemented. The laboratory's work stands at the meeting point between the fields of materials (chiefly ceramics), and process engineering. SPCTS is one of the major participants in the European Center of Ceramics.

Lux Research: a research and advisory firm, providing advice, and up-to-date intelligence on emerging technologies. Its approach is predicated on collecting information at the source, and a wide-ranging global network.



Matériaux: Ingénierie et science (MATEIS): the MATEIS (Materials Engineering and Science) Laboratory, part of the Lyon- (southeastern France) based National Institute of Applied Sciences (INSA: Institut national des sciences appliquées), conducts research for the purposes of optimizing the utilization properties of existing structural materials, or creating new materials, with a view to reducing structural weight, and promoting sustainable development. It is actively collaborating with laboratories based in Lyon, and more widely in the Rhône-Alpes Region, under the aegis of the "Materials and Utilization Properties" research federation (CNRS FR 2145), and of the "Materials and Design for Sustainable Development" regional research cluster. It is an associate member of the Lyon Institute of Chemistry (CNRS FR 3023).

Max-Planck-Gesellschaft zur Förderung der Wissenschaften: named after German physicist Max Planck (1858–1947), 1918 Nobel laureate in Physics, the Max Planck Society for the Advancement of Science has a remit to carry out fundamental research; it brings together 80 specialized institutes, funded by the German federal state, and the regional states (*Länder*).

Mecachrome: a central player in the aerospace, automotive, and motor racing fields, the group has been active for 70 years, designing, and manufacturing high-value-added components, and structural units. Mecachrome, headquartered in Tours (central France), operates six production sites, in Europe and North America. It employs a workforce of some 2,000.

National Institute for Occupational Safety and Health (NIOSH): a US federal organization, charged with carrying out research, and formulating recommendations with respect to the prevention of occupational injuries, and diseases; for that purpose, NIOSH conducts investigations, produces recommendations, disseminates information, and responds to requests for assessment of working environments presenting hazards to health.

Northwestern University: sited in Evanston (Illinois) – a suburb of Chicago – this university is consistently ranked among the top ten US universities, alongside Harvard, or Princeton.

OCAS: based in Belgium, the OCAS metallurgical research center was newly set up in 2004 as a joint venture between Arcelor, subsequently ArcelorMittal, and the Flemish Region. ArcelorMittal, a worldwide steelmaking group, employing a workforce of close to 310,000, across more than 60 countries, was set up in 2006, as a result of the merger of Arcelor, and Mittal Steel.

OSEO: a public-sector establishment set up for the purposes of assisting innovation by putting up guarantees for financial backing from the banking sector, or from equity funds, or partnership funding.

Plansee Group: comprising four divisions, the Austria-based Plansee Group, founded in 1921, is present in 16 countries. It is one of the chief producers of high-performance materials fabricated by powder metallurgy.

PSA Peugeot-Citroën: French private-sector automotive manufacturer, the holding group for companies trading under the Peugeot and Citroën brands; present in 160 countries, it ranks as the second European manufacturer, the seventh worldwide; with more than 670,000 automobiles sold, in 2009, in Europe, emitting less than 120 g CO₂/km, the group stands as the leading maker of low-emission vehicles, and offers an ensemble of complementary products (constantly improved thermal engines, electric vehicles from 2010, and subsequently hybrid diesel-powered, and rechargeable hybrid vehicles).

Raigi: a French firm, specializing in the formulation of epoxy, and polyurethane systems, for batch quantities ranging from a few kilograms to several tonnes.

Safran: a French industrial group, its chief activities lying in the fields of aerospace propulsion (SNECMA), and electronics and telecommunications (SAGEM). SNECMA Propulsion solide (SPS) is a subsidiary of the group.

Sandvik: a Swedish corporation, specializing in high-technology tooling, and metal alloys, founded in 1862 by Göran Fredrik Göransson, in Sandviken (Sweden) – hence the corporate identity. Sandvik employs a workforce of some 44,000, in 130 countries.

SGN: a nuclear engineering company (Société générale pour les techniques nouvelles: General-purpose Company for New Technologies), a subsidiary of Areva NC, active in process engineering (bringing to the industrial scale processes developed by research organizations, first and foremost by CEA), engineering for industrial plant construction, service engineering, and dismantling engineering.

Soitec: founded in 1992, the firm has risen to a leading position, worldwide, as a supplier to the microelectronics industry, through the development, and industrialization of an innovative material, silicon on insulator (SOI), used to fabricate the chips that are revolutionizing our daily life; 15 years after it was set up, Soitec had become a central player in this market, owing to the unique position it had achieved, both as a supplier, and as partner for its customers; its capability, in terms of technological innovation, and materials engineering, its R&D policy, and industrial production capacity have made Soitec a world leader, for innovative products for the electronics industry.

Spintec (Spintronique et technologie des composants): the Spintronics and Components Technology Laboratory is a joint research unit, bringing together CNRS, and CEA; Spintec, dedicated as it is to spin electronics components, is developing innovative magnetic components, for mass storage, and random-access memories for computers, and telecommunications equipment, thus bringing a novel impetus to the microelectronics of the future.

STMicroelectronics: an international corporation of French-Italian origin, registered in the Netherlands (and headquartered in Switzerland), active in the development, fabrication, and commercialization of electronic chips (semiconductor materials); it stands as one of the leading players in the global semiconductor production sector.

ThyssenKrupp: a German steelmaking group, set up in 1997 as a result of the merger of Krupp, and Thyssen, and headquartered in Düsseldorf (Germany); it employs a workforce more than 180,000 strong, active in five branches: steel, automotive, elevators, technologies, and services.

University of California, Berkeley: with 33,000 students, and a faculty of 1,800, this US university was ranked third in the world's best universities by 2007.

University of Manchester: UK university, set up in 2004 through the bringing together of The Victoria University of Manchester, and the University of Manchester Institute of Science and Technology (UMIST).

University of Texas at Austin: bringing together nine colleges, and six medical schools, with an enrolment of more than 50,000 students, and more than 2,700 faculty members; a highly selective institution, UT Austin is reputed for its technology, and computer science programs.

XLIM: Limoges- (central France) based laboratory, bringing together 350 teacher/researchers, CNRS research scientists, and PhD students, working in the areas of information technology, mathematics, optics, electromagnetism, and electronics.

Yale University: named after its early benefactor, Elihu Yale, this university, sited in New Haven (Connecticut), ranks as one of the most prestigious in the USA; it is a great rival of Harvard University.

Glossary

A

ab-initio calculation: calculation carried out on the basis of theoretical data, without the use of simplifying **models** adjusted to fit experiments, and intended to be fully predictive.

abrasion: the wear undergone by a coating, or surface layer through the removal of matter by the repeated passage of an abrasive part over it.

absorption: the process whereby the intensity of **radiation** decreases as it passes through a material medium, to which it transfers all or part of its energy. See also **molar absorption**.

actinides: natural, and/or artificial **radioelements**, of **atomic number** ranging from 89 (actinium) to 103 (lawrencium); **major actinides:** heavy nuclei – uranium, plutonium – present in, or generated within nuclear **fuel**; **minor actinides:** heavy nuclei, generated in relatively small amounts in reactors, through successive **neutron captures** by fuel nuclei. The main such elements are neptunium, americium, and curium.

activation: the process whereby certain initially stable **nuclides**, particularly in reactor, and **fuel element** structural materials, are made **radioactive**, through **neutron** bombardment (**neutron activation**), or bombardment by other particles.

activity: the number of **decays** per unit time within a **radionuclide**, or a mixture of radionuclides, expressed in **becquerels (Bq)**. **High activity** may reach several billion becquerels per gram.

adsorption: a surface phenomenon, whereby **molecules** from a gas, or liquid become attached to the solid surfaces of **adsorbents**, by way of a variety of processes, of diverse intensities; this phenomenon is of major importance, with regard to the evolution of many chemical reactions; **desorption** is the reverse phenomenon.

aerosol: an ensemble of solid, or liquid particles of a given chemical species, held in suspension in a gaseous medium.

alkali metals: the metals belonging to group IA (IUPAC group 1) in the periodic table of **elements**: lithium, sodium, potassium, rubidium, cesium, francium.

alkaline earth metals: the metals belonging to group IIA (IUPAC group 2) in the periodic table of **elements**: beryllium, magnesium, calcium, strontium, barium, radium.

allotropic: a solid substance occurs in allotropic forms if it exhibits two or more **thermodynamically** stable **crystal** structures, depending on certain temperature, and pressure conditions. An allotropic transformation is a process whereby a solid substance transforms from one stable crystal structure into another.

alloy: a metallurgical product, yielded by the incorporation, into a base metal, of one or more **elements**, metallic or otherwise.

aluminosilicate: a **silicate** containing **aluminum (Al)**.

aluminum: a chemical **element**, of symbol Al, and **atomic number** 13, occurring with a high terrestrial abundance (accounting for 1.5% of the Earth's total mass); it is a silvery metal, highly malleable, and remarkable for its resistance to **oxidation**, and its low density.

aluminum nitride (AlN): a **refractory**, wide-bandgap (6.2 eV) **semiconductor** material; it is an electrical insulator, exhibiting high **thermal conductivity**, and affording high **oxidation**, and abrasion resistance.

amaranth: a purple azo anion-active dye, used in cosmetics, and as a food coloring agent, in which respect (as a food additive) it is known under E-number E123.

amine: an organic compound derived from **ammonia**, by replacing some **hydrogen atoms** by **hydrocarbon** groups (alkyls); if one of the **carbon** atoms bonded to the **nitrogen** atom belongs to a carbonyl group, then the resulting **molecule** belongs to the amide family.

ammonia: a gaseous compound of **nitrogen** and **oxygen**, with a sharp, irritating odor.

amorphization: the process whereby a substance is brought to a state characterized by an absence of order in the arrangement of particles of matter (**amorphous** state), as opposed to the **crystalline** state.

ampere (A): a unit of electric current intensity, taking its name from French physicist André-Marie Ampère (1775–1836), a major figure in the history of **electromagnetism**.

analogs (natural, archeological): materials of natural, or engineered provenance (glasses, metals, cements), investigation of which may yield information as to the long-term behavior (over timescales of hundreds, or even thousands of years) of similar, more recent materials.

angstrom (Å): 1 Å = 10⁻¹⁰ meter.

anisotropic: exhibiting properties that vary according to the direction (antonym: **isotropic**).

annealing: a heat treatment operation – effected either by heating, or through **irradiation** – applied to a material, inducing **grain precipitation**, restoration, and/or growth phenomena.

antibody: a complex **protein**, used by the immune system to detect, and neutralize antigens, in a manner specific to each antigen. See also **monoclonal antibodies**.

aromatic: any compound containing one, or more **benzene** nuclei. Aromatic compounds occur in tars, and provide reactants that are essential for chemical **synthesis**. These compounds owe their name to their odor, or aroma, since the more volatile such substances exhibit a characteristic odor.

arthropods: representatives of the phylum Arthropoda, i.e. invertebrate animals with segmented, articulated bodies, covered with a rigid integument, forming an outer skeleton (**exoskeleton**), consisting, in many instances, of chitin.

aryl: in an organic compound, an aryl group is a functional (or substitution) group derived from an **aromatic** nucleus (ring).

assembly (fuel): a structure comprising a set of **fuel elements**, loaded into a nuclear reactor as a single unit.

atom: the basic constituent of ordinary matter, comprising a **nucleus** (made up of **neutrons**, and **protons**) around which **electrons** orbit.

atom-probe tomography: a technique that makes it possible e.g. to determine the spatial distribution of the various constituent **atoms** in an **alloy**, by stripping, one at a time, **ions** from a tip made from this alloy, accelerating these ions in an electric field, and measuring their time of flight to a detector.

atomic-force microscopy (AFM): a **microscopy** method based on the measurement, along all three spatial directions, of a force, or of a force gradient, arising between a probe (the extremity of which consists of a few **atoms**), and a solid surface. The probe, taking the form of a finely tapered tip, is fitted onto a thin strip (the cantilever), acting as a spring, the deflection of which is measured by the deflection of a laser beam, a computer system then allowing the data to be visualized.

atomic-layer deposition (ALD): a process used for the deposition of **atomic thin films**, involving the exposure of a surface, successively, to various chemical precursors, to obtain ultrathin films. It is used in the **semiconductor** industry.

atomic mass unit (amu): 1 amu is – by definition – equal to 1/12 of the mass of an unbound **atom** of **carbon-12**, i.e. about 1.6606·10⁻²⁷ kg (also noted u, for “unified amu”).

atomic number: the number of **protons** in the **atomic nucleus** of a given **element**.



austenite: in steels, a phase exhibiting a **face-centered cubic structure** (**austenitic structure**).

austenitic steels: iron-base grades, exhibiting a **face-centered cubic crystal structure**, and containing, as a rule, 15–25% **chromium**, 7–20% **nickel**, small quantities of **carbon**, and – depending on cases – some **molybdenum**, **titanium**, or **niobium**.

B

band theory: in a solid body, **electrons** may occupy ranges of energy levels, making up the so-called **allowed bands**. A given allowed band may be empty, full (i.e. all the states within it are occupied by pairs of electrons of opposite **spin**), or partly occupied. The gap arising between two consecutive allowed bands is known as a **forbidden band**, or **band gap** – a term serving to refer to a gap arising between any two consecutive allowed bands. In a solid, the following bands are identified: the **core band**, or **normal band**, i.e. the band formed by electrons occupying the lowest energy levels, or **core levels** (**core electrons** remain close to the **atom's nucleus**, and are virtually unaffected by neighboring atoms); the **valence band**, i.e. the band occupied by **valence electrons** (involved in the setting up of bonds between atoms); and the **excitation band**, i.e. the set of levels that may be accessed by electrons, as a result of excitation of the core band. A **conduction band** is a band that remains empty, or is partly occupied by almost free electrons (**conduction electrons**), which are able to pass from one atom to the next. By considering the electronic structure of lowest possible energy, known as the **atom's ground state** – corresponding to the energy exhibited by atoms in the material at absolute zero (0 **kelvin**) – the **Fermi energy** (or **Fermi level**) is defined as the minimum value for energy levels accessible to an electron added to the system. This level lies between the valence, and conduction bands. In a **metal**, the valence, and conduction bands overlap. Electrons can directly cross over from the valence to the conduction band, and are thus able to circulate around the solid. The material is a **conductor**. In an **insulator**, the gap arising between the valence, and conduction bands (the latter remaining empty) is large. Electrons are unable to pass from the valence to the conduction band. In a **semiconductor**, the gap between the valence, and conduction bands is smaller. If energy is supplied to the electrons (by heating the material, or illuminating it...), this gives them the ability to jump from the valence band to the conduction band, and thus to circulate in the material.

basalt fiber: a material made of extremely fine basalt fibers, i.e. fibers consisting of such minerals as plagioclase, pyroxene, and **olivine**; such fibers are similar to **carbon fibers**, and **glass fibers**, albeit exhibiting physicochemical properties that are better than those of glass fiber, while proving less expensive than carbon fiber.

becquerel (Bq): a unit – named after French physicist Henri Becquerel – of nuclear **activity** (1 Bq = 1 **atomic nucleus** decay per second). The becquerel is an altogether minute unit! Nuclear activity was formerly measured in curies: 1 **Ci** = $3.7 \cdot 10^{10}$ Bq.

benzene (C₆H₆): a monocyclic **aromatic hydrocarbon**; a colorless organic compound, benzene is a carcinogenic liquid; it is a **solvent** widely used by the chemical industry, and a major precursor for the purposes of effecting the chemical **synthesis** of drugs, **plastic** materials, synthetic rubber, or dyes. Benzene occurs as a natural constituent in petroleum.

biocompatible: the quality of a substance, or device that is compatible with biological tissues.

biokinetics: the study of the evolution of substances inside an organism (absorption, distribution across organs, and tissues, **metabolism**, excretions).

biomimetism: an approach endeavoring to mimic, by means of engineered materials, or devices, the essential properties of one, or more biological systems.

biosignal: a generic term, used to refer to any kind of electric signal of physiological provenance that may be measured in living organisms.

biotechnology: the controlled, large-scale utilization of biological, possibly genetically engineered materials.

body-centered cubic structure: a **crystal** structure in which the constituent **atoms** are located at the eight corners of a cube, and at the center of the cube.

boiling-water reactor (BWR): a type of nuclear reactor in which water boils directly inside the **core**.

boron: chemical **element**, of symbol B, and **atomic number** 5.

bottom-up: the “bottom-up” approach, in **nanotechnologies**, involves the controlled assembly of **atoms**, and **molecules**, for the purposes of forming components of larger size.

brass: an **alloy** of copper, and **zinc**, in varying proportions.

brazing: an operation involving the joining of two parts by the interposition of a filler material applied in the liquid state (the **solder**).

bronze: 1. an alloy of copper, and **tin**; 2. a type of structural arrangement.

Brownian motion: taking its name from British botanist Robert Brown (1773–1858), this involves a mathematical description of the random motion of a “large” particle, immersed in a fluid, and subjected to no interaction, other than the impacts from the “small” **molecules** of the fluid around it; this results in a highly irregular motion of the large particle.

burnable neutron poison: a substance exhibiting a high **neutron capture** capability (i.e. acting as a **neutron** absorber), deliberately introduced into a nuclear reactor for the purposes of contributing to the control of long-term variations in **reactivity**, as the poison gradually vanishes (its disappearance counteracting the loss of reactivity due to **fuel** depletion). **Gadolinium** is found to be a particularly neutron-absorbent **element**.

burnup: the ratio, usually expressed as a percentage, of the number of **atomic nuclei** of a given **element**, or ensemble of elements disappearing through **fission**, over the number of such nuclei initially present in the **fuel**. This is then expressed in at.%. This quantity is commonly used to evaluate *specific burnup*, i.e. the quantity of **thermal energy**, per unit mass fuel, obtained in reactor, from fuel loading to discharge; it is then expressed in **megawatt**-day per tonne (MW·d/t), or **gigawatt**-day per tonne (GW·d/t).

C

cadmium: chemical **element**, of symbol Cd, and **atomic number** 48, taking its name from the Greek word for calamine, i.e. smithsonite (zinc carbonate); **cadmium telluride**: a compound of cadmium, and tellurium: a **crystalline** material, exhibiting a **body-centered cubic structure** (a II–VI **semiconductor**).

Callovo–Oxfordian: a geological stage in the Jurassic, dating back 155 million years. It arises in the form of clay formations in eastern France, in particular in the area straddling the Meuse, and Haute-Marne **départements**, where an underground laboratory has been set up, to investigate the **disposal** of **radioactive waste** in **deep geological formations**.

carbide: a chemical compound of **carbon**, and another **element**, in most cases a metal.

carbon: a chemical **element**, a member of the so-called crystallogenic group (group IVA, IUPAC group 14), of symbol C, and **atomic number** 6, with an atomic weight of 12.0107.

carbon dioxide (or carbon gas): a **chemical compound**, consisting of one **carbon atom**, and two oxygen atoms, of molecular formula CO₂.

carbon felt: a nonwoven agglomerate, formed from **carbon fibers**.

carbon fiber: a material consisting of extremely fine filaments, 5–15 **microns** in diameter; chiefly consisting of **carbon atoms**, agglomerated into microscopic **crystals**, aligned more or less parallel to the fiber's longitudinal axis; this alignment of the crystals makes the fiber incredibly strong, for its dimensions; several thousand carbon fibers are bundled together to form a yarn (typically, from 6,000 to 24,000 unit carbon fibers), which may be used as such, or woven; carbon fibers are characterized by their low **density**, high tensile, and compressive strength, high flexibility, good electrical, and **thermal conductivity**, and their high-temperature resistance, and chemical inertness (except with respect to **oxidation**).

carbon nanotube: a **crystalline** structure, consisting of one or more rolled up **graphene** sheets, involving a **nanometer**-scale diameter, of a length however that may be as long as several, or even several hundred **micrometers**. Depending on the angle at which the tube is rolled, relative to the graphene lattice, the nanotube may be either metallic, or **semiconducting**.

carboxyl: in organic chemistry, a carboxyl group is a functional group consisting of one **carbon atom**, bonded by way of a double bond to a first oxygen atom, and by a single bond to a second oxygen atom, itself bonded to a **hydrogen** atom (**hydroxyl** group).

cascade (atomic displacement): a sequence of **atom** ejections, away from their equilibrium sites in the **crystal** structure of a material, subsequent to a collision with an incoming particle. If the energy yielded by the latter is close to the **threshold displacement energy**, a single atom will be expelled, leaving a **defect** known as a **Frenkel pair**. If the energy imparted to the first atom impacted is much higher than this threshold, a displacement cascade occurs, the ejected atoms being endowed with sufficient energy to dislodge further atoms.

Castaing microprobe: an electron-probe microanalysis (EPMA) technique used for chemical analysis purposes, devised by Raimond Castaing in 1951, which involves bombarding a region about 1 **micron** in diameter, in a sample, with a focused **electron** beam, and analyzing the spectrum of the **X-ray** emission generated in response to that excitation.

catalysis: a process involving a substance (the **catalyst**) having the ability to accelerate a chemical reaction without itself being altered, or only temporarily so.

cathode sputtering: the formation of **thin films** by way of the ejection of **atoms** from a target material, as it is bombarded by noble-gas **ions**, accelerated under high **voltage**. See also **magnetron cathode sputtering**.

cathodic arc evaporation: a **thin-film** deposition technique, involving the vaporization, or sublimation, by means of an electric arc, of a negatively **polarized** target material, the vapor subsequently undergoing condensation on the part subject to coating. This makes it possible to obtain high-**density**, high-adhesion films.

centrifugation: a technique making use of centrifugal force to effect the separation of fluids of different **densities**, or to isolate solid particles held in suspension in a fluid.

cephalopods: representatives of the class Cephalopoda, in the phylum Mollusca, in which the foot, now subdivided into arms, or tentacles, is positioned above the head; well known types of cephalopods include octopuses, squids, and cuttlefish.

ceramic: any inorganic, nonmetallic material exhibiting a **crystalline** structure featuring a regular, periodic arrangement of the constituent **atoms**, and involving **ionic**, and/or **covalent bonds**.

cermet: a **ceramic**-metal composite; for HTE purposes, the metal involved is **nickel**, the ceramic being yttria-stabilized-**zirconia** (i.e. **zirconium** oxide [ZrO₂] stabilized with **yttrium** oxide [Y₂O₃]), or scandia- (**scandium** oxide: Sc₂O₃) stabilized zirconia, or **gadolinia-doped ceria**.

chain reaction: a sequence of nuclear **fissions**, in the course of which the **neutrons** released cause further fissions, which in turn yield further neutrons causing further fissions, and so on.

charge carrier: an **electron**, or a hole (i.e. a position where an electron is missing), the motion of which sets up an electric current.

chemical vapor deposition (CVD): a method used to obtain layers (featuring thicknesses ranging from a few tens of **nanometers** to 100 **micrometers** or so) by vapor deposition, the deposit forming, by way of a chemical reaction, from a gaseous medium of different composition.

chemical vapor infiltration (CVI): a densification process, involving the infiltration of a precursor vapor into a fiber preform, to fabricate the **matrix** of thermostructural **composites**.

chirality: in chemistry, a compound is said to be chiral if it may not be superposed with a mirror-image of itself; more specifically, the handedness of such a **molecule**; for **carbon nanotubes**, a parameter defining the angle made by the **graphene** lattice relative to the tube axis (i.e. helicity).

chlorine: chemical **element**, a member of the halogen group (group VIIA, IUPAC group 17), of symbol Cl, and **atomic number** 17.

chromatography: a technique used in analytical chemistry, whereby the sample, containing one or more species, is entrained by a current set up by a mobile phase (liquid, gas, supercritical fluid), across a stationary phase (paper, gelatin, silica, **polymer**, grafted silica...): each species moving with its own specific velocity, depending on its own characteristics, and those exhibited by the two phases; **liquid chromatography** involves the separation of compounds entrained by a liquid across a solid phase, held inside a tube (chromatography column), or fixed on an inert surface.

chromium and chromium oxide: chromium is the **element** (symbol Cr, **atomic number** 24) which, when added to steel to obtain **stainless steels**, provides these with their resistance to **oxidation**, due to the formation of a layer of chromium **oxide** (chromia: Cr₂O₃).

chromophor: a chemical group causing the **molecule** carrying it to be colored; a molecule so colored.

clad, cladding: a leaktight envelope, encasing the **fuel** material, having the purpose of **containing radioactive** materials, of ensuring fuel mechanical strength, inside a reactor core, and serving to carry heat from the fuel to the **coolant**.

cleavage: the property, exhibited by certain minerals, of splitting along certain well defined planes. In metallurgy, **ferritic**, and/or **martensitic steels** are found to exhibit a low-temperature (< 20 °C) **ductile-to-brittle** transition, with respect to their rupture mode, rupture then occurring through cleavage, preferentially along the (100) base planes of the **body-centered cubic structure**. **Cleavage planes** follow the direction of the plane of least cohesion, i.e. across the weakest bonds arising between each unit in the **crystal** structure.

CMOS (complementary metal-oxide-semiconductor): a technology used for the fabrication of **electronic components**; more generally, the term is used to refer to any component fabricated according to this technology.

CMOS (complementary metal-oxide-semiconductor) varactor: a variable capacitor, making use of active circuits.

coal gas: a gas generated during the transformation of coal into **coke**.

coalescence: the phenomenon whereby two identical, albeit separate objects, or substances (e.g. two droplets) tend to merge.

coating: a surface treatment, involving the application of a covering layer, in liquid form as a rule (varnish, paint, oil...), onto a substrate (paper, textile, **plastic** film, steel...).



cobalt: chemical **element**, of symbol Co, and **atomic number** 27, with a mass number of 59; cobalt fluorophosphate: a compound of cobalt, **fluorine**, phosphorus, and oxygen; cobalt **oxide**: a compound of cobalt, and oxygen.

coke: a derivative of coal, obtained through the distillation of coal, in the absence of air, in a coking oven.

complexation: the process whereby, from extractant (**complexant**) systems, and a species that is to be extracted, a structure (a **complex**) is formed, comprising one central metal **ion**, to which other **atoms**, ions or **molecules** are bonded.

composite: a material formed by the assembly of several materials, and exhibiting properties that these initial materials do not individually possess. It may consist, e.g. of a fibrous structure (the **reinforcement**) serving to withstand mechanical **stresses**, and an encapsulating material (the **matrix**).

computation code (or software): the assembly, in a computer software, in the form of coded mathematical expressions, of the simplified representation, in **numerical** form (**model**), of a system, or a process, for the purposes of **simulation**.

condensation: the process whereby a body, initially occupying a certain volume, is reduced to a smaller volume.

conditioning (of radioactive waste): the ensemble of successive operations that must be carried out in order to turn **waste** into a stable, safe form, allowing its subsequent management, whether it be by way of **storage**, **transmutation**, or **disposal**. These operations may include, in particular, compaction, encapsulation, melting, **vitrification**, and containerization.

conductivity: a quantity characterizing the capacity for (**heat**, or **electrical**) **conduction** exhibited by a material. See also **thermal conductivity**.

containment: the physical, and/or chemical capability to keep **radioactive**, and/or toxic **elements** and compounds to a given location, or within a given object (by restricting dispersion, or release).

containment barrier: a setup having the ability to prevent, or restrict the dispersion of **radioactive** materials.

contamination (radioactive): the undesired presence of a **radioactive** substance, coming into contact with a surface, or penetrating into the interior of a medium.

convection: an energy transfer mode involving a movement of matter across a medium.

coolant: a fluid (gas, or liquid) used to remove the heat generated by **fission** processes inside a nuclear reactor.

coordination number: the number of bonds an **ion** is able to set up with **electron-donor atoms**.

core: in a nuclear reactor, the region containing the nuclear **fuel**, with a layout designed to ensure it is host to a sustained **fission chain reaction**.

corrosion: the slow process whereby the surfaces of materials are attacked by the activity of chemical agents; in metals, corrosion takes the form of **oxidation**.

covalent bond: a bond set up between two **atoms** that thereby fill their outermost orbital, by sharing one or more **electron** pairs.

creep: the gradual deformation undergone by a solid body, due to a **stress** field applied to it over extended timescales. Creep may be activated by heat (**thermal creep**), and/or **irradiation** (**irradiation creep**).

cross-linking: the formation of one or more cross-linked three-dimensional networks – i.e. linked by bonds from which at least four chains emanate – by a chemical, or physical route.

crosstalk: the interference of one signal with another, due to phenomena of **electromagnetic** induction, or capacitive coupling.

cryogenics: the branch of physics concerned with the production of, and the effects arising from, very low temperatures.

crystal: an assembly of **atoms**, **ions**, or **molecules** arrayed in regular, **periodic** fashion across all three space directions; **cell (crystal):** the elementary repeat unit of a crystal; **crystallization:** the process whereby a substance is brought to the crystalline state; **crystallinity:** the quality, or degree of crystalline order.

crystallite: a material domain (**grain**) exhibiting the same structure as a **single crystal**, with sizes ranging from a few tens of, to several hundred **nanometers**, the dividing surface between two crystallites being a **grain boundary**.

crystallography: the science concerned with the study of **crystalline** substances at the **atomic** scale.

cyanides: a class of compounds featuring the cyanide (CN) group, e.g. potassium cyanide (KCN).

cycling: going through an alternating sequence, e.g. of charges, and discharges.

cytoskeleton: a complex network of **protein** filaments, present inside biological cells, endowing them with their mechanical properties. It ensures a degree of rigidity in the cell, and enables organelle transport, and cell contraction, and deformation, along with cell mobility.

D

damage dose: a measure of the degradation undergone by a material, expressed in **dpa**.

defect: see **point defect**, **dislocation**.

delamination: the separation of a stratified material into individual plies; the term may refer, more specifically, to separation at the interface between two distinct layers (e.g. an **electrolyte**, and **electrode**).

density: the mass of a given substance per unit volume; **relative density** (or **specific gravity**): the ratio of the density of a material to that of a standard, reference material, as a rule water at 4 °C.

deoxyribonucleic acid (DNA): a **molecule** serving as the carrier of hereditary genetic information; its unique structure, consisting of two complementary, helically intertwined strands (the double helix), allows DNA to replicate itself, yielding two **molecules** that are identical with one another, and with the parent molecule; it is one of the constituents of chromosomes; genes are DNA segments.

deprotonation: a chemical reaction whereby a **proton** (H⁺) is removed from a **molecule**, the residue forming the proton's conjugate base; the tendency of a molecule to give up a proton is measured by its pK (serving as a measure of acidity).

diazonium (salts): positively charged **ions**, comprising an organic radical (typically an **aromatic** ring) carrying a "diazo" group (N₂); these compounds are very widely used for the purposes of dye **synthesis**, and – more recently – as precursors for **aryl** groups, for surface **functionalization** purposes.

dielectric: a material bearing no electric charges able to move across it, and that is thus unable to conduct electric current; synonym of "insulator."

dielectric constant: a quantity, noted κ , expressing the response of a **dielectric** to an electric field; also known as relative **permittivity** (by reference to the permittivity of vacuum).

diffraction: the deflection affecting the direction along which (acoustic, light...) waves travel, as they come across an obstacle, or an aperture involving a size of the order of their wavelength;

electron diffraction: the deflection of an **electron** beam by matter, as a rule by a **crystal**. See also **X-ray diffraction**.

diffusion: the transport of matter, and/or charges, induced by a difference in concentration; **diffusion (defect):** the migration of **point defects** within a material, due to a concentration gradient. This conforms to a $t^{1/2}$ law.

dilatometry: the measurement of the expansion undergone by bodies.

diode: an **electronic component** that lets electric current through in one direction only.

dislocation: a defect concerning the arrangement of **atoms** in a **crystalline** solid. The usual distinction is between dislocations associated to a half-plane of atoms inserted into the crystal (**edge dislocations**), and dislocations associated to a half-plane cut through the crystal, with atoms being displaced in the crystal parallel to the edge of that half-plane (**screw dislocations**).

dislocation loop: a **dislocation** along a line forming a circular, or closed polygonal figure.

dispersion: a blend of small particles (organic, or inorganic) distributed across a homogeneous medium.

disposal (of radioactive waste): the operation involving placing **radioactive waste** in a facility specifically engineered to hold it on a possibly final basis. This term is also used to refer to the facility (also known as a repository) inside which waste is kept, when no retrieval is planned, at a later date. Retrieval would nonetheless still be feasible, in the case of a reversible disposal facility (see also **storage**). The **disposal** of radioactive waste in **deep geological formations** involves consigning that waste to disposal in an underground repository specially designed for that purpose.

doping: the introduction, into a **crystal** lattice, or an **amorphous** substance, of a small quantity of extraneous **atoms** (the **dopant**), for the purposes of modifying its properties.

dose: a term used to estimate, in a material, the integrated **flux** of particles (i.e. the **fluence**), over its **irradiation** time.

dpa: the number of displacements per **atom**, induced in a material under **irradiation**. This unit of damage indicates that, for 1 dpa, every atom in the material has undergone 1 displacement, on average, over the duration of irradiation.

ductility: the ability of a material to undergo plastic deformation, while resisting any propagation of induced **defects**.

E

effluents: waste in liquid, or gaseous form.

electroacoustics: the technique of sound production, recording, and reproduction by electrical means.

electrochemical cell: a unit comprising an **electrolyte**, an **ion conductor** (not itself conducting **electrons**), and two **electrodes**: the anode, and cathode.

electrochemistry: the scientific discipline concerned with the study, and description of chemical phenomena that are coupled with interchanges of electrical energy.

electrode: the locus where **electrochemical** reactions take place; the conducting pieces, known as the anode (positive electrode), and cathode (negative electrode), allow the circulation of **electrons**.

electrodeposition: a deposition method involving the **electrochemical** generation of reactive species, which deposit onto an **electrode**. When it is used to deposit a metallic film, this method is known as electroplating.

electrografting: the “organic” counterpart of electroplating; the **electrochemically** generated species are organic reactants, serving as precursors for an organic film that is **covalently** grafted onto the **electrode**.

electroluminescence: an optical, and electrical phenomenon, whereby a material emits light in response to an electric current passing through it, or to a strong electric field; used e.g. in **light-emitting diodes (LEDs)**.

electrolysis: a method serving to carry out chemical reactions, used to split compounds, by way of electrical activation, and conversion processes, transforming electrical energy into chemical energy.

electrolyte: a substance that acts as a conductor, owing to the mobility of the **ions** it contains.

electromagnetic (radiation, or wave): a radiation (or wave) that propagates, in a vacuum, at the speed of light, through the interaction of oscillating electric, and **magnetic fields**, and transports energy (**photons**).

electromagnetic field: a field involving two vector **fields** (the electric, and **magnetic fields**), which exerts an electromagnetic force (known as the **Lorentz force**) on moving particles exhibiting a nonzero electric charge.

electromechanical coupling coefficient: a figure of merit for **piezoelectric components**, e.g. acoustic resonators, as a measure of their ability to convert energy of one kind into another (mechanical to electrical energy, or vice-versa).

electron: a negatively-charged elementary particle. One of the constituents of the **atom**, orbiting around the **nucleus**.

electron cyclotron resonance (ECR) source: this type of source is fitted to many **heavy-ion accelerators**, for the purposes, in particular, of delivering **multicharged ions** (i.e. **atoms** from which several **electrons** have been stripped). A **plasma** is set up inside a magnetized vacuum chamber, by injecting an **electromagnetic wave** with a frequency matching the electrons' **Larmor precession frequency**. This wave yields high-energy electrons, having the ability to **ionize** atoms down to their core shells.

electron diffraction and microdiffraction (microscopy): with the **transmission electron microscope**, it is possible to observe, at the same time, the image of the illuminated region, and the associated **diffraction** patterns. By looking at the focal plane of the **electron** beam, rather than the image plane, a **diffraction image** is obtained. This makes it possible to visualize the directions along which electrons travel, and thus characterize the **crystals** involved. The image may be formed solely by nondiffracted electrons (**bright-field mode**), or by electrons diffracted at a particular angle (**dark-field mode**). In the electron **microdiffraction** technique, the electron beam is focused onto a very small region (10–1 **nm**). This method is well suited to the study of small **precipitates**.

electron, or ion conduction: the phenomenon whereby an **electron**, or an **ion** moves across a material.

electronegativity: this quantity is a measure of the capacity, exhibited by a given **atom**, to attract **electrons** to itself. **Fluorine** is the most highly electronegative **element**.

electronic component: a unit designed to be assembled with other such units, to provide one or more electronic functions.

electronvolt (eV): unit of energy, corresponding to the energy gained by an **electron** accelerated by a potential of 1 **volt**, i.e. $1 \text{ eV} = 1.602 \cdot 10^{-19} \text{ joule}$. Main multiples: the **kiloelectronvolt (keV)**: 10^3 eV , the **megaelectronvolt (MeV)**: 10^6 eV , and the **gigaelectronvolt (GeV)**: 10^9 eV .

electroreduction: the transfer of **electrons** from a cathode (acting as the negative pole) to a chemical compound held in solution, close to the cathode.



electrostatics: the branch of science concerned with the study of electric charges at rest, and their interactions.

element (chemical): the ensemble of all **atoms** having the same **atomic number** (i.e. all atoms having **nuclei** containing precisely the same number of **protons**, irrespective of the number of **neutrons**). A distinction is made between **light elements** (**hydrogen**, **helium**, **lithium**, **beryllium**, **boron**), and **heavy elements** (the others, from **carbon** to **uranium**, as far as natural elements are concerned – though more specifically those elements of atomic number equal to or greater than 80).

elution: a term used, in **chromatography**, to refer to the migration of a substance across a porous solid medium, under the flushing effect of a **solvent**.

empiricism: a method that gives pride of place to experience, and experiment, rather than first principles.

enantiomers: two isomers (i.e. **molecules** that have the same molecular formula, but different structures) that may not be superposed, but stand as the mirror image of one another, being of opposite **chirality**.

endoskeleton: an internal skeleton, i.e. contained within an animal's body; in vertebrates, the endoskeleton consists of calcareous bones.

enrichment: the process whereby, for an **element**, content is increased with respect to one of its **isotopes**.

epoxy and epoxide: the **epoxy** chemical group gives its name to the epoxy, or **epoxide molecules**, or **monomers**, and, by extension, to **polymers** known as **polyepoxides** (epoxy resin), commonly used in glues, and paints; once "dry", epoxy resin practically ceases to react with **oxygen**, and takes on a rigid form, a property made use of to strengthen components, by coating them with epoxy.

Evolutionary Power Reactor (or European Pressurized-Water Reactor) (EPR): a third-generation **pressurized-water reactor (PWR)** concept, developed by Areva NP, featuring improvements in terms of safety, **fuel** utilization, and operating economics.

exciton: a pseudoparticle, consisting of a paired **electron**, and hole (i.e. a position where an electron is missing, which behaves as a positively-charged particle).

exoskeleton: an external anatomical feature, serving to support, and protect an animal; many invertebrates, e.g. insects, crustaceans, and molluscs, feature an exoskeleton; the abdominal portion of the exoskeleton is commonly known as a "carapace."

extended defect: a cluster of point **defects**.

extracellular matrix (ECM): a network of **molecules**, lying in the extracellular medium, and interacting with one another; it chiefly consists of fibrillar **proteins** (collagen, elastin), cellular adhesion proteins (fibronectin, laminin), and proteoglycans (hyaluronic acid).

extrusion: a method used to form metals, once they have been rendered **ductile**, through hot forging, by drawing them through a die.

F

face-centered cubic structure: a **crystal** structure in which the constituent **atoms** are located at the eight corners of a cube, and at the centers of all of the faces of that cube.

fast neutrons: **neutrons** released at the time of **fission**, traveling at very high velocity (20,000 km/s). They have an energy of around 2 MeV.

fast reactor (FR): a type of nuclear reactor using no **moderator**, in which most **fissions** are caused by **fast neutrons**, i.e. **neutrons**

involving energies of the same order as that imparted to them when they are yielded by fission.

ferrite: this term is commonly used to refer to α -iron itself, this being the stable phase, for pure iron, at temperatures below 914 °C. This phase exhibits a **body-centered cubic structure** (**ferritic structure**).

ferritic steels: such steels, exhibiting a **body-centered cubic crystal structure**, feature, as a rule, low **carbon** contents (~0.05–0.20%), and varying concentrations of **chromium**. Involving, in most cases, no **nickel** content, these are iron–chromium, or iron–chromium–**molybdenum** (or tungsten) **alloys**, featuring chromium contents in the 12–25% range.

ferroelectric (material): a material exhibiting a permanent electric dipole moment (permanent polarization: i.e. the center of gravity of positive charges, in the material, is offset relative to the center of gravity of negative charges), even in the absence of any external electric field.

ferromagnetism: the property, exhibited by certain substances, of giving rise to strong magnetization under the effect of an external **magnetic field**, and, in some materials (magnets, hard magnetic materials), of retaining a strong magnetization, even when the external field is removed.

fertile: a term used to refer to a **nuclide** the **nucleus** of which may be transformed, directly or indirectly, into a **fissile** nucleus, through **neutron capture**.

field-effect transistor: a **semiconductor** device, coming under the general class of **transistors**, which makes use of an electric field to control the shape, and thus the **conductivity**, of a "channel," in a semiconductor material.

fireproofing: a treatment having the purpose of making a naturally flammable material nonflammable.

fissile: a term used to refer to a **nuclide**, the **nucleus** of which is liable to undergo **fission** through **neutron** absorption. Strictly speaking, it is not the so-called fissile nucleus that undergoes fission, rather it is the compound nucleus formed subsequent to a **neutron capture**.

fission: the splitting of a **heavy nucleus** into two fragments, with concomitant emission of **neutrons**, radiation, and a considerable release of heat.

fission products: **nuclides** yielded either directly, by nuclear **fission**, or indirectly by the **decay** of fission fragments. They may be gaseous (**fission gases**), or solid (volatile or otherwise).

flagellum: the mobile filament featured by certain cells (bacteria, algae, fungi, spermatozoa), for which it acts as a locomotor organelle.

flank wear: this type of wear is due to the mechanical, and thermal **stresses** generated by the relative motions affecting the part, the tool, and the chip. Flank wear is observed on the main flank face, taking the form of a striated, shiny wear band – average band width being noted VB – parallel to the cutting edge. This is due to friction from the machined part.

fluence: the total number of incoming particles (e.g. **ions**, **neutrons**) per unit surface, over the duration of **irradiation**. A measure of **dose**, used to quantify the irradiation of materials.

fluidized bed: a technique using the rising current of a fluid column to counterbalance the apparent weight of a bed of particles of a powdered product, which then flows like a fluid.

fluorescein (C₂₀H₁₂O₅): a complex chemical substance, consisting of two **phenol molecules**, bonded to a **furan** ring, which is bonded in turn to a benzoic acid group; this substance is **fluorescent**, emitting light under reflection, when excited by **ultraviolet** radiation. Commonly used in the form of fluorescein sodium (C₂₀H₁₀Na₂O₅).

fluorescence: the emission of light, induced by the **absorption** of an incident flux (of light, of **electromagnetic X-radiation**, or of **electrons**), and subsequent rapid deexcitation of electrons in the outer **atomic** shells of the luminescent substance, this loss of energy taking the form of an emission of fresh electromagnetic radiation. Should its wavelength lie in the visible part of the spectrum, **luminescence** occurs.

fluorine and perfluorocarbon: fluorine is a chemical **element**, of symbol F, and **atomic number** 9; it is the first element in the halogen group (group VIIA, IUPAC group 17), with a mass number of 19; a perfluorocarbon is a **molecule** obtained from a **hydrocarbon**, by replacing all the **hydrogen atoms** in it by fluorine atoms.

flux (and damage dose rate): the number of incoming particles (e.g. **ions**) per unit surface, per unit time; **neutron flux:** the number of **neutrons** passing across the unit surface, per unit time. This determines the speed with which **damage** occurs.

fossil energy: energy yielded by a fossil fuel, i.e. by a substance formed within rock beds, over several million years, from vegetable, animal, and mineral detritus.

fourth-generation nuclear reactor: a new generation of nuclear energy systems currently being investigated on an international basis, and affording, at the same time, improved qualities in terms of economics, safety, **waste** minimization, and proliferation resistance, compared to the reactors now in service, or under construction. Six **reactor lines**, most of them involving a **closed fuel cycle**, and using **fast neutrons**, have been selected for further in-depth study, these lines differing in terms of the **coolant** used: **sodium**, lead, supercritical water, gas (**helium**), or molten salts.

friction stir welding: a solid-state joining process, whereby a rapidly rotating tool is used to exert friction as it is inserted at the seam plane between the two parts, causing the two materials to soften. The tool then penetrates down into the seam, and proceeds along it, intimately mixing the materials.

fuel (nuclear): a **fissile** material that enables, through use of an appropriate geometry, a **chain reaction** to be sustained inside the **core** of a reactor; **fuel element:** the smallest core component having a distinct structure of its own, containing nuclear fuel; **spent fuel:** fuel which, being unable to further sustain the nuclear reaction, is discharged from the reactor.

fuel cycle: the ensemble of steps undergone by nuclear **fuel**. The fuel cycle includes ore extraction, concentration of the **fissile** material, **enrichment**, **fuel element** fabrication, in-reactor use of these elements, **spent fuel treatment**, **recycling**, if required, of the **heavy atoms** thus recovered, and the **conditioning**, and **storage**, or **disposal** of the **radioactive waste**.

fullerene: a **molecule**, consisting of **carbon atoms**, which may take on a shape reminiscent of a sphere, an ellipsoid, a cylindrical tube (known as a **nanotube**), or a doughnut; fullerenes are akin to **graphite**, consisting as they do of sheets of bonded hexagonal carbon rings, though they do feature pentagonal, or even heptagonal rings, this ensuring the sheet cannot lie flat.

functionalization: in the broader sense of the word, the adaptation of a chemical, physical, or biological object, for the purposes of enabling it to fulfill the desired functions. More narrowly, the term surface functionalization, for instance, is used to refer to the appending of certain chemical **functional groups** to a surface.

furan (C₄H₄O): a simple, fundamental heterocyclic **compound**, consisting of an **aromatic** ring comprising 5 **atoms**, including one oxygen atom; it is used in organic chemistry as a reagent, or as a precursor.

fusion: an energy production process involving the fusion of **light-element nuclei** [**hydrogen isotopes**].

G

gadolinia-doped ceria: cerium **oxide** (ceria: CeO₂) **doped** with gadolinium oxide (gadolinia: Gd₂O₃); noted GDC.

gadolinium: chemical **element**, of symbol Gd, and **atomic number** 64, a member of the **rare earth** group of elements.

gallium: chemical **element**, of symbol Ga, and **atomic number** 31; gallium arsenide: a chemical compound of gallium, and arsenic (a III–V **semiconductor** material, used, in particular, for the fabrication of **microwave**, and optoelectronic components, infrared **light-emitting diodes**, or **photovoltaic cells**).

gas-cooled fast reactor (GFR): a high-temperature, gas-cooled **fast reactor** (the coolant as a rule being **helium**), allowing the **homogenous**, or **heterogeneous recycling** of **actinides** to be carried out. This is one of the six concepts selected by the Generation IV International Forum (GIF), an international collaboration dedicated to the development of **fourth-generation nuclear systems**.

genotoxicity: the property, exhibited by certain chemical, or physical toxic agents, of triggering mutations affecting the genetic material, in organisms exposed to them.

germanium: a chemical **element**, a member of the so-called crystallogen group (group IVA, IUPAC group 14), of symbol Ge, and **atomic number** 32; a **semiconductor** metalloid.

glass fiber: an inorganic fiber, obtained by melting, drawing through a die, and stretching.

global analysis: an analysis that involves addressing every aspect of an issue, in a gradual – albeit not sequential – manner.

grains: the elementary **crystallites**, in a **crystalline** material, “adhering” to one another by way of **grain boundaries**.

granulometry: the measurement of grain sizes, and determination of grain shapes in powdered products, or products in suspension.

graphene: a two-dimensional (single-sheet) **carbon crystal**; **graphite** consists of stacked graphene sheets.

graphite: one of the three **allotropic** forms of **carbon**, exhibiting a **crystal** structure consisting of **graphene** sheets, in which every **atom** is bonded to three of its neighbors.

gravimetry: a term used to refer either to a so-called potentiometric geophysical method, serving to study spatial variations in the gravitational field; or an ensemble of analytical, or separation techniques, based on differences in **specific gravity**.

greenhouse gases: gases, present in the Earth’s atmosphere, which contribute to global warming (water vapor, and **carbon dioxide**, in particular).

H

hafnium: chemical **element**, of symbol Hf, and **atomic number** 72.

half-life (radioactive): the time required for one half of the **radioactive atoms** initially present in a sample of a given radioactive **nuclide** to disappear, through natural **radioactive decay**.

hardening (of a material): the raising of the yield stress value, for a material.

hardness: the strength exhibited by a material, enabling it to withstand penetration by another body, assumed to be rigid. This is expressed in terms of specific scales of hardness (e.g. Vickers hardness). See also **spectrum hardness**.

heat conduction: the phenomenon whereby, in a medium, heat flows from a higher-temperature region to another, lower-temperature region, or from one medium to another coming into contact with it. See also **thermal conductivity**.



heavy ions: in a **particle accelerator** context, positively-charged **atom nuclei**, with a mass higher than that of the **helium-4** nucleus (**alpha** [α] **particle**).

heavy nuclei: a term used to refer to **isotopes** of **elements** of **atomic number** equal to or greater than 80. All **actinides**, together with their *daughter products*, fall into this category.

helium: chemical **element**, of symbol **He**, and **atomic number** 2, the lightest element, after **hydrogen**. **Helium-4**, the **nucleus** of which – i.e. the **alpha** [α] **particle** – comprises two **protons**, and two **neutrons**, is by far the most common **isotope**. **Helium-3**, featuring a nucleus comprising two protons, and a single neutron, exhibits nonzero **nuclear spin**.

hertz: a unit of frequency (**Hz**), equal to 1 cycle per second, for alternating phenomena. The chief multiples include the **megahertz** (1 **MHz** = 10^6 **Hz**), and the **gigahertz** (1 **GHz** = 10^9 **Hz**).

heterologous: produced by a different organism.

hot isostatic pressing: a process involving the simultaneous application, to a material, of high pressures (10^8 – $1.5 \cdot 10^8$ **Pa**), and high temperatures (around 1,000 °C), by means of a neutral gas, or fluid.

hot pressing: a forming process involving subjecting the product to pressure at high temperature.

hydrides: compounds of **hydrogen**, and any other **element**, other than **oxygen**.

hydrocarbon: a **molecule** consisting solely of **atoms** of **carbon**, and **hydrogen**.

hydrodynamics: the part of fluid mechanics concerned with the flow of incompressible, or poorly compressible fluids; with the forces, and pressures arising during such flows; and with turbulence.

hydrogel: a network of **hydrophilic polymer** chains, initially soluble in water, but rendered insoluble subsequent to **cross-linking**.

hydrogen: chemical **element**, of which three **isotopes** occur, one of which is an **atom** solely consisting of one **proton**, and one **electron** (^1H), the other two being **deuterium** (^2H), and **tritium** (^3H); **proton** ($^1\text{H}^+$): the ^1H **nucleus**.

hydrolysis: the decomposition of a substance, through bonding with H^+ and OH^- **ions** yielded by the dissociation of water **molecules**.

hydrophilic/hydrophobic: terms used to refer to substances which attract/repel water.

hydroxide: one of the two constituent **ions** (OH^-) of water, spontaneously produced, together with hydronium ions (H_3O^+), through the autodissociation of water **molecules**; the larger the hydroxide (or **hydroxyl**) ion (OH^-) content, in an aqueous solution, the higher its **hydrogen** potential (**pH**) is.

hyperfrequency: a **radio frequency** sufficiently high to allow techniques such as waveguides, or cavities to be employed (3 –300 **GHz**). See also **microwave**.

hysteresis: a property exhibited by a system that tends to remain in a given state, once the external cause that occasioned the change has been removed, and thus lags behind it, depending on previous history.

I

ilmeneite: a mineral consisting of an **oxide** of iron and **titanium**, of formula FeTiO_3 , conforming to the trigonal **crystal** system.

immunoglobulin: a type of **antibody**, produced by certain white blood cells (lymphocytes, plasmocytes).

impedance: a measure of the opposition that an electrical circuit presents to the passage of a sinusoidal alternating current.

indium: chemical **element**, of symbol **In**, and **atomic number** 49.

infrared (IR) radiation: a segment of the **electromagnetic** spectrum covering **radiation** of wavelengths ranging from 760–780 **nm** to 1 mm.

insulin: a **polypeptide** hormone, secreted by cells in the pancreas; classed as a hypoglycemic agent, its role is to keep blood glucose concentration constant; when insulin secretion is insufficient, diabetes ensues.

integrated circuit (or electronic chip): an **electronic component**, serving to reproduce one or more electronic functions, of varying complexity, and commonly integrating a number of basic electronic components within a restricted volume, making for ease of use of the resulting circuit.

interaction: a mutual action involving two or more objects, or factors.

intercalation: a phenomenon involving the reversible insertion of **atoms**, or **ions**, e.g. **lithium** ions, into a host structure, initially exhibiting a lamellar structure.

interdiffusion: the exchange of chemical species between two systems.

interstitial loop: under the effects of **irradiation**, **interstitials** may form up into a loop, through planar condensation.

ion: an **atom**, or **molecule** that has lost, or gained, one or more **electrons**, and thus exhibits an electric charge (**cation**: positive ion; **anion**: negative ion). See also **heavy ions**.

ion conductor: a conductor in which the charge carriers involved are **ions**.

ion-exchange resin: an **ion** exchanger is a solid substance having the ability to exchange the ions it contains for other ions, yielded by a solution, by effecting a shift in equilibrium. In order to speed up exchanges, and reach that state of equilibrium, the substance must present the largest possible contact surface area with the solution. Initially, the first ion exchangers to be used were zeolites (natural inorganic compounds). Nowadays, synthetic organic, or inorganic compounds serve that purpose. An ion-exchange resin consists of a three-dimensional network of a high-density **polymer**, most commonly polystyrene, onto which **ionized**, or ionizable **functional groups** are grafted, endowing it with the characteristics of an ion exchanger.

ion implantation: a process whereby **ions** can be implanted into a solid substance, thus modifying its properties, by causing both a chemical alteration of the target body, and, possibly, a change in its **crystal** structure. The implantation system comprises an ion source, an **electrostatic accelerator** (the implanter), and a chamber, inside which the target is positioned.

ionic bond: a bond characterized by the *transfer* of **electrons** from one **atom** to another, the electrons however not being *shared*, as is the case in a **covalent bond**.

ionization: a state of matter in which **electrons** are separated from the **nuclei**; the process whereby **ions** are produced, through collisions with **atoms**, or electrons (*collision ionization*), or interaction with **electromagnetic radiation** (*photoionization*).

ionomer: an “ionically **cross-linked**” thermoplastic copolymer: **cross-linking** enhances the **polymer**’s cohesion, and electrical conductivity.

iridium: chemical **element**, of symbol **Ir**, and **atomic number** 77.

irradiation: exposure to an **ionizing** radiation, and, more broadly, the outcome of such exposure.

irradiation cycle (in-reactor): the time interval over which a nuclear reactor is operated, between two successive loadings (whether partial, or otherwise) with nuclear **fuel**.

isotopes: forms of one and the same chemical **element**, for which the **nuclei** have the same number of **protons** (and hence of

surrounding **electrons**], but different numbers of **neutrons**. **Heavy isotopes** are isotopes of high-**atomic-number** elements.

isotropic: showing identical physical properties in all directions (antonym: **anisotropic**).

J

joule (J): derived unit of work, of energy, and of heat in the International System of Units (SI). The joule is defined as the work done by a force of 1 newton, when the point of application moves a distance of 1 meter in the direction of the force; or the work done when a current of 1 **ampere** passes through a resistance of 1 ohm for 1 second.

Joule effect: the release of heat, due to the **resistance** exhibited by a conductor to the passage of an electric current.

K

kelvin: unit of temperature (symbol **K**). The Kelvin scale features a single fixed point, this being, by convention, the thermodynamic temperature of the triple point of water (i.e. the point at which the three phases, solid, liquid, and vapor, coexist) at 273.16 K, i.e. 0.01 °C. 0 K = -273.15 °C is known as “absolute zero,” at which temperature every form of matter is frozen still.

kinetic energy: the energy possessed by a body, because of its actual motion; it is equal to the work required to bring that body from rest to its current state of translational, or rotational motion.

L

lamellar oxides: compounds of oxygen, a **transition element** (cobalt, nickel...), and, as a rule, an **alkali metal** (lithium, sodium), exhibiting structures featuring a stack of successive layers of transition elements, and alkali metal layers.

lanthanides: the series of **elements** of **atomic number** ranging from 57 (lanthanum) to 71 (lutetium). Lanthanides exhibit chemical properties that are very close to those of **actinides**.

lanthanum: chemical **element**, of symbol La, and **atomic number** 57.

lead zirconate titanate (PZT): a material, of chemical formula $\text{Pb}(\text{Zr}_x\text{Ti}_{1-x})\text{O}_3$, widely used for industrial applications, owing to its **ferroelectric**, **piezoelectric**, and **pyroelectric** properties.

ligand: an **atom**, **ion**, or **molecule** featuring chemical functions that enable it to form bonds with one or more central atoms, or ions.

light-water nuclear reactors (LWRs): a family of nuclear reactors in which light water (i.e. ordinary water) serves both as **coolant**, and **moderator**. The LWR family covers both **pressurized-water reactors (PWRs)**, and **boiling-water reactors (BWRs)**.

liposome: a naturally occurring (e.g. in egg cytoplasm), or artificially prepared lipid vesicle.

liquefaction: the change of state undergone by a substance, which passes from the gaseous to the liquid state; or, through the effects of heat, passes from the solid to the liquid state.

lithium: chemical **element**, of symbol Li, and **atomic number** 3, similar to **sodium**, though less chemically active, and used as a constituent in **alloys**.

long-lived: a term used to refer to **radionuclides** having a **half-life** longer than 30 years.

Lorentz force (and Laplace force): the Laplace force is the force exerted by an **electromagnetic field** on all the charges contained in a conducting material; it is a special aspect of the Lorentz force, which applies to any charged particle.

loss of primary coolant accident (LOCA): loss of tightness in the **primary circuit** of a **water nuclear reactor**, resulting in a rapid rise in **cladding** temperature – with a concomitant rise in internal pressure – causing accelerated high-temperature **oxidation** to occur, prior to final quenching, i.e. the final reflooding of the **core** by the emergency injection systems – forming part of the safety systems – provided for that purpose.

M

macro-: a prefix meaning “large,” used to refer, in particular, to objects of a size akin to the human scale, i.e. larger than 1 mm; for instance, a macromolecule is a large **molecule**.

magnesium spinel: a **crystal** structure exhibited by **oxides**, of formula $[\text{Mg}^{2+}][\text{Al}^{3+}]_2[\text{O}^{2-}]_4$, in which the oxygen **ions** form a compact lattice, of the **face-centered cubic** type, while the Mg^{2+} , and Al^{3+} **cations** occupy, respectively, the tetrahedral, and octahedral sites in these structures.

magnetic field: a force field, defined, at every point, in its intensity, and direction, set up by the motion of electric charges. It is expressed in **amperes** per meter (A/m), or in oersteds (Oe); **magnetic flux density** (or **magnetic induction**): the total magnetic field set up within a magnetic material placed in an external magnetic field; this quantity, noted B , is expressed in **teslas** (T), gauss (G), or webers per square meter (Wb/m²).

magnetic moment: a quantity, noted M – described, in mathematical terms, as a vector having the dimension of a current intensity (measured in **amperes**), multiplied by a surface area (A·m²) – related to the torque Γ to which a magnet of moment M is subjected, when placed in a uniform **magnetic field** B , by the formula: $\Gamma = M \cdot B \cdot \sin \theta$, where θ is the angle between M , and B .

magnetic permeability: the capacity, noted μ , of a material to give rise to an increase in **magnetic flux density** B , when placed in an external **magnetic field** H : $B = \mu H$.

magnetism: a physical phenomenon, giving rise to attractive, or repulsive forces between objects, or affecting moving electric charges.

magnetron cathode sputtering: a **cathode sputtering** technique using a magnetron (i.e. a set of permanent magnets, positioned under the target), in order to increase **ion** density around that target. The magnetron effect makes it possible to sustain the discharge at lower pressure, resulting in enhanced sputtering quality.

manganese: a chemical **element**, of symbol Mn, and **atomic number** 25; a hard, brittle gray-white metal, of similar appearance to iron, which melts at a low temperature, but is readily **oxidized**; it takes its name from Magnesia, a city forming part of the ancient Greek province of Thessaly, from which was likewise derived the Greek word *magnes*, i.e. “magnet.”

martensitic steels: such steels, exhibiting a **body-centered cubic crystal structure** (or a body-centered **tetragonal** structure, for high **carbon** contents), feature **chromium** contents, in most cases, of less than 13% (8–12% as a rule), with a maximum 0.2% carbon. As they are rapidly cooled down from a high-temperature domain, the initial **austenitic** phase undergoes a martensitic transformation, causing the emergence of a structure consisting of very thin platelets, or laths.

martensitic structure: a **body-centered cubic structure**, found in certain metal **alloys**, in particular in certain steels.

mass spectrometry: a physical analytical technique, making it possible to detect, and identify **molecules** of interest, by measuring their mass, and to characterize their chemical structure; its principle involves the gas-phase separation of charged molecules (**ions**), according to their mass/charge (m/z) ratio.



massively parallel supercomputer: a high-power computer, consisting of a large number of interconnected processors, simultaneously carrying out different tasks, in order to boost its performance, or its capacity.

matrix (composites): a material encapsulating the **reinforcement** (fibers, as a rule), its chief functions being to provide cohesion for the **composite** material as a whole, and to allow **stresses** to be transmitted to the mechanical reinforcement.

matrix (waste): an organic, or inorganic matrix (**glass**, bitumen, hydraulic binder, **ceramic**), having the purpose of immobilizing **waste**, to prevent its dispersion, and/or of ensuring the long-term **containment** of **radionuclides**.

mechanistic: pertaining to mechanism, as a school of thought, i.e. to the philosophical theory that holds that all phenomena are produced by the mechanical properties of matter.

mesoscopic: occurring at a scale intermediate between the **nanoscopic**, and **microscopic** scales: a **mesostructure** is a structure characterized by features at that scale.

metabolism: the ensemble of coupled reactions arising within the cells of an organism; metabolism serves either to extract energy from nutrients (catabolism), or to synthesize the constituents required for the cells' structure, and their proper operation (anabolism).

methane: a **hydrocarbon**, of molecular formula CH_4 , the simplest compound in the alkane family; it is a gas generated by living organisms, which may be used as a fuel, and equally as a refrigerant fluid; it is also recognized as one of the main **greenhouse gases**.

methyl orange: a color indicator, used in chemistry to indicate the presence of an acid medium (when it turns pink-red), or of a basic medium (when it turns yellow-orange); it is employed for acid-base titration purposes.

metric: a function serving to define a distance between elements in a set.

micelle: a spheroidal aggregate of so-called **surfactant molecules**, each comprising a **hydrophilic** polar head, and a **hydrophobic** chain, or tail.

micro-: a prefix (symbol: μ) representing one millionth (10^{-6}). 1 **micrometer** (μm), or **micron** = 10^{-6} meter.

microelectronics: the specialized branch of electronics concerned with the study, and fabrication of **electronic components** at the **micrometer** scale.

microscopy: the ensemble of techniques used for the purposes of imaging small objects, by means of instruments known as microscopes; three types of microscopy are in use: optical microscopy, **electron microscopy**, and local-probe microscopy.

microstructure: when applied to nuclear **fuel**, or to any material, this term refers to the shape, size, and arrangement of that material's constituent features (**grains** in a **polycrystalline** material, minerals), as of its voids (**porosity**, **vacancies**...).

microwave: an **electromagnetic** wave having a wavelength in the 1–100 cm range. See also **hyperfrequency**.

modeling: the simplified representation (**model**) of a system, or a process, for the purposes of **simulating** it, which is then drawn up in a computation software [often referred to as a **code**], in the form of mathematical expressions. Mesh **cell** size, across space, and time, yields the model's **resolution**.

moderator: a material consisting of light **nuclei**, serving to slow down **neutrons** by way of elastic scattering. The moderator should have a low **capture** capability, to avoid neutron "wastage," while being sufficiently dense to ensure effective slowing down.

molar absorption: a quantity, denoted by the Greek letter ϵ (epsilon), and expressed in liters per **mole**, per centimeter ($\text{L}\cdot\text{mol}^{-1}\cdot\text{cm}^{-1}$) by biochemists, or in square meters per mole ($\text{m}^2\cdot\text{mol}^{-1}$) [by chemists working with the International System of Units]. Its value is a function of wavelength, temperature, and the nature of the solute, and **solvent**.

molar mass: the mass of 1 **mole** of a substance [a chemical **element**, or a compound], expressed in grams per mole ($\text{g}\cdot\text{mol}^{-1}$ or g/mol).

mole: a unit of the amount of substance (symbol: **mol**), viz. the amount of substance of a system which contains as many elementary entities as there are **atoms** in 0.012 kg **carbon-12**, i.e. $6.03\cdot 10^{23}$ (Avogadro's number). For concentrations: **M** = mole/liter.

molecular dynamics: a method involving the **simulation** of the motions of **atoms** within **molecular** systems, through the application of the laws of classical mechanics, for the purposes of predicting the evolution, over time, of their spatial configuration. These motions correspond to vibrations around an energy minimum, or transitions from one energy minimum to another. This method makes it possible to determine structural properties, and **thermodynamic** quantities.

molecular-beam epitaxy: a technique making use of **molecular** beams, to deposit, onto the surface of a **single-crystal** substrate, kept at high temperature, films consisting of a few **atomic** planes. The process involves effecting the evaporation of the various pure constituents of the material being fabricated, within a chamber held under high vacuum.

molecule: a group of **atoms**, held together by chemical bonds.

molybdenum: chemical **element**, of symbol Mo, and **atomic number** 42.

monoclonal antibodies: **antibodies** that are homogeneous, as a result of being produced by genetically identical cells.

monomer: a substance, organic in most cases, serving in **polymer synthesis**, where it is used in a **polymerization** reaction.

Monte-Carlo (method): a statistical method, used to obtain an approximation for the value of an integral, by way of a set of points, randomly distributed in accordance with a certain probability. This involves repeatedly assigning a numerical value, dependent on the ongoing operation of a process in which chance events are a factor, and then calculating a mean, and the corresponding statistical dispersion (as a measure of accuracy) over the set of values so obtained. **Kinetic Monte-Carlo simulations** serve to reproduce, and equally to predict, a wide variety of kinetic behaviors, at a **mesoscopic** scale.

N

Nafion: a **polymer** conventionally used as an **electrolyte**, in PEM fuel cells fabricated by **DuPont de Nemours**.

nano-: a prefix (symbol: **n**) representing one billionth (10^{-9}); 1 **nanometer** (**nm**) = 10^{-9} meter.

nanoparticle/nanostructure: a **nanometer**-scale particle/structure.

nanophotonics: the study of light at the **nanometer** scale.

nanstructuring: the formation of structural patterns at the **nanometer** scale.

nanotechnology: the ensemble of fabrication, and handling processes used for **nanometer**-scale structures, devices, and material systems; and likewise for **nanoaerosols**, **nanomaterials**, **nano-objects**, **nanoparticles**, **nanoproducts**, **nanotracers**...

nanotoxicology: the study of the toxicity exhibited by ultrafine (1–100-**nanometer**) particles.

natural uranium-graphite-gas (UNGG) reactor: a nuclear reactor line using a **natural-uranium-metal-based fuel**, **graphite**

as the **moderator**, and pressurized **carbon dioxide** (CO₂) as **coolant**. Such reactors were operated in France in the 1960s and 1970s.

negative reactivity: a process causing a drop in **reactivity**, i.e. as induced by devices designed for that purpose – e.g. **neutron-absorber rods** – or due to physical phenomena.

neutron: an electrically neutral fundamental particle, having a mass of $1.675 \cdot 10^{-27}$ kg. Neutrons are the constituents, together with **protons**, of **atomic nuclei** (**nucleons**). They can cause the **fission** of **fissile** nuclei, in nuclear reactors. See also **fast neutrons**, **thermal neutrons**.

neutron capture: the absorption of a free **neutron** by a **nucleus**, not resulting in **fission**.

neutron spectrum: the energy distribution of the **neutron** population present in a reactor **core**.

nickel: chemical **element**, of symbol Ni, and **atomic number** 28; a silvery white metal, belonging to the iron group of elements; highly resistant to **oxidation**, and **corrosion**, nickel enters in the composition of many **alloys**.

nickelates: **nickel**-containing **oxides**, e.g. with the composition Ln₂NiO_{4+δ} (with Ln = Nd, La, Pr).

nitride: a compound of **nitrogen**, and another **element**, in many instances a metal.

nitrogen: a chemical **element**, a member of the pnictogen group (group VA, IUPAC group 15), of symbol N, and **atomic number** 7, forming the main constituent of the Earth's atmosphere (4/5 of the air mass, 78.06% by volume).

nitrogen dioxide (NO₂): a toxic gas, and an atmospheric pollutant able to absorb **ultraviolet** (UV) **radiation**, which is then prevented from reaching the Earth's surface.

nonpolar: in chemistry, polarity is a characteristic serving to describe the distribution of negative, and positive charges in a dipole; this is due to differences in **electronegativity** between the various constituent chemical **elements** of that dipole, to the diverse charges induced by this differential electronegativity, and the spatial distribution of these charges; the more highly asymmetrical the charge distribution, the more polar the bond is said to be; if the charges are symmetrically distributed (no separation of positive, and negative charges), the **molecule** is said to be nonpolar.

normal cubic meter (Nm³): a unit of volume, allowing comparisons to be made, for gases, between quantities measured under different actual conditions, by converting these values to the so-called normal temperature and pressure conditions: 0 °C, 1 bar absolute.

nuclear glass: an inorganic **matrix**, used for the **containment** of high-level (**high-activity**) **nuclear waste**. Glass exhibits the structure of a frozen liquid, i.e. a structure featuring short-range order (the concatenation of **silica** tetrahedra), and an absence of medium-range order, enabling it to accommodate most of the **fission products**, and **minor actinides** yielded by the **treatment** of **spent fuel**. See also **R7T7 glass**.

nuclear magnetic resonance (NMR) spectroscopy: a **spectroscopy** technique based on the nuclear magnetic resonance phenomenon, which involves making a **radiofrequency** (RF) wave interact with the system being investigated – the RF frequency varying, depending on the **magnetic field**, and the **nucleus** being looked at – in order then to detect the signal reemitted from the sample (the **NMR signal**), this yielding information as to the local structure, around the nucleus involved.

nucleus (atomic): the central constituent in an **atom**, bearing a positive charge and consisting of **protons**, and **neutrons** (except in the case of **hydrogen**), around which **electrons** orbit. See also **heavy nuclei**.

nuclide: a nuclear species, characterized by its number of **protons** *Z* [i.e. its **atomic number**], number of **neutrons** *N*, and mass number *A*, this being equal to the sum of the number of protons, and number of neutrons (*A* = *Z* + *N*).

numerical simulation: the reproduction, by way of computation, of the functioning of a system, subsequent to its prior description through a **model**, or an ensemble of models.

O

ohmic: a characteristic involved in charge transport (resistance, contact, loss...).

olivine: a magnesium iron **silicate**, taking its name from its olive-green hue, of general formula (Mg, Fe)₂SiO₄; it crystallizes at high pressure, in the absence of water, in quartz-poor environments; by extension, compounds featuring similar structures, e.g. LiFePO₄, are commonly referred to as olivines.

opportunistic radio: a radio transmission system in which the radiolink equipment, constructed so as to be as simple as feasible, in hardware terms, is able to reconfigure dynamically through its software, to cater for any type of signal.

optical fiber: a very fine glass, or **plastic** filament exhibiting the property of acting as a light conductor; optical fibers are used for transcontinental, and transoceanic communications, for which purpose they enable high data transmission rates; they may be used to transmit, indifferently, television, telephony, videoconferencing signals, or computer data.

organometallic compound: an organic compound featuring at least one **carbon**–metal bond.

osteogenesis: the process of bone formation.

oxidation: a reaction whereby an **atom**, or an **ion** loses **electrons**. The most common such reaction is the one whereby a compound combines with one or more oxygen atoms, yielding an **oxide**.

oxidation–reduction: a chemical reaction involving a transfer of **electrons**; the chemical species accepting the electrons is known as an oxidizing agent (oxidant), the electron-donor species as a reducing agent (reductant). See also **redox**.

oxide-dispersion strengthened (ODS) alloy: an **alloy** reinforced by means of **oxide nanoparticles**.

P

package: a unit comprising a transportation, **storage**, or **disposal** container, and a well-defined content of **radioactive waste**.

palladium: chemical **element** of scarce terrestrial abundance (0.015 ppm in the Earth's crust), a member of the platinum group of elements, of symbol Pd, and **atomic number** 46.

particle accelerator: a machine designed to generate, shape, and accelerate a beam of charged particles, directed onto targets, or other beams of accelerated particles. Accelerators may use, for acceleration purposes, **electrostatic** (Van de Graaff accelerator, **Pelletron**™), or **electromagnetic** forces (cyclotrons, **synchrotrons**).

pascal: the international unit of pressure [Pa]. Multiples include the **megapascal** (1 MPa = 10⁶ Pa), and the **gigapascal** (1 GPa = 10⁹ Pa). 1 bar = 10⁵ Pa = 0.987 **atmosphere**.

passivation: a surface treatment applied to a metal, for the purposes of proofing it against attacks by certain chemical agents.

passive (or passivation) layer: a barrier having the ability to restrict the access of corrosive species (H₂O₂, O₂...) to a surface. It thus contributes to bringing down the rate of **corrosion** undergone by the underlying material.



pellet: a cylindrical **fuel element**, made from a **ceramic**, a stack of which, inside a **cladding** tube, forms the **fissile** column (in a **rod**, or **pin**), in a reactor.

peptide: a chain comprising fewer than 50 amino acids linked by peptide bonds.

percolation: a critical physical process, serving to describe, for a system, a transition from one state to another: in particular the ability, for certain materials (platinum grains, **catalysts**, **polymer** chains...), to set up bonds with one another, to form a continuous chain.

perfluoropolyether (PFPE): a **polymer** rich in **fluorine atoms**, widely used as a lubricant.

permeability: for a material, this is an intrinsic quantity; it is a measure of its capacity to let a fluid through, and is independent of the fluid involved. See also **magnetic permeability**.

permittivity: a quantity expressing the capacity of a material to store electrical energy, in the presence of an electric field. It is noted by the symbol ϵ . See also **dielectric constant**.

perovskite: named after Russian mineralogist L. A. Perovski, this refers to a **crystal** structure that is common to numerous **oxides**, of general formula ABO_3 . Perovskites exhibit a variety of electrical, and magnetic properties, depending on the nature of **elements** A, and B.

pH: a measure of the concentration in **hydrogen ions**, in a liquid. Below pH 7, the measure is said to be that of an **acidic** pH, an **alkaline** pH above that value.

phenol: also known as hydroxybenzene, phenylic acid, or carbolic acid, this is the simplest of all **molecules** in the class of phenolic compounds (phenols); it comprises an **aromatic benzene** ring (i.e. it is an **aromatic hydrocarbon**), and a **hydroxyl** function.

phosphate and lithium iron phosphate: phosphates are compounds of phosphorus, oxygen, and another **element**; lithium iron phosphate: a compound of phosphorus, oxygen, iron, and **lithium**.

photon: the **quantum** of energy of an **electromagnetic radiation**. An elementary particle, having zero mass and no electric charge, associated to such radiation; **X-photons:** the constituent particles of **X-radiation**.

photovoltaic cell: an **electronic component** which, when exposed to light (i.e. to **photons**), generates an electric current.

photovoltaic effect: the effect whereby the energy of light is directly converted into electrical energy, within a **semiconductor**.

physical chemistry: also known as physicochemistry: the part of chemistry that makes use of the laws of physics to interpret chemical phenomena.

physical vapor deposition (PVD): a deposition technique, used for coating purposes, involving the generation, in a vacuum chamber, of a vapor of various substances, combined with reactant gases, so as to yield compounds. This vapor is transferred under vacuum conditions, condensing onto the parts that are to be coated. One vapor generation method is evaporation, which may be initiated by means of an **electron** beam, emitted by a charged tungsten filament, so as to bombard a target **anode** (**electron-beam physical vapor deposition [EB-PVD]**).

pi-conjugation: a chemical system is said to be conjugated when it consists of **atoms** bonded in **covalent** fashion, with an alternation of single, and multiple bonds; a pi- (π -) conjugated system features at least one delocalized π bond

piezoelectric effect: the property, exhibited by certain **crystals**, of undergoing strain proportional to an applied electric field; the inverse effect, which is invariably present, involves the generation of electric charges when mechanical **stress** is applied.

piezoresponse-force microscopy (PFM): this involves a special operating mode of the **atomic-force microscope (AFM)**, known as the *piezoresponse mode*, which makes it possible to map the **polarization** states of **ferroelectric** domains in a sample. By applying a direct **voltage** between the AFM tip, and the sample, it is feasible, locally, to effect a polarization of the sample.

pin: a form of **fuel element**, akin to the **rod** used in **PWRs**, more specifically used in **fast reactors**.

plasma: the state of matter prevailing, when matter is heated to a temperature such that most, or all **atoms** become **ionized**.

plasma forming: a technique whereby a material is sprayed, by means of a **plasma** torch, onto a support matching the internal geometry of the shape desired.

plasma spray deposition: the principle of this deposition method involves using a high-energy **plasma** to melt a powder of the **element**, or compound that is to be deposited, and spray it onto the substrate, prior to resolidification.

plastic material: a blend comprising a base material (a **polymer**) amenable to being formed, as a rule at high temperature and under pressure, to yield a semi-finished product, or an end-object.

plenum (in a pin): a free volume, inside a **pin**, holding no **fuel** material. It serves to **confine fission gases** released by the fuel, preventing such release from causing an excessive pressure rise, within the pin.

plutonium: chemical **element**, of symbol **Pu**, and **atomic number** 94, having **isotopes** ranging from ^{232}Pu to ^{247}Pu . Five of these isotopes are important, for the nuclear industry: from ^{238}Pu to ^{242}Pu – especially ^{239}Pu , a **fissile** element, generated inside reactors from **uranium-238**.

point defect: a defect localized at one point in a **crystal** lattice, due either to a missing **atom** (**vacancy**), or to an extra atom located between the normal positions for atoms in the lattice (**interstitial**), or to an extraneous atom being substituted for one of the atoms in the lattice. A **Frenkel pair** is generated by the displacement of an atom away from its site in the lattice, thus resulting in one vacancy, and one interstitial; **irradiation defect:** a point defect attributable to **irradiation**.

polarization: the alignment, along one and the same direction, of the **magnetic moments** – and thus of the **spins** – of all, or part of the **nuclei** of a given substance, or of the particles in a beam; **polarity:** the assignment of a plus, or minus sign, serving to distinguish the poles of a magnet, or the terminals of an electrical generator.

polyacrylic: a term used to refer to **polymer** derivatives of acrylic acid, and polyacrylates.

polyamide: a **polymer** featuring amide functions, yielded by a polycondensation reaction involving **carboxylic** acid, and amine functions.

polyanionic: a term referring to an anion featuring multiple negative charges, commonly used to refer to compounds comprising oxygen **atoms** bonded, in part at least, to phosphorus, **silicon**, sulfur, or **germanium** atoms.

polycarbonate: a **polymer** formed by the polycondensation of bisphenol A, and phosgene, or a carbonate, or by ester interchange – yielding a **plastic material** exhibiting outstanding mechanical properties, and heat resistance such as to allow it to be used at temperatures ranging from $-135\text{ }^{\circ}\text{C}$ to $+135\text{ }^{\circ}\text{C}$.

polyethylene (PE): also known as polythene: one of the simplest, and cheapest **polymers** on the market, belonging to the class of polyolefins.

polyethylene terephthalate (PET): a **polymer** obtained through polycondensation of terephthalic acid, and ethylene glycol; put simply, this is a refined petroleum product.

polymerization: the gradual addition, and concatenation of **monomer molecules** linked by **covalent bonds**, to form a **polymer**, i.e. a **macromolecule** of high molecular weight, consisting of a number of identical repeat units (antonym: **depolymerization**).

polymethyl methacrylate (PMMA): a transparent **thermoplastic polymer**, obtained from the **monomer** methyl methacrylate (MMA); this polymer is better known under its original trade name: Plexiglas®.

polypeptide: a **polymer** consisting of a large number (> 50) of amino acids (see **peptide**).

polyphenyl ether (PPE): a **polymer** obtained from the reaction e.g. of sodium phenate with bromobenzene; fluorinated PPE is a polymer rich in **fluorine atoms**, widely used as a lubricant.

polypropylene $[-CH_2-CH(CH_3)-]_n$: a semi-**crystalline thermoplastic polymer** (symbol: PP), mass-produced to meet a wide demand.

polysaccharides: complex sugars, formed through the **polymerization** of monosaccharides (i.e. **oses**).

polyurethane: a **thermoplastic polymer** of urethane (a compound yielded by the reaction of an isocyanate with an alcohol); polyurethanes are **plastic** materials for which applications abound: glues, paints, synthetic rubber, foams, fibers...

polyvinyl chloride (PVC): an **amorphous**, or slightly **crystalline thermoplastic polymer**, mass-produced to meet a wide demand.

porosity: the ensemble of interstices, or **pores**, whether connected or otherwise, within a material. The **porosity fraction** is equal to the ratio of the total volume of voids, over overall material volume. **Porosity** is said to be **closed** when pores are not accessible to outside agents. It is termed an **open porosity** when pores connect with the material's external environment.

powder metallurgy: a process used for the fabrication of metal **alloys** – differing from the more conventional process, which involves melting the constituents – or **ceramics**, involving the blending of elementary powders, a compaction step, and a heat treatment step, with or without concomitant compaction (densification by **sintering**, or **extrusion**).

ppm: part per million; **ppb:** part per billion (10⁹).

precession: a motion involving the gradual change in direction (i.e. an angular velocity) of the axis of rotation of an object, or of a vector, due to an outside action; this is the case, in particular, for a particle possessing a **magnetic moment**, acted on by a **magnetic field** (**Larmor precession**), or for the **spin** of an accelerated particle (**Thomas precession**).

precipitation: in a solution, the formation of an insoluble, solid substance (a **precipitate**), as a result of a chemical reaction between two or more compounds.

pressurized-water reactor (PWR): a type of nuclear reactor in which heat is transferred directly from the **core** to a heat exchanger, by water kept at high pressure in the **primary circuit**, to prevent its boiling.

primary circuit: a closed, leaktight loop, the primary circuit contains the reactor **core**, and serves to circulate, by means of circulators, pumps, or compressors, the **coolant**, the heat from which is transferred to a secondary circuit, by way of a heat exchanger.

propane: a saturated **hydrocarbon**, belonging to the class of paraffin (alkane) compounds, of chemical formula C₃H₈; it is a gas which is heavier than air, and readily liquefied.

protease: an enzyme serving to degrade **proteins**.

protein: a biological **macromolecule**, consisting of one or more **polypeptide** chains.

proteolysis: the degradation of **proteins**, through the action of enzymes.

proton: a particle – a constituent of the **atomic nucleus** (i.e. a **nucleon**) – bearing a positive electric charge, equal to that of the **electron**, and of opposite sign. A proton is 1,836 times heavier than an electron.

pyrocarbon (or pyrolytic carbon): a form of **carbon** produced through the high-temperature decomposition of a gaseous **hydrocarbon**; pyrocarbon is used as a coating layer, in the makeup of **fuel** particles.

Q

quadrupole interaction: **nuclei** with a **spin** higher than ½, known as **quadrupoles**, exhibit a nuclear electric quadrupole moment. Consequently, they are subject to a specific interaction, with the local electric field gradient. This interaction does not arise for the most commonly used nuclei, in biology, and organic chemistry in particular, e.g. ¹H, ¹³C, ¹⁵N, ²⁹Si, ³¹P. On the other hand, with respect to **glasses**, all the nuclei involved (except ²⁹Si) are quadrupolar nuclei.

quantum: relating to the theory developed on the basis of Planck's quantum principle – whereby any manifestation of energy can only be expressed in terms of **discrete** (discontinuous) values, known as **quanta** (i.e. indivisible quantities) – and **Heisenberg's uncertainty principle**, whereby it is not possible to measure precisely, at one and the same time, both the position, and velocity of a particle.

quantum mechanics: the ensemble of principles, and operational rules worked out, in physics, from the observation of properties exhibited by radiation, found to be incompatible with classical mechanics.

quantum numbers: in **quantum mechanics**, an **electron** is characterized by four numbers. The **principal quantum number** *n*, a positive integer (≥ 1), corresponding to the electron shell number, largely specifies the electron's energy, and the size of the orbital, which increases with *n*. The **orbital angular momentum quantum number** *l*, which may take any integer value from 0 to *n* – 1, chiefly specifies the shape of the orbital: *s* orbital (*l* = 0), *p* orbital (*l* = 1), *d* orbital (*l* = 2), *f* orbital (*l* = 3)... The **magnetic quantum number** *m*, which may take any integer value in the range –*l* to +*l*, specifies the orientation of the orbital the electron keeps to. Finally, the **spin quantum number** *s* specifies the electron's **spin**, i.e. ±½. In XPS and XPEEM practice, the notation used for an electron configuration is *n**l*_{*i**s*}.

quenching: a thermal treatment process applied to certain materials (historically, this involved plunging hot metals into a cold liquid), endowing them with new properties, by freezing some of their high-temperature characteristics, and/or inducing a **martensitic-type** (i.e. diffusionless) phase transformation.

R

R7T7 glass: a type of borosilicate **glass**, produced for the purposes of **containing waste** yielded by the **treatment** of **spent fuel**, taking its name from the R7, and T7 workshops at the La Hague (western France) plant, where it is produced.

radio frequency (RF): any frequency lying in the range 9 kHz–3,000 GHz.

radiofrequency (RF) component: an **electronic component** carrying out signal processing, for signal frequencies lying in the **radio frequency** range.

radioactive decay: 1. the falloff, over time, of the **activity** exhibited by a **radioactive** substance, owing to the **radioactive disintegration**, or **decay** of its constituent **nuclei**. 2. the process whereby a **nucleus**, or a particle decays (disintegrates) into a number of fragments (particles, and nuclei, forming its **decay products**, and **photons**), to reach a lower-energy – and consequently more stable – state, the characteristics of this transformation only being dependent on the state of the initial nucleus (or particle), not on the process that gave rise to it.

radioactive disintegration: see **radioactive decay**.



radioactive marking: the introduction of **radioactive** chemical **elements** into a **molecule**, a substance, or a living organism, for the purposes of studying its movements.

radioactive waste: a **radioactive** substance for which no further use is foreseen, or contemplated. **Ultimate radioactive waste** is radioactive waste that is not amenable to further **treatment**, in the techno-economic conditions prevailing at a given time, in particular in terms of extracting its recoverable fraction, or bringing down its polluting, or hazardous character.

radioactivity: the property, exhibited by a **nuclide**, of spontaneously transforming into another nuclide, this involving an emission of radiation (particles, **X-radiation**, gamma radiation...), or of undergoing spontaneous **fission**, with a concomitant emission of particles, and gamma radiation.

radioelement: an **element** all **isotopes** of which are **radioactive**.

radionuclide: an unstable **nuclide** of an **element**, which undergoes spontaneous **decay**, with a concomitant emission of radiation.

Raman spectrometry: the spectrum of light scattered by a substance illuminated by a monochromatic **infrared radiation** features lines arising from the coupling between the radiation emitted, and the vibrations, and rotations affecting the **molecules** that light has passed through (Raman effect). Analysis of such lines yields information as to the molecules present.

rare earths: a family of **elements**, chiefly comprising the **lanthanides**, together with **yttrium** (39), and **scandium** (21). The rare earths include, in particular, europium, **gadolinium**, and **erbium**.

reactivity: the deviation, relative to unity, of the ratio of the number of **neutrons** generated by **fission**, over the number of neutrons disappearing, within a nuclear reactor.

recycling: the recovery, for value-added purposes, of reusable materials, subsequent to a production process. In a nuclear reactor, the reuse of **fissile** materials (generated **plutonium**, residual **uranium-235**...) yielded by a previous cycle, after **treatment** of the **spent fuel**. Recycling may be **homogeneous** (the materials being blended into all of the fuel), or **heterogeneous** (the materials are held in target **assemblies**).

redox (oxidation-reduction): the redox potential characterizes a **molecule's** affinity for **electrons**; redox center: a molecular group participating in electron transfers between molecules.

refraction: the phenomenon whereby a wave is deflected as its velocity changes, when it passes from one medium to another – this occurring, as a rule, at the interface between these two media – or as the medium's **density**, or **impedance** varies.

refractory: the quality of a substance that is able to withstand certain physical, or chemical conditions, in particular very high temperatures.

resistance welding: a process making use, as its means of heating, of the **Joule effect** generated by a high-intensity current – delivered by copper-**alloy electrodes** – passing through the assembly. The electric current heats the material to melting point. This technique is thus dependent on the materials' **resistivity**, overall assembly thickness, and on the diameter of the electrodes.

resistivity (of a material): as a rule noted ρ , this quantity accounts for a material's ability to resist the passage of an electric current. It corresponds to the resistance exhibited by a segment of that material 1 m long, with a cross-section of 1 m², and is expressed in **ohm-meters** ($\Omega\cdot\text{m}$).

resolution: also known as *resolving power*, i.e. the ability to discriminate, in a detection device. It may be **spatial** (i.e. the measure of the smallest angular, or linear separation between two objects, characterizing in particular the ability of an optical system to distinguish, or reproduce, details in a scene, or its image), or **temporal** (the shortest time interval separating two successive

instances of a signal over time, allowing these to be perceived as separate). A detection system's **spectral resolution** specifies its ability to discriminate between **electromagnetic radiations** of different frequencies.

rheology: the study of the deformation, and flow of matter, under the effect of applied **stress**.

rod: a small-diameter tube, closed at both ends, used as a component of a nuclear reactor **core**, holding a **fissile**, **fertile**, or **neutron-absorbent** material. When containing fissile material, the rod is a **fuel element**.

ruthenium: chemical **element**, of symbol Ru, and **atomic number** 44, a member of the platinum group of elements (forming part of the **transition metals**).

S

samarium: chemical **element**, of symbol Sm, and **atomic number** 62; a silvery metal, of scarce abundance, relatively stable in the open air, but undergoing spontaneous combustion in air at 150 °C.

scandium: chemical **element**, of symbol Sc, and **atomic number** 21.

scanning electron microscope (SEM): in scanning microscopes, the image is built up point by point, by scanning a small **electron** probe across the object. For every position of the probe, a signal is recorded by one or more detectors; and a software suite, or an acquisition card processes the signals detected, to yield a cartography. The **resolution** achieved is close to 1 nm.

scanning tunneling microscope (STM): this instrument makes it possible to explore, at the **atomic** scale, the topography of the surfaces of **conducting** solids, by means of a finely tapered tip – so fashioned that its extremity consists of just a few atoms – moving across the surface. Tip-surface interaction is measured by way of the number of **electrons** traveling, by the tunnel effect, between the metal probe, and the conducting surface. Scanning tunneling microscopy relies on the fact that there is a nonzero probability that a particle with an energy lower than a potential barrier will nonetheless be able to cross it, by "tunneling" through it (**tunnel effect**). STM also allows surfaces immersed in a liquid to be studied.

selenium: chemical **element**, of symbol Se, and **atomic number** 34, a member of the chalcogen group (group VIA, IUPAC group 16).

self-assembly: the spontaneously occurring formation of complex, hierarchical structures, from simple "building blocks." In nature, **molecular self-assembly** is the process governing, e.g., the formation of cell walls, and **protein** folding.

self-diffusion: the movement of **atoms** within the very material of which they are constituents.

self-interstitial: a **point defect**, corresponding to the presence, within a **crystal** lattice, of an extra **atom**, of the same nature as the atoms forming the lattice.

semiconductor: a material featuring a **forbidden band** (**band gap**), which is neither solely an **insulator**, nor solely a **conductor** at nonzero temperatures, and the electronic properties of which may be made to vary. Some of its **electrons**, being very weakly bound to their **atoms**, may become **conduction electrons**. A semiconductor may be of the *n* type (with electrons as the majority **charge carriers**), or of the *p* type (holes as majority carriers), depending on the **dopants** used.

silanols: chemical compounds featuring at least one **silicon atom** directly bonded to a **hydroxyl** group; they are similar to alcohols, just as silanes are similar to alkanes.

silicate: a chemical compound, formed by combining **silica** (SiO₂) with another **oxide**.

silicon: chemical **element**, of symbol Si, and **atomic number** 14, a member of the so-called **crystallogen** group (group IVA, IUPAC group 14); it occurs in the noncrystalline state (**amorphous** silicon), as in the **crystalline** state (in various forms); it is not found in a free, native state, only occurring in the form of compounds: silicon dioxide (SiO₂), i.e. silica (in sand, quartz, cristobalite), or in other **silicates** (feldspars, kaolinite...); it has long been used as an essential constituent of glass, and has now found new uses in electronics, and for the production of such materials as silicones, or of solar **photovoltaic** modules.

silicon on insulator (SOI): a technology that involves transferring (by the Smart Cut™ process, patented by CEA/LETI) an ultrathin **silicon** film onto an insulator, acting as a mechanical support, this making it possible, in particular, to boost performance, and bring down microprocessor power consumption.

siloxanes: a class of **silicon** compounds (taking its name from silicon, oxygen, and alkane), of formula R₂SiO, where R is a radical group, which may be organic; these compounds may occur as hybrid organic-inorganic forms. The organic chains endow the compound with **hydrophobic** properties, while the main -Si-O-Si-O- chain is purely inorganic.

simulant: the complications of procurement, for work in a **radioactive** environment, frequently leads to stable isotopes of the same element being used, or **isotopes** of **elements** exhibiting chemical characteristics similar to those of the **radionuclides** being investigated. Such elements are known as simulants.

single crystal (or monocrystal): a **crystal** standing, as a single unit, i.e. with no discontinuity, as an assembly of **atoms**, **ions**, or **molecules** arrayed in regular, periodic fashion across all three space directions, by contrast to a **polycrystal**.

sintering: an operation involving welding together the grains of a powdered precursor (a metal, and/or inorganic compound), by carrying out a heat treatment, at a temperature lower than the melting point of the main constituent, in order to turn it into a continuous solid mass. The latter is termed a **ceramic**, when nonmetallic inorganic precursors are involved (ceramic powders).

sodium: an **alkali metal** (of symbol Na, and **atomic number** 11), used in the liquid state as a **coolant** for **fast-neutron** reactors (i.e. **fast reactors**), owing to its "transparency" to **neutrons**.

sodium-cooled fast reactor (SFR): a liquid-sodium-cooled **fast reactor**, associated to a closed **fuel cycle**, allowing the full **recycling** of all **actinides**, and **plutonium** regeneration. This is one of the six concepts selected by the Generation IV International Forum (GIF), an international collaboration dedicated to the development of **fourth-generation nuclear systems**.

solvent: a substance having the ability to dissolve another substance;
solute: a substance that has been dissolved.

source term: in a **radioactive waste** management context, the nature, and quantity of **radioactive** products released, or liable to be released, by a nuclear installation, or by a **package** of radioactive materials. The source term, as implemented in computation **models**, is used, in particular, to evaluate the consequences of an accidental release of radioactivity into the environment.

spark plasma sintering (SPS): a process used to join components, involving high-temperature **sintering**, achieved by means of a pulsed electric field.

specific energy: the quantity of energy available per unit mass.

specific gravity: see **density**.

specific surface area: the ratio of the actual surface area of an object – as opposed to its apparent surface area – over its mass.

spectrometry: the measurement, and interpretation, of the **spectra** exhibited by quantities related to the physical, or chemical composition of a substance, or to the analysis of a wave.

spectroscopy: the study of substances on the basis of radiations emitted by them, or of the transformations undergone by such radiation as it passes through other substances.

spectrum hardness: a term used to specify the mean energy level exhibited by particles (e.g. **neutrons**). A "hard spectrum" involves highly energetic particles, while spectrum "softening" involves a falloff in particle energies.

spin: the intrinsic angular momentum (or rotational momentum) of a particle, taking on integer, or half-integer values; **electron spin:** the spin of an **electron**; **nuclear spin:** the spin of an **atomic nucleus**. Atoms featuring a nucleus comprising an even number of **protons**, and an even number of **neutrons** have zero spin, as is the case e.g. for **carbon-12** (6 protons + 6 neutrons). By contrast, the **hydrogen** nucleus, consisting as it does of just a single proton, has a spin of ½. The **oxygen-17** nucleus (8 protons + 9 neutrons), on the other hand, has a nuclear spin of 5/2.

spintronics: a discipline making use of the **spins**, rather than the charges of **electrons** as carriers.

stainless steel: an alloy of iron and **carbon**, to which an addition is made, chiefly, of **chromium**, which, for contents of more than 12–13%, provides the desired resistance to **oxidation**.

steric: relating to the spatial configuration of a **molecule**.

stoichiometry: the study of the proportions according to which, in a chemical reaction, reactants combine, and products are formed. A reaction is said to be **stoichiometric** when the quantities of reactants involved stand in **molar** proportions identical to those specified in the chemical equation.

storage (radioactive waste): an operation involving holding **radioactive waste**, temporarily, in a facility specifically engineered for that purpose, on the surface, or at low depth, pending retrieval. The term is also used to refer to a facility inside which waste is stored, with the prospect of retrieving it at a later date (see also **disposal**).

stress: a force acting on a structure, whether constantly, or in transient fashion. This is expressed in newtons per square meter (N/m²), or, in mechanics of materials practice, in **megapascals** (1 MPa = 1 N/mm²).

strontium: chemical **element**, of symbol Sr, and **atomic number** 38; a soft, malleable, yellowish-gray substance, strontium forms a protective **oxide** layer, when it comes into contact with air; in air, it readily bursts into flame, and combusts, and it reacts with water.

strontium titanate: an **oxide** of **titanium** and **strontium**, of formula SrTiO₃; this compound crystallizes with a **perovskite** structure – **cubic** at ambient pressure, and temperature – and occurs in the form of transparent **crystals**; it is used in **microelectronics** as a substrate, in **single-crystal** form, or, in **ceramic** form, for its properties as a **dielectric**.

superconductor: a metal, or **alloy** the **resistivity** of which abruptly drops to a value close to zero, at a **critical** temperature (**superconductivity**).

surfactant: a substance every **molecule** of which, comprising a **hydrophilic** part, and a **hydrophobic** part, has the property of reducing surface tension, for a liquid in which it is dissolved, and of making immiscible products soluble in water, through the formation of **micelles**.

swelling: a deformation, due to **irradiation**, caused by the nucleation, and growth of cavities, formed by the accumulation of **vacancies**.

synchrotron (radiation): the characteristic radiation emitted by any charged particle subjected to acceleration. In the case of particles moving at relativistic velocities, this radiation exhibits exceptional properties (continuous spectral range, from **infrared** to **X-rays**, low divergence, **polarization**, coherence, temporal structure), which may be put to use to probe the structure, and electronic properties of matter.



synthesis: the preparation of a chemical substance (e.g. the active material for an **electrode**), obtained from elementary constituents.

T

tantalum: chemical **element**, of symbol Ta, and **atomic number** 73.

Teflon: a trade name, registered by DuPont de Nemours, for tetrafluoroethylene.

tesla: the unit (symbol: T) of **magnetic flux density**, in the International System of Units (SI), corresponding to the generation of a magnetic flux of 1 weber, across a surface area of 1 m², by a uniform magnetic induction. Submultiples include the **nanotesla** (nT), which is equal to 10⁻⁹ T.

tetragonal (phase): having the shape of a square-based rectangular prism. The **tetragonal** (or **quadratic**) **structure** is a **crystal** system the unit **cell** of which is a square-based rectangular prism.

thermal conductivity: a quantity characterizing the resistance to the flow of heat, in a given homogeneous material; it expresses, in **watts** per meter, per **kelvin** (W/m·K), the rate at which heat flows across a surface, per unit temperature variation, along a direction perpendicular to that surface. See also **heat conduction**.

thermal diffusivity: the penetration, and attenuation rate of a thermal wave, in a given medium.

thermal energy: the **kinetic energy** corresponding to the random **microscopic** agitation, within an object, of its constituent **molecules**, and **atoms**; it contributes part of that body's internal energy.

thermal neutrons: also known as slow (or thermalized) **neutrons**, these are neutrons in thermal equilibrium with the material within which they travel, at a velocity of some 2–3 km/s. Their energy stands at less than 1 eV.

thermal spraying: a surface treatment technique by a dry route, allowing thick coatings, of diverse kinds, to be obtained, on a variety of substrates. A carrier gas serves to accelerate, and transport fine (typically 5–100 **micrometers**) particles of a material in molten form onto the surface that is to be coated. The droplets are deposited directly onto the surface, where they solidify. The energy input is provided by a flame, or an electric arc.

thermodynamics: the branch of physics concerned with the description, and study of energy transfers in matter.

thermomechanics: the scientific discipline concerned with the study of physical energy, and changes of state in matter, as governed by the laws of mechanics.

thermoplastic: the quality of a substance which softens (i.e. becomes plastic) when heated.

thermosetting: the quality of a substance which loses all plasticity (i.e. "sets") when heated.

thin film: a layer, or coating, having a thickness that may range from a few **atomic** layers to 10 **micrometers** or so, which modifies the properties of the substrate onto which it is deposited; thin films may serve as very thin **electrodes**.

thorium: chemical **element**, of symbol Th, and **atomic number** 90; it is relatively abundant in nature, occurring with **isotopes** from ²²³Th to ²³⁵Th. Isotopes ²²⁷Th, ²²⁹Th, and ²³³Th are **fissile** when bombarded by **thermal neutrons**.

tin: chemical **element**, of symbol Sn, and **atomic number** 50.

titanate: any of a class of compounds of general formula ATiO_{3+δ}.

titanium: a metallic chemical **element**, of symbol Ti, and **atomic number** 22.

toluene: also known as methylbenzene, or phenylmethane: an **aromatic hydrocarbon**, taking the form of a transparent liquid, very widely used as an industrial feedstock, or as a **solvent**.

tomography: an imaging technique that makes it possible to obtain, from a recorded, and duly processed signal, a three-dimensional image. In mathematical terms, the technique may be broken down into a direct **model** of the physical processes measured, and an inverse model – or reconstruction – based on the output from the direct model. See also **X-ray tomography**.

tracer: a chemical **element**, or compound, readily identifiable by **physicochemical** means; tracing involves using such a substance (a tracer) to monitor the movements of matter during a chemical reaction, or in the environment.

transcriptomic and proteomic analyses: the investigation of gene expression, by way of two approaches: the analysis of the transcriptome, consisting of the ensemble of ribonucleic acid (mRNA) transcripts present in a cell, in a given situation; and the analysis of the proteome, as represented by all the proteins coded for by these mRNA sequences. These approaches make it possible to identify, and quantify the products of gene expression, in a cell, or a tissue, at a given point in time, and for a given environment, with a view to allowing comparisons to be made between different biological states.

transducer: a device serving to convert one physical quantity into another.

transistor: the fundamental active **electronic component**, in electronics, where it is used for switching purposes, or for amplification, **voltage** stabilization, signal modulation... See also **field-effect transistor**.

transition elements (transition metals): a general term, used to refer to the ensemble of **elements**, in the periodic table of elements, that are characterized by a partly filled *d*, or *f* shell, whether in the elemental state, or in a stable state; also known as transition metals, this is a family comprising 38 elements, of **atomic numbers** 21 to 30, 39 to 48, 72 to 80, and 104 to 112, and including **manganese**, **iron**, **cobalt**, **nickel**, **chromium**, **platinum**... Elements from the first transition series [Sc, Ti, V, Cr, Mn, Fe, Co, Ni, Cu, Zn] are found to be the most advantageous, for use in Li-ion storage batteries (involving as they do lower masses than elements from the second, and third transition series).

transmission electron microscope (TEM): an **electron beam** (electron probe) is directed onto the sample, passing through it prior to being detected. A system of lenses (coils generating a **magnetic field**, which deflects the electrons) serves to focus the beam onto the sample, a second set of lenses then being used to modify the outgoing beam, to form a magnified image of the object. The **resolution** achieved may be as high as 0.1 nm, i.e. at the **atomic** scale. Just as the **scanning electron microscope**, the TEM is found to be a choice instrument, for the purposes of visualizing bulk structures, interfaces, and chemical composition.

transmutation: the transformation, by means of a nuclear reaction, of one **nuclide** into another. The transmutation being considered, for **radioactive waste** management purposes, would be aimed at transforming a **long-lived** nuclide (i.e. one involving a long **half-life**) into a shorter-lived, or stable nuclide.

treatment, or reprocessing (of spent fuel): the selective sorting of substances contained in **spent fuel**, in order to extract those that are recoverable, and **recyclable** (**uranium**, and **plutonium**), or possibly amenable to **transmutation**, while **conditioning** the **ultimate waste**.

U

ultratrace: a trace is an **element** occurring at a low concentration; this notion varies, with the ongoing evolution of the sensitivity of the techniques employed – nor does it have the same meaning for

a biologist, a geochemist, or a metallurgist: the term “trace” is used when the element subject to measurement occurs at concentrations ranging from a few tens of milligrams per kilogram (mg/kg) to a few tens of micrograms per kilogram (µg/kg), “ultratrace” for concentrations that are lower still.

ultraviolet (UV) radiation: a segment of the electromagnetic spectrum covering radiation characterized by wavelengths ranging from 400 nm to 10 nm, and in turn subdivided into a number of domains: the **near ultraviolet** (400–250 nm), **far ultraviolet** (250–180 nm), and **vacuum ultraviolet (VUV)** (180–100 nm). **Extreme ultraviolet (EUV)** corresponds to wavelengths of 100–10 nm.

uniaxial diffusion welding (U–DW): a solid-state joining process, involving the application of a force, at high temperature, on the parts that are to be welded, for a set time. This makes it possible to obtain particularly strong homogeneous, or heterogeneous joints, including for materials reputed not to be amenable to welding to one another.

uranium: chemical element, of symbol U, and atomic number 92, occurring naturally (**natural uranium**), in the form of a mixture of three isotopes: ²³⁸U, a **fertile** isotope (99.28%), ²³⁵U, a **fissile** isotope (0.71%), and ²³⁴U (traces).

V

Van der Waals force: taking its name from Dutch physicist Johannes Diderik van der Waals, 1910 Nobel laureate in Physics, this force is a weak electrical interaction arising between **atoms**, or **molecules**, or between a molecule and a **crystal**.

varactor: see CMOS (**complementary metal–oxide–semiconductor**) varactor.

viscosity: the degree of resistance to flow exhibited by a fluid.

vitrification: the operation involving the incorporation of **radioactive waste** into **glass**, to ensure **conditioning** in a stable form, as **packages** amenable to **storage**, or **disposal**.

volt (V): a unit of electromotive force, or electric potential difference (i.e. of **voltage**), taking its name from Italian physicist Alessandro Volta (1745–1827), famed for his invention of the electric battery, in 1800.

voltage: (*general definition*) the circulation of an electric field around a circuit; (*usual definition*) the difference in electric potential arising between two points of an electrical circuit (e.g. between the positive, and negative **electrodes**).

voltage-controlled oscillator (VCO): an oscillator of the inductance–capacitance type, **voltage** control being effected by means of a tunable **varactor**.

voltammetry: an electroanalytical method, based on the measurement of the current flow generated by the reduction, or **oxidation** of test compounds occurring in a solution, as a result of a controlled variation in the potential difference arising between two specific **electrodes**; this makes it possible to effect the identification, and quantitative measurement of a large number of compounds (cations, certain anions, organic compounds), simultaneously for some of them. It further makes it possible to study chemical reactions involving these compounds.

W

watt (W): a unit of power, corresponding to the production, or consumption of 1 **joule** per second. Chief multiples: the kilowatt (1 kW = 10³ watts), the megawatt (1 MW = 10⁶ watts), the gigawatt (1 GW = 10⁹ watts), and the terawatt (1 TW = 10¹² watts); **watt–hour (Wh):** the amount of energy consumed, or delivered by a system, corresponding to 1 W power for 1 hour.

wave filter: a device that makes it possible to allow only a certain range to go through, out of the **electromagnetic** waves reaching it, depending on wavelength.

whey: also known as “lactoserum,” this is the liquid fraction yielded by the curdling of milk, containing no casein, and virtually no fat.

X

X-radiation: **electromagnetic radiation** involving wavelengths, comparable to interatomic distances, lying in a range from a few fractions of a **nanometer** (0.005 nm) to 1–100 nm, with energies ranging from a few **kiloelectronvolts (keV)** to a few hundreds of keV.

X-ray absorption spectroscopy: this technique allows variations in the **X-ray absorption** coefficient to be measured, over an energy range extending a few hundreds of **electronvolts** beyond the **ionization** threshold of a given chemical **element**. It yields information as to the **electronic** characteristics of the element subjected to analysis [X-ray absorption near-edge structure [XANES]], and on its **atomic** environment (extended X-ray absorption fine structure [EXAFS]).

X-ray diffraction: a method used for the structural investigation of substances occurring in **crystal** form, since **X-ray** wavelengths are of the same order as internuclear distances, being sufficiently small to result in **diffraction** patterns, due to the – more or less densely packed – crystal planes.

X-ray tomography: a nondestructive technique that makes it possible to obtain “cross-sectional” views of a three-dimensional object. Its principle relies on the multidirectional analysis of the interaction of an **X-ray** beam with a material, by way of the radiation transmitted, once it has passed through the object, as recorded by detectors.

Y

Young’s modulus (or tensile elastic modulus): for an “elastic” material subjected to tensile, or compressive stress, this is the ratio, as measured longitudinally, between variations in **stress**, and strain. Derived as it is from Hooke’s law (strain is proportional to stress), this ratio is expressed in terms of a pressure, measured as a rule in **megapascals (MPa)**, or **gigapascals (GPa)**.

yttrium: chemical element, of symbol Y, and atomic number 39.

Z

Zeeman effect: an effect arising in certain **atoms**, when subjected to a **magnetic field**, resulting in the splitting of characteristic spectral lines (due to a splitting of energy levels), into a number of frequency-shifted, **polarized** sublevels (**Zeeman levels**), the offset (the **Zeeman transition**) being proportional to the intensity of the ambient field.

zinc: chemical element, of symbol Zn, and atomic number 30; a naturally occurring metal, combined with sulfur in zinc blende (sphalerite), and in hydrated oxide form in calamine (hemimorphite).

zirconia: the name commonly used for **zirconium oxide** (ZrO₂), a technical **ceramic** material of opaque appearance, known as cubic zirconia (CZ) when it is transparent, in which form it is used to imitate diamond.

zirconium: a metallic chemical element, of symbol Zr, and atomic number 40. Zirconium **alloys** are widely used as a **fuel cladding** material for **water nuclear reactors**.